sciendo

DOI: 10.1515/sspjce-2021-0001

Effect of cohesion, the friction angle and the time under static loading on the behavior of piles

Hacene Benyaghla

University 08 may 45, P.B N°401, Guelma, 24000 Algeria
Faculty of science and technology, Department of civil Engineering and Hydraulics
e-mail: benyaghla@yahoo.fr.

Abstract

The calibration chamber of the 3SR INPG laboratory in Grenoble used to study the point stress and the shear, mobilized along the shaft of the pile under monotonic axial loading. The physical model used for the various tests is a standard mini-pile installed in standard sand: Fontainebleau sand. This article explores the induced effects on the bearing shear capacity of the pile as a function of time, up to the point of failure, under different monotonic loads applied after periods of rest. A series of monotonic static loading tests, were performed on the pile. Tensile load tests, uplift, were performed before and after each series of static loads. A Lateral stress was observed at the start of the experiment at the pile-soil interface. It disappears as soon as the pile is driven into the soil, due to the dilatancy of the soil. This observed phenomenon is probably due to a decrease in non-mobilized lateral friction at the start of the experiment. A study of this phenomenon will be described in this article. Likewise, the effect of the mechanical characteristics of the soil and the effect of time will be presented in the bearing capacity of the soil, as well as the total bearing capacity of the pile under monotonic static loading.

Key words: calibration chamber, pile, soil, sand-pile interface, monotone axial-loading

1 Introduction

Calculation at fracture aims to identify a potentially bearable loading zone for a structure, whose load depends on a finite number of parameters. In its research applications, it is a question of knowing the state of stresses and deformations of the ground at a given stress level. We use in this case a criterion of rupture and not a constitutive law. This is of great convenience given the difficulty of developing such a sufficiently realistic law. The stability of a configuration can only be established with strict assumptions on the material. In the charge space, the domain of these charges is convex, and does not contain any charge. Any load, outside the domain, will cause the system to fail. The monotonic static loading experimental approach undertaken, is in the sense of security. It presentis a statically admissible stress field and expresses that it satisfies the fracture criterion Several studies have

been carried out on this subject, both for purely cohesive soil,[1], and for detrital soils, [2]. Piles are very often used to support structures made on soils with low mechanical characteristics (bridges, very tall buildings, ect) These large structures transmit considerable forces of inertia to the foundation system, including static and dynamic loads. When they are subjected to a movement of the ground (earthquake), they transmit horizontal forces, and cyclic bending moments. In this case, the piles are subjected to a cyclic axial load which can affect its bearing capacity. It is therefore important to analyze the mechanisms involved at the pile-soil interface during a static or dynamic loading in the sand on the bearing capacity of a pile. Several authors have demonstrated this type of phenomena, during the installation of piles by dynamic driving, or by monotonous driving [3], [4], [5], [6], [7]. In certain cases, these observed disturbances could, by hypothesis, be compensated by a process of recovery over time of the bearing capacity of the pile around it. This appens due to a modification of the mechanical characteristics of the soil particles proposed by certain authors,[8]. For dynamic loading [9], list the main factors influencing the behavior of the pile. This article is devoted to the study of the various parameters, influencing the bearing capacity of the soil and the bearing capacity of the pile to the mobilized forces. It will be devoted to an experimental approach and a numerical calculation for the determination of the point stress, the shear stress, the angle of friction and the cohesion. The pile will undergo a monotonic axial loading.

2 Experimental trials

2.1 Introduction

The foundation tests on a real model are generally very expensive and in the majority of cases are impossible to perform. In order to overcome this handicap, the real structure is scaled down, believing that the reduced model and the real model have a analogous behaviour. The rheological behavior of a model in loose sand under a weak constraint will be the same as that of the prototype model in dense sand and strong pressure if the two points, that of the model and that of the prototype are located on a parallel to the critical line, That is to say if these two points have the same value of the state parameter ψ.This state parameter includes both the influence of soil density and stress level. It allows the unique correlation of peak resistance between the model studied and the prototype by a standardized penetrometer test, [10], [11], figure 1. For this experimentation, the Sand used is dense. The density of the sample is of the order of 72% for a void index of e= 62% (3SR, Laboratory, INPG Grenoble. To ensure a similar rheological behaviour between the model and the prototype, the choice of the initial vacuum index of the soil in the laboratory is important because it limits the reinterpretation of the results obtained in the laboratory. The soil of model cannot be placed at a void index greater than the maximum void index. Likewise, the soil of model cannot be placed at an index lower than the soil of prototype characterized by a minimum void index [12], figure 1.

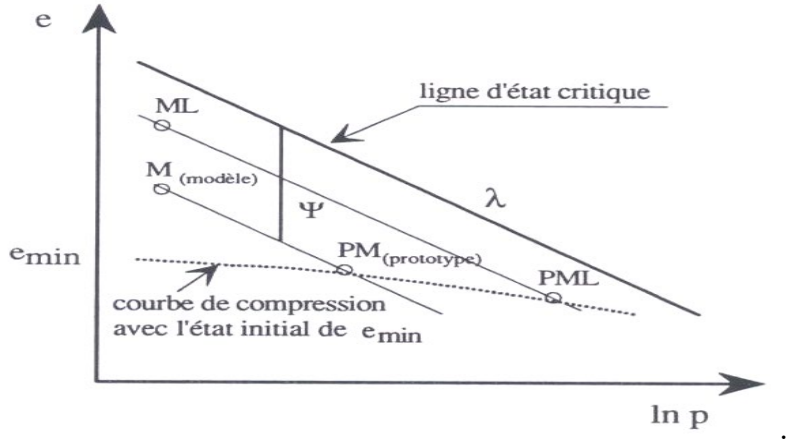

Figure 1: Principle of interpretation of the results of laboratory tests at 1g (the gravity scale g* = 1/1*) [13].

2.2 Description of the calibration chamber

The calibration chamber has been designed for the dual purpose of : Calibrate the response of recognition devices (piozo-cone, pressuremeter, dilatometer), in situ in a material with well-known parameters (confined condition and controlled compactness), to constitute a physical simulation tool for the behaviours of inclusions with axisymmetric geometry in the soil The realization of this type of test can be conceived in a good condition only if the mass of soil located in the calibration chamber has the same behaviour as a slice of ground in place at a given depth. The conditions at the limits of the calibration chamber must be as close as possible to those of the ground in situ. This can be done since the upper and lower borders, as well as on lateral chamber boundaries are installed in the chamber. This allows the control of the boundary conditions. The membranes at the upper and lower borders, apply vertical pressure to the mass of soil simulating the weight of the overlying soil. The membranes on laterals chamber boundary allow the application of variable boundary conditions, (Figure2).

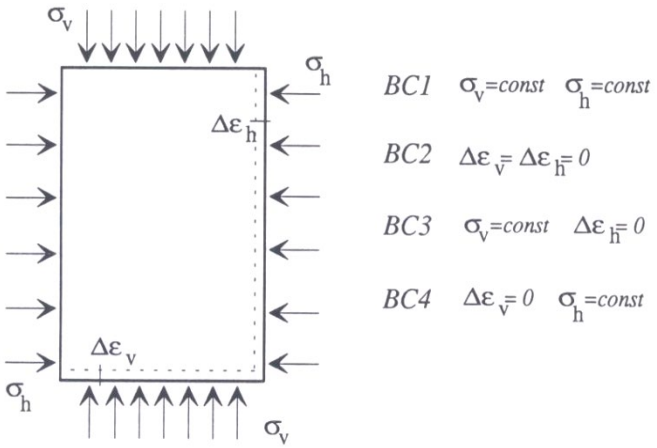

Figure 2: Boundary condition of the calibration chamber

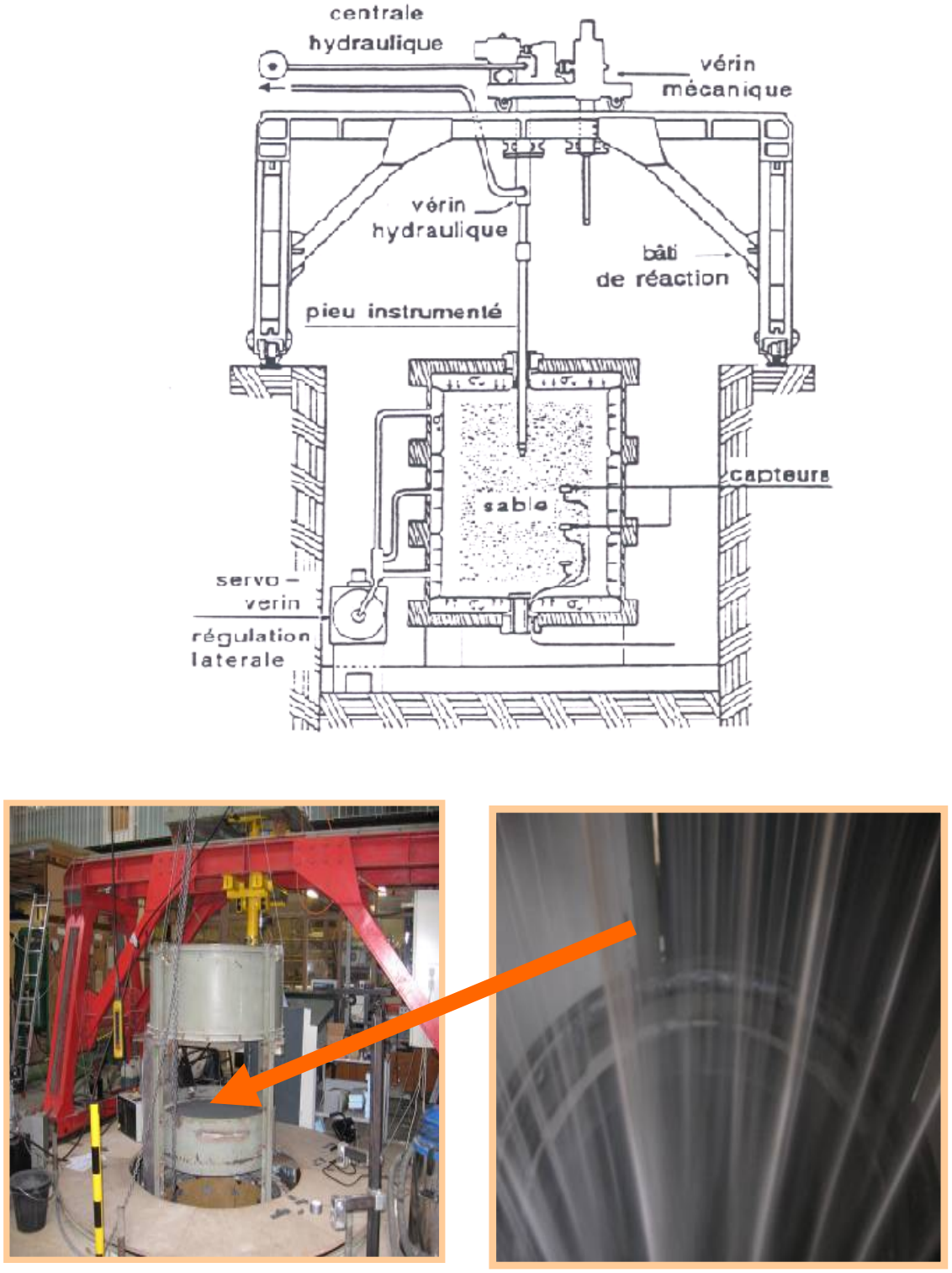

Figure 3: Calibration chamber of the 3SR laboratory

2.3 Static tests

For this test, two horizontal membranes fixed on the internal face of the upper and lower plates, and filled with water apply the vertical stress conditions. Depending on the degree of filling of this area, the depth of the desired area of the test is obtained. The membranes on the side walls provide the boundary conditions required for the test. The boundary conditions for the experiment carried out ensured by the lateral membranes are: The lateral stress remains constant throughout the period of the experiment with zero lateral strain ($\varepsilon_h = 0, \sigma_h = cte$). The horizontal, lower and upper membranes ensure the following limiting conditions: the vertical stress remains constant throughout the test period with zero vertical strain ($\varepsilon_v = 0, \sigma_v = cte$) (Figure 4).

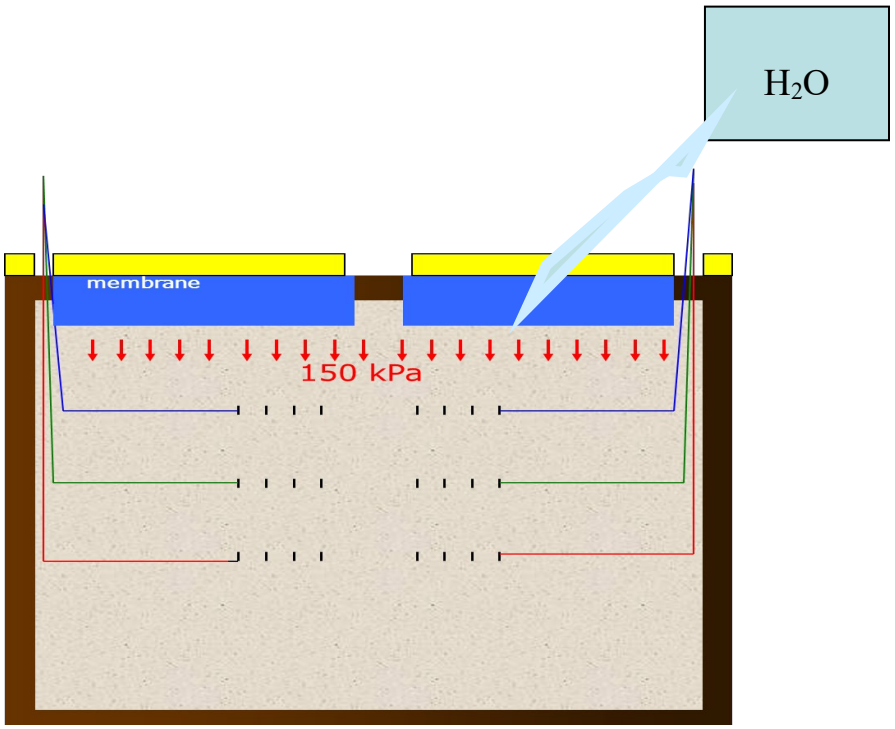

Figure 4: Pressurizing system, laboratory 3SR INPG Grenoble

2.4 Test sand

The Sand use in this experiment is a sand of Fontainebleau N34. This sand is well characterized as uniform. This sand is pure (99.7% silica). The test sample is placed in the calibration chamber by the pluvassions technique in order to guarantee a homogenization of the soil. The density of the sample is of the order of 72% for a void index of e= 62% (3SR, Laboratory, INPG Grenoble).

Table 1 Index properties of Fontainebleau NE34 sand (Laboratory 3SR Grenoble

Grain shape	GS	D10(mm)	D50(mm)	D60(mm)	emax	emin
Granulometric test	2.65	0,15	0,21	0,23	0,90,	0,51

2.5 Piles

The characteristics of piles are:

Table 2 the geometry of the selected pile is conical 3SR, Laboratory, INPG Grenoble. These characteristics are:

Type of pile	Length The shaft (m)	Length of tip (m)	Diameter at the top (m)	Diameter in foot (m)	weight (g)
Conical	1.40	0.100	0.100	0.100	36

Table 3 Type of pile

Type of pile	Surface Area in foot (m^2)	Lateral surface (m^2)	Pile volume (m^3)
Conical	0,006	0,229	0,005

2.6 Soils sensor

Soil stress sensors of different capacities and types were installed inside the chamber. They are installed on 2 or 3 different levels, top (T), middle (M) and bottom (B). At each level, sensors (TML PDA / PDB and Kyowa PS / D) were placed to monitor the vertical stress and the frictional stress. Loading and unloading tests were carried out on the piles after defined periods of time. These tests gave results which will be presented in this article.

3 Experimental tests

3.1 Static loading test

Recording are made after a initial static loading, which determines the test area. The load is 150 kPa. It is common for the new grain arrangement caused by the start of the test to cause soil expansion. The test is said to be unconfined and a minimal lateral stress appear. As soon as this phenomenon disappears, a contraction of the ground appear and the vertical stress is mobilized, the test is then said confined tests. The recordings are made at two levels, the upper part or the main plane, and the lower part or the secondary plane, for static loading. The

results of thése tests are presented in this article for a monotonic static loading
The axial static loading tests were carried out by a hydraulic cylinder for monotonic and continuous soil penetration. the Results obtained for the peak stress (qc), the friction stress (qf) and the total stress (Q_T) obtained, are shows in Figures 5, Figure 6 and Figure 7.

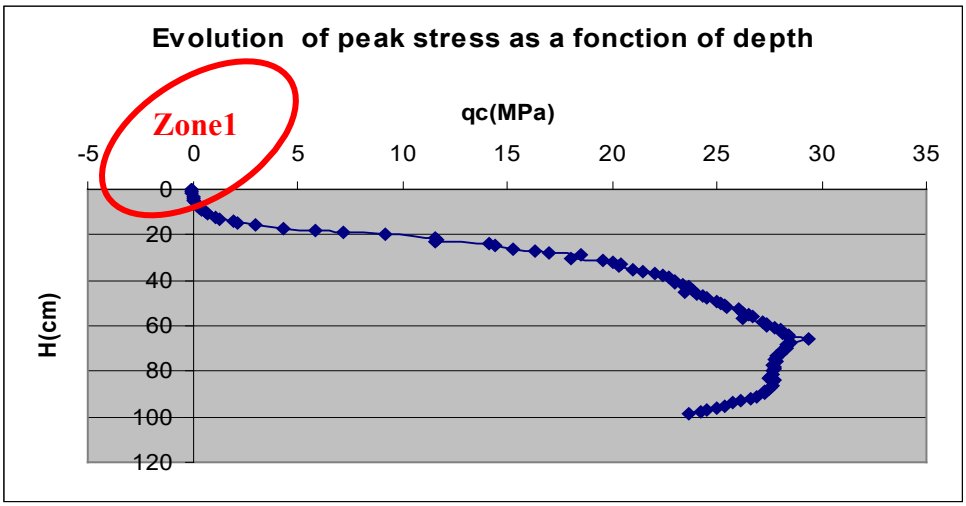

Figure5: Evolution of peak stress as a function of deep

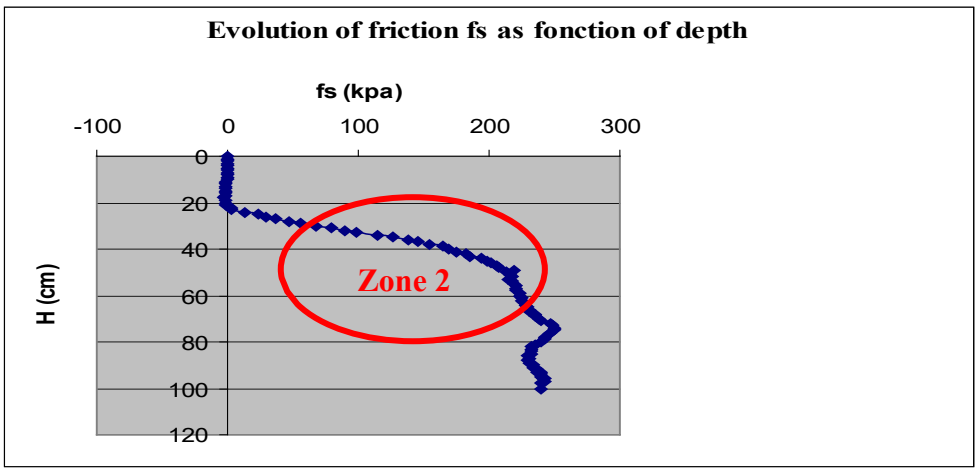

Figure 6: Evolution of friction under axial static load

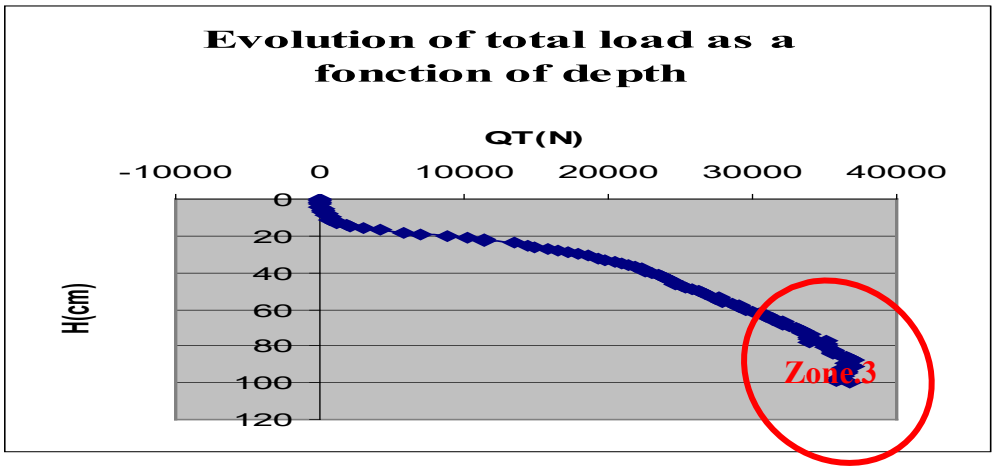

Figure 7: Evolution of the total stress in the soil under static load

3.1.1 Comment

3.1.1.1 Zone 1

At the level of the zone located at the base of the mini-pile, one notice at the time of the beginning of the sinking of the pile, an expansion of the soil around the shaft of the pile. An upward movement of the ground over a certain height is observed which will be defined during the numerical calculation of the lateral friction according to the results obtained experimentally. Likewise, the calculation of the friction angle will be performed at the same time. The start of the test will be considered as an unconfined test. This was previously announced. The earth passive pressure at this time will not be mobilized.

3.1.1.2 Zone 2

We notice a beginning of downward movement of the ground. A new arrangement of grains is triggered, one then speak of the beginning of compressibility of the soil. The mobilization of the friction angle and of the cohesion allows the mobilization of the earth passive pressure.

3.1.1.3 Zone 3

The grain arrangement triggered at the start of the second zone becomes effective. The ground stabilizes and the lift of the ground will be ensured successively but limited just before rupture as a function of the critical friction angle, the critical cohesion, and the effective depth. We observe that at the end of the curve, a plateau is reached and therefore a constant value of the peak pressure.

Table 4 Partial results of the stresses of extraction and monotonous driving-in of a pile

Depth (cm)	0	0,4	0,9	2	6,5	8,5
Q_T(Draving in) (N)	0	14700	27400	30300	32800	32500
Q_T(Extraction)(N)	31500	0	-7200	-8800	-10900	-11500

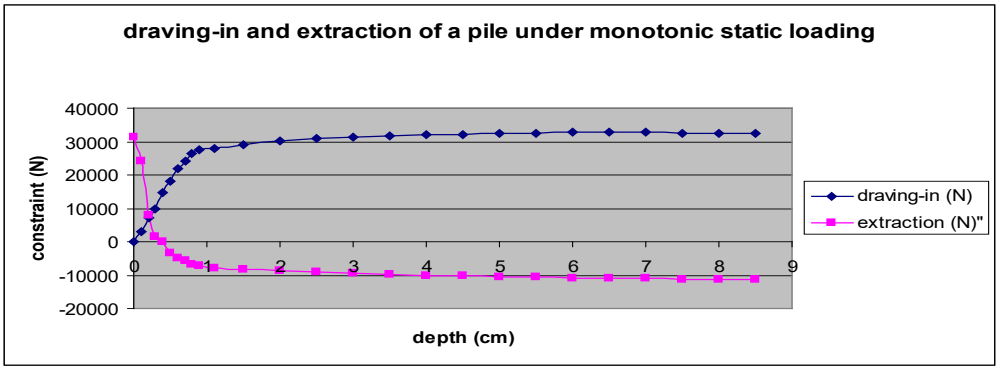

Figure 8: Draving and extraction of a pile static loading

Table 5 Partials results of the shear stresses and a peak stress of a pile

Depth (cm)	0	3	10	50	76	87	99
Friction stress (N)	-0,24	0,36	-1,7	171,5	201,9	185,6	185,6
shear stress(N)	-0,24	0,32	-2,45	128,35	149,1	132,3	132,3

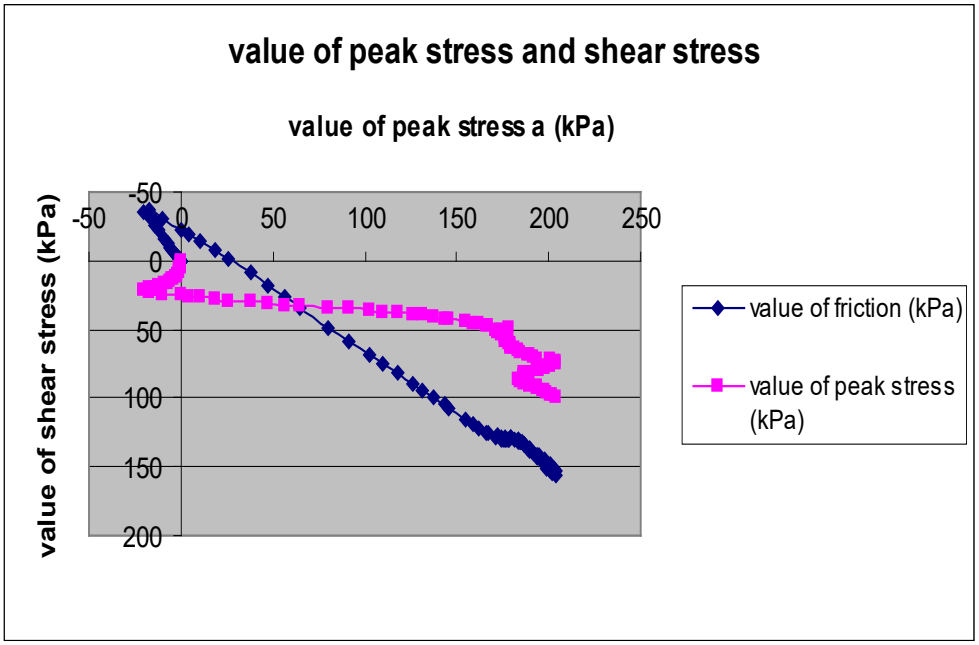

Figure 9: Value of shear stress and peak stress of a pile

3.2 Comment

[11], [14], [15], and others have established the relationship between the monotonous driving-in of a driven pile, and the extraction of a driven pile. the assumptions of the time affirmed, that the various setting up of a stake induce negative constraints, Figure 9. During sinking, the mobilization of friction first involves the cancellation of negative stresses, while during extraction, the shear stresses always keep the negative sign ,Figure 9.At the start of the test, a displacement due to the mobilization of a weak lateral stress is recognized, which disappears as soon as the pile sinks into the ground, leaving room for the mobilization of the passive pressure of the earth. This Observation has already been announced above. It should be noted that the value of the shear stress around the shaft of the pile is lower than the peak stress, which allows us to conclude that the soil is loosened at the point.

Figure 10: Crushed grain of sand

3.3 Comment

Experimentally, after having reassembled the pile, we observe that the soil around the shaft of the pile is crushed. The soil, here the sand has changed color, he goes from yellow to gray Figure 10. The attempt at granulometric analysis of this crushed sand has failed, because part of this sand is stuck on the shaft of the pile, on the one, hand and on the other hand, the quantity recovered is very low for this type of analysis. For that one carried out an analytical calculation of the cohesion and of the angle of friction via the modified formula of [16], starting from the experimental results to try to include understand this phenomenon
One carries out, a numerical calculation by the modified formula, [16], and the formula of calculation of Mohr Coulomb using the total forces successively mobilized, according to the depth for a monotonic axial loading.

4 Influence of cohesion, friction angle and time

One carries out, a numerical calculation by the modified formula, [16], and the formula of calculation of Mohr Coulomb using the total forces successively mobilized, according to the depth for a monotonic axial loading.

$$Log(tg\varphi_c) = Log\left\{\frac{A}{BLog\dfrac{Q_{(n+1)}}{Q_n}}\right\} \qquad (1)$$

$$\tau = \sigma \times tg\varphi + c$$

Dr Density	A	B
70	0.9275	0.08630
50	0.7630	0.0795

Table 6 Partial values of the friction angle as a function of the depth

Depth(m)	1	4	7	10	13	16	20
friction angle (degree)	36,7	36,76	36,72	36,68	36,5	36,08	31,4

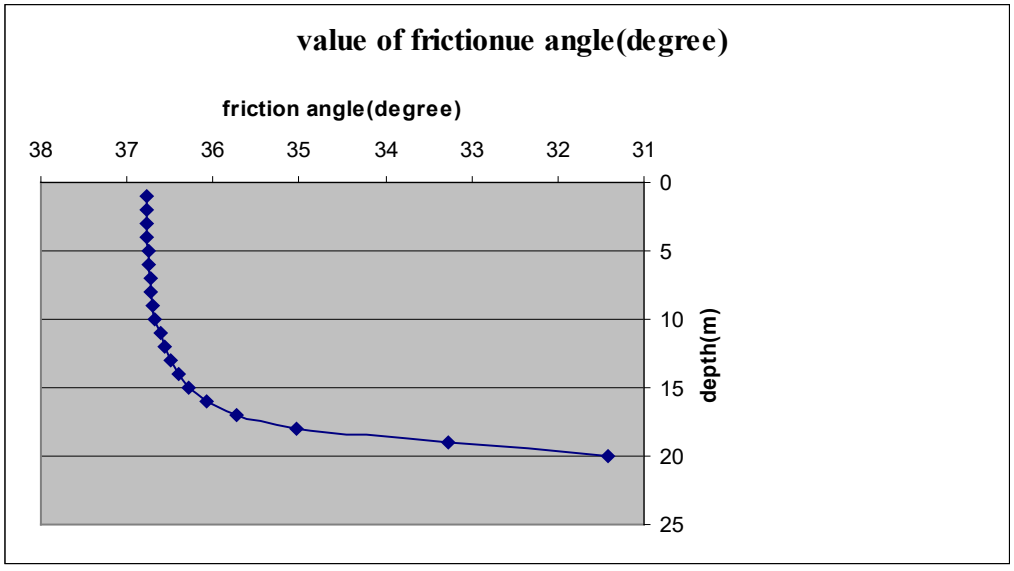

Figure 11: Calculation of the friction angle as a function of the depth

4.1 Comment

The Figure 11 shows a decrease in the friction angle as a function of the depth, to reach a level from which, the value of the friction angle becomes a constant. This will be the critical value φ_C (critical value of the friction angle), before deterioration of the lift of the soil.

Table 7 Partial values of cohesion as a function of depth

Depth(cm)	56	138	185	217	237	243
Cohesion(kPa*10-1)	25,74	102,50	145,97	173,88	194,18	204,04

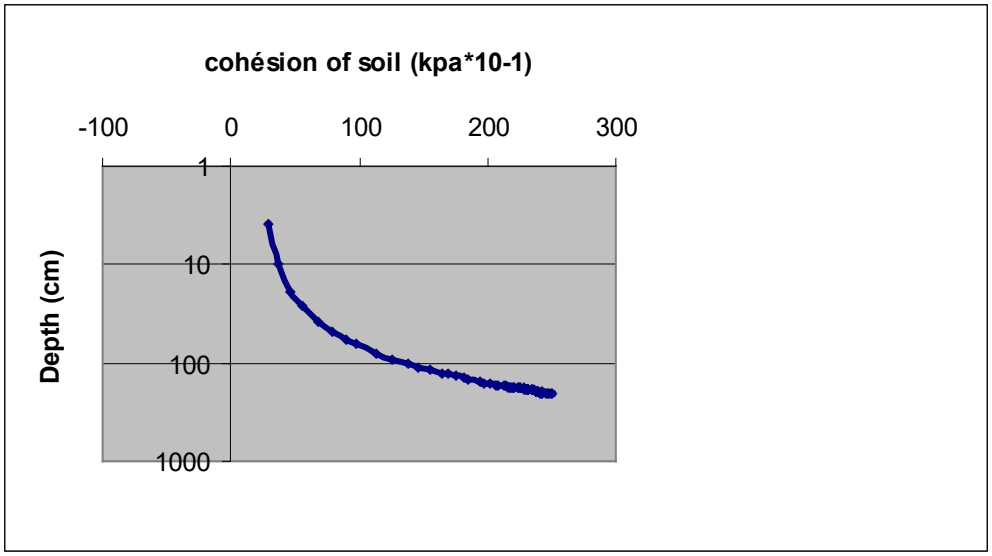

Figure 12: Calculation of the cohesion as a function of the depth

4.2 Comment

On the other hand, figure 12 shows an increase in the cohesion of the soil as a function of the depth, to reach a level from which the value of the cohesion of the soil becomes a constant: it will be the critical value of, thus increasing the stress of shear applied. On the shaft of the pile, which can affect its bearing capacity? This result confirms the comment of figure 11. Indeed the calculation of the shear stress by the Coulomb criterion becomes really imprecise.

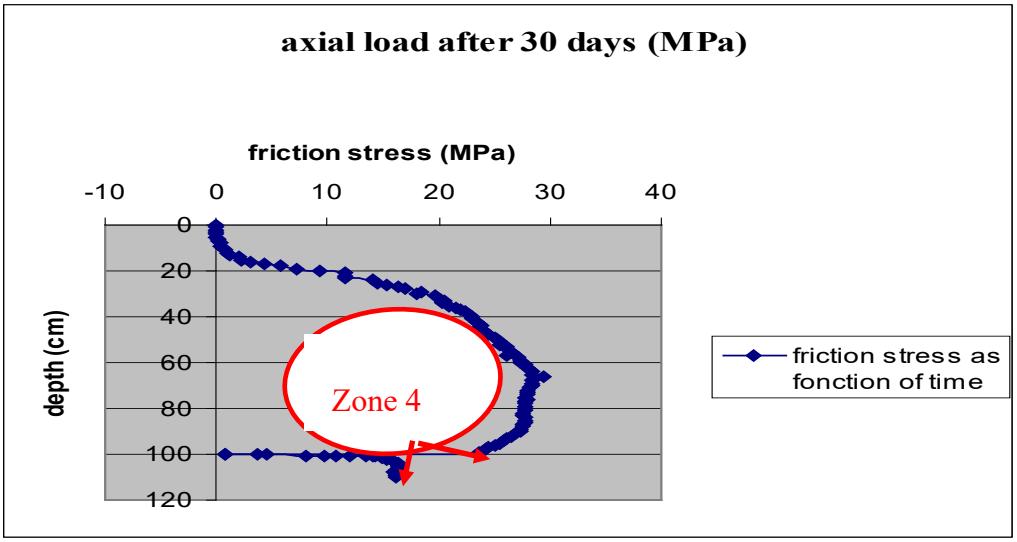

Figure 13: Evolution of the friction stress as a function of time under monotonic axial loading

4.3 Comment

A pile driving-in test was carried out in two steps, A first driving-in at 50 cm from a depth of 15 m simulated by the pressurization system Figure 13, and thirty days (30) later, the driving-in was taken backwas carried out above the remaining depth, i.e. 50 cm. The results obtained in Figure11 of the frictional stress start from the value obtained during the first test. A slight subsidence of the ground is observed, the influence of which on the values of the frictional stress does not appear. However, we notice that the curve follows a path which will join the path obtained during the first experiment. This allows us to conclude as a hypothesis, that time plays no role in the values of the friction constraint.

5 Conclusion

Experimentally, after having reassembled the pile, we observe that the soil around the shaft of the pile has been crushed (Figure 10). The attempt to analyze the granulometric, or sedimentological of this powdery soil, obtained from the sand used for the experiment has failed. It was stuck on the shaft of the pile; on the one hand, on the other hand, the amount of this soil recovered was very low for this type of analysis. The initial soil became a very fine soil completely linked to the shaft of the pile. The study of the sedimentology or granulometry, for to obtain, the physico-mechanical characteristics of this soil, is difficult to determine. The all studies which have been devoted to it have failed. From the experimental results at this level, the analytical study of the friction angle and the cohesion shows a decrease in the value of the friction angle, and an increase in the value of the cohesion as a function of the depth. The two values separately reach a plateau, where their respective value becomes constant. It is then assumed that the angle of friction and the cohesion respectively reach a critical value. These two friction angle and cohesion values define the limit load bearing capacity of the soil before failure. At the start of the penetration of the pile into the soil under monotonic axial loading, the test is considered as an unconfined test at the start of

soil expansion. After a random arrangement of the soil particles and significant penetration, the test becomes confined and the soil cohesion as well as the earth passive stress is gradually mobilized due to the contractancy of the soil. From the experimental results of friction angle and cohesion, the analytical formulations for the calculation become applicable, which was not the case at the time of soil dilatancy. This is reported by the experimental results represented in the Figures 10 and Figure11 obtained for the frictional stress and the cohesion. Eurocode 7 allows the calculation of tangential stress as a function of normal stress, by application of the Mohr-Coulomb principle. This study shows that the linearity between the normal stress and the tangential stress is not assured. The friction angle and the cohesion are a function of the depth. They respectively reach their critical values at a predefined depth for each of these two Parameters. Their respective diagrams are curve Figure 11 and Figure 12.These results confirm the non-linearity of the normal stress by relation to the tangential stress. In the end, the increase in soil lift over time is a hypothesis put forward by several authors. We could not confirm this in this study. The physico-mechanical characteristics of the soil around the pile shaft have not been determined. It would be possible, by hypothesis, for this soil to serve to increase the cohesion at the soil-structure interface. If this is verified, soil lift will increase as and as cohesion increases with time at the soil-structure interface. This is an interesting research perspective to affirm and refute the conclusions drawn regarding the increase in the bearing capacity of the soil, as a function of time by some authors.

Acknowledgements

The author gratefully acknowledge Professor Emeritus Pierre Foray who died recenthly for his help in carrying out this work during the years of training the author spent at the 3SR INPG Grenoble laboratory. Thanks

Reference

[1] Aboshi,H, Ichimoto, E, Enoki M and Harada, K 1979. The “composer”, a method to improve characteristics of soft clay by inclusion of large diameter sand columns, .R. International symposium. on soil building: Army Land and other methods 1, 211-216

[2] Airey, D. W., Al-Douri, R. H., Poulos, H. G. (1992). Estimation of pile friction degradation from shearboxtests. Geotechnical Testing Journal 15(4): 388-392

[3] Axelson, G. (2000). Long-term set-up of driven piles in sand, PhD Thesis, Department of civil and Environmental Engineering: Stockholm Royal Institute of Technology

[4] Foray P. (1991). Scale and Boundary Effects on Calibration Chamber Pile Test, Calibration ChamberTesting, pag 147-160

[5] Jardine, R.J., Zhu, B.T, Foray, P., & Dalton, C.P. (2009). Experimental arrangements for the investigation of soil stresses developed around a displacement pile Soil and Foundations 49(5) pp. 661-673

[6] Bullock, P.J., Schmertmann, J.H., McVay, M.C. & Townsend, F.C. (2005). Side Shear Setup. I: Test Piles Driven in Florida. Journal of Geotechnical and Geoenvironmental Engineering131(3): 292-300

[7] Bowman, E, T, and Soga, K, (2005), Mechanisms of set-up of displacement piles in sand: Laboratory creep tests, Canadian Geotechnical Journal 42(5): 1391-1407

[8] Yang, Z, X, Jardine, R, J, Zhu, B, T, Foray P and Tsuha, C, H, C,(2010): Sand grain crushing and interface shearing during displacement pile installation in sand in Press for publication in

the Géotechnique Themed Issue
[9] Chow, F, C, Jardine R, G, Brucy, F, and Nauroy, J, F (1998): Effect of time on capacity of pipe piles in dense marine sand. Journal of Geotechnical and Geoenvironmental Engineering, ASCE 124(3): 254-264
[10] Chan, S, and Hanna, T, H, (1980): Repeated loading on single piles in sand American Society of civil Engineering Division: 106(2): 171-188
[11] Mokrani , L;(1991) Simulation physique de comportement de pieux à grande profondeur en chamber de calibration , thése de doctorat à INPG, Grenoble
[12] Altaee,A,Fellenus,B,H,Eving,E,(1992) Axial load transfer for pile in sand I&II, Canada geotechnical J.29
[13] Zelikson, a leguay, P (1986). Some basic data on piles under statique and dynamique loading from stress conserving models.Proc of 3rd int.conf on Numerical methods in offshore Piling Nante, pp.105-124
[14] De Nicolas, a; Randolph,mf(1993); tensile and compressive shaft capacity of piles in sand, JGE,vol 119 n°2
[15] Benyaghla H (2009), Calculating the rupture of pile under static loading by method of analysis, World journal of Engineering 10(02) (2013) 145-158
[16] Baligh, M (1975). Cavity expansion insand with curved envellopes, journal of the Soil Mechanic and Fondations Division,ASCE,vol.102,N°GT11

DOI: 10.1515/sspjce-2021-0002

The effect of steel fiber size on the properties of fresh and hardened self-compacting concrete incorporating marble powder

Naima Haddadou[1, 2], Messaouda Boulkhiout[3], Malika Sabria Mansour[2], Rabah Chaid[2] and Youcef Ghernouti[2].

T1 Department of architecture, University of Algeria I Benyoucef Ben Khedda, Algeria
2 Department of civil engineering, Polytechnic National School, Algiers, Algeria
3 Department of civil engineering, research unit: materials, process and environnement, University M'Hammed Bougura of Boumerdes,. Algeria
e-mail: n.haddadou@univ-alger.dz

Abstract

The current study aims at highlighting the fresh and hardened characteristics of self-compacting concrete (SCC) incorporating marble powder and steel fibers at different sizes. Seven SCC mixtures were investigated with two different types of steel fibers were used in combination at different proportions, keeping the total fiber content constant at 72 kg/m3, 400 kg/m3 of cement and 80kg of marble powder was substituted by weight of fine and coarse aggregate. Slump flow time and diameter, L-Box, and sieve segregation test were performed to assess the fresh properties of the concrete. Compressive strength, splitting tensile strength, fracture energy and ultrasonic pulse velocity of the concrete were determined for the hardened properties.
The results indicate that marble powder with high fineness can be used with steel fiber to produce reinforced self-compacting concrete (RSCC) with an improvement in the hardened properties, even though there is some reduction in the fresh properties because of the use of large steel fibers.

Key words: Self-compacting concrete, marble powder, steel fiber, workability, strength.

1 Introduction

The Self-compacting concrete (SCC) is a concrete that has a high flowability and settle into the heavily reinforced deep sections and can be placed without vibration; it is able to flow under its own weight [1].
Though, one of the disadvantages of SCCs is the cost, associated with the use of the high volumes of Portland cement and chemical admixtures. One alternative to minimize the cost of self-compacting concrete is the incorporation of cementitious minerals which are finely pulverized such as limestone powder, marble powder, natural pozzolan, fly ash and slag, added to concrete as separate ingredients either before or during mixing [2]. The compactness

of the SCC matrix, due to the higher amount of fine and extra-fine particles, may improve interface zone properties [3, 4].
On the other hand, effect of mineral admixtures on the strength, durability and environmental effect of SCC and RSCC (fiber reinforced self-compacting concrete) has been extensively investigated under different environmental conditions [5, 3, 6, and 7]. The assessment of the fiber reinforced SCC by the researchers shows improvement of compressive strength, flexural strength, splitting tensile strength, elastic modulus, creep and shrinkage, as compared to conventional normally vibrated concrete, self-compacting concrete and normally vibrated fiber reinforced concrete under statically applied loads [5, 8, 9, 10, 11, and 12].
The addition of fibers to self-compacting concretes extends its possibilities, that since it may take advantage of its superior performance in the fresh state to achieve a more uniform dispersion of fibers, which is critical for a wider structural use of fiber-reinforced concrete. Some useful, mainly empirical, guidelines are available for mix design of fiber-reinforced SCC [13].
The character and performance of RSCC changes depending, on the properties of concrete and the fibers. The particularities of fibers that are usually of interest are fiber concentration, fiber geometry, fiber orientation, and fiber distribution. Using a single size of fiber may improve the quality of FRSCC to a limited level. However, the concept of combination, adding two or more sizes of fiber into concrete, can offer more attractive engineering properties as the presence of one size of fiber.
Corinaldesi et al. [14] stated that since its high degree of fineness, MP was proved to be very effective in providing very good cohesiveness of mortar and concrete, and consequently the fiber-matrix bond, leading to enhanced post-cracking toughness and energy absorption capacity [15]. Even though, the suitability of using such a substandard marble powder in fiber reinforced self-compacting concrete needs much detailed investigations.
The objective of this study is to assess the effects of steel fibers with different length on the fresh and hardened properties of SCC incorporating marble powder with high fineness.

2 Experimental procedure

2.1 Materials

The fibers used in the present work are made of steel with low strength (Yield Stress 260MPa) for economical reason. The two types of fibers that have been used are of rectangular section and L=30 and 15mm lengths respectively (Fig.1). Type of cement used is 42.5 CEM II/A With high proportion of clinker and the characteristic strength at 28days is a minimum of 42.5 MPa, from M'sila (Algeria) factory. It is the type of binder used for making concrete for the purpose of the work undertaken and marble powder from Fil Fila is used as substituting fine and coarse aggregate. Workability improvement of SCC was obtained thanks to the polycarboxylate superplasticizer (MEDAFLOW 30) used and a viscosity modifying admixture (Medacol BSE). Continuous graded coarse aggregates (3/8 and 8/15) were used with specific gravity and water absorption of 2.56 g/cm3 and 1.03% respectively. Natural dune sand and river sand were used. Selected sands and coarse aggregates are subjected to grain size distribution analysis according to XP P 18-540 standard [16]. Physical properties of used sands are given in table 2. The gradation of coarse and fine aggregates was determined by sieve analysis. The water used was tap drinking water.

Table 1: Chemical and Physical Properties of Cement and Marble Powder

Chemical	Cement	Marble Powder
SiO_2	16,52	0.34
Al_2O_3	4,08	0.04
Fe_2O_3	2,89	0.13
CaO	58,49	54.93
MgO	1,47	0.73
K_2O	0,47	0.01
Na_2O	0,24	0.01
SO_3	1,98	0.06
TiO_2	0,22	0.01
P_2O_5	0,14	0.02
Insoluble	1,09	/
Loss of ignition	7,45	43.72

Table 2: Properties of used sands (DS and RS)

	DS	RS
Fineness modulus	1.29	2.85
Sand equivalent	48	90
Absorption (%)	2.43	0.63
Moisture content (%)	1	0.42

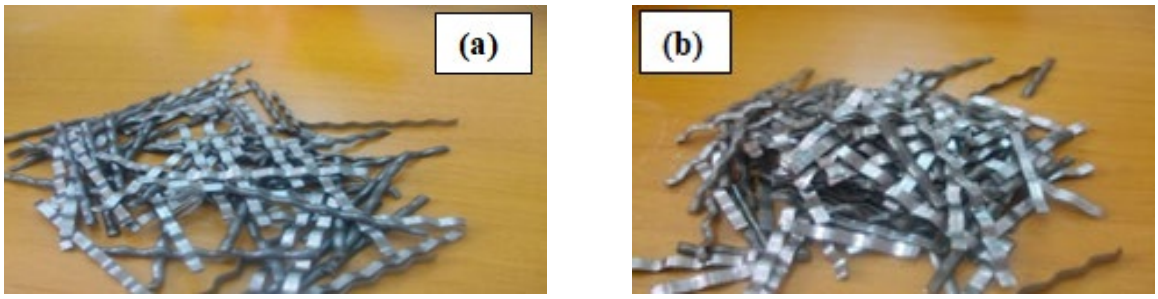

Figure 1: (a) Long Steel Fibers (LSF), (b) Short Steel Fibers (SSF)

2.2 Mix proportions

The Seven mixtures, two controls, the first with marble powder and the second with limestone powder as addition and five fibers reinforced self-compacting concrete, were prepared for investigating the effect of marble powder and sizes of steel fiber. Water/binder (cement+ MP or LP) ratio was designed as the ratio of 0.32 for all concrete mixtures. All of the mixtures

had the same amount of marble powder 80 Kg witch was replaced by fine and coarse aggregates. These were named as SCC1with marble powder, SCC2 with limestone powder, RSCC1 with SSF, RSCC5 with LSF and RSCC2, RSCC3 and RSCC4 with SSF and LSF in combination, indicating the two different values of aspect ratios (Steel fiber length: 30 and 15 mm), and the same percentage of volume fraction (Steel fiber volume: 1%) of steel fiber incorporated in the mixture. For all the mixtures, the total amount of binder (Cement + Marble powder), cement, marble powder, water and the amount of steel fiber were all kept constant as listed in table3. The chemical admixture was added to the mixture until the SCC characteristics were obtained According to Specification and Guidelines for SCC set by EFNARC [17] (European Federation of National Trade Associations), a slump flow diameter ranging from 650 to 800 mm can be accepted for SCC.
In addition to the slump flow test and L-Box test, sieve stability test to assess the flow ability, passing ability and stability of SCC. The L-Box blocking ratio ranging from 0.8- 1.0 and the sieve segregation test values range of 0-15 %.

Table 3: Mix Proportions

Mix ID	**Water**	**C (kg/m^3)**	**Fillers**		**Fine aggregates F.A (kg/m^3)**		**Coarse aggregates C.A (kg/m^3)**		**Steel fibers SF (kg/m^3)**		**superplasti zer SP (l/m^3)**	**VMA (l/m^3)**
			MP (kg/m^3)	**LP (kg/m^3)**	0/1	0/5	3/8	8/15	SSF	LSF		
SCC1	154	400	80	0	202	706	374	410	0	0	6.82	1.58
SCC2	154	400	0	80	202	706	374	410	0	0	6.82	1.58
RSCC1	154	400	80	0	190	720	379	405	72	0	6.82	1.58
RSCC2	154	400	80	0	190	720	379	405	50.4	21.6	6.82	1.58
RSCC3	154	400	80	0	190	720	379	405	36	36	6.82	1.58
RSCC4	154	400	80	0	190	720	379	405	21.6	50.4	6.82	1.58
RSCC5	154	400	80	0	190	720	379	405	0	72	6.82	1.58

2.3 Preparation and casting of test specimens

In the production of SCC, mixing sequence and duration are very important, thus the mixing process was kept constant for all concrete mixtures.
In this investigation the filling ability was evaluated by slump flow time and diameter. The passing ability was measured by L-Box. The resistance to segregation was measured by sieve stability test [18].
For each concrete mix six 150 mm cubes, six prisms of 70*70*280 mm and fifteen 150*300 mm cylinder specimens were cast.

2.4 Tests on fresh concretes

Slump flow time and diameter test, L-Box and sieve stability test on fresh concrete were carried out. The first and second test procedures were discussed by Sahmaran and Yaman [5].
The slump flow is used to evaluate the horizontal free flow (deformability) of SCC in the absence of obstructions. During the slump flow test, the time required for the concrete to reach a diameter of 500 mm is also measured and recorded as t500. This parameter is an indication of the viscosity of concrete and indicates the stability of the concrete. A lower time points to a greater fluidity or smaller workability loss.
According to Nagataki and Fujiwara [19], a slump flow diameter ranging from 500 to 700 mm is considered as the slump required for a concrete to be classified as SCC.
Good flowability and stable concrete would consume short time to flow around the obstruction. According to Khayat [20], flow times were in the range of 0-5sec.

Sieve segregation test

Slump flow test

L Box blocking test

Figure 2: Fresh properties test of SCC

2.5 Test on hardened concrete

Concrete specimens have been batched, molded and cured according to AFNOR standard [21]. A testing program has been elaborated and consisted of determining the essential properties of hardened self-compacting concretes as shown in Fig.3.
For the determination of compressive strength and ultrasonic pulse velocity, concrete cubes of 150 x 150 x 150 mm [22, 23] were used. It was measured at 7, 28 and 56 days and, to determine split tensile strength, 150 x300 mm (diameter 150 x300 length) cylinder specimens [24] were used at 28 and 56 days, using a testing machine with a maximum load capacity of

3000 KN. For flexural strength, Three-point bending tests were carried out at 28 and 56 days old, using a classical machine, with a capacity of 100 kN, on prismatic specimens (70 × 70 × 280 mm) [25].
The fracture energy of the SCC and RSCC is based on the area under the complete load versus displacement at mid span curve. The notch to depth ratio (a/D) of the specimens was 0.30 and the notches were formed using a special saw.

Compressive strenght test of SCC

Compressive strength test of RSCC

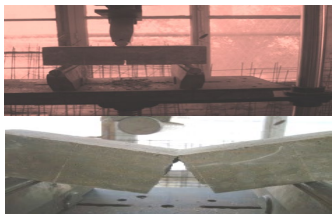

Flexural strength test of SCC

Flexural strength test of RSCC

Figure 3: Hardened tests on SCC and RSCC

3 Results and discussion

3.1 Fresh concrete properties

To classify a concrete as self-compacting, the requirements for filling and passing ability as well as segregation resistance must be satisfied in order to provide easiness of flow when unconfined by formwork or reinforcement, and an ability to remain homogeneous in fresh state. It is specified that the filling ability and stability of self-compacting concrete in the fresh state can be defined by four required characteristics namely flow ability, viscosity, passing ability, and segregation resistance [26].
The results obtained are reported in Table 4. It can be seen that, the fresh properties are in the range of 654-745mm for slump flow diameters, 2.9-5s for slump flow times, 0.82-0.98 for the L-box ratio and 3.07-5.62% for the sieve stability. All concrete mixtures were considered as Self compacting concrete (SCC). In all of the SCC mixtures, there was no segregation of aggregate near the edges of the spread-out concrete as observed from the slump flow test.
From a comparative study between SCC1 and SCC2, marble powder can be considered as limestone powder (LP) which is one of the materials that have extensively been studied in the literature [27–28, 29] and have improved the mechanical and durability features of concretes by providing more compact structure through its pore-filling effect. Marble powder helps to evenly disperse fibers during mixing. Although the angular shapes with rough surface texture of MP particle, it provides ball bearing effects and reduces internal friction in fresh concrete and these increase the flow ability (workability) and compaction of the concrete.
The steel fibers have affected slightly the fresh properties of the concrete mixtures. The addition of short steel fibers did not affect the water requirement of the mixture for the same workability. The fresh properties decreased with increased long steel fiber content, similar loss in workability was observed by [30, 31] with the addition of high volume of steel fiber. However, this could be explained by the geometry of the fibers. Short fibers had smaller

dimensions when compared to long fibers, thus had lower potential to prevent the movement of aggregates. Therefore, the shorter size of fibers reduced the energy loss during the movement of concrete ingredients.

Table 4. Fresh properties of self-compacting concretes.

Mix ID	Slump flow (mm)	T500 (s)	L-Box ratio (%)	Sieve stability (%)
SCC1	723	3.2	0.95	5.62
SCC2	745	2.9	0.98	5.22
RSCC1	706	3.8	0.95	4.9
RSCC2	703	4.3	0.94	4.89
RSCC3	686	5	0.9	4.6
RSCC4	668	4.46	0.87	4.43
RSCC5	654	4.7	0.82	3.07

3.2 Hardened concrete properties

The hardened concrete test results are summarized in table 5 and presented in Figures 4. (a-b), 5.(a-b), 16.(a-b), 7.(a-b), 8 and 9, which includes the 7, 28 and 56 days for compressive strength, 28 and 56 days for split tensile strength, flexural strength and ultrasonic pulse velocity and ending with 56 days for fracture energy.

It can be thus noted that, the most significant changes were observed on the flexural strength, splitting tensile strength, fracture energy and later on the compressive strength. Differently, ultrasonic pulse velocities did not seem to be affected by the size of fibers in this research. However, the UPV could be used to assess the hardening of the SCC mixtures. It was clear from Fig. 7(a-b) that as hydration continued, the UPV increased for all the SCC and RSCC mixtures.

Substituting FA and CA by MP with high fineness and steel fibers resulted in lower compressive strength and increased splitting tensile and flexural strengths both at 28 and 56 days, even though the fresh properties were reduced. The decrease in compressive strength was 7.36% at 56 days. This reduction could be attributed to the orientation of fibers mostly when their size was large. However, as seen in Figs. 4. (a, b), as the volumetric ratio of the SSF type fibers increased the compressive strength increased. This was due to the relatively small dimensions of SSF type fibers, which gave these fibers the ability to delay the micro-crack formation and to stop and prevent its propagation. Another explanation to the increase in the compressive strength could be the decrease of fresh properties as the amount of LSF type fibers increased. Nonetheless, it should be pointed that, when the splitting tensile strength was examined Fig.5. (a, b), there was a reduction in the splitting tensile, flexural strengths and fracture energy as the volume of SSF type fibers was increased or the fresh properties decreased. The reduction in the splitting tensile strength was interpreted by the absence of LSF fibers. Therefore, LSF fibers were mainly responsible for the increase in tensile and flexural strengths and fracture energy. Otherwise, when the tensile stress is transferred to LSF fibers, the macro-cracks propagation stops and considerably improves the tensile strength of the concrete.

The addition of steel fibers to the SCC mixes has a moderate positive effect on the ultrasonic pulse velocity. This enhancement was obviously observed from Fig.7.(a, b), which shows RSCC1 have higher value. This increase is noticeable because the shape and size of the SSF witch improve their anchoring and their adhesion.

As shown in Fig.8. Fracture energy, which is defined as the area under the load-deflection curve, seemed to be affected by the LSF and the effect of fiber combination can be observed on the obtained test results. Highest fracture energy obtained in RSCC5. This indicates the energy absorption capacity of RSCC in the event of intense stress. The negligible variation fracture energy test results can be considered as an indication of the uniformity of the mixes of the SCC1 and 2.

All the results founded in this research are summarized in Fig.9 and which meet the requirements of self-compacting concrete.

Table 5: Hardened properties of self-compacting concretes

Mix ID	**Compressive strength (MPa)**			**Splitting tensile strength (MPa)**		**Flexural strength (MPa)**		**Ultrasonic pulse velocity (m/s)**		**Fracture energy (N/m)**
	7 d	28 d	56 d	28 d	56 d	28 d	56 d	28 d	56 d	56 d
SCC1	39.35	49.56	54.33	2.42	2.75	4.45	4.79	4178	4297	81.42
SCC2	37.18	49.02	52.87	2.35	2.83	4.37	4.71	4158	4269	79.04
RSCC1	36.63	47.72	52.02	2.56	3.11	4.6	4.89	4432	4598	502.14
RSCC2	40.45	47.85	49.36	2.85	3.38	5.08	5.28	4342	4443	570.95
RSCC3	33.82	45.38	47.54	3.32	3.82	5.43	5.81	4322	4577	657.14
RSCC4	34.08	45.33	48.08	3.48	4.02	5.69	5.97	4411	4549	727.38
RSCC5	35.49	49.22	48.35	3.63	4.23	5.93	6.29	4424	4558	914.76

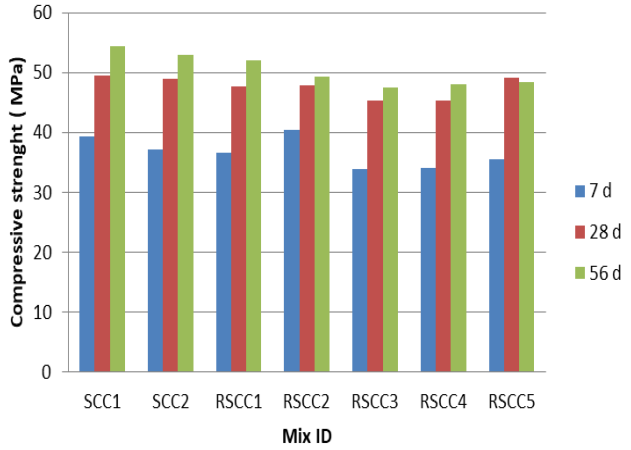

Figure 4: a. Effect of MP and steel fibers on the compressive strength

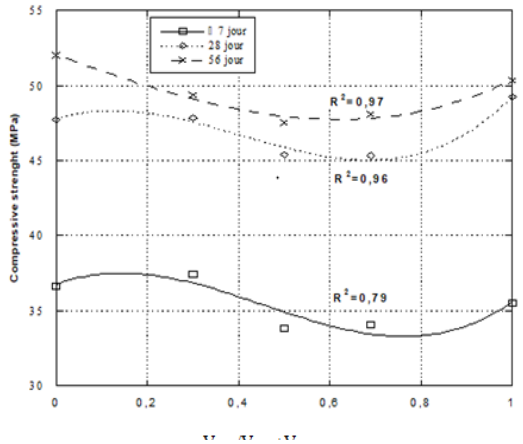

Figure 4: b. Effect of steel fibers size on the compressive strength

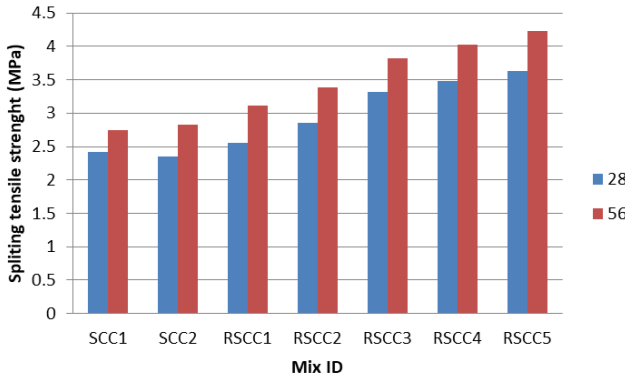

Figure 5: a. Effect of MP and steel fibers on the splitting tensile strength.

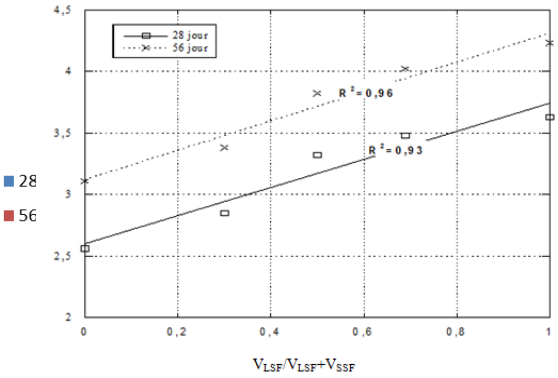

Figure 5: b. Effect of steel fibers on the splitting tensile strength

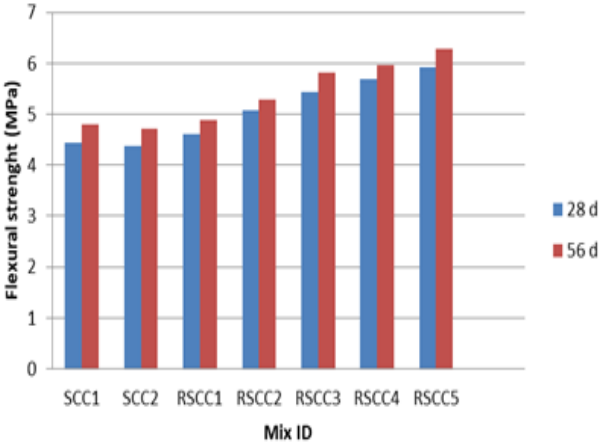

Figure 6:.a. Effect of MP and steel fibers flexural on the flexural strength

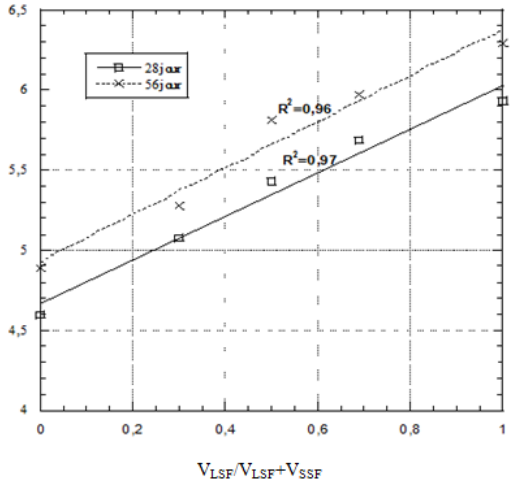

Figure 6:.b. Effect of steel fibers on the strength

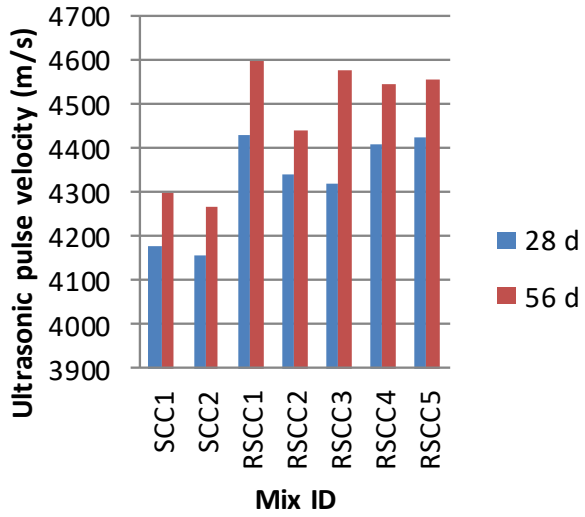

Figure 7:.a. Effect of MP and steel fibers on the ultrasonic pulse velocity

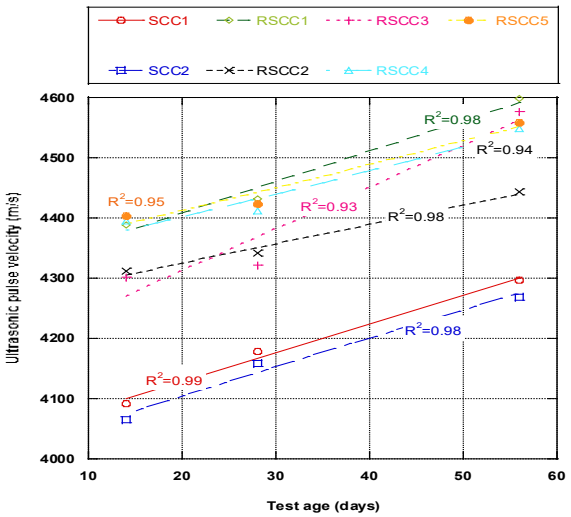

Figure 7:.b. Strength gain of SCC mixtures

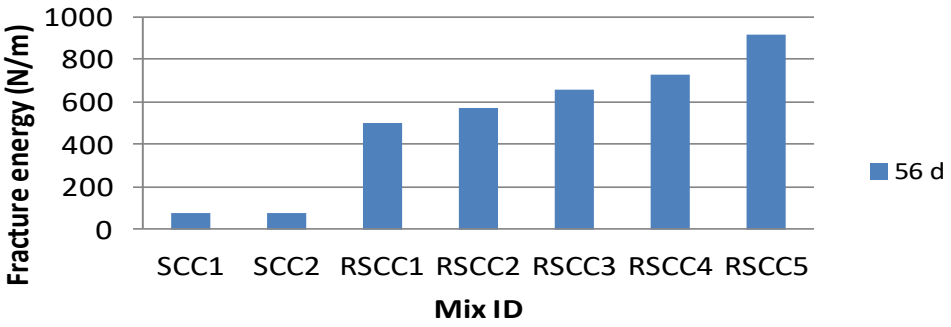

Figure 8: Effect of MP and steel fibers on the fracture energy

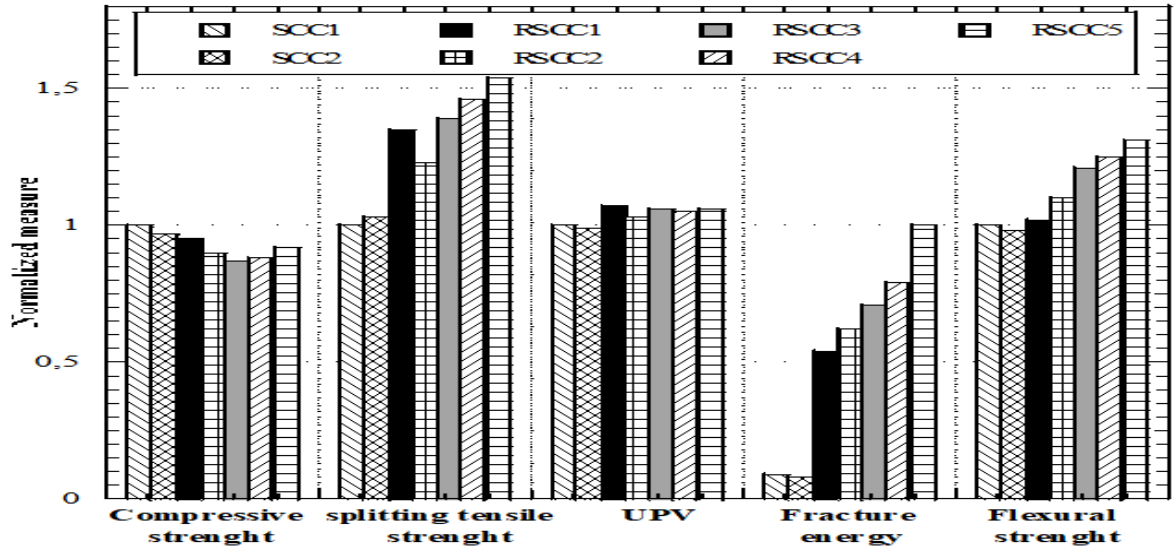

Figure 9: 56 days hardened properties of the RSCC–SCC

4 Conclusion

An experimental program has been undertaken to investigate the performance of self-compacting concrete containing marble powder and steel fibers as a partial replacement of sand and coarse aggregates.
The experimental results showed that:

- The use of marble powder and steel fibers at different sizes in self-compacting concrete as a structural material is possible but it requires the addition of high reducer water in order to reach a good workability.
- Marble powder can replace limestone powder with success.
- Increasing the short fiber content in the SCC mixtures slightly reduced the workability of RSCC.
- Incorporating steel fibers is essential in changing the brittle failure mode of SCC into a more ductile one. Based on the experimental tests conducted, it can be concluded that smaller sized fibers in concrete function as a bridge to reduce the micro-cracks; however, they have small effect on the post-peak response of load versus displacement at the midspan of the prism.
- The LSF have no significant effect in barring the formation of micro-cracks; nonetheless, they effect on the post-peak response part of load versus displacement curve, whose results in high value of fracture energy.
- The concrete with high strength and large size steel fibers showed a behavior of enhanced toughness and ductility compared to the SCC with shorter size of steel fibers.
- The effects of marble powder replacement and steel fibers on the ultrasonic pulse velocity (UPV) seemed to be slightly effected. Therefore, it could be concluded that the fiber geometry affected the properties of SCC mixtures not only in the hardened state but also in the fresh state.
- Mechanical properties are enhanced by the adding of steel fibers in SCC, especially splitting tensile strength, flexural strength and fracture energy. The improvement increases as the larger fiber volume fraction increases.

References

[1] Ghezal A, Khayat KH. Optimizing self-consolidating concrete with limestone filler by using statistical factorial design methods. ACI Mater J 2002; 99:264–72.

[2] Sahmaran M, Christianto HA, Yaman IO. The effect of chemical admixtures and mineral additives on the properties of self-compacting mortars.CemConcr Compos 2006; 28(5):432–40.

[3] Corinaldesi V, Moriconi G. Durable fiber reinforced self-compacting concrete, Cement and Concrete Research 34 (2004) 249–254.

[4] Moriconi G, Corinaldesi V. Rheological study of blended cement concrete' in "cement combinations for durable concrete. In: Dhir RK, Harrison TA, Newlands MD, editors. Procs of the sixth int. congress on 'global construction: ultimate concrete opportunities'. Thomas Telford, London, UK; 2005. p. 211–8.

[5] Sahmaran M, Yaman IO. Hybrid fiber reinforced self-compacting concrete with a high volume coarse fly ash. Constr Build Mater 2007; 21:150–6.

[6] Rao PS, Seshadri ST, Sravana P. Durability studies on glass fibre SCC. IndConcr J 2009; 83:44–52.

[7] Hwang, J.P., Jung, M.S., Lee, C.K., Jin, S.H., Ann, K.Y., 2015. Risk of environmental contamination arising from concrete structures, part I: CO2 emission. KSCE J. Civ. Eng. 2015 (19), 1224–1229.
[8] Ambroise J, Rols S, Pera J. Properties of self-leveling concrete reinforced by steel fibers. In: Proceedings of 43rd Brazilian congress of the concrete (IBRACON). Brazil; August 2001.
[9] Dhonde HB, Mo YO, Hsu TCC, Vogel J. Fresh and hardened properties of self-consolidating fiber reinforced concrete. ACI Mater J 2007; 104:491–500.
[10] Cunha VMCF, Barros JAO, Sena-Cruz JM. Pullout behavior of steel fibers in self-compacting
[11] concrete. J Mater Civil Eng – ASCE 2010; 22:1–9.
[12] Greengough T, Nehdi M. Shear behaviour of fiber reinforced self-consolidating concrete slender beams. ACI Mater J 2008; 105:468–77.
[13] Torrijos MC, Barragan BE, Zerbino RL. Physical–mechanical properties and
[14] mesostructure of plain and fiber reinforced self-compacting concrete. Constr
[15] Build Mater 2008; 22:1780–8.
[16] Liberato F, Yong D P,Surendra P S. A method for mix-design of fiber-reinforced self-compacting concrete, Cement and Concrete Research 34 (2007) 957–971.
[17] Corinaldesi V, Moriconi G, Naik T. Characterization of marble powder for its use in mortar and concrete. Construct Build Mater 2010; 24:113–7.
[18] Ferrara L, Park Y-D,Shah S. Amethode for mix-design of fiber-reinforced self-compacting concrete.cemconcr res2007;37:957-14
[19] XP P 18-540 Standard, Granulats : Définitions, conformité, spécifications, Association Française de Normalisation (AFNOR), Paris, 1997 (In french).
[20] EFNARC.European guidelines for self-compacting concrete: specification,production and use. Self-compacting concrete European project group: 2005
[21] EFNARC.European guidelines for self-compacting concrete:specification,production and use. Self-compacting concrete European project group: 2005
[22] Nagataki S, Fujiwara H. In; Malhotra VM, editor.Self-compacting property of highly flowable concrete, Vol. Sp 154. American Concrete Institute: 1995. P. 301-14.
[23] Khayat KH, GuizaniZ.Use of viscosity-modifying admixture to enhance stability of fluid concrete. ACI Mater J 1997; 94(4); 332-41.
[24] EN 12390-2. Testing hardened concrete – Part 2: Making and curing specimens for strength tests; 2001.
[25] EN 12390-3. Testing hardened concrete – Part 3: Compressive strength of test specimens; 2001.
[26] EN 12504-4. Testing hardened concrete – Part 4: Ultrasonic pulse velocity of test specimens; 2005.
[27] EN 12390-6. Testing hardened concrete – Part 6: Splitting tensile strength of test specimens; 2001.
[28] EN 12390-5. Testing hardened concrete – Part 5: Flexure strength of test specimens; 2001.
[29] Barr B, Gettu R, Al-Oraimi SKA, Bryars LS. Toughness measurement – the need to think again.CemConcr Compos 1996; 18(4):281–97.
[30] Elkhadiri I, Diouri A, Boukhari A, Aride J, Puertas F. Mechanical behaviour of various mortars made by combined fly ash and limestone in Moroccan Portland cement. CemConcr Res 2002; 32:1597–603.
[31] Petit JY, Wirquin E. Effect of limestone filler content and superplasticizerdosage on rheological parameters of highly flowable mortar under light pressure conditions. Cem ConcrRes 2010; 40:235–41.
[32] Tennich M, Kallel A, Ben Ouezdou M. Incorporation of fillers from marble and tile wastes in the composition of self-compacting concretes. Constr Build Mater. 91 (2015) 65–70
[33] Madandous R, Ranjbar M.M, Ghavidel R, Shahabi S. F. Assessment of factors influencing mechanical properties of steel fiber reinforced self-compacting concrete, Mater. Des. 83 (2015) 284–295.
[34] Khaloo A, Molaei Raisi E, Hosseini P, Tahsiri H. Mechanical performance of self-compacting concrete reinforced with steel fibers. Constr Build Mater.51 (2014) 179–186

DOI: 10.1515/sspjce-2021-0003

Estimation of pile displacements anchored in sand after a large number of cycles

Assia Bellayoune[1], Salah Messast[2]

[1]Ph.D.Student, Department of Civil Engineering, LMGHU Laboratory, University 20 August 1955 of Skikda, BP 26, Road Elhadeik, 21000 Skikda,Algeria.
Corresponding Author. E-Mail: assia_blio@yahoo.fr
[2]Professor of Civil Engineering, Civil EngineeringDepartment, LMGHU Laboratory, University 20 August 1955 of Skikda, BP 26, Road Elhadeik, 21000 Skikda,Algeria.
E-Mail: msalah2007msalah@gmail.com

Abstract

Taking into account the soil-structure interaction in the design of structures is a very decisive factor in the safety and durability of these structures. Several studies have been carried out in this direction to better describe the behavior of soil-structure interfaces.

This paper presents an analysis of the maximum and minimum displacement as a function of the number of cycles of a bored pile under the effect of cyclic tensile loading. In this study, the cyclic stiffness and the displacement of the pile are expressed by a simple formulation according to the cyclic parameters, based on the exploitation of the experimental tests carried out by Benzaria (2013) on a bored pile.The proposed formulation well predicts the displacement of piles in cyclic tensile. The approach presented in this paper can be used to evaluate the maximum and the minimum displacement of the head of pile foundation subjected to large number of shear cycles.

Keywords: stiffness, displacement, cyclic amplitude, loading average, number of cycles, sand

1 Introduction

Piles are commonly used as foundations for special civil engineering works such as towers, bridges, silos. The study of their response and the verification of their stability require an adequate modeling of the soil-pile contact. Generally, the piles are subjected to cyclical stresses which can be of environmental type (wind, swell, tides, earthquakes, etc.) or of industrial type such as road and rail traffic or vibrating machines etc. Many structures are liable to be subjected to cyclic loads in normal or accidental situations such as roads, bridges, railways, silos, reservoirs, foundations for vibrating machines etc [1]. These forces can have a significant influence on the stability and the behavior of these foundations during their lifetime [2]. The loading and unloading of the pile cause a very significant modification of the behavior of the pile-soil system and lead to a degradation of the bearing capacity as well as to the accumulation

of irreversible displacements [3]. The national SOLCYP project (2009-2012) aims to develop a methodology and calculation procedures to take into account the effect of cyclic loads on the response of the pile [4].

The behavior of deep foundations, mainly piles, under cyclic loading, depends on several factors whose influence is more or less important. In the majority of cases, the piles are vertically embedded in soil. The cyclic loading applied on the foundation can be characterized by five parameters: the direction of the loading (lateral or axial), the number of cycles N, the maximum cyclic loading applied, the amplitude of the cyclic loading and the type of loading (alternately or not) [5].

The soil-structure interfaces for a small number of cycles typically less than 100 cycles, have been studied in the laboratory by many researchers [6, 7, 8, 9, 10, 11]. The formulation of cyclic stresses at soil-structure interfaces has been widely invested by several researchers [12, 13, 14, 15, 16, 17, 18]. But the case of the large number of shear cycles of soil-pile interfaces is relatively little studied in the laboratory and in situ, due to the complexity of the tests [19].

The load displacement response of piles is different if they are performed individually or in groups. When carried out in groups, interactions occur between several piles during the transfer of load to the mass of the soil. This interaction creates a superposition of stresses which affects the load-displacement response of the pile group [20].

The rigidity of a pile influences its behavior when subjected to axial loading, particularly in terms of head displacement. Indeed, the overall displacement of an axially loaded pile depends not only on the mechanical properties of the surrounding soil but also on the axial compressibility inherent in the pile [21, 22, 23].

This paper presents a simple approach to formulate stiffness and displacement as a function of the number of shear cycles of the soil-pile interface. This approach makes it possible to evaluate the effect of rigidity and displacement on the resistance of the piles. Moreover, this formulation will be compared with the experimental values by [21].

2 The Behavior of the Piles Under Cyclic Loading

The bearing capacity of a pile in compression Q_{uc} is considered to be the sum of the mobilizable resistance at the soil-pile interface (lateral friction along the shaft Q_s) and the resistance available under the point Q_p [21]. In tension, neglecting the weight of the pile, the bearing capacity Qut is equal to the lateral friction along the shaft Q_s.

$$Quc = Qs + Qp \textbf{ et } Qut = Qs \quad (1)$$

Three essential characteristics, generally recognized, in the response of piles under cyclic loads which are [24]:

- ✓Degradation of the resistance of the pile-soil interface (friction);
- ✓The accumulation of displacements (degradation of rigidity);
- ✓The effects of loading speed.

3 Analysis

From the experimental tests carried out by Benzaria, the test program based on two bored piles of diameter D = 420 mm and length L = 10.5 m the two piles F1 and F2 were tested in tension which are compatible with the program general of the SOLCYP project. The objective of this simulation is to determine a relation between the cyclic rigidity and the displacement according to the cyclic parameters (the cyclic amplitude, the average loading, the number of cycles), and the influence of these parameters on the Maximum and minimum displacement. Table 1 summarizes the parameters of the tests carried out on two piles.

Table 1: Tensile Load Test Program On Bored Piles [21].

Pile	**Test**	**Type**	**Effort**	**f (HZ)**	**Qm (kN)**	**Qc (kN)**	**N (cycles)**
F1	Test N°1	Cyclique	Tension	0.5	160	120	126
	Test N°2			0.5	75	50	500
	Test N°3			0.5	100	50	760
F2	Test N°4	Cyclique	Tension	0.5	320	240	367
	Test N°5			0.5	120	80	315

Qm : Average cyclic vertical loading ;

f : is the frequency

Qc : Cyclic vertical loading amplitude.

3.1 Formulation Of The Cyclic Stiffness

The rigidity of a pile influences the behavior of the pile when subjected to axial loading, particularly in terms of head displacement [21]. It is recalled that the cyclic rigidity is defined by the relation (2):

$$Kc = \frac{Q\max,N - Q\min,N}{Z\max,N - Z\min,N} \qquad (2)$$

$Q_{max,\,N}$: Maximum cyclic vertical loading during the N^{th} cycle;

$Q_{min,\,N}$: Minimum cyclic vertical loading during the N^{th} cycle.

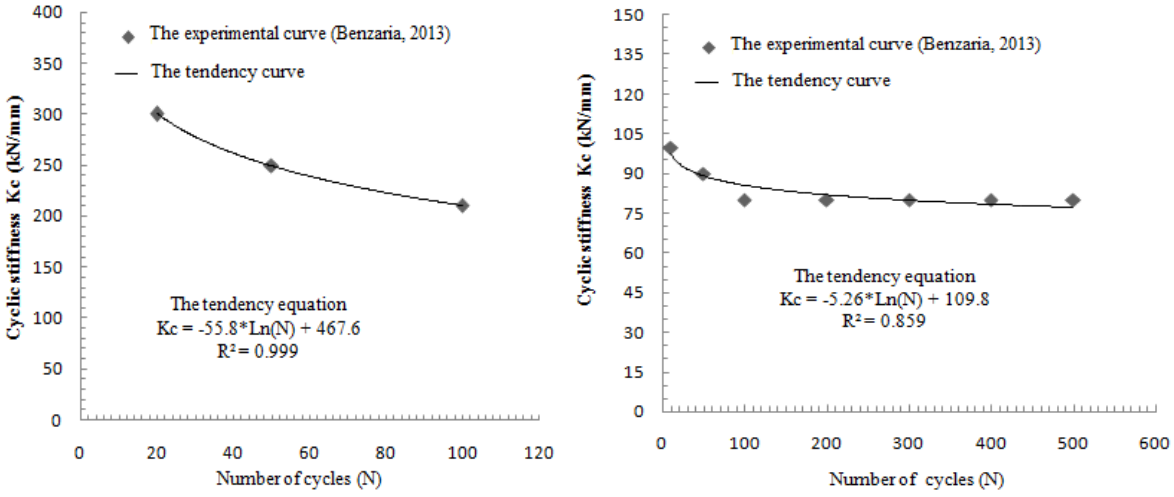

Test N°1 Test N°2

Figure 1: Evolution of cyclic stiffness as a function of the number of cycles for pile F1.

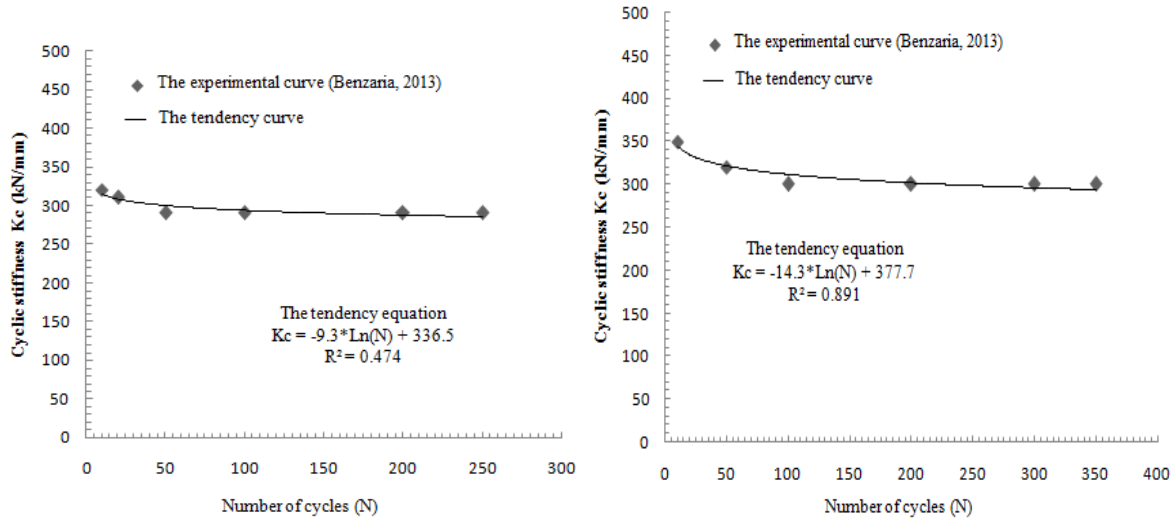

Test N°4 Test N°5

Figure 2 : Evolution of cyclic stiffness as a function of the number of cycles for pile F2.

Figures 1, 2 show for all the tests carried out on the two piles F1 and F2, the evolution of the cyclic stiffness of the pile as a function of the number of cycles. These curves can be expressed by a logarithmic equation as presented in equation (3).

$$Kc = A.\,Ln(N) + B \qquad (3)$$

Table 2 : The different values of the parameters used for the formulation of cyclic stiffness.

N°(Test)	A	B	Qm (kN)	Qc (kN)
1	-55.8	467.6	160	120
2	-5.26	109.8	75	50
4	-14.3	377.7	320	240
5	-9.3	336.5	120	80

The exploration of table 2 allows to plot point by point the curves A = f(Qc/Qm) and B = f(Qc/Qm)for the set of cyclic tests in tension.The tendency curves of A = f(Qc/Qm) and B = f(Qc/Qm) can be expressed by equations 4 and 5 :

$$A = -5136.5\left(\frac{Q_c}{Q_m}\right)^2 + 6680\left(\frac{Q_c}{Q_m}\right) - 2177 \qquad (4)$$

$$B = \left(-105.135\left(\frac{Q_c}{Q_m}\right)^2 + 152.126\left(\frac{Q_c}{Q_m}\right) - 54.556\right).10^3 \qquad (5)$$

After substitution of the Equations 4 and 5 into Equation 3. The cyclic stiffness can be expressed by equation 6 as:

$$K_c = \left(-5136.5\left(\frac{Q_c}{Q_m}\right)^2 + 6680\left(\frac{Q_c}{Q_m}\right) - 2177\right).\ln(N) + \left(\left(-105.135\left(\frac{Q_c}{Q_m}\right)^2 + 152.126\left(\frac{Q_c}{Q_m}\right) - 54.556\right).10^3\right) \qquad (6)$$

3.2 Formulation Of The Maximum Displacement (Zmax)

To study the evolution of displacements under cyclic loadings, it can be chose to calculate the cyclic maximum relative displacement Zmax :

$$Z_{max} = Z_{max,N} - Z_{max,1} \qquad (7)$$

Where : $Z_{max,\,N}$: maximum displacement at the head of the pile during the N^{th} cycle;
$Z_{max,\,1}$: maximum displacement at the pile head during the first cycle.

The evolution of the displacement as a function of the number of cycles performed on the two piles F1 and F2 is shown in Figure 4. This dependence have an exponential form, It can be expressed by the general form of equation (8) :

$$Z_{max} = C.exp(D.(N)) \qquad (8)$$

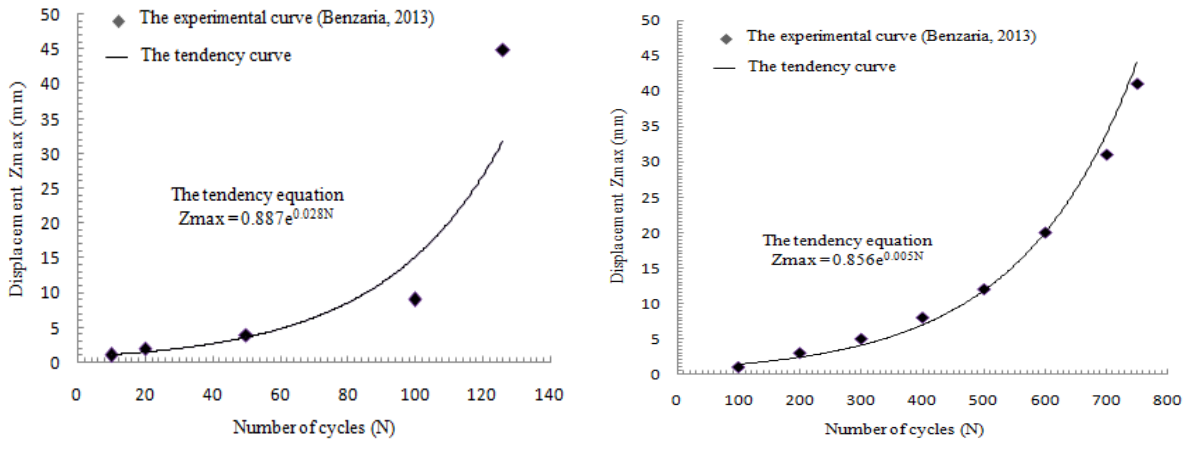

Test N°1 Test N°3

Figure 3: The evolution of displacement as a function of the number of cycles for the piles F1.

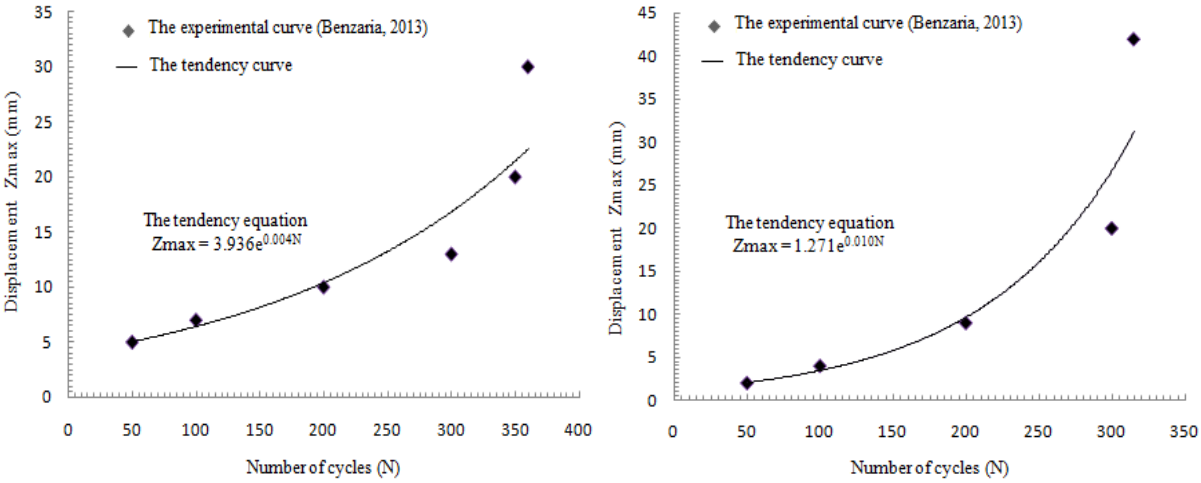

Test N°4 Test N°5

Figure 4: The evolution of displacement as a function of the number of cycles for the piles F2.

Table 3 give different values of C and D from equation of tendency curves of tests considered in this study.

Table 3: The different values of the parameters used for the formulation of Zmax.

N°(Test)	C	D	Qm (kN)	Qc (kN)
1	0.887	0.028	160	120
3	0.856	0.005	100	50
4	3.936	0.004	320	240
5	1.271	0.010	120	80

The exploration of table 3 allows to plot point by point the curves C=f(Qc/Qm) and D=f(Qc/Qm) for the set of cyclic tests in tension. The tendency curves of C=f(Qc/Qm) and D=f(Qc/Qm) can be expressed by equations 9 and 10 :

$$A = -28.36\left(\frac{Q_c}{Q_m}\right)^2 + 35.77\left(\frac{Q_c}{Q_m}\right) - 9.94 \qquad (9)$$

$$B = 0.803\left(\frac{Q_c}{Q_m}\right)^2 - 0.92\left(\frac{Q_c}{Q_m}\right) + 0.24 \qquad (10)$$

After substitution of the Equations 9 and 10 into Equation 8, the maximum diplacement an be given by equation 11 :

$$Z_{max} = \left(-28.36\left(\frac{Q_c}{Q_m}\right)^2 + 35.77\left(\frac{Q_c}{Q_m}\right) - 9.94\right).\exp\left(0.803\left(\frac{Q_c}{Q_m}\right)^2 - 0.92\left(\frac{Q_c}{Q_m}\right) + 0.24\right) \qquad (11)$$

From equation 2 , the minimum displacement can be expressed by equation 12.

So :

$$Z_{min} = Z_{max} - \frac{\Delta Q}{K_c} \quad \text{Then : } Z_{min} = Ce^{D.(N)} - \frac{\Delta Q}{A\ln(N)+B} \qquad (12)$$

Using the expressions of the maximum and the minimum displacement of the head of the pile from equations 11 and 12 respectively, it can be ploted Zmax = f(N) and Zmin = f(N) like it shown in figures 5 and 6.

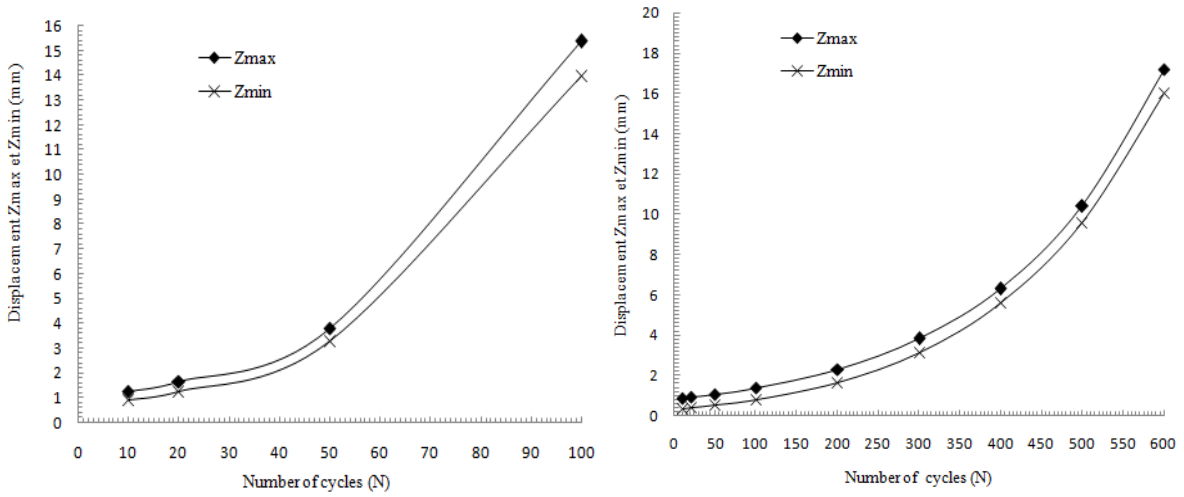

Test N° 1 Test N°3

Figure 5:The comparison between maximum and minimum displacement by pile F1.

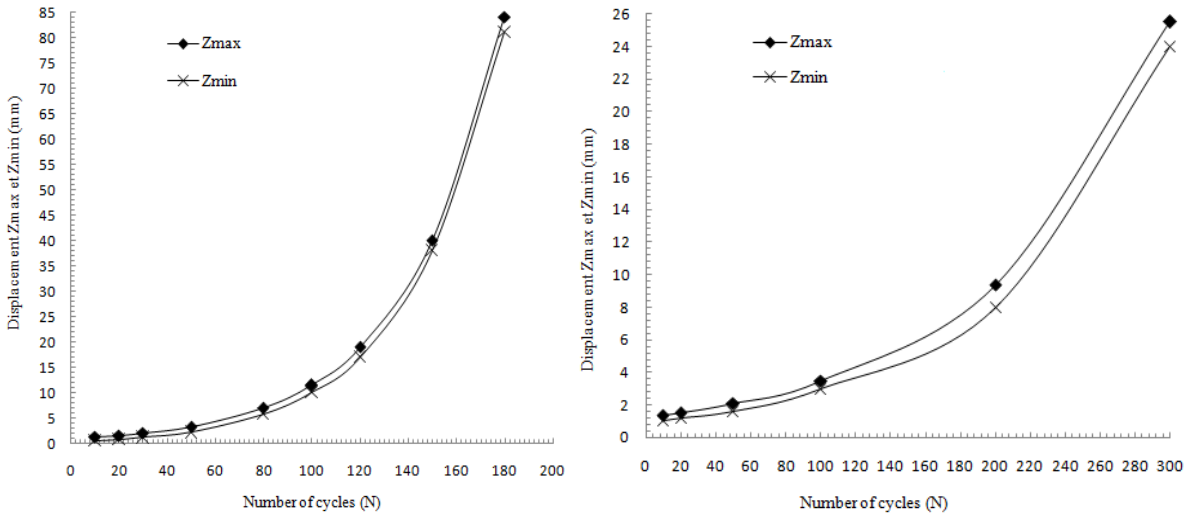

Test N°4 Test N°5

Figure 6 : The comparison between maximum and minimum displacement of the pile F2.

Figures 5, 6 present the maximum and the minimum displacement versus the number of cycles. It can be concluded that increase with a variable space, witch confirm the consistency of this approach with the cyclic behavior of this type of problems.

4 Conclusion

The behavior of piles under a large number of cycles can be characterized by the variation of their stiffness and their displacement according to the number of cycles. This research was based on the exploitation of the results of the tests carried out by Benzaria (2013) on the cyclic loading of a pile.

The analysis made in this study made it possible to express the cyclic stiffness and the maximum and the minimum displacements according to the number of cycles for a pile foundation in the same test conditions and of the soil (sand). The results presented in this paper are much more qualitative than quantitative. The estimated minimum displacements have an evolution which resembles that of the maximum displacements but with a variable spacing, which confirms the consistency of this approach with the cyclic behavior of this type of problems. This study can be extended to examine the case of group of piles.

References

[1] Messast, S., Boulon, M., & Flavigny, E. (2008).Constitutive Modeling of the Cyclic Behaviorof Sands In Drained Condition. *Studia Geotechnica And Mechanica,1(2),*131-137.

[2] Benzaria,O., Kouby, A., L, & Puech, A. (2010). Physical and Numerical Modelling of Cyclic Axial LoadingResponse of Piles.*National Days of Geotechnics and Geology of the Engineer JNGG,*7-9 juillet 2010, Grenoble, 555-562.

[3] Bekki, H., Tali, B., Canou, J., Dupla, J.C., & Bouafia, A. (2014). Behavior of soil-structure interfaces under cyclic loading for large numbers of cycles: Application to Piles, *J. Appl. Eng. Sci. Technol, 1(1),*11-16.

[4] Puech, A., Canou, J., Bernardini, C. (2008) SOLCYP : Un projet national de recherche sur le comportement des pieux sous chargement cyclique. *JNGG 2008*.

[5] Rakotonindriana, M. H. J. (2009). *Behavior of piles and groups of piles under cyclic side loading*, Ph.D. dissertation, National School of Bridges and Roads. Central Laboratory of Bridges and Roads.

[6] Desai, C., Drumm, E., & Zaman, M. (1985). Cyclic Testing and Modeling of Interfaces, *ASCE JGE, 111(6),* 793-815.

[7] Johnston, I., Lam, T., & Williams, A. (1987). Constant Normal Stiffness Direct Shear Testing For Socketed Pile Design In Weak Reak. *J. Géotechnical , 37(1),* 83-89.

[8] Al-Douri, R. H., & Poulos, H. G. (1991). Static And Cyclic Shear Tests On Carbonate Sands. *ASTM-GTJ , 15(2),* 138-157.

[9] Tabucanon, J., Airey, D., & Poulos, H. (1995). Pile Skin Friction In Sand From Constant Normal Stiffness Test, *ASTM GTJ, 18(3),* 350-364.

[10] Fakharian, K., & Evgin, E. (1997). Cyclic Simple Shear Behaviour of Sand-Steel Interfaces Under Constant Normal Stiffness Condition, *ASCE JGGE, 123(12),* 1096-1105.

[11] Mortara, G. (2001). *An Elastoplastic Model for Sand-Structure Interface Behaviour Under Monotonic and Cyclic Loading*, Ph.D dissertation, Politecnico Di Torino- Italy.

[12] Desai, C., & Nagaraj, B. (1988). Modeling for Cyclic Normal and Shear Behavior of Interfaces, *ASCE JGE, 114(7),* 1198-1217.

[13] Aubry, D., Modaressi, A., & Modaressi, H. (1990). A Constitutive Model for Cyclic Behavior of Interfaces with Variable Dilatancy, *J. Computers and Geotechnics, 9(1/2),* 47-58.

[14] Boulon, M., & Jarzebowsky, A. (1991). Rate Type and Elasto-Plastic Approaches for Soil-Structure Interface Behavior : A Comparison, *Proc7th Int. Conf IACMAG,* Carins, Australia, 305-310.

[15] Mortara, G., Boulon, M., & Ghionna, V. (2002). A 2-D constitutive model for cyclic interface behaviour, *International Journal for Numerical and Analytical Methods in Geomechanics, 26,* 1071-1096.

[16] Shahrour, I., & Rezaie, F. (2002). An Elasto-Plastic Constitutive Relation for Soil-Structure Interface Under Cyclic Loading, *J. Computers and Geotechnics, 52 (1),* 41-50.

[17] Pra-ai, S., Martin, A., & Boulon, M. (2010). Soil-Structure Direct Shear Involving a Large Number of Cycles, Experiments and First Steps of Modelling,*Procceding National Days of Geotechnics and Geology Engineering,* 7-9 juillet, Grenoble, pp. 327-334.

[18] Amrane, M., & Messast, S. (2017). Modeling the Behavior of Geotechnical Constructions Under Cyclic Loading With a Numerical Approach Based on J. Lemaitre Model, *Indian Geotechnical Journal, 48,* 520-528.

[19] Boulon, M., & Puech, A. (1984). Numerical Simulation of the Behavior of Piles Under Cyclic Axial Loading, *J. French Geotechnical Review, 26,* 7-20.

[20] Melchior Filho, J., Bonan,V.H.F., Moura, A.S. (2020). Experimental Study of the Group Effect on the Bearing Capacity of Bored Piles in Sandy Soil, *Soils and Rocks, 43(1),* 11-20.

[21] Benzaria, O. (2003).*Contribution to the Study of the Behavior of Isolated Piles Under Axial Cyclic Loadings*, Ph.D. dissertation, Unversity of Pais-Est.

[22] Rouhanifar, Salman, et al. (2020). Strength and deformation behaviour of sand-rubber mixture. *International Journal of Geotechnical Engineering*: 1-15.

[23] Majedi MR, et al. (2021). A micromechanical model for simulation of rock failure under high strain rate loading. *International Journal of Civil Engineering*. 19(5): 501-15.

[24] Poulos, H.G. (1981). Cyclic Axial Response of Single Pile. *JnI. Geot. Eng. Divn, ASCE, 107(7),* 41-58.

DOI: 10.1515/sspjce-2021-0004

Experimental Study on the Sol-Bentonite mixture stabilized by different types of Polymers

Saida Belouahem[1], Souhila Rehab Bekkouche*[1], Mohamed Salah Nouaouria[2], Salah Messast[1], Imane Idoui[3]

[1]LMGHU Laboratory, University 20 August 1955, Skikda, Algeria.
[2]Laboratory of Civil Engineering and Hydraulics (LGCH), University 8 May 1945 Guelma, Algeria.
[3]LGG Geological Engineering Research Laboratory (Geotechnical Team), University Mohamed Seddik Benyahia- Jijel, Algeria.
* Corresponding Author: solrehab@yahoo.fr

Abstract

Coherent soils are very responsive in nature and are part of many human activities. They change in volume considerably with changes in moisture content. These soils are characterized by the presence of a large proportion of highly active clay minerals of the montmorillonite group which are responsible for the pronounced volume change capability of the soils. The objective of this paper is to investigate the influence of different polymers on the plasticity properties of swelling clays. A study of their physicochemical properties based on an experimental protocol in the laboratory was carried out, the results obtained showed that the addition of the different types and amounts of polymers favourably influences the behaviour of expansive soils and reduces swelling.

Key words: Atterberg limits, Clay, plasticity, polymers, swelling.

1 Introduction

The problem of soil swelling is a serious danger for buildings and specific to certain clay soils. It is mainly linked in the first place to their mineralogical composition. Other factors such as soil structure, density, initial water content can significantly affect the swelling pressure or deformation of these clays. These phenomena are more pronounced when they occur in regions where significant climatic variations happen, in particular strong gradients of evaporation and seasonal moisture deficits. Soil swelling problems are especially evident in arid and semi-arid regions which are characterized by long periods of drought followed by short periods of rainfall [1, 2, 3, 4].
In Algeria, several cases of very damaging disorders, linked to this problem, mainly affect structures built on the surface (building, shallow foundation, retaining structure, embankments, etc.) [2].

In order to improve the behavior of expansive soils, geotechnical engineers seek help from soil science and geology. Today, a detailed literature is available, and a worldwide research on expansive soil stabilization using a wide array of classical and emergent materials is still in progress [5–13].
Simple compaction reduces soil porosity by expelling trapped air. The optimum soil compaction characteristics are determined by the normal Proctor test, which are the optimum water content and maximum dry density, these data are used and applied in studies of stabilization of problematic soils on site.
A large number of researchers and scientists have concentrated their efforts on the swelling clays and the methods and techniques of apparatuses which have been developed, to know the influence of the effectiveness of a solution or a product on the stabilization and improvement of the behavior of a swelling soil [14-20].
The use of polymers has become more and more common in many fields of activity. The choice of a polymer material is now made from a wide range of polymer species associated with many shaping possibilities. The lightness and low cost of polymers make them widely used materials, each field of activity exploiting specific properties that meet their specifications. The stability of these properties over time is a determining factor for use industrial [21].
Other researchers have studied the effect of different types of polymers in aqueous solutions [22, 23]. These analyzes often assess the potential of polymers for use as dust suppressants, anti-corrosion agents, and crack inhibitors in waste containment barrier materials. The sorption and the interaction between aqueous molecules and clay surfaces have also been studied. This paper presents an experimental investigation of the use of several types of polymer with different rates and in different shapes and sizes, in order to evaluate their effects on the plasticity properties of swelling soils, The state of mixing of soil with different levels of bentonite (6%, 12%, 20% and 25%) was studied by analyzing the variation in the properties of the mixtures.

2 Experimental Procedure

2.1 Materials

2.1.1 Site and Sampling

The soil used in this study was collected from the municipality of Ramdane Djamel in the wilaya of Skikda (North east of Algeria). Six samples were obtained from 6 m below ground surface, plastic bags to maintain the moisture content unchanged and transported to the National Habitat and Construction Laboratory (NHCL) situated in Skikda city, Algeria), table 1 summarizes the clay soil properties.

Table 1: Index properties of the studied soil

Physical and chemical properties	Value
Moisture content(%)	16.8
Liquid limit (%)	62.84
Plastic limit (%)	31.36

Plasticity index (%)	31.48
Maximum dry density (t/m^3)	1.75
Compressibility index (%)	15.99
Swelling index (%)	5.8
Preconsolidation pressure (kPa)	158
Friction angle (°)	15.12
Cohesion (kPa)	15
Methylene Blue	6.12

The soil was classified as a plastic clay (class A3) soil, according to the classification system AASHTO [24].

2.1.2 Bentonite

Bentonite shows swelling plastic properties, which promote the introduction of water molecules due to the presence of bulky cations between the sheets.
These clay materials are characterized by the superposition of elementary layers. Between these sheets are exchangeable cations, mainly Ca^{2+} and Na^{+}.
The interest in this material is explained by the following properties:
- A swelling capacity in certain liquids and in particular in water, allowing it to fix ten to fifteen times its volume of water.
- A cation binding capacity comparable to that of all natural ion exchangers [25].
In this work, the goal of using bentonite with multiple percentages is to increase the rate of swelling of the original soil, and afterwards to explore what type and rate of polymer is adequate to stabilize swelling.
Figure 1 shows the bentonite used in this study.

Figure 1: Bentonite

The properties of bentonite are shown in Tables 2 and 3.

Table 2: The properties of Bentonite

Properties	value
Humidity (%)	12
Fine particle size (%)	95
Water content (%)	9
Swelling rate (mL/2g)	25 - 27
Liquid limit (%)	181
Plasticity limit (%)	30
Plasticity index (%)	151

Table 3: Chemical compositions of Bentonite

Chemical characteristics	value
SiO_2 (%)	58.89
TiO_2 (%)	0.28
Al_2O_3 (%)	17.37
Fe_2O_3 (%)	3.32
MnO (%)	0.07
MgO (%)	3.37
CaO (%)	1.06
Na_2O (%)	1.32
K_2O (%)	1.30
H_2O (%)	9.00
P_2O_5 (%)	0.05
SO_3 (%)	0.68

2.1.3 Polymers

In this study we used five types of polymers: Polyvinyl chloride, Low density polyethylene and High density polyethylene, Polyethylene terephthalate and Polypropylene, their properties are described in the section below. Figures 2, 3, 4 and 5 show the polymers used in this study.

Figure 2: Polyvinyl chloride

Figure 3: Polypropylene

Figure 4: Polyethylene terephthalate

Figure 5: Polyethylene

2.1.3.1 Polyvinyl chloride

Polyvinyl chloride (PVC) is the leading thermoplastic material that can be considered as a third widely produced polymeric material in the world that is formed by free radical polymerization of vinyl chloride [26, 27]. This resin shows low thermal, thermoxidative and photostability and becomes colorless due to the genesis of a conjugated polyene series ina zipper-like technique [27]. In addition, PVC is assumed to be a relatively low-cost, it has huge industrial interests due to the ability to access the basic raw materials and its superior properties [28].
The properties of PVC are shown in Table 4.

Table 4: The properties of Polyvinyl chloride

Properties	Value
Density (g/cm^3)	1.38
Water Absorption (%)	0.2
Hardness	D 80
Resilience (kJ/m^2)	8-10
Modulus of elasticity in tension (MPa)	2500
Melting point (°C)	160
Degree of crystallinity (%)	10 - 15
Max temperature (°C)	90
Transition temperature (°C)	80
Thermal conductivity (W/m.K)	0.12

2.1.3.2 Polyethylene

Polyolefins, especially polyethylenes, are widely used thermoplastics because they have good mechanical properties, they are transformed and allow tubes to be welded together easily. Polyethylene is widely used for the manufacture of pipes for transporting water or town gas [29]. In this study we used two resins, High density polyethylene and Low density polyethylene, their properties are presented in tables 5 and 6.

Table 5: The properties of High density polyethylene

Properties	Value
Density (g/cm^3)	0.95 - 0.98
Carbon content (%)	2.0 - 2.5
Water absorption (%)	< 0.01
Young's modulus (GPa)	0.55 - 1
Tensile strength (MPa)	15-40
Thermal conductivity (W/m.K)	0,45-0,52
Transition temperature (°C)	300

Table 6: The properties of Low density polyethylene

Properties	value
Density(g/cm^3)	0.92
Carbon content (%)	2.0 - 2.5
Water absorption (%)	< 0.015
Young's modulus (GPa)	0,1-0,3
Thermal conductivity (W/m.K)	0.33
Tensile strength (MPa)	5-25

2.1.3.3 Polyethylene terephthalate

Polyethylene terephthalate (PET or PETE) is a general-purpose thermoplastic polymer which belongs to the polyester family of polymers. Polyester resins are known for their excellent combination of properties such as mechanical, thermal, chemical resistance as well as dimensional stability. Polyethylene terephthalate is one of the most recycled thermoplastic, and has the number "1" as its recycling symbol [30].
The properties of PET are shown in Table 7.

Table 7: The properties of Polyethylene terephthalate

Properties	value
Density (g/cm^3)	1.38
Melting point (°C)	> 250
Thermal conductivity (W/m.K)	0.15 - 0.24
Young's modulus (MPa)	2800–3100
Elastic limit (%)	50- 150
Tensile strength (MPa)	55–75
Water absorption	0.16

2.1.3.4 Polypropylene

This material is one of the most widely used synthetic materials for reinforcing soil because of it’s nontoxicity, corrosion resistance, and high tensile strength [31].
The properties of Polypropylene are shown in Table 8.

Table 8: The properties of Polypropylene

Properties	value
Melting point (°C)	160-163
Density (g/cm^3)	0.905
Thermal conductivity (W/m.K)	0.17 - 0.23
Tensile strength (MPa)	31 - 45
Tensile modulus (MPa)	1350 - 1800
Water absorption (%)	0.01 - 0.03

2.2 Preparation of test samples

To prepare the clay soil for test, the soil was first dried in an oven at 50°C for 24 h, then manually mixed with 6%, 12%, 20% and 25% respectively of bentonite for at least 10 min to create a series of test mixtures.
The experimental methodology followed in this study consists of adding the five types of polymers (High density Polyethylene, High density Polyethylene, Polypropylene, Polyethylene terephthalate and Polyvinyl chloride) with the different percentages: 3%, 6%, 12 % and 20%, with the soil-bentonite mixtures already prepared.
The percentage of polymers was calculated regarding to the overall mass of the soil-bentonite mixtures. All the prepared specimens were tested in the same manner and under the same laboratory conditions.

3 Results and Discussions

3.1 Effect of the addition of Bentonite on Atterberg limits

The Atterberg limits are used to determine the plasticity of a soil, which is defined as the property of the earth to undergo deformations without noticeable elastic reaction characterized by cracking or sputtering. The results of the Atterberg limits are presented in Figure 6:

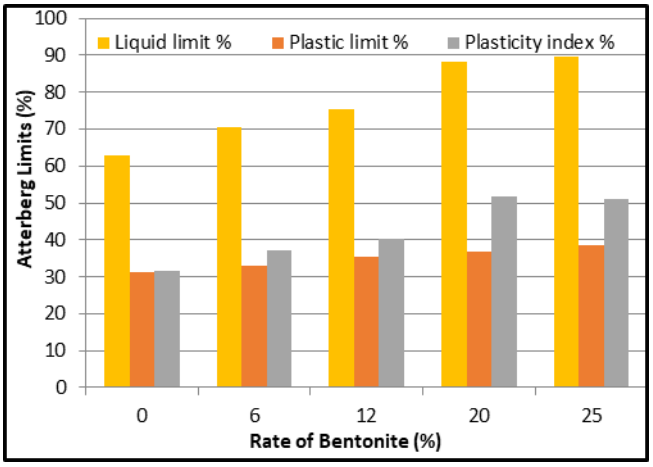

Figure 6: Variation of the Atterberg limits according to the bentonite content

From figure 6, it can be seen that bentonite has a considerable effect on the results of the Atterberg limits, the addition of 25% of bentonite increased the plasticity index by 31.48% to the value of 50.99%, this is justified by the increase in the quantity of fine particles which are not very permeable and that the quantity of water absorbed enters into their composition and modifies the structure of the clay, because it can penetrate inside their crystal lattice.

3.2 Effect of polymers on the plasticity of swelling soils

A series of seventy-five Atterberg limit tests was carried out on the various test pieces mixed with several levels of bentonite, then mixed with the polymers (Polyvinyl chloride - High density polyethylene- Low density polyethylene- Polyethylene terephthalate and Polypropylene) at a percentage of (0%, 3 %, 6%, 12% and 20%).
The test results are shown in Figures 7, 8 and 9:

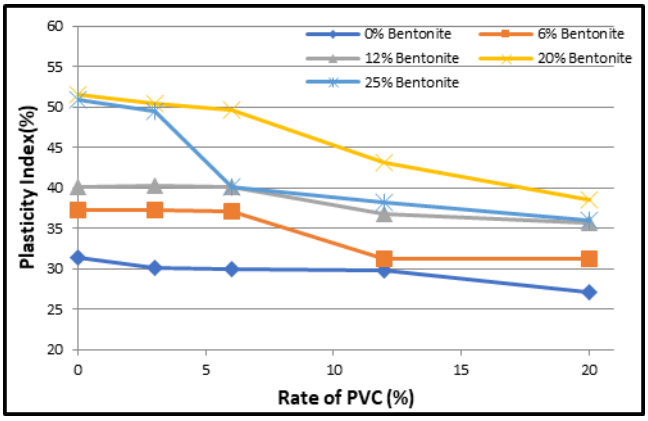

Figure 7: Plasticity Index variation as a function of the Polyvinyl chloride rate

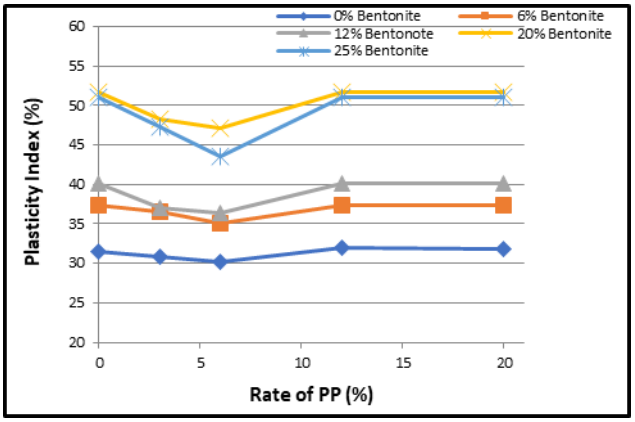

Figure 8: Plasticity Index variation as a function of the Polypropylene rate

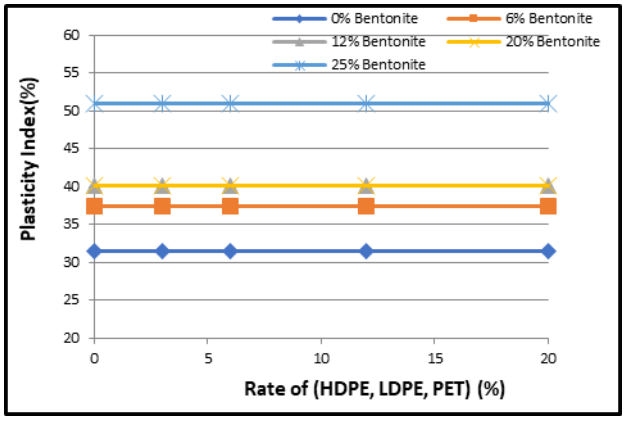

Figure 9: Plasticity Index variation as a function of the High density polyethylene, Low density polyethylene and Polyethylene terephthalate rate

The study of the effect of polymers on the plasticity properties of clay soils shows that the quantity, quality and shape of the grains play an important role in the characterization of the final product. These effects are much more noticeable for Polyvinyl chloride and Polypropylene. In the case of Polyvinyl chloride, we observe that the plasticity index goes from the value of 50.99% to the value of 36.05% so about 30% drop in plasticity, the observed decrease in the Plasticity index when Polyvinyl chloride is first introduced in the soil could be attributed to the effect of the resulting interlocking and friction between the Polyvinyl chloride and soil particles.

Consequently in the case of Polypropylene, one notices that the curves which represent the variation of the index of plasticity have the same pace, at the beginning and with a rate of 3% and 6% of addition, the index of plasticity decreases then it increases and takes the initial value before stabilization, so the best stabilization rate in this case is 6%.

The results of the tests also made it possible to see the effect of High density polyethylene, Low density polyethylene and Polyethylene terephthalate on the plasticity of the soil, the variations of Plasticity index are very negligible, practically one notices the same values before and after stabilization, for example in the case of High density polyethylene, at the beginning and with 0% of addition PI = 31.48% and it takes the same value with a rate addition of 12%.

These results were confirmed in the specialized literature [3, 16, 17, 18] studying the effect of polymer mixed with the soil on the behaviour of swelling clays.

4 Conclusion

In this study, the effects of different polymers content on the plasticity properties of swelling soils were investigated using a series of laboratory tests, with a comparison of unstablized and stabilized swelling soil with 0%, 3%, 6%, 12% and 20% of (Polyvinyl chloride, Polypropylene, High density polyethylene, Low density polyethylene and Polyethylene terephthalate).

The conclusions and recommendations from this study are given in the following sections:

- Mixing the soil with amounts of bentonite from 0% up to 25%, allowed us to investigate the

relationship between plasticity properties and the presence of swelling minerals, The increase in Atterberg limits observed in this study depending on the addition of different bentonite levels is due to the increase in specific surface area due to the addition of finer particles compared to the soil studied.
- As the Polyvinyl chloride content increased, the plasticity index decreased. The decrease in plasticity index improved the stability and reduced swelling of the soil.
- Up to a rate of 6% Polypropylene has a favorable effect in stabilizing the swelling soil.
- The effect of High density polyethylene, Low density polyethylene and Polyethylene terephthalate on plasticity is negligible
- Optimal solutions for stabilizing soil swelling by the addition of polymers require intimate mixtures between soil and reinforcement at optimal dosages studied and tested.

References

[1] Rapport final, (2009). Analyse du Retrait-Gonflement et de ses Incidences sur les Constructions. Projet ARGIC BRGM/RP 57011-FR.
[2] Hachichi. A, Bourokba S, et al. (2009). Etude des phénomènes retrait-gonflement et stabilisation des sols gonflants de la région d'Oran, 19 ème congrès français de mécanique, Marseille.
[3] Rehab Bekkouche S and Boukhatem G. (2016). Experimental Characterization of Clay Soils behavior stabilized by polymers. J. Fundam. Appl. Sci., 8(3), 1193-1205.
[4] Christopher M Geiman, (2005). Stabilization of soft clay subgrades in Virginia phase I, laboratory study, Thesis Master of Science Faculty of the Virginia Polytechnic Institute.
[5] K. Yan and L. Wu, (2009). Swelling behavior of compacted expansive soils, recent advancement in soil behaviour, in Proceedings of the Situ Test Methods, Pile Foundations, and Tunneling: Selected Papers from the 2009 GeoHunan International Conference, pp. 1–6, Changsha, China.
[6] C. C. Ikeagwuani and D. C. Nwonu, (2019). Emerging trends in expansive soil stabilisation: a review, Journal of Rock Mechanics and Geotechnical Engineering, vol. 11, no. 2, pp. 423–440.
[7] Yilmaz and B. Civelekoglu, (2009). Gypsum: an additive for stabilization of swelling clay soils, Applied Clay Science, vol. 44, no. 1-2, pp. 166–172.
[8] C. Kurtulus, F. Sertcelik, M. M. Canbay, and İ. Sertcelik, (2010). Estimation of Atterberg limits and bulk mass density of an expansive soil from P-wave velocity measurements, Bulletin of Engineering Geology and the Environment, vol. 69, no. 1, pp. 153-154.
[9] P. Priyadharshini, K. Ramamurthy, and R. G. Robinson, (2018). Reuse potential of stabilized excavation soil as fine aggregate in cement mortar, Construction and Building Materials, vol. 192, pp. 141–152.
[10] M. L. Nehdi, (2014). Clay in cement-based materials: critical overview of state-of-the-art, Construction and Building Materials, vol. 51, pp. 372–382.
[11] E. Celik and Z. Nalbantoglu, (2013). Effects of ground granulated blastfurnace slag (GGBS) on the swelling properties of lime-stabilized sulfate-bearing soils, Engineering Geology, vol. 163, pp. 20–25.
[12] M. Sol-Sánchez, J. Castro, C. G. Ureña, and J. M. Azañón, (2016). Stabilisation of clayey and marly soils using industrial wastes: pH and laser granulometry indicators, Engineering Geology, vol. 200, pp. 10–17.
[13] M. F. Iqbal, Q.-F. Liu, I. Azim et al., (2020). Prediction of mechanical properties of green concrete incorporating waste foundry sand based on gene expression programming, Journal of Hazardous Materials, vol. 384, p. 121322.
[14] Inyang H, Bae S, Mbamalu G, and Park S, (2007). Aqueous Polymer Effects on Volumetric Swelling of Na-Montmorillonite J. Mater. Civ. Eng., 19, Special Issue: Geochemical Aspects of Stabilized Materials, 84–90.
[15] L Hammadi , N Boudjenane, M Belhadri, (2014). Effect of polyethylene oxide (PEO) and shear rate on rheological properties of bentonite clay, Applied Clay Science. , 99, 306–311.
[16] Mpofu P, Addai-Mensah J and Ralston J, (2004). Flocculation and dewatering behaviour of smectite dispersions: effect of polymer structure type, Minerals Engineering, 17, 411-423.
[17] R L Anderson, I Ratcliffe, H C Greenwell, P A Williams, S Cliffe, P V Coveney, (2010). Clay swelling, A

challenge in the oilfield, Earth-Science Reviews, 98, 201–216.

[18] Jin Liu, Bin Shi, Hongtao Jiang, He Huang, Gonghui Wang, Toshitaka Kamai. (2011). Research on the stabilization treatment of clay slope topsoil by organic polymer soil stabilizer, Engineering Geology, 117, 114–120.

[19] Waseim Ragab Azzam. (2014). Durability of Expansive Soil using Advanced Nanocomposite Stabilization, Int. J. of GEOMATE, Sept, 7 (1), 927-937

[20] Rehab Bekkouche Souhila, Boukhatem Ghania, Mendjel Djenette. (2018). Mechanical Behavior of Clay Reinforced by Layers of Polymer, International Invention of Scientific Journal, [S.l.], v. 2, n. 04, p. 130-133.

[21] X. Lefebvre, (2002). Fissuration fragile lente du Polyamide 11: mécanisme et durée de vie en fluage, Thèse de doctorat, Ecole Nationale Supérieure des Mines de Paris.

[22] M. A. Mohsin and N. F. Attia, (2015). Inverse emulsion polymerization for the synthesis of high molecular weight polyacrylamide and its application as sand stabilizer, International Journal of Polymer Science, 10 pages.

[23] P. V. Barry, D. E. Stott, R. F. Turco, and J. M. Bradford, (1991). Organic polymers' effect on soil shear strength and detachment by single raindrops, Soil Science Society of America Journal, vol. 55, no. 3, pp. 799–804.

[24] American Association for State Highway and Transportation Officiais (AASHTO).(1990). Standard Specification for Transportation Materials and .wethods of Sampling and Testing. 15e éd., Washington, D.C. Partie 1, Spécifications, 828 p.; Partie Il, Essais, 998 p.

[25] Boukhedimi Mohamed Amine, (2008), Origine du processus de bentonitisation des terrains volcaniques rhyolitiques de hammam boughrara (Maghnia ; Algérie Nord occidentale), Thèse de Magister, Université d'Oran.

[26] Abdelghany AM, Meikhail MS, Hamdy R. (2018). Enrichment of polyvinyl chloride (PVC) biological uses through sodium chloridefiller, density functional theory (DFT) supported experimental study. J Adv Phys; 14(3):5682–92.

[27] Khan W, Ahmed Z. (1996). Cadmium chloride catalyzed degradation of PVC: UV-visible spectrophotometric and thermogravimetric studies. Polym Degrad Stab; 53(2):243–9.

[28] Abdelghany AM, El-Damrawi G, El-Shahawy AG, Altomy NM. (2018). Structural investigation of PVC/PS polymer blend doped with nanosilica from a renewable source. Silicon: 1–7.

[29] Rehab Bekkouche Souhila, (2010). Etude de l'interaction des différents types de sols avec des structures polymériques enfouies, Thèse de Doctorat, Université de Annaba.

[30] Kako Linda Nait-Ali. (2008). Le PET recyclé en emballages alimentaires: approche expérimentale et modélisation. Matériaux. Université Montpellier II - Sciences et Techniques du Languedoc. Français.

[31] Mazahir M. M. Taha, Cheng Pei Feng and Sara H. S. Ahmed, (2020). Influence of Polypropylene Fibre (PF) Reinforcement on Mechanical Properties of Clay Soil. Advances in Polymer Technology, 15 pages.

DOI: 10.1515/sspjce-2021-0005

Use of construction waste and recycled rubber for the preparation of cement composites

Jakub Charvát[1], Jakub Svoboda[1], Kateřina Máčalová[1], Radek Papesch[1], Tomáš Dvorský[1], Vojtěch Václavík[1]

[1] Department of Environmental Engineering, VŠB-TU Ostrava, Czech Republic;
e-mail: jakub.charvat@vsb.cz

Abstract
This article presents the results of the possible utilization of construction waste as the filler substitute in the production of cement composites. It describes the representation of the individual material components in the sample of mixed construction recyclate with the fraction of 0/4 mm. It also presents the results of a grain analysis of mixed construction recyclate, experimental formulations of cement composites, test specimen preparation procedure, results of compressive and flexural strength tests of the individual mixtures which were tested after 28 and 90 days.

Key words: recycling, construction waste, cement, rubber.

1 Introduction

Up to 820 million tonnes of construction and demolition waste are produced in Europe each year. This amount corresponds to 46% of the total waste produced in Europe. For example, in the United Kingdom, 50% of landfill material represents this type of waste. If we look overseas, around 1/3 of the volume of landfills is occupied by this type of material in the USA [1-3]. According to surveys, construction waste stored in this way consists mainly of concrete, brick material and ceramics, followed by wood and plasterboard [1]. The current setting of the economy in this field still favours the use of new resources for new constructions and landfilling of the used material. Landfilling charges were supposed to encourage the use of construction waste, but as a result of the introduction of this measure, some companies began to process this waste in and illegal way, such as filling in sacrificial formwork or for various types of sub-bases [3, 4]. With respect to this situation, the European Commission is seeking to gain control over construction and demolition waste, for example by reducing its generation or by promoting its recycling [1-3]. Many research projects have studied the possibilities of recycling construction waste. There were research projects dealing with the use of industrial waste in the field of civil engineering [5-9]. In Asia, they were looking at the possibility of using construction waste as a secondary raw material [10-12], or using construction waste as an admixture in concrete to replace Portlad cement [13], or to create new building materials [14,15].

2 Materials and Methods

Two mixtures (R1 and R2) were designed on the basis on the identified properties. The designed mixtures were left to cure for 28 and 90 days and their strength characteristics were examined afterwards.

2.1 Cement

One type of cement was used for the designed mixtures, namely Blast Furnace Cement III / A 32.5N from the manufacturer Považská cementáreň a.s. The cement properties are presented in Tab.1.

Table 1: Composition of experimental mixtures of cement composites

Cement CEM III/A 32.5N				
		Measuring unit	Required values EN 197-1	Achieved values in PCLA, a.s., Ladce
Setting start:		minute	min. 60	229.0 (+- 10.0)
Compressive strength:	2 days	$N \cdot mm^{-2}$	min. 10	21.8 (+- 0.9)
	28 days	$N \cdot mm^{-2}$	min. 42.5 - max. 62.5	47.4 (+- 0.7)
Specific surface:		$m^2 \cdot kg^{-1}$	not prescribed	339.0 (+- 7.0)
Content Cr (VI):		ppm	max. 2	0.0 (+- 0.0)

2.2 Mixing water

Water from the water supply system, which had met all the monitored parameters set by the standard ČSN EN 1008 - mixing water for concrete, was used for the preparation of mixtures based on mixtures R1 and R2 [16].

2.3 Filler

2.3.1 Rubber granulate

Rubber granulate from waste tires in the fractions of 1/1 mm and 1/3 mm mixed in the ratio of 50:50 (mixture R1) and 40:60 (mixture R2) was used as the filler.

2.3.2 Construction recyclate

Sorted construction waste fr. 0/4 mm, which contained burnt brick, ceramics and mortar, was used as the second type of filler. The representation of the individual components is described and illustrated in Fig.1.

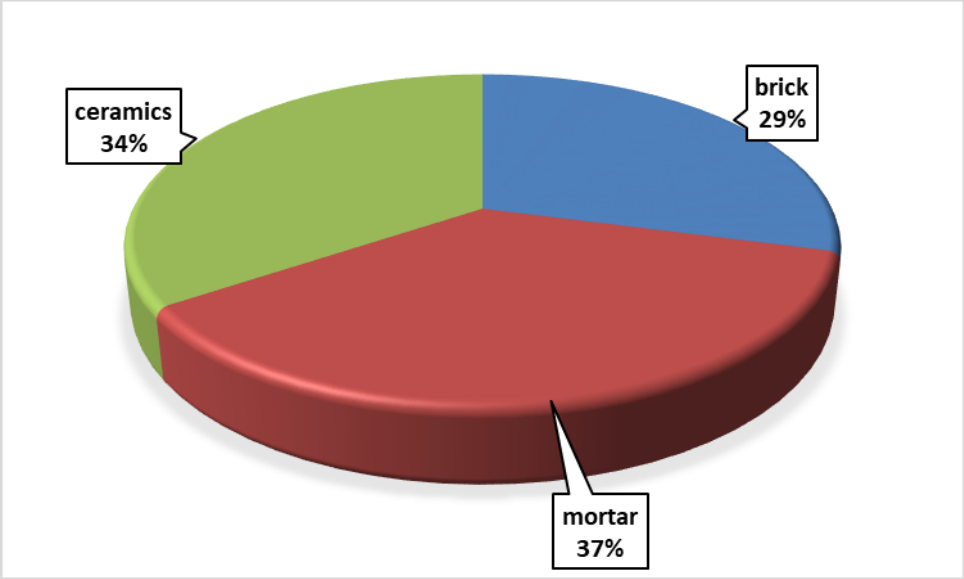

Figure 1: – Content of the individual components of mixed construction recycled material

2.4 Mixture design

Two mixtures (R1 and R2) have been designed in order to produce the concrete test specimens based on recycled rubber and construction waste. The filler was replaced in the amount of 10, 20, 30% in each mixture. The compositions of the individual mixtures are presented in Tab. 2.

Table 2: Composition of experimental mixtures

Mixture	Cement CEM III/A 32,5N [g]	Mixing water [g]	Mixed construction recyclate [g]	Rubber granulate fr. 0/1 and 1/3 in ratio 50:50 [mL]	Rubber granulate fr. 0/1 and 1/3 in ratio 40:60 [mL]
R1 + 10%	569	285	181	990	0
R1 + 20%	569	285	362	880	0
R1 + 30%	569	285	543	770	0
R2 + 10%	569	285	181	0	990
R2 + 20%	569	285	362	0	880
R2 + 30%	569	285	543	0	770

2.5 Sieve analysis of mixed construction recyclate

HAVER EML 300 digital plus sieving machine was used to determine the granulometry of the crushed sample of the mixed construction recyclate and a series of sieves with the mesh size of 0.063, 0.125, 0.25, 0.5, 1, 2, 4 mm was selected.

2.6 Strength characteristics

Flexural strength and compressive strength tests were performed in accordance with ČSN EN 196-1 [17]. Beams measuring 40x40x160 mm were used as the test specimens. Formtest testing instrument with a compressive force of 100KN and 300KN was used as the testing device.

3 Results and discussion

3.1 Sieve analysis of mixed construction recyclate

The mixed construction recyclate rubble was subjected to a sieve analysis, the result of which is the grain size curve presented in fig. 2. The mean grain size of the construction recyclate d50 = 0.68 mm was determined on the basis of the sieve analysis, the mean grain size of the rubber granulate fr. 0/1 mm d50 = 0.78 mm and the mean grain size of the rubber granulate fr. 1/3 mm d50 = 2.50 mm.

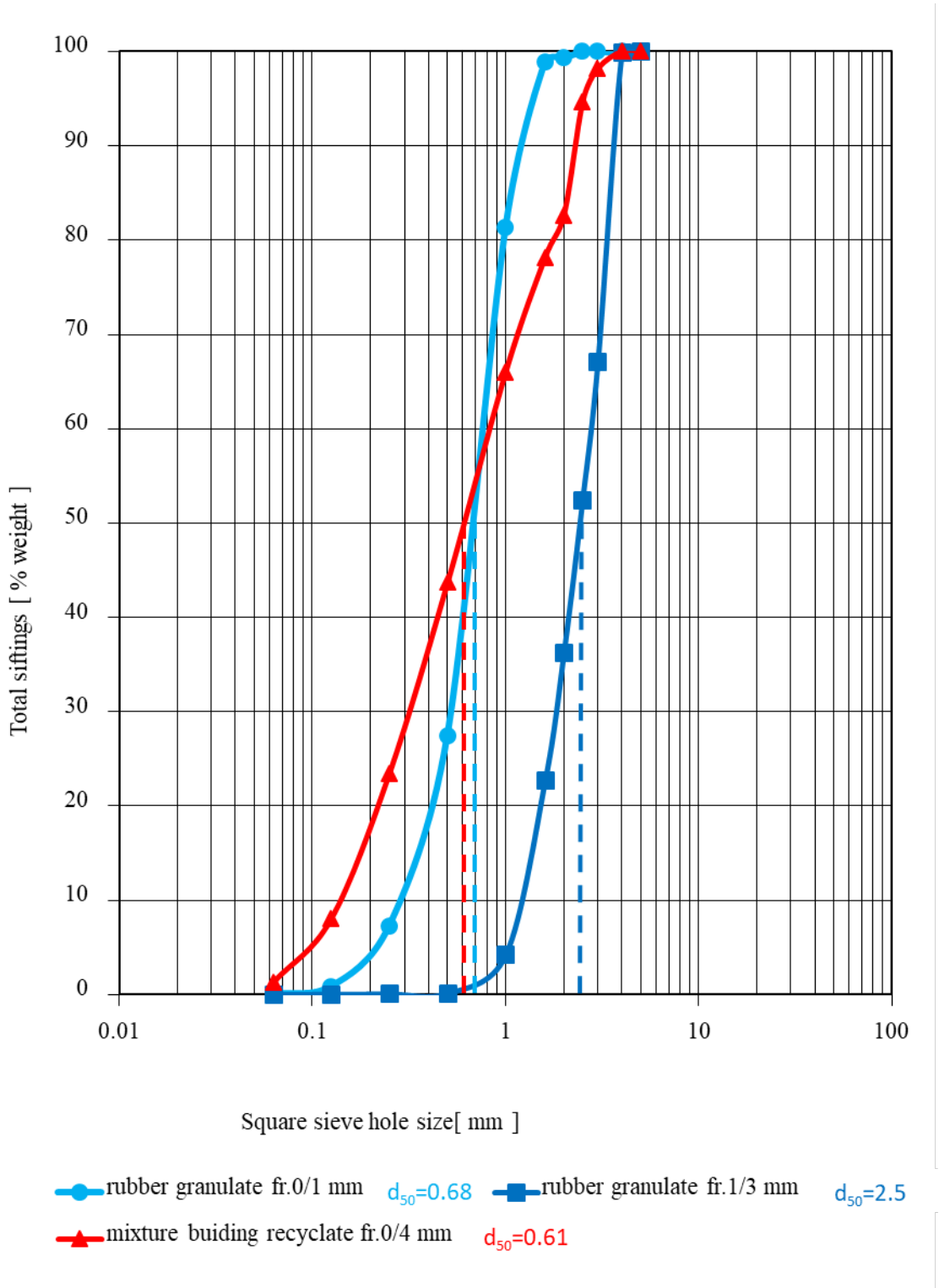

Figure 2: Results of grain-size curve determination: grain-size curve for fr. 0/4 mixture; rubber granulate sample with the grain-size of 0/1 mm; rubber granulate sample with the grain-size of 1/3 mm.

3.2 Strength characteristics

Test specimens measuring 40x40x160 mm were used to test the flexural and compressive strengths. The determination of the flexural strength and compressive strength was performed on samples after 28 and 90 days of age. The measured values of the flexural and compressive strengths are presented in Fig. 3-6.

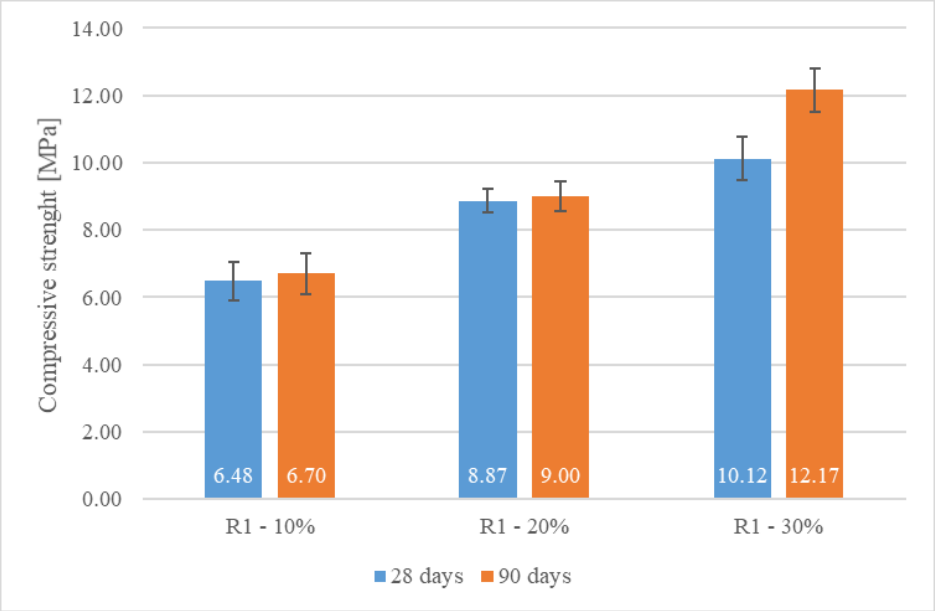

Figure 3: Overview of compressive strengths of cement composites of mixture R1.

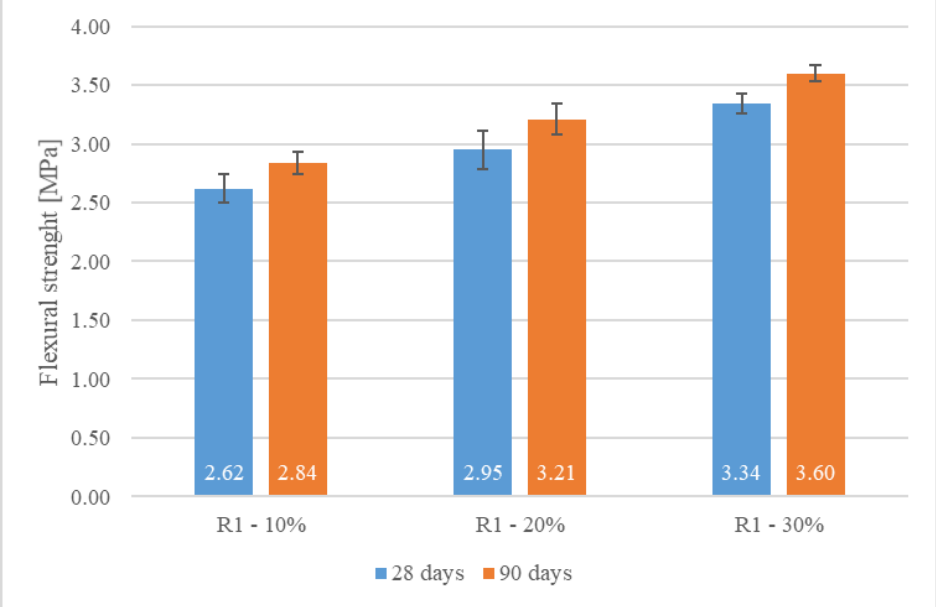

Figure 4: Overview of flexural strengths of cement composites of mixture R1

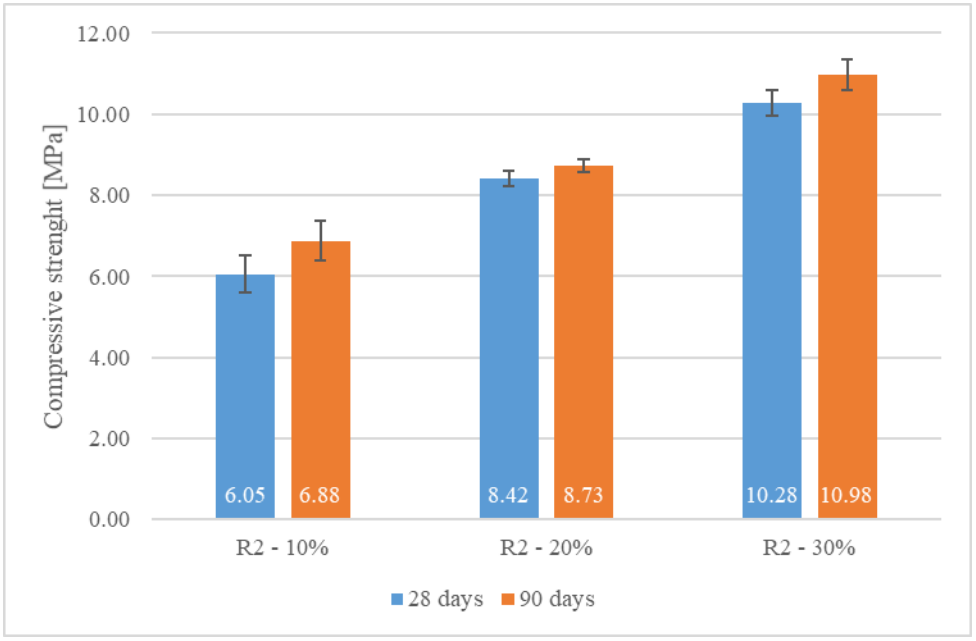

Figure 5: Overview of compressive strengths of cement composites of mixture R2

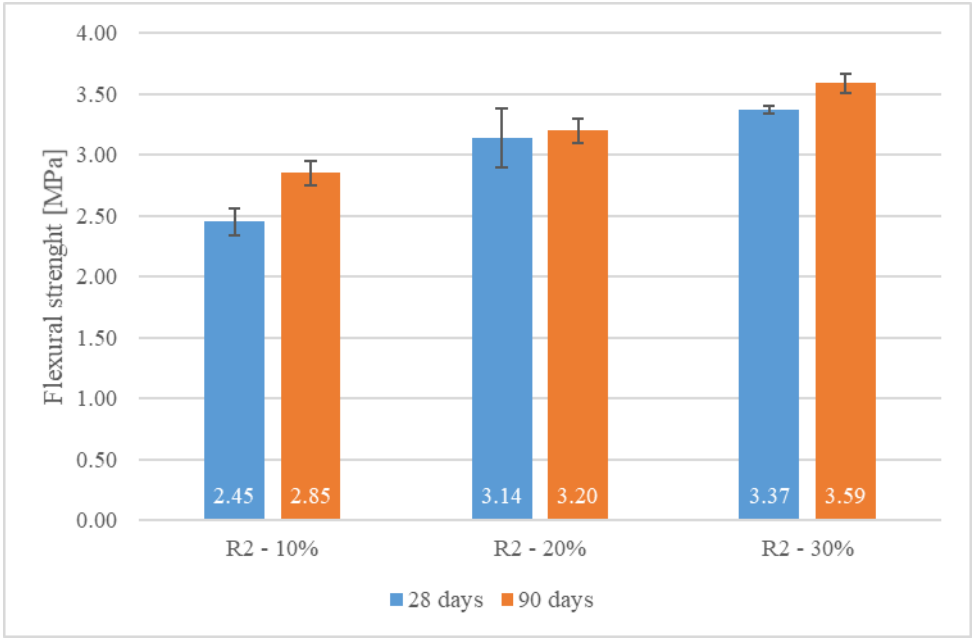

Figure 6: Overview of flexural strengths of cement composites of mixture R2.

Tab. 3 shows a percentage comparison of the increases in compressive and flexural strength of the test specimens prepared according to mixtures R1 and R2 in the time interval after 28 and 90 days.

Table 3: Comparison of the increases in compressive and flexural strength of the test specimens

Mixtures	10% substitute	20% substitute	30% substitute
R1 – Compressive strength	3.39 %	1.46 %	20.25 %
R1 - Flexural strength	8.39 %	8.81 %	7.78 %
R2 - Compressive strength	13.70 %	3.68 %	6.81 %
R2 - Flexural strength	16.32 %	1.91 %	6.52 %

The table shows that the mixture R1 achieved the highest percentage increase in compressive strength with 30% substitute of the filler, however the mixture R1 with 30% substitute had the lowest flexural strength. The results of the R1 mixture with 20% substitute were opposite. This mixture achieved the best percentage increase in flexural strength, but it had the lowest compressive strength.
In case of the R2 mixture, we can clearly state that the largest percentage increase in strength occurred in the mixture with 10% substitute. This mixture achieved the largest percentage increase in both compressive and flexural strength.

4 Conclusion

This paper presents the results of an experimental research dealing with the design of a new type of cement composite based on the by-products arising from the recycling of tires at the end of their life cycle with the fractions of 0/1 mm and 1/3 mm and construction recyclate with the fraction of 0/4 mm prepared from construction waste. Based on the performed tests of strength characteristics, we can draw the following conclusions:

- The increasing share of replacement of rubber recyclate fr. 0/1 mm with mixed recyclate fr.0/4 mm in the amount of 10, 20 and 30 % of weight (see mixtureR1) is accompanied by increasing compressive and flexural strength after 28 and 90 days, as shown in Fig. 3 and 4.
- The largest increase in compressive strength of R1 mixture in the time interval of 28 and 90 days was detected in case of 30 % replacement of rubber recyclate with mixed construction recyclate. It increased by approx. 20 %.
- The largest increase in flexural strength of R1 mixture in the time interval of 28 and 90 days was detected in case of 20 % replacement of rubber recyclate with mixed construction recyclate. It increased by approx. 9 %.
- The increasing share of the replacement of rubber recyclate fr. 1/3 mm in the amount of 10, 20 and 30 % of weight (see mixture R2) is accompanied by the increasing compressive and tensile strength after 28 and 90 days, as shown in Fig. 5 and 6.
- The largest increase in compressive strength of R2 mixture in the time interval of 28 and 90 days was detected in case of 10 % replacement of rubber recyclate with mixed construction recyclate. It increased by approx. 14 %.
- The largest increase in flexural strength of R2 mixture in the time interval of 28 and 90 days was detected in case of 10 % replacement of rubber recyclate with mixed construction recyclate. It increased by approx. 16 %.
- Cement composite based on rubber granulate from waste tires and recycled aggregate can

be used for example as cladding panels in the building interiors for sound and thermal isolation.

- Another benefit is saving the natural non-renewable materials as experimental mixture fillers by replacing them with secondary products from tire recycling and construction waste according to the policy of secondary materials in the Czech Republic and according to the European material strategy Raw Materials Initiative.

Acknowledgements

This article was partially supported by

- Grant of SGS No. SP2020/30, Faculty of Mining and Geology, VSB – Technical University of Ostrava, Czech Republic.
- Moravian-Silesian Region – grant number RRC/10/2018 and RRC/02/2020
- Považská cementáreň, a.s.,, Ul. Janka Kráľa,, 018 63 Ladce, Slovakia

References

[1] GÁLVEZ-MARTOS, J., D. STYLES, H. SCHOENBERGER & B. ZESCHMAR-LAHL. 2018. Construction and demolition waste best management practice in Europe. *Resources, Conservation and Recycling*.*18*(5), 507-512.10.1016/j.resconrec.2018.04.016.

[2] CHEN, J., C. HUA & C. LIU. 2019. Considerations for better construction and demolition waste management: Identifying the decision behaviors of contractors and government departments through a game theory decision-making model. *Journal of Cleaner Production*. *212*, 190-199. 10.1016/j.jclepro.2018.11.262.

[3] ESIN, T. & N. COSGUN, 2007. A study conducted to reduce construction waste generation in Turkey. *Building and Environment*.*42* (4), 1667-1674. 10.1016/j.buildenv.2006.02.008.

[4] LU, W., 2019. Big data analytics to identify illegal construction waste dumping: A Hong Kong study. *Resources, Conservation and Recycling*. *141*, 264-272. 10.1016/j.resconrec.2018.10.039.

[5] JUNAK, J., 2015. Utilization of Crushed Glass Waste in Concrete Samples Prepared with Coal Fly Ash. *Solid State Phenomena*. *244*, 102-107. 10.4028/www.scientific.net/SSP.244.102.

[6] HOSPODAROVA, V., N. STEVULOVA, J. BRIANCIN & K. KOSTELANSKA, 2018. Investigation of Waste Paper Cellulosic Fibers Utilization into Cement Based Building Materials. *Buildings*. *8* (3), 43. 10.3390/buildings8030043.

[7] STEVULOVA, N., A. ESTOKOVA, M. HOLUB, E. SINGOVSZKA & K. CSACH, 2020. Characterization of Demolition Construction Waste Containing Asbestos, and the Release of Fibrous Dust Particles. *Applied Sciences*. *10* (11), 4048.10.3390/app10114048.

[8] SMOLAKOVA, M, A ESTOKOVA, V VACLAVIK, K SOUCEK & V ZAJICOVA, 2018. Determination of durability of mortar with slag exposed to bacterial environment. IOP Conference Series: *Materials Science and Engineering*. *385*. 10.1088/1757-899X/385/1/012052.

[9] ONDOVA, M., N. STEVULOVA & A. ESTOKOVA, 2012. The Study of the Properties of Fly Ash Based Concrete Composites with Various Chemical Admixtures. *Procedia Engineering*. *4*2, 1863-1872. 10.1016/j.proeng.2012.07.582.

[10] TAM, V.W.Y., M. SOOMRO & A. CATARINA J. EVANGELISTA, 2018. A review of recycled aggregate in concrete applications (2000–2017). *Construction and Building Materials*. *172*, 272-292. 10.1016/j.conbuildmat.2018.03.240.

[11] DUAN, Z. H. & C. S. POON, 2014. Properties of recycled aggregate concrete made with recycled aggregates with different amounts of old adhered mortars. *Materials & Design*. *58*, 19-29. 10.1016/j.matdes.2014.01.044

[12] BUI, N. K., T.i SATOMI & H. TAKAHASHI, 2018. Recycling woven plastic sack waste and PET bottle

waste as fiber in recycled aggregate concrete: An experimental study. *Waste Management*. *78*, 79-93. doi.org/10.1016/j.wasman.2018.05.035.

[13] XIAO, J, A D SINGH, Z DUAN, Y PAN & J QIN, 2019. Overview of recycled concrete research through development years (2004-2018). IOP Conference Series: Earth and Environmental Science. *323*. 10.1088/1755-1315/323/1/012134.

[14] LU, J.-X., Xi. YAN, P. HE & C. S. POON, 2019. Sustainable design of pervious concrete using waste glass and recycled concrete aggregate. *Journal of Cleaner Production*. *234*, 1102-1112. 10.1016/j.jclepro.2019.06.260

[15] SAINZ-AJA, J. A., I. A. CARRASCAL, J. A. POLANCO, I. SOSA, C. THOMAS, J. CASADO & S. DIEGO, 2020. Determination of the Optimum Amount of Superplasticizer Additive for Self-Compacting Concrete. *Applied Sciences*. *10* (9), 3096. 10.3390/app10093096.

[16] ČSN EN 1008 Mixing water for concrete (2003) - Specification for sampling, testing and assessing the suitability of water, including water recovered from processes in the concrete industry, as mixing water for concrete. ÚNMZ, Prague.

[17] ČSN EN 196-1 Methods of testing cement - Part 1(2016): Determination of strength. ÚNMZ, Prague.

DOI: 10.1515/sspjce-2021-0006

Investigation on the use of crushed waste of ceramic tiles and clay brick as aggregate in dune sand based mortars

A. Ghrieb[a,b], [a*]Y. Abadou, [c] R. Bustamante

[a] Civil Engineering Department, University of Djelfa, Algeria
[b] Laboratory of Development in Mechanics and Materials, University of Djelfa, Algeria
[c] School of Architecture of Universidad Politécnica de Madrid (UPM), Spain.

Abstract

This present study aims to examine the possibility of using the dune sand which is abundant in Algeria in the manufacture of mortars having sufficient physical and mechanical performances to exploit them in different applications in the field of construction of buildings. The improvement of the mortars based on dune sand was made through the addition of crushed wastes of ceramic tiles and red clay brick. The formulation of mixtures is based on the substitution of dune sand with crushed wastes at different weight contents; 5, 10, 15, 20 and 25%. The W/C ratio is fixed at 0.7. The results obtained show that the incorporation of these additions improves the compactness, the mechanical strengths and the sulphate resistance, and enhancement the dynamic modulus of elasticity with 15% ratio of waste incorporation. Further to this, it was also observed that the inclusion of the used wastes with determined percentages can provide physical and mechanical performances exceed that given by the mortar made with alluvial sand, which demonstrate their effectiveness to the improvement of the various properties of the mortar.

Keywords: Dune sand, ceramic waste, clay brick waste, mortar, Mechanical strength, water absorption, dynamic modulus of elasticity, sulphate resistance.

1 Introduction

In Algeria, there is an abundant presence of noble aggregates. However, the excessive exploitation of these materials can cause long-term problems, especially on the environment.

The exploitation oriented towards to dune sand, clean and present in abundance. Its use could be related to its very high silica content. This sand is also of great economic interest, environmental and ecological. For these reasons which push to the valorization of dune sand.

The dune sand, which constitutes almost 60% of the Algerian territory, is characterized by its good cleanliness and high grain hardness [1-3]. These characteristics have encouraged researchers to further study this material in order to apply it to various fields of civil

engineering, such as road construction [4,5] and concrete and mortar manufacturing [6,7]. Due to the poor particle size distribution of dune sand [4,8], these researches were all focused on finding a way to correct the granular distribution of this sand, with the aim of reducing its porosity, and consequently improve the physical and mechanical characteristics of the mixtures based on this sand.

The waste materials aggregates can be used as well as in mortar and concrete. These waste materials play a very important role in solving present ecological problems. The waste of ceramic tiles and red-clay brick were produced during manufacturing industry, transportation and placing. The production of these wastes has seen a very significant increase in the world over the past few years. This increase was accompanied by an increase in interest in the valorization of these materials, for the purpose to use them as additives in the production of cement [9], or as active additions in the manufacturing of mortars and concretes [7,10,11]. Due to their pozzolanic activity reaction of clay brick powder in blended cement mortars contributes to the compressive strength of mortars and the microstructure of blended pastes became compact [12], the use of these wastes in the manufacture of cementitious mixtures can contribute to improving the physical and mechanical properties, reducing the cost, saving energy and protecting the environment [13]. Y.F. Silva et al [14] revealed that the addition of residue mortar composed of red clay bricks and cement mortar aggregate as cement substitute less than 37.5% can improve compressive strength and from 12.5% to 50% as cement substitute has good workability and self-compaction. Y. Ogawa et al [15] investigated in another study the cement hydration, compressive strength, shrinkage and carbonation properties of concrete made with porous ceramic waste coarse aggregate and 40% of fly ash. The results of this study showed that the porous ceramic waste and fly ash can be used to improve the compressive, drying shrinkage properties and carbonation resistance of concrete. With PCWA incorporation, cement hydration enhancement and fly ash reaction in steam-cured concrete. On the other hand, they can also be generated with other kinds of building materials. The residue of sintered clay brick and aerated concrete blocks generated to manufacture other kinds of building materials. Q. Liu [16] have shown that the use of 10% of recycled powder as cement replacement could be considered the best proportion to enhance the properties of mortar. However, Li et al. [17] demonstrated that mortar with ceramic polishing waste added as paste substitute can significantly enhance sulphate resistance, shrinkage and compressive strength resistance of mortar. Moreover, Pachta et al. [18] concluded that the usage of brick dust and crushed brick enhanced the layered as well as increased adhesion mortars performance and higher compressive strength and Huseien et al. [19] demonstrated the properties of self-compacting, alkali-activated concrete incorporating ceramic tile powder waste could substantially improve the low carbon by using high volume ceramic powder and concrete strength but have better workability performance resistances of concrete as well as, enhancement of concrete durability.

This study focused on the feasibility of correcting the dune sand particle size by the incorporation of crushed waste of ceramic tiles and red clay brick in the production of mortar. To evaluate the influence of waste addition on important physical and mechanical characteristics of modified mortars, the dune sand was replaced by several replacement ratios of waste. The performance of these modified mortars was compared with control mortar (made solely of alluvial sand, cement and water). The results obtained show that the inclusion of these crushed wastes with determined percentages can provide physical and mechanical performances exceed that given by the control mortar, which demonstrates their effectiveness

to the improvement of the various properties of the mortar.

2. Materials

2.1. Cement

The cement used in this study is of ordinary Portland cement CEM I 42.5 class, conforming to the NF EN 197-1 standards [20]. It was manufactured by the Algerian cement company. Its specific gravity is 3.11 g/cm^3 and its Blaine surface specific area is equal to 3118 cm^2/g. The potential mineralogical composition of the clinker (Table 1) is calculated according to the empirical formula of Bogue [21].

Table 1: Mineralogical composition of clinker (%)

C_3S	C_2S	C_3A	C_4AF
52.02	28.97	6.71	12.28

2. 2. Studied sands

In this work, the experiment was undertaken on two types of sand; dune sand noted by DS and alluvial sand designed by AS (Fig. 1). The dune and alluvial sand comes from the southern region of Algeria.

Figure. 1. Used materials

The different results of the physical characteristics of the sands studied are summarized in Table 2. The AS presents a good value of the fineness modulus (2.36), but the DS has a low value (0.86), which means that the AS provides a reasonable compromise between the workability and the resistance [22].

Table 2: Physical characteristics of the studied materials

Physical characteristics	AS	DS	CW	BW
Bulk density (g/cm^3)	1.61	1.46	1.02	1.19
Specific density (g/cm^3)	2.60	2.53	2.43	2.50
Porosity (%)	38	43	58	52
Compactness (%)	62	57	42	48
Water absorption (%)	0.87	2.15	12.73	5.61
Visual sand equivalent (%)	81	79	--	--
Sand equivalent with the piston (%)	80	75	--	--
Maximum size (mm)	5.00	0.63	2.50	2.50
Fineness modulus	2.36	0.86	--	--
Fine particles percentage (%)			47	37

The sand equivalent test carried out in accordance with the NF P 18-598 standard, set values above the recommended limits for concrete and mortar. This allows us to use AS and DS in our investigation.

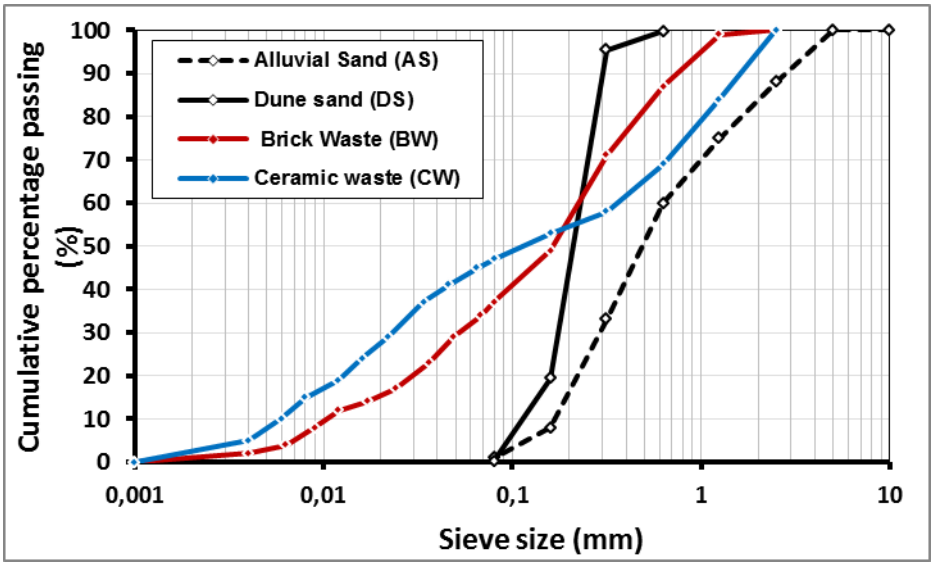

Figure. 2. Particle size distribution of the materials used

The dune sand (DS) presents a continuous distribution of particle sizes from 0 to 0.63 mm (Fig.2). It can be clearly seen that 90% of the sand grains in the dunes are below 0.3 mm. From a granular point of view, this sand can be classified as fine sand [23]. The grading is very tight; almost 90 % of the grains have dimensions ranging from 0.1 mm to 0.5 mm. The sand alone could not have sufficient compactness and therefore not have sufficient mechanical strength (compressive and tensile strength). It should be noted that the sand considered must therefore be granularly corrected [1].

In this investigation, the X-ray diffraction was performed using a random powder method for the bulk sample. The results obtained by the XRD analysis of the sands studied to demonstrate the essentially siliceous nature of DS and AS (Fig. 3.a and 3.b).
The contents of the essential harmful substances (Table 3) are within the tolerable limits recommended by AFNOR standard FD P 18-011[24]. This enables us to use ordinary Portland cement as a binder.

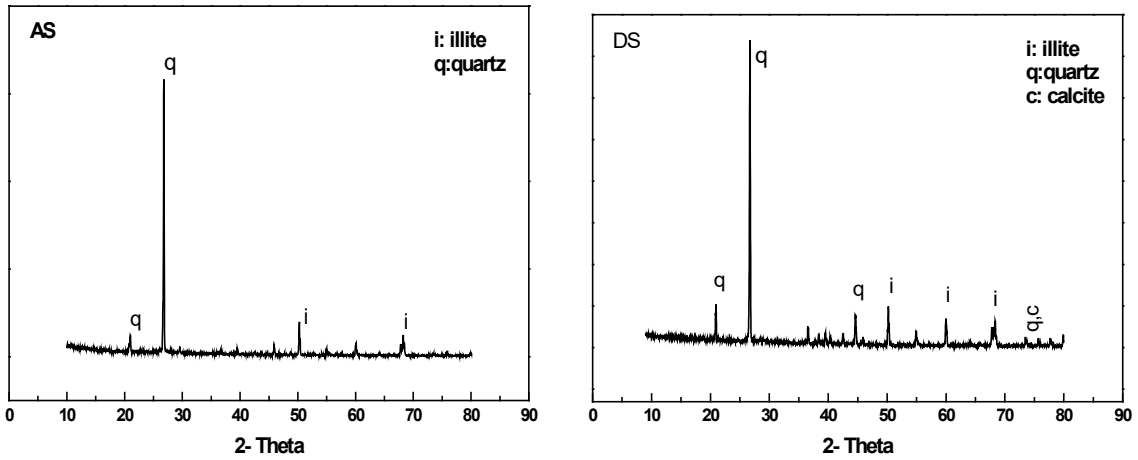

(a) (b)

Figure. 3: X-ray diffraction patterns of sands: (a) Alluvial and (b) dune

2. 3. Additions

In our study, two additions from two different origins were chosen. The additions used in the experiments are; crushed ceramic tile waste and crushed Red-clay brick waste noted respectively by CW and BW (Fig. 1). The reduction of the particle size of the CW and BW was made in the laboratory by crushing and grinding using a ball mill. It should be noted that for the same grinding time, the ceramic waste offers more resistance during the crushing operation. The particle size distribution of studied additions which is shown in Fig. 2, has been determined by sieving method according to NF P94-056 [25] for the fraction higher than 0.080 mm, and by sedimentation method according to NF P94-056 [26] for the fine fraction (smaller than 0.080 mm). The CW and BW present a continuous particle size distribution ranging from 0 to 2.5 mm. The percentage of fine particles is respectively, 47% and 37%. The additions used have a relatively lower bulk density and higher water absorption compared to AS and DS aggregates, as can be seen in Table 2. The higher water absorption of crushed wastes aggregates is due to the higher porosity of the original wastes.

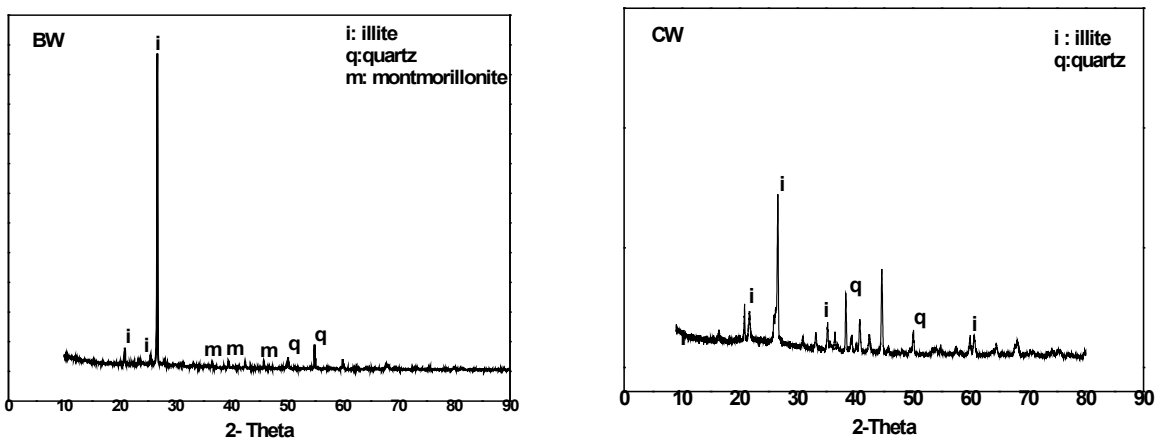

(d) (c)

Figure. 3. X-ray diffraction patterns of additions; (c) CW and (d) BW

The XRD analysis mentioned in Fig. 3.c and 3.d shows that CW and BW are comprised of mainly crystalline phase of illite. The chemical analysis shows that these additions contain almost no harmful elements (Table 3).

Table 3: Contents of the essential harmful substances

Essential harmful substances	AS	DS	CW	BW
Sulphates (%)	traces	traces	traces	traces
Chlorides (%)	0.16	0.82	traces	traces

3. Mix proportions and sample preparation

The mix proportion used to prepare the mortars was the same as used to make the normal mortar, according to the NF EN 196-1 Standard [27]. The additions CW and BW were used as dune sand replacement. To study the effect of the waste incorporation on mortar characteristics, the percentages used were 0%, 5%, 10%, 15%, 20% and 25% by weight of dune sand. A fixed water-cement ratio of 0.70 was used for all mixtures. Cement-aggregate ratio was 1:3. A reference mixture (control mortar) using cement and alluvial sand was prepared to be compared with the CW and BW mortars. Twelve (12) mixtures are to be studied in this investigation. Details of the proportions of mixtures are given in Table 4.

Table 4: Ponderal composition of designed mortars

Symbol of mortar	Mix proportions	Cement (g)	DS (g)	AS (g)	CW (g)	BW (g)	W/C
MA0 (control mortar)	100% AS	450	-	1350	-	0	0.7
MD0	100% DS + 0% CW	450	1350	-	-	0	0.7
MC5	95% DS + 5% CW	450	1282.5	-	67.5	-	0.7
MC10	90% DS + 10% CW	450	1215	-	135	-	0.7
MC15	85% DS + 15% CW	450	1147.5	-	202.5	-	0.7
MC20	80% DS + 20% CW	450	1080	-	270	-	0.7
MC25	75% DS + 25% CW	450	1012.5	-	337.5	-	0.7
MB5	95% DS + 5% BW	450	1282.5	-	-	67.5	0.7
MB10	90% DS + 10% BW	450	1215	-	-	135	0.7
MB15	85% DS + 15% BW	450	1147.5	-	-	202.5	0.7
MB20	80% DS + 20% BW	450	1080	-	-	270	0.7
MB25	75% DS + 25% BW	450	1012.5	-	-	337.5	0.7

Upon completion of the mixing process, the fresh mortar was placed in molds of dimensions (40×40×160) mm^3, which were then clamped onto a vibrating table for 20s. During the first 24 hours, the samples were stored in the normal laboratory environment. After 24 h, these samples were demoulded, and they were then immersed in drinking water at laboratory temperature (23 ± 2 °C), until testing.

4. Testing details

4.1. Tests on fresh mortars

The workability of fresh mortars was investigated using the NF P18-452 LCPC workabilymeter [28]. The test consists of measuring the time necessary for the flow of mortar under the effect of the specified vibration until the reference line is reached. This time is going to be all the shorter as the mortar will be more fluid. The bulk density of fresh mortars was determined in accordance with NF EN 1015-6[29].

4.2. Tests on hardened mortars

Mechanical testing of the prepared samples was carried out using an electromechanical universal press TE 300 kN, in accordance with the NF EN 196-1 standard [27]. Mechanical properties were performed on mortar samples of dimensions (4×4×16) cm^3 at different curing times 7, 28 and 90 days. The flexural strength was measured using a three point bending test. The distance between supporting pins is 100 mm. The half-specimens resulting from bending test were then subjected to compression on a 4×4 cm^2 test section. The dry bulk density and water absorption of hardened mortars were performed in accordance with the standard NF EN 1015-10 [30] and NF EN 1015-18 [31] respectively.
The methods used in most of the tests complied with European standards, rendering mortars may be classified according to the Dynamic modulus of elasticity categories (determined in accordance to EN 14146 [32]) Three prisms (40x40x160) mm^3 per mortar presented in figures 10.a and 10.b. respectively, measure the velocity of ultra-sonic waves according to Fe Pa 43 (2010) [33].
The sulfuric acid immersion test was determined on mortar samples of dimensions 40×40×160 mm^3, in accordance with the standard ASTM C267 [34], using the Vol 5% acid solution (H_2SO_4). The mortar samples were conserved in water until the age of 28 days, at laboratory temperature (23 ± 2 C°). The samples were then immersed in the sulfuric solution. The masse loss of the mortar samples was monitored at 15, 30, 45, 60, 75 and 90 days after immersion, and the sulfuric acid solution was renewed every 2 weeks.
The sulfuric acid resistance is evaluated by the cumulative percentage of mass loss (CPLM), which is given by the following formula:
$CPLM\ (\%) = ((M_t - M_0)/M0)\ x100\%$
Where; M_t is the mass of the sample at time t, and M_0 is the initial sample mass before immersion in sulfuric acid solution.

5. Test results and discussion

5.1. Workability of mixtures

The curves of Fig.4 show the evolution of the flow time (workability) according to the quantity of crushed waste added. We notice that for a fixed water-cement ratio (W/C = 0.7), the dune sand mixture (MD_0) presents low workability (16 seconds) compared to the control mortar (2 seconds), this is mainly due to the size of sand dunes, which is very fine compared to alluvial sand (fine sands require more water).
It was also noted that the progressive substitution of dune sand by CW and BW addition with percentages of less than 15%, has a significant negative influence on the workability. This may be explained by the increase in the specific surface area of the fine particles in mixtures after adding crushed wastes, thereby increasing the water requirement to wetting the fine waste aggregates [35]. However, beyond 15% of CW and BW addition, the dune sand replacements by used additions have a positive influence on the workability of the fresh mortars. This improvement in workability may be related to the fine fraction of the additions filling the voids and releasing the trapped water, which therefore improves the consistency of the mortar [36].

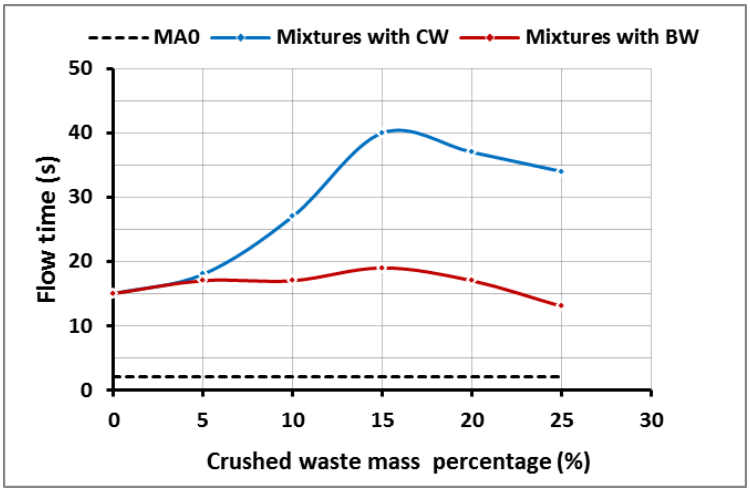

Figure. 4. Evolution of workability as a function of the substitution rate

In the curves shown in Fig. 4, it can also be observed that, beyond 5 % crushed waste replacement, the effect of the type of waste on workability becomes very significant; the mixes containing BW exhibit good to very good workability (13 to 19 seconds), however, it is medium to low (27 to 40 seconds) for those based on CW. This can be explained by the distinct fine particles percentage and water absorption for each addition (Table 2).

5.2. Dry bulk density of fresh mortars

Fig. 5 displays bulk density results of fresh mixtures as a function of crushed wastes amounts. It should be noted that, for a constant W/C ratio, the bulk density of mortar containing dune sand is lower than that of control mortar. The reason for this difference is mainly attributed to the bulk density of dune sand that is lower than that of alluvial sand by 10%. Furthermore, the bulk density generally decreases according to the percentage of incorporated additions. This appears to be due essentially to the lower bulk density of CW and BW (1.02 g/cm^3 and 1.19 g/cm^3 respectively) as compared with dune sand. This observation was already reported by several authors [11, 37, 38].

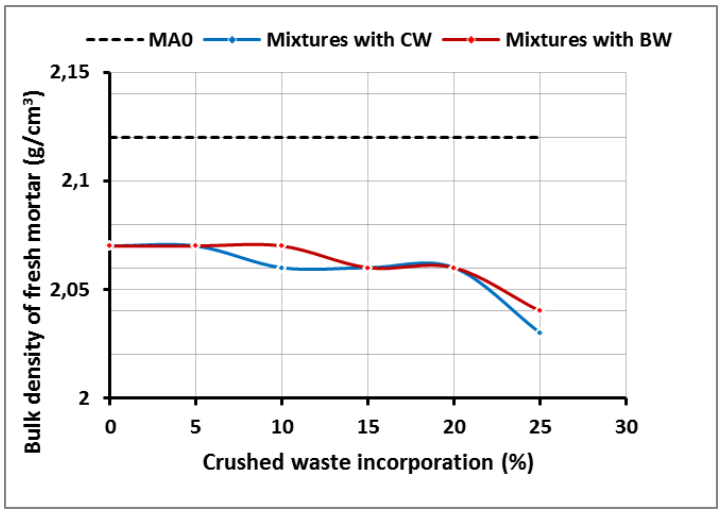

Figure. 5. Evolution of the bulk density of fresh mortar according to the incorporation rate

5.3. Dry bulk density of hardened mortars

The evolution of dry bulk density of hardened mortars with additions percentage is shown in Fig. 6. It was observed that, for a fixed water quantity the dry bulk density of mixture based on dune sand (MD_0) is lower than that of the mixture based on alluvial sand (control mortar). This is principally caused by the distinct porosity (Table 2) for each sand (the DS contains a higher void volume).

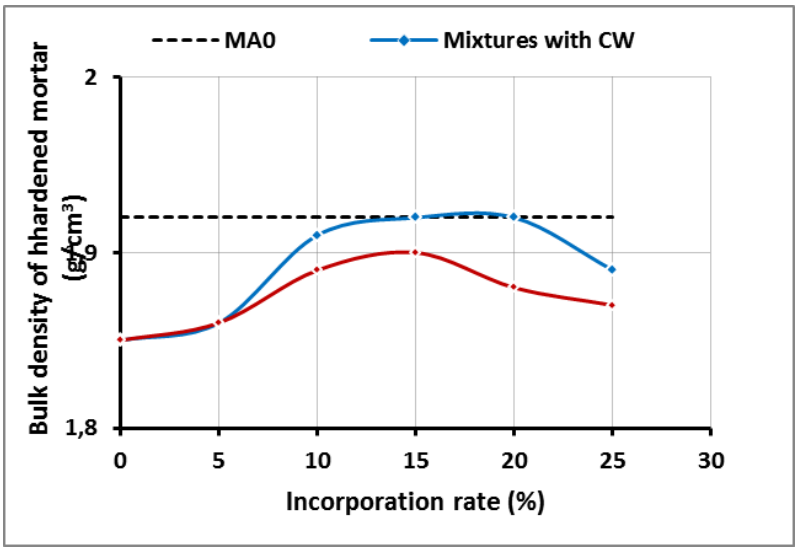

Figure.6. Evolution in bulk density of hardened mortar versus addition rate

It was also observed that, by increasing the replacement rate of the crushing wastes, the bulk density of the hardened mortars increased until a certain optimum and then decreased (Fig. 6). The increase in bulk density for replacement rates from 5% to 15% is linked to the decrease of voids volume within the mortars due to the addition of the fine particles [11]; which explains the effectiveness of the used granular correctors (CW and BW) to improve the compactness of the mixtures. A replacement rate equal to 15%, the bulk density of the modified mortars reaches maximum values of 1.92g/cm^3 and 1.9g/cm^3 for CW and BW respectively; these values correspond to the optimal filling of the spaces between grains of dune sand [39]. The decrease in bulk density for incorporation percentages beyond 15% and 20% of BW and CW respectively is ascribed to the fine particles which begin to occupy the place of the dune sand grains [36], which increased the overall volume (for the same mass, the volume of the crushed waste is greater than that of dune sand), and consequently, The apparent density of modified mortars decreased.
From Fig. 6, it may also be noted that beyond 5 % of addition replacement the effect of the type of waste on the bulk density becomes very significant; at the same replacement level, the incorporation of CW in the mortars results in a higher bulk density compared to that of mortars containing BW; Due to the higher percentage of fine particles and water absorption capacity of CW compared with BW (Table 2), at fixed W/C ratio, the amount of the water in excess in mortars containing CW is lower than that mortars containing BW, which gives after evaporation a smaller voids volume, and consequently greater compactness.
Finally, it should be noted that the dune sand correction with 15 to 20 per cent CW makes it

possible to obtain a bulk density equal to that of the control mortar (MA_0).

5.4. Compressive strength

The development of compressive strength with additions content and with time is given in figures 7.a and 7.b. A number of comments on these results may be made;
At 7 days, the incorporation of CW and BW as partial replacements of dune sand leads to lower compressive strengths than that of a mortar without addition (MD_0). As seen in Fig. 7.a and Fig.7.b, the use of 25% CW and BW induces a loss in compressive strength of 15% and 52.7% respectively. These results show that, at this age, the use of the studied additions has significantly delayed cement hydration (chemical effect) and consequently decreased the compressive strength of mortars.
The increase in CW content at 28 days leads to a continuous increase in compressive strength.

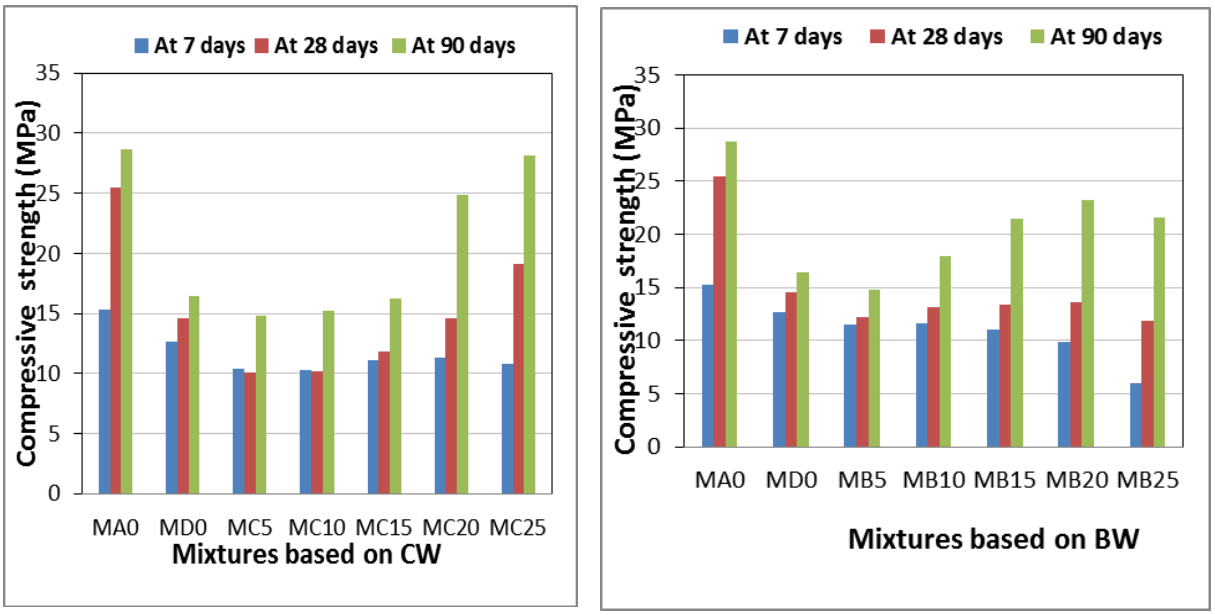

(a) (b)

Figure. 7. Influence of the incorporation of CW (a) and BW (b) on compressive strength

This shows that the chemical effect of CW on the evolution of compressive strength, due to its possible pozzolanic reactivity, is most dominant, as its filling effect normally leads to compressive strength. To a maximum strength between 15% and 20% of CW (the percentages for which the compactness is maximum (Fig.6)). We can also add that the compressive strength does not reach that of the mortar without addition (MD_0) that as from 20% CW and the incorporation of 25% CW induces a gain in compressive strength of 30.8%. On the other hand, it is also observed that the compressive strength increased up to a certain optimum (15% of BW) and then decreased with increasing amounts of BW (evolution similar to that of compactness). Furthermore, it is noted that the correction of dune sand with BW does not participate in the giving of strengths at 28 days higher than that of a mortar without addition (MD_0), but there is a decrease in the strength loss rate compared with 7 days; for 15%, 20%

and 25% of BW, it is observed a strength loss of 8.2%, 6.8% and 19.2% at 28 days versus 13.4%, 22% and 52.7% at 7 days respectively.

At 90 days, the same observation may be noted concerning the evolution of the compressive strength as a function of the percentage of CW, Which remains an increasing function. We also note that the use of CW as a dune sand substitute is only 20 per cent effective for CW. The strength gain rate is 50 per cent and 70 per cent respectively for 20 per cent and 25 per cent for CW. The strength gain rate is of the order of 50% and 70% for 20% and 25% of CW respectively. On the other hand, it is also observed that the increase in BW, causing the same evolution of the compressive strength at 28 days, but with an optimum corresponds to 20% of BW; which shows that the use of this addition is less effective for percentages greater than 20%, and its incorporation becomes effective only from 10%. The strength gain rate is of the order of 10%, 30%, 40% and 30% for 10%, 15%, 20% and 25% of BW respectively.

The incorporation of CW and BW can give maximum improvements in compressive strength at 90 days of the order of 70% and 40% for 25% CW and 20% BW respectively. These improvements make it possible to reach compressive strength close to that of the control mortar (MA_0) in the case of CW and to attain 81% of its strength in the case of BW. These results clearly indicate the effectiveness of the CW and BW in improving the compressive strength of the dune sand-based mortars.

Finally, it is found that the effect of the addition of CW and BW on the evolution of compressive strength as a function of time is very significant, especially after 28 days. Where it is observed that the proportion of the increase in compressive strength for mortars without incorporation is from 28 days to 90 days. for mortars without incorporation (MA_0 and MD_0) is approximately 12%, whereas, it is 70% and 47% for 20% and 25% of CW respectively, and 36%, 60%, 71% and 83% for 10%, 15%, 20% and 25% of BW respectively; This can be attributed to the pozzolanic activity that is becoming more important after 28 days.

5.5 Flexural strength

The flexural strength results of mortars mixes made with and without CW and BW were given in Fig. 8.a and Fig. 8.b. From these results, it can be seen that the flexural strength of CW mortars, were higher than the mortar without addition (MD_0) at all ages. It is evident from Fig 8a that this characteristic increases continuously until reaching its maximum value at 25% CW, with the rate of increase of strength about 69%, 32% and 56% at 7 days, 28 days and 90 days respectively. It can be seen also that the flexural strength of BW mortar mixes with 10%, 15% and 20% replacement were higher than the mortar without addition at all ages. Maximum strength at all ages occurred at 15% CW replacement, with the rate of increase of strength about 44%, 19% and 33% at 7 days, 28 days and 90 days respectively.

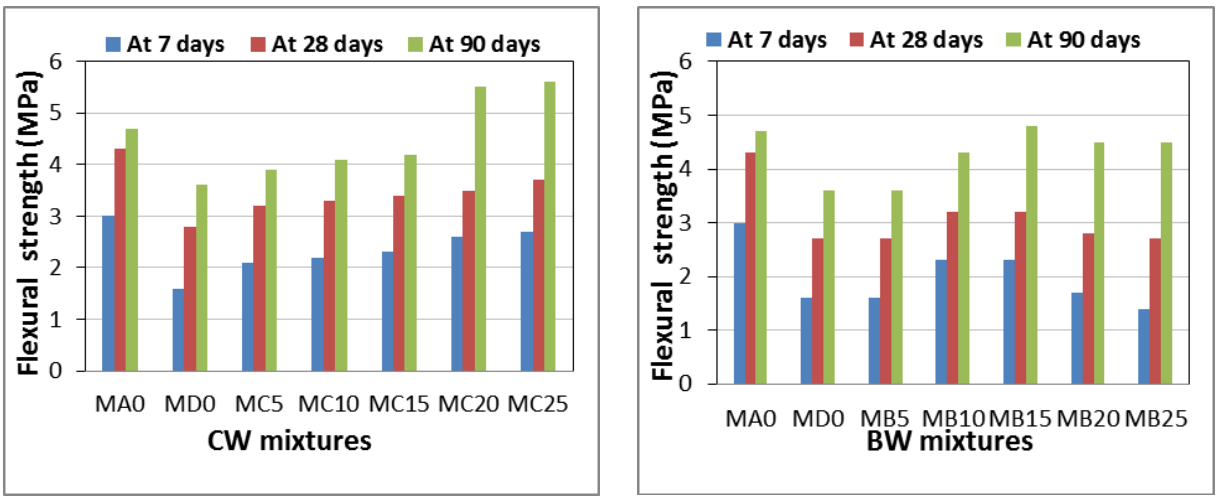

(a) (b)

Figure. 8. Influence of the incorporation of CW (a) and BW (b) on flexural strength

The inclusion of CW and BW as a partial replacement of dune sand makes it possible to achieve flexural strengths at 90 days higher than that of the control mortar (MA_0); the 90-days strengths at 20% and 25% of CW and 15% of BW exceed that of the control mortar by 17%, 19% and 2%, respectively. These values vividly demonstrate the effectiveness of the additions used to improve the flexural strength of dune sand mortars. These results may be explained, by a higher compactness of the hardened mortar (filler effect) and a potential pozzolanic effect of this construction and demolition waste.

5.6. Water absorption of hardened mortars

The results of water absorption of the mortar mixes are shown in Fig. 9. It was observed that, by increasing the rate of incorporation of CW and BW, the water absorption coefficient of the mortars decreased to 15% and then increased. The decrease in water absorption is mainly due to the filling effect of CW and BW. The increase of this characteristic may be related to the increase of the quantity of free water in the mixtures after the filling of the voids. The mortars with 15% CW and BW (MC_{15} is MB_{15}) are those that exhibit the lowest workability for each type of addition (Fig. 4). The amount of free water in the mixtures is thus reduced for these mortars, which decreased the volume of voids and therefore the water absorption coefficient (Fig. 9). This means that the porosity at 15% CW and BW is the lowest (the compactness is the highest), which confirms the results of the other tests (workability, bulk density of hardened mortars, compressive and flexural strength).

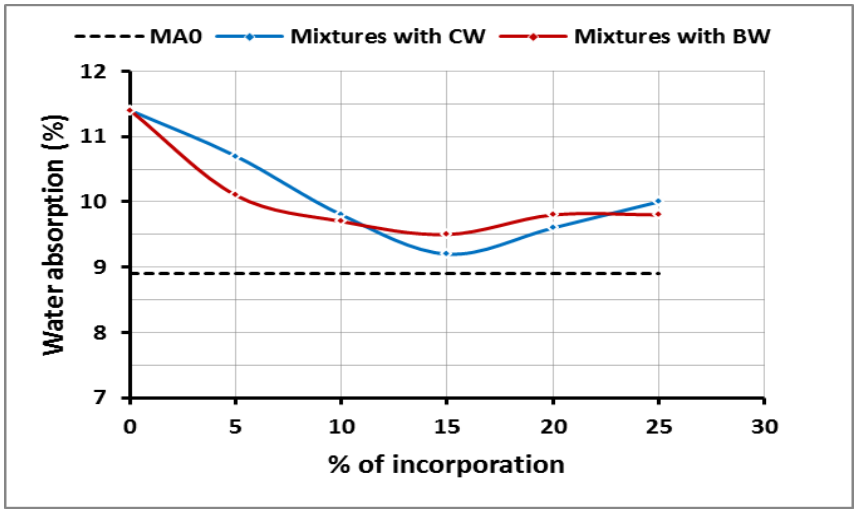

Figure. 9. Effect of addition amount on water absorption

Finally, it can be seen that the correction of studied dune sand granulometry by the use of CW and BW does not make it possible to obtain water absorption coefficients lower than that of the control mortar (MA_0). This is mainly due to the good particle size distribution of the alluvial sand.

5.7. Dynamic modulus of elasticity of hardened mortar

The results of the dynamic modulus of elasticity test are presented in Fig. 10.a. The dynamic modulus of elasticity, considered of the materials waste used, increased with the type of waste incorporation (ceramic tile and crushed red-clay brick). This is due to the fine particles that occupy the voids between sand aggregates. Thus, mortars become more compact, the irregularity shape of waste materials provides a higher bond between waste aggregates and the cement paste and as a consequence, the modulus of elasticity increased. The dune sand mortar with 15% rate incorporation of ceramic tile and red clay brick had a modulus of elasticity 28%, 10% and 24%, 0.6% higher than that of the references mortars (MD_0, MA_0). This denotes higher compactness of the modified dune sand mortar (15%) when compared with a reference mortar and as well consistent with higher lower water absorption and mechanical strength.

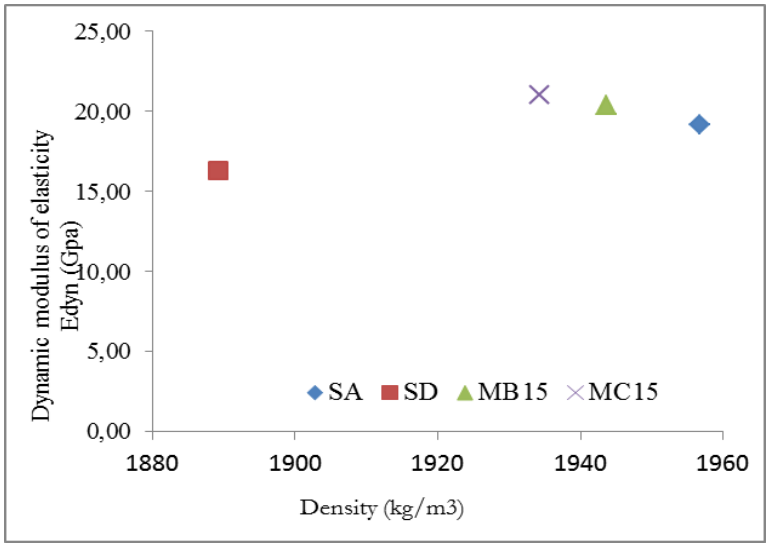

Figure. 10.a. Dynamic modulus of elasticity of mortar tested

5.8. Ultra-sound of hardened mortar

The effect of adding aggregates waste (CW, BW) on these tests of a dune sand mortar has been presented on Fig.10.b, an increase in ultra-sound pulse velocity in the modified dune sand mortars with incorporation of ceramic tile and red clay brick waste. This result of agreeing with the modulus of elasticity test. These experimental strengthen the concept that the incorporation of ceramic tile and crushed red-clay brick wastes produced a dune sand mortar with a lower volume of pores, which higher mechanical resistance, and lower water absorption.

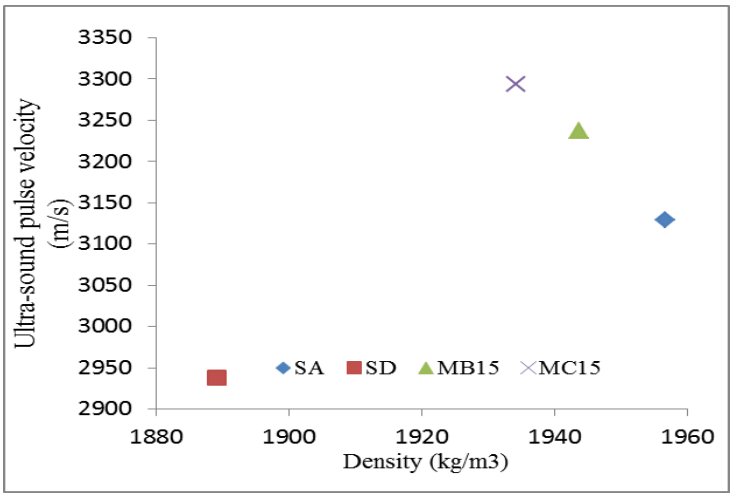

Figure. 10.b. Ultra-sound pulse velocity of the mortar tested

5.9. Resistance to sulfuric acid attack

The mass loss is commonly used as an acceptable indicator to evaluate the deterioration of mortars and concretes under acid attack [40, 41]. Fig. 11.a and 11.b represent the mass loss (negative means mass loss) of specimens exposed to sulfuric acid up to 90 days. From these results, it can be observed that the mass is gradually decreased with the increase in exposure time for all studied mortars. This deterioration of the mortar structure is mainly due to the reaction between the calcium hydroxide ($Ca(OH)_2$) present in cement and the sulphuric acid, which can induce tensile stress, resulting in mortar cracking and scaling [42].

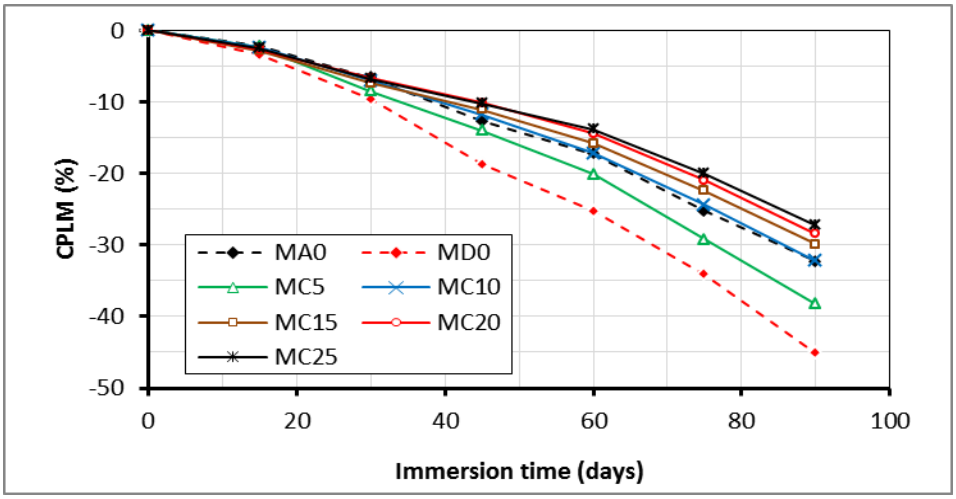

Figure. 11.a. Mass loss of mortar samples made with CW

As shown in Fig. 11.a, the replacement of part of dune sand by CW increased the mortar's ability to resist to acid attack. A mortar containing 10% of CW (MC_{10}) may have the same acid resistance as a control mortar. Beyond 15% the CW mortars exhibited higher acid resistance than that of control mortar. At the end of the test period, the incorporation of 25 % of CW results in an acid resistance improvement of approximately 40 %.

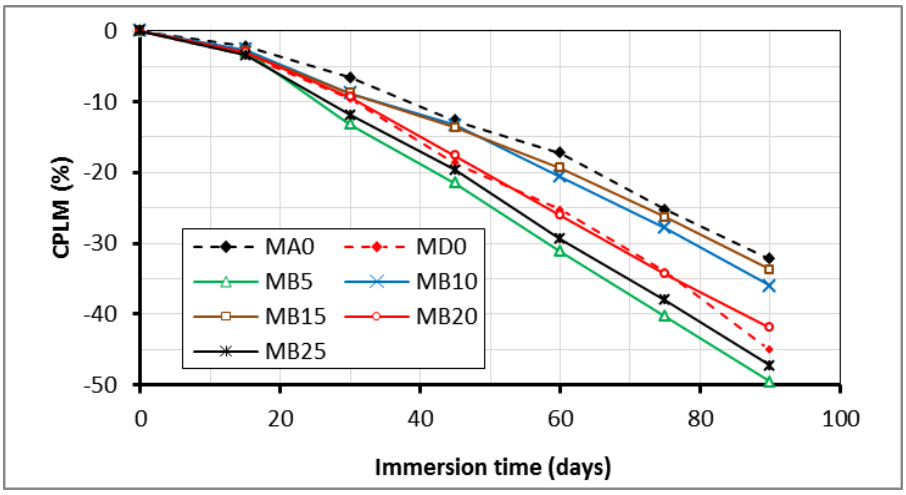

Figure. 11.b. Mass loss of mortar samples made with BW

Concerning BW, as illustrated in Fig. 11.b, the amelioration of the resistance to sulfuric acid attack is only possible for incorporation rates of 10% and 15%. These gains are not sufficient to achieve the results obtained by the control mortar.

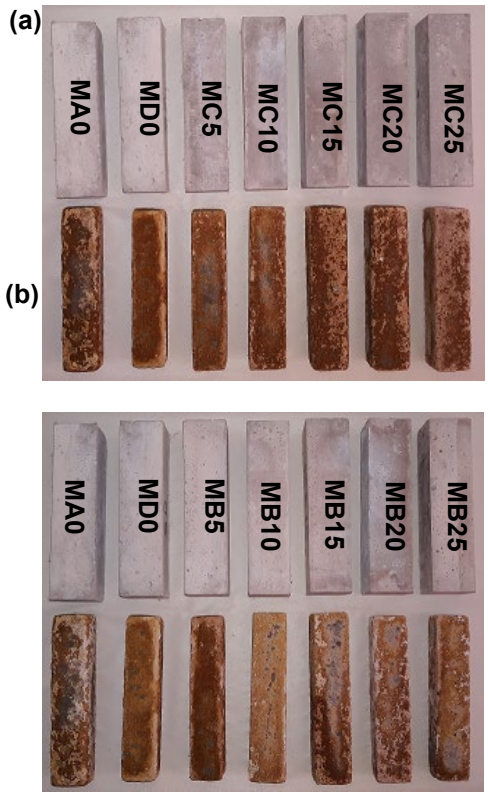

Figure. 12. Deterioration of CW (a) and BW (b) samples after 90 days of immersion in 5% H_2SO_4 solution

After 90 days of immersion in sulfuric acid solution, the correction of dune sand with 15 % BW contributes to reducing the deterioration of mortar structure by 25%. Visually, the fig. 12.a 12b reflects the deterioration of mortar samples in sulfate environment, particularly for the mortar with 5% of BW.

6. Conclusion

This study was conducted to assess the possibility of utilizing crashing waste of ceramic tiles (CW) and red clay brick waste (BW) as a partial replacement of dune sand for valorizing them in mortar manufacturing. Based on the results of the experimental program conducted in this investigation, the following main conclusions are drawn:

- At the same W/C ratio, the progressive substitution of dune sand by CW and BW addition with percentages of less than 15%, has a significant negative influence on the workability, however, beyond 15%, it has a positive effect. The mixes containing BW exhibit good to very good workability, however, it is medium to low for those based on CW.
- The incorporation of CW results in a higher bulk density of hardened mortars compared to

that of mortars containing BW. The optimal filling of the voids between grains of dune sand, which corresponds to maximum compactness and bulk density, is obtained for CW content between 15% and 20%, and for 15% of BW.

-The use of CW and BW as a partial replacement for dunes sand can lead to very good improvements in compressive strength at 90 days; around 70% and 40% for 25 % CW and 20 per cent BW respectively. These improvements make it possible to reach compressive strength close to that of the control mortar in the case of CW and to attain 81% of its strength for BW. The effect of the addition these crushed wastes on the evolution of compressive strength with time is very significant, especially after 28 days; this is mainly attributed to the pozzolanic activity that has become important in this period.

- The correction of dune sand with the studied additions makes it possible to achieve flexural strengths at 90 days higher than that of the control mortar (MA_0); the 90-days strengths at 25% of CW and 15% of BW exceed that of the control mortar by 19% and 2%, respectively; This reflects the efficiency of CW and BW to improve this characteristic.

- The results of drying shrinkage at an early age show that the incorporation of CW leads to a clear reduction in the drying shrinkage (reduction of 26% for 20% incorporation) in comparison with that the mortar MD_0, The opposite effect was noticed with the incorporation of BW.

- The addition of CW increased the mortar's ability to resist to acid attack; this is not possible in the case of BW except for incorporation rates 10% and 15%. Beyond the incorporation rate of 15%, the CW mortars exhibited higher resistance to sulfuric acid attack than that of mortar based on alluvial sand (control mortar).

References

[1] Ghrieb A, Mitiche-Kettab R, Bali A (2014) "Stabilization and utilization of dune sand in road engineering". *Arabian Journal for Science and Engineering*; 39 (3): 1517-1529. doi.org/10.1007/s13369-013-0721-z

[2] Ghrieb A, Mitiche-Kettab R (2013) "Stabilized Dune Sand for Road Foundation Layers - Case of the Dune Sand of the Region of Djelfa (Algeria)". *Applied Mechanics and Materials.* 319: 263-277. doi .10.4028/www.scientific.net/AMM.319.263

[3] Capdessus H, Chauvin JJ (1973) "Traitement des sables des Landes". Bulletins de Liaison de Laboratoire des Ponts et Chaussées. ; 67 : 85-103.

[4] Al-Abdul Wahhab HI, Asi IM. (1997) "Improvement of marl and dune sand for highway construction in arid areas" *Building and Environment*; 32 (3): 271-279. doi.org/10.1016/S0360-1323(96)00067-4

[5] Khay SE, Neji J, Loulizi A (2011) "Compacted dune sand concrete for pavement applications*". Proceedings of the Institution of Civil Engineers - Construction Materials*; 164 (2): 87-93. doi.org/10.1680/coma.900049

[6] Kettab R, Ghrieb A, Bali A. (2003) "A study of dune sand concrete for aeronautical runways" *International symposia, advances in waste management and recycling*; September 9-11; Dundee, Scotland.

[7] Abadou Y, Mitiche-Kettab R, Ghrieb A (2016) "Ceramic waste influence on dune sand mortar performance" *Construction and Building Materials*. 125: 703–713. doi: 10.1016/j.conbuildmat.2016.08.083

[8] Charman JH, West G. (2011) "Particle size distribution of dune sand from Libya" *Quarterly Journal of Engineering Geology and Hydrogeology*. 44 (2): 277-280. doi: 10.1144/1470-9236/09-045

[9] Ay N, Ünal M. (*2000)"* The use of waste ceramic tile in cement production". *Cement and Concrete Research.; 30: 497-499*. doi: 10.1016/S0008-8846(00)00202-7

[10] Binici H. (2007) "Effect of crushed ceramic and basaltic pumice as fine aggregates on concrete mortars properties". *Construction and Building Materials*; 21: 1191–1197. doi.org/10.1016/j.conbuildmat.2006.06.002

[11] Silva J, De Brito J, Veiga R. (2009) "Incorporation of fine ceramics in mortars" *Construction and Building Materials.* ; 23: 556–564. doi.org/10.1016/j.conbuildmat.2007.10.014

[12] J. Shao, J. Gao, Y. Zhao, X. Chen (2019) "Study on the pozzolanic reaction of clay brick powder in blended cement pastes" *Construction and Building Materials* 213; 209–215. doi.org/10.1016/j.conbuildmat.2019.03.307.

[13] Pašalić S, Vučetić S, Zorić D, Ducman V, Ranogajec J. (2012) "Pozzolanic mortars based on waste building materials for the restoration of historical buildings". *Chemical Industry and Chemical Engineering Quarterly*.; 18 (2): 147−154. doi: 10.2298/CICEQ110829056P

[14] Y.F. Silva, David A. Lange, S. Delvasto (2019) " Effect of incorporation of masonry residue on the properties of self-compacting concretes" *Construction and Building Materials* 196 277–283. doi.org/10.1016/j.conbuildmat.2018.11.132

[15] Y. Ogawa, P.T. Bui, K. Kawai, R. (2020) Sato "effects of porous ceramic roof tile waste aggregate on strength development and carbonation resistance of steam-cured fly ash concrete". *Construction and Building Materials* 236 117462. doi.org/10.1016/j.conbuildmat.2019.117462

[16] Q. Liu, B. Li, J. Xiao, A. Singh (2020) "Utilization potential of aerated concrete block powder and clay brick powder from C&D waste" *Construction and Building Materials* 238 117721. doi.org/10.1016/j.conbuildmat.2019.117721

[17] L.G. Li, Z.Y. Zhuo, J. Zhu, A.K.H. Kwan (2020)" Adding ceramic polishing waste as paste substitute to improve sulphate and shrinkage resistances of mortar. 362 ; 149-156 doi.org/10.1016/j.powtec.2019.11.117.

[18] Vasiliki Pachta, Pinelopi Marinou, Maria Stefanidou (2018) " Development and testing of repair mortars for floor mosaic substrates" *Journal of Building Engineering* 20 501–509. doi.org/10.1016/j.jobe.2018.08.019.

[19] G.F. Huseien, Abdul R.M. Sam, K.W. Shah, J. Mirza (2020) "Effects of ceramic tile powder waste on properties of self-compacted alkali-activated concrete" *Construction and Building Materials* 236 117574. doi.org/10.1016/j.conbuildmat.2019.117574.

[20] NF EN 197-1; AFNOR standards organisation (2012) Cement - Part 1: composition, specifications and conformity criteria for common cements.

[21] Bogue R.H (1955), Chemistry of Portland cement. New York (NY): Reinhold Publishing.

[22] Dreux G, Festa J. (1998) Nouveau guide du béton et de ses constituants. France : Eyrolles.

[23] Chauvin JJ. (1987). Les sables, guide technique d'utilisation routière. France : ISTED.

[24] FD P18-011; AFNOR standards organization (2009) Concrete - Definition and classification of chemicaly aggressive environments - Recommendations for concrete mix design.

[25] NF P 94-056; AFNOR standards organization (1996): Soil: investigation and testing. Granulometric analysis. Dry sieving method after washing.

[26] NF P 94-057; AFNOR standards organization (1992). Soils investingation and testing. Granulometric analysis. Hydrometer method.

[27] NF EN 196-1, AFNOR standards organization (2006)"Methods of testing cement - Part 1: determination of strength".

[28] NF P18-452, AFNOR standards organization (1988) "Concretes - Measuring the flow time of concretes and mortars using a workabilitymeter

[29] EN 1015-6, European Standard (1999) ''Methods of test for mortar for masonry – Part 6: Determination of bulk density of fresh mortar'', European Committee for Standardization (CEN).

[30] EN 1015-10, European Standard (2000), ''Methods of test for mortar for masonry - Part 10: Determination of dry bulk density of hardened mortar'', European Committee for Standardization (CEN)

[31] EN 1015-18, European Standard (2003), ''Methods of test for mortar for masonry – Part 18: Determination of water absorption coefficient due to capillary action of hardened mortar'', European Committee for Standardization (CEN).

[32] EN 14146, European Standard (2004). Natural stone test methods. Determination of the dynamic elastic modulus of elasticity (by measuring the fundamental resonance frequency). European Committee for Standardization (CEN).

[33] FE Pa 43, Test form (2010). Test of evaluation of the mechanical characteristics by ultra-sounds (in Portuguese). National Laboratory of Civil Engineering (LNEC), Lisbon; September 2010.

[34] American Society for Testing and Materials (ASTM) C 267 (2003). Standard test methods for chemical resistance of mortars, grouts, and monolithic surfacings and polymer concretes.

[35] Nazari A, Riahi S. (2011) "Improvement compressive strength of concrete in different curing media by Al_2O_3 nanoparticles". *Materials Science and Engineering*; 528 (3): 1183-1191.

doi.org/10.1016/j.msea.2010.09.098.
[36] Bédérina M, Khenfer MM, Dheilly RM. Quéneudec M.(2005)"Reuse of local sand: effect of limestone filler proportion on the rheological and mechanical properties of different sand concretes", *Cement and Concrete Research*; 35: 1172–1179. doi.org/10.1016/j.cemconres.2004.07.006
[37] Neno C, De Brito J, R. Veiga (2014). Using Fine Recycled Concrete Aggregate for Mortar Production. *Materials Research*. 17: 168-177. doi.org/10.1590/S1516-14392013005000164
[38] Penacho P. De Brito J, Veiga MR (2014). Physico-mechanical and performance characterization of mortars incorporating fine glass waste aggregate. *Cement & Concrete Composites* ; 50: 47–59. doi.org/10.1016/j.cemconcomp.2014.02.007
[39] Chauvin JJ, Grimaldi G, (1988) "Les bétons de sable", *Bull. Liaison Lab. Ponts et Chausseés*.; 157: 9-15.
[40] Attiogbe KE, Rizkallah HS. (1988) "Response of concrete to sulphuric acid attack". *ACI Materials Journal*; 85 (6): 481–488.
[41] Fattuhi NI, Hughes BP. (1988) "SRPC and modified concretes subjected to severe sulphuric acid attack". *Magazine of Concrete Research*; 40 (144): 159–166. doi.org/10.1680/macr.1988.40.144.159
[42] Sata V, Sathonsaowaphak A, Chindaprasirt P. (2012) "Resistance of lignite bottom ash geopolymer mortar to sulfate and sulfuric acid attack". *Cement and Concrete Composites*, 34: 700–708. doi:10.1016/j.cemconcomp.2012.01.010.

DOI:10.1515/sspjce-2021-0007

Behaviour of cemented and compacted clayey sand reinforced with two types of fibers

Adjabi Souhila[*1a], Nouaouria Mohamed Salah[1b]

(1) University of 8 May 1945, Guelma, Algeria
(1) Civil Engineering and Hydraulic Laboratory
e-mail: ([*a]) adjabi.souhila@univ-guelma.dz,([b])nouaouria.mohamed@univ-guelma.dz

Abstract

Considering Soil reinforcement techniques have been rapidly developed because of its efficiency in geotechnical engineering. The goal of this experimental work is to improve the characteristics of a collapsible soil with polyethylene fibers in the aim of reducing the number of plastic bottles thrown in nature and with natural materials such as sisal fibers. Polyethylene fibers contents in mass were used in this investigation, namely: 5%, 10% and 15%; Sisal fibers contents: 0.5% and 1% respectively. Oedometer apparatus is used to study the reinforcing fibers effect on the Collapse Potential, and direct shear box is used to determine the intrinsic characteristics of this treated soil. Results show that when the fiber reinforcement is combined with other processing procedures such as compaction and the addition of APC cement decrease the collapse potential until a non-collapsible soil is obtained.

Key words: Collapse potential, Polyethylene fiber, sisal fiber, collapsible soil, compaction energy, shear strength, cohesion

1 Introduction

Buildings a civil engineering structures on collapsible soils is not safe because such soils can settle suddenly when are loaded and wetted.

It is quite common to find soils that do not meet the basic necessities of an engineering project technically, economically or in terms of timing. Economic issues have raised interest in the development of alternative materials that fulfill design specifica¬tions. The well-established technics of soil stabilization and soil reinforcement are generally used to obtain improved geotechnical materials, either through the addition of cementitious agents or through the inclusion of randomly distributed discrete elements such as fibers. Stabilized and reinforced soils are composite materials that result from the combination and optimization of the properties of individual constituent materials.
Many investigators have studied stress-strain characteristics of reinforced soil by using

triaxle, direct shear, and plane strain tests since the early 1970's. From 1977, extensive experimental work has been performed on geotextile-reinforced sand. Incorporating reinforcement inclusions within soil is also an effective and reliable technique that can be used to improve the engineering properties of soil. Many investigators have used various types of fibers under different test conditions. A state of art of some investigations is cited as follow:

Maher and Ho [1] evaluated the effect of randomly distributed fiber reinforcement on the response of cemented sand to load. The results of the test indicated that fiber reinforcement have significantly increased the compressive and shear strength of cemented sand.

Consoli N.C. [2] assessed the effect of randomly distributed fiber reinforcement and cement inclusion on the response of a sandy soil to load. The results showed that the addition of cement to the soil results in the increase of stiffness, brittleness and peak strength. The addition of fibers increases both the peak and residual triaxial strength, and decreases stiffness and changes the cemented soil's brittle behaviour to a more ductile material.

Ayadat and Dahili [3] improved the properties of a collapsible soil. They examined the bituminous treatment of collapsible soil at a depth of less than 4m ha, the results indicated that for obtaining no collapsible soil, a minimum water content of 4%, a bitumen content between 10 and 12 % and a high compacting energy (more than 80 blows by layer for a total of two layers in oedometer ring) have been applied.

Yetimoglu T. and Salbas O. [4] studied the effect of the fiber reinforcement content on the shear strength. The results of the tests indicated that the peak shear strength and the initial stiffness of the sand were not affected significantly. However, the fiber reinforcement could reduce soil brittleness providing smaller loss of post-peak strength, and increase the residual shear strength angle of the sand.

Chauhan M.S and Mittal S. [5] investigated the effect of reinforcement with coir fiber and synthetic fiber in subgrade soil on the strength; they reported that the permanent and resilient strains in all materials decrease with confining pressure but increase with the number of load cycles and deviator stress in reinforced and unreinforced conditions.

Ahmed F. and Batni F.[6] evaluated the response of randomly distributed oil palm empty fruit bunch (OPEFB) fiber on the strength of reinforced silty sand. The results indicated that the shear strength parameters of the soil- fiber mixture (Ø' and c') can be improved significantly, but (OPEFB) fibers are biodegradable and must be protected from any circumferential agents to ensure long-term performance.

Al Adili A. and Azzam R. [7] studied the effect of soil reinforced with randomly included papyrus fiber on the strength behaviour. The results of these tests have shown a significant improvement in the failure deviator stress and shear strength parameters of the soil with 10% of papyrus fiber. This addition also reduced the deformation of the soil under loading.

Chegenizadeh A. and Nikraz H. [8] investigated the effect of paper inclusion on the modulus of elasticity of subgrade material; the results indicated that the increase of paper percentage in mass slightly increases the modulus of elasticity

Cristelo. N, Glendinning S [9], investigate the role of calcium content in fly ash used to stabilize soft soils through alkaline activation with sodium-based alkaline activators, the

results that low calcium fly ash is a better source for long term soft soil stabilization with alkaline activation than high calcium fly ash.

Zhang M., and al [10], studied, stabilization of lean clay with metakaolin based geopolymer at different concentration (ranging from 3 to 15 wt. % of unstabilized soil at its optimum water content) to examine the feasibility of geopolymer in stabilizing soils. Geopolymer stabilized soil specimens were characterized with compressive strength testing, volume measurements during curing .The results indicated that with geopolymer concentrations, compressive strength, failure strain and Young's modulus of the stabilized soil specimens increased, and shrinkage strains during curing decreased.

Botero E. and Ossa A.[11] investigated the mechanical behaviour of a silty soil that was reinforced with randomly distributed PET fibers. The results indicated that the reinforced specimens presented increase of shear strength that was associated with the increasing quantities of the PET fiber.

In comparison with conventional geosynthetics (strips, geotextiles, geogrids, etc.), there are some advantages in using randomly distributed fibers as reinforcement. Firstly, the discrete fibers are simply added and mixed randomly with soil, in the same way as cement, lime, or other additives. Secondly, randomly distributed fibers limit potential planes of weakness that can develop parallel to oriented reinforcement.

The objective of this paper is to determine the effect of randomly distributed short polyethylene-fiber, glass fibers and sisal fibers, respectively, on the collapse behaviour of a clayey sand material. A series of compression tests were carried out in the Oedometer apparatus, on soil samples made of sand, fibers and Kaolinite. Three lengths of fibers were respectively used, such as: 5mm, 10mm and 25 mm.

This paper describes a study of the collapse behaviour of Kaolinite-sand mixed samples reinforced with randomly distributed polyethylene fibers, sisal fibers and glass fibers respectively, under Oedometer loading conditions. The specific objectives of the present work are to evaluate the effect of fiber insertion on the collapse potential of sand samples mixed with Kaolinite in different proportions such as: 0 %, 5%, 10%, 15%, 20%, 25% and 30% respectively, to determine the optimum content of Kaolinite giving the maximum potential collapse.

In order to get healthier drinking water, millions of people use bottled water. The annual global consumption of bottled water has reached billions of liters. This requires the production of innumerable quantities of large and small bottles which are generally thrown in the nature. This act is harmful to the environment. Only about 20% of plastic bottles are recycled; 80% end up in landfills, or in nature. Plastic bottles begin to decompose in nature only after hundreds of years. In order to reduce the quantity of used plastic bottles, we undertake this study based on the use of these bottles to treat the collapsible soil.

This is in order to protect the environment and to address this type of soil problems by finding economic solutions; soil was reinforced with polyethylene fibers contents of 5%, 10% and 15% respectively. For each content three different lengths were used (5 mm, 10mm and 25 mm respectively), and 0.5%, 1% (5mm, 10mm and 25mm long) for sisal and glass fibers.

2 Materials, Equipment and Experimental Program

2.1 Materials

2.1.1 Soil

The reconstituted soil in the laboratory used in this experimental work is composed of sand with the grain size distribution curve is unlisted in Fig.1.

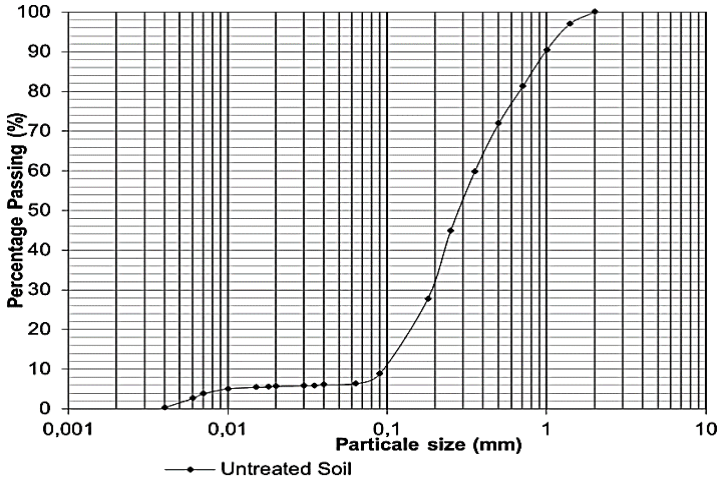

Figure1. Particle size distribution curve of kaolinite and sand

It is mixed with kaolinite or china clay, its chemical formula is $Al_2O_3.2SiO_2.2H_2O$, in proportions of 25% which is the optimum content of Kaolinite giving the maximum potential collapse [12&13]. The properties of this material are indicated in table 1.

Table 1. Properties of Kaolinite used in the study

Properties	value
Liquide limit WL [%]	60
Plastic limit W_P [%]	45
Plasticity Index IP [%]	15
Specific gravity G_s	2.60
SPECIFICATION: SiO_2 Al_2O_3 H_2O Density:	 53% 43% 0.5% max 2.5 g / cm^3

2.5.1 Treatment Materials

The materials used for the treatment in this study are:

a. Cement

Artificial Portland Cement (APC) type CEM I with strength class 42.5 complying with Algerian Standard NA433-2002 was used. The absolute density and specific surface area of the cement were 3.15 and 3200 cm2/g respectively.

b. Polyethylene Fibers

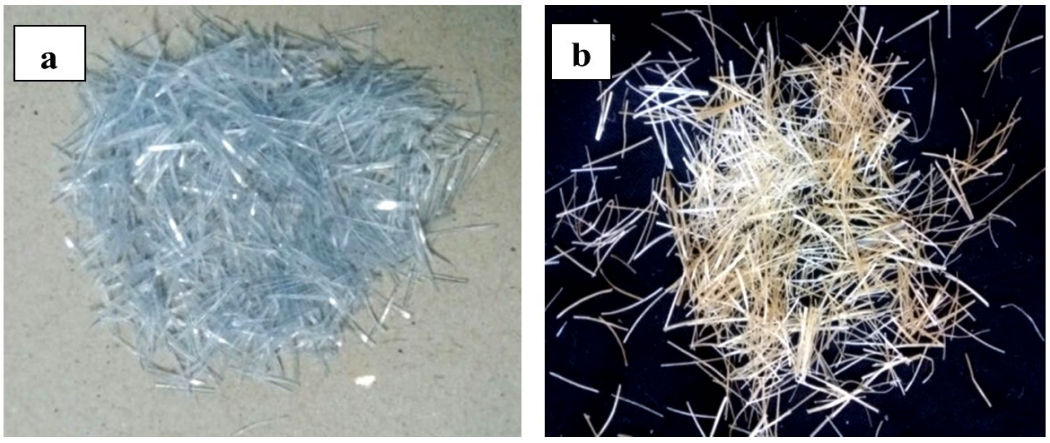

Figure2. Fibers used for reinforcement: (a) Polyethylene fibers, (b) Sisal fibers

Another processing material is Polyethylene fibers (abbreviated PE); it is a recycled material from the plastic bottle. This plastic decomposes completely in nature after hundreds of years (see Fig. 2(a)). Fibers of 5 mm long were used because they gave the minimum collapse potential against fibers of 10 mm and 25mm long.

Sisal Fibers

Sisal, shown in Fig. 2(b), is a natural fiber; the botanical name is sisalan, which produces rigid fibers used in the manufacture of various products. Sisal is biodegradable, so it is environmental friendly fiber based on the results of the previous paper [12], in this study the sisal fiber content used is 0.5% with 5 mm length.

2.2 Equipment

2.2.1 Compacting Device.

The compaction apparatus first designed by Ayadat. (1998) [3], consists of a vertical stem of 150 mm long and 12.2 mm in diameter. It is attached to a horizontal disk of 50.25 mm in diameter and 5 mm thick. A movable disc slides along the vertical stem of 136g, 16.4mm thick and a diameter of 39.2 mm.

2.3 Sample Preparation

Collapse potential increases as the initial water content decreases. In this investigation, the collapse behaviour is assessed with an initial water of 4%.
According to the tests results that investigate the impact of the Kaolinite content on the collapse potential, it was noted that the Kaolinite content of 25% has clearly given maximum collapse potential, as presented in Fig. 3. These findings confirm the observations made by Lawton [13], who stated that the maximum collapse is found with clay content between 10 % and 40 % and are in concordance with results of the investigation undertaken by Nouaouria et al [14] who have indicated that the maximum collapse potential was obtained with an optimal content of about 25% of Kaolinite.
Who have indicated that the maximum collapse potential was obtained with an optimal content of about 25% of Kaolinite.

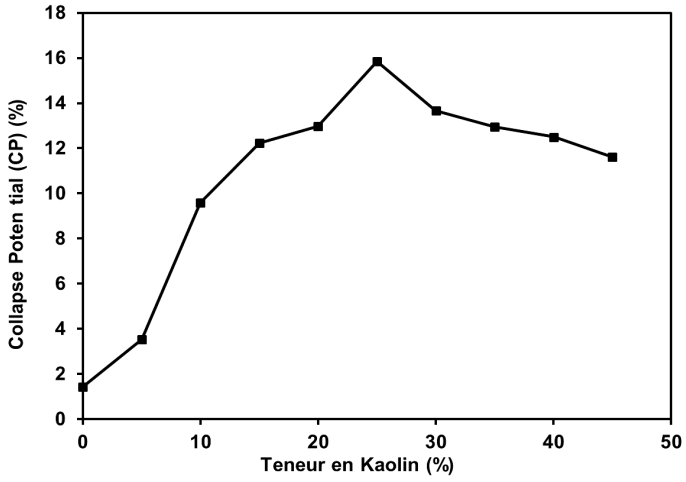

Figure 3. Effect of the kaolinite content on the collapse potential

The reconstituted soil is well mixed with 15% of polyethylene fibers or with 0.5% of sisal fibers of 5mm long both. In the first series of tests, the mixture is placed into Oedometer ring and compacted with different values of compaction energy as illustrated in table 2 in order to examine the effect of compaction. In the second set of specimens, the cement is added into three different contents, namely 1, 2 and 5% to examine the effect of cement on the collapse potential. Finally, a combination is made of cement and compaction energy to assess the influence of these two parameters on the collapse potential.
The hydro-collapse tests were carried out based on the procedure of Jennings and Knight [15]. According to Ayadat [3], the compaction is undertaken using dropping, hollow disk from a constant height of H = 150 mm. This disk slides freely along the vertical rod until it hits the circular base of the device that transmits the shock to the sample.

Direct shear tests were performed for the treated samples. The samples are subjected to different normal pressures (σ= 100, 200, 300 kPa) respectively to obtain the cohesion c and the internal friction angle φ. Two types of samples were tested unsaturated samples and saturated samples in order to investigate their behaviour before and after collapse.

3 Results and Discussions

3.1 Effect of Energy of Compaction on Collapse Potential (CP)

The effect of compaction energy on the collapse potential, of soil treated with polyethylene fibers is shown in Table 2. It is clearly seen that the CP decreases with increasing the number of blows/layer.

$$CP = [\Delta e / 1 + e_o] * 100\ \% \quad (1)$$

Where:
Δe : Change in void ratio resulting from saturation
e_o: initial void ratio

Table 2. Compaction effect on the collapse potential of reinforced soil with fibers

Number of blows/ layer	**5**	**10**	**15**	**20**	**25**
Compaction Energy [KJ/dm^3]	0,065	0,13	0,195	0,261	0,326
CP (%) (Polyethylene Fibers)	9,41	8,67	7,51	6,64	5,34
CP (%)(Sisal Fibers)	12,39	11,73	10,31	9,07	/

The collapse potential is then considered to cause trouble according to Jennings and Knight Classification [15]. The decrease of collapse potential is within the limits of 70% (see Fig. 4). As far as the compaction effect on the collapse potential of sisal fibers reinforced soil is concerned, the results are shown in Fig. 4 and table 2.

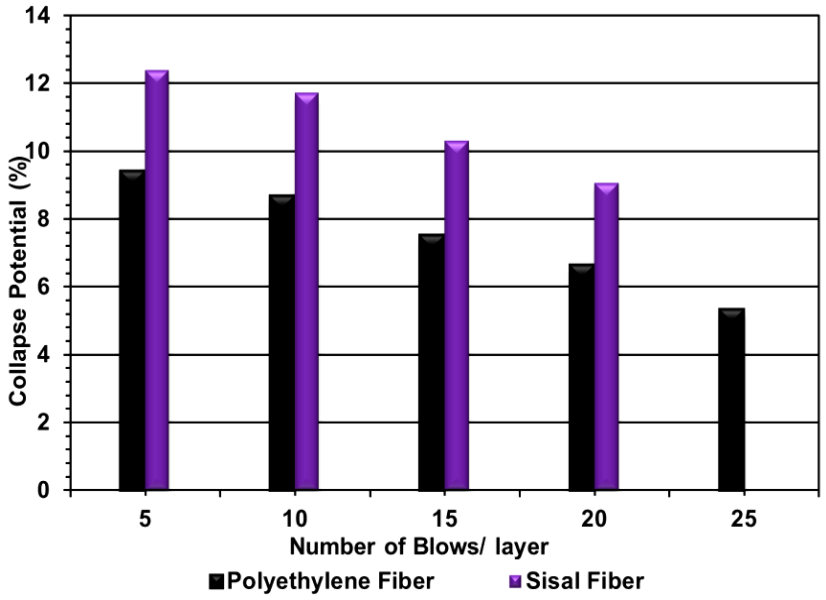

Figure 4. Compaction effect on the collapse potential of polyethylene and sisal fibers reinforced soil

The collapse potential is approximately ranging between 12.39 % and 9.07 %, it can be pointed out that the treatment of soil with sisal fibers content of 0.5% and 5mm long has decreased the collapse potential to 9.07% with a compaction energy corresponding to 20 blows/ layer. Compacted soil at energy of 5 blows/ layer still have an open structure with a relatively high void ratio, facilitating the migration of fine particles from a level to another in the soil sample. Now, compaction with 20 blows/layer makes it dense, and the destruction of intergranular bonds and movement of fine particles become relatively difficult, but the potential collapse is still high (9.07%), according to the Jennings and Knight classification [15], the collapse potential is considered to cause “disorders” to "severe troubles".

3.2 Effect of Cement Content on the Collapse Potential (CP)

To decrease the collapse potential, addition of another agent of treatment is considered, which the Artificial Portland Cement (APC).
To improve the characteristics of the reinforced soil with polyethylene fibers and sisal fibers, an amount of Artificial Portland Cement is added in three different proportions such as: 1, 2 and 5% respectively. The results are illustrated in Fig. 5 and table 3.

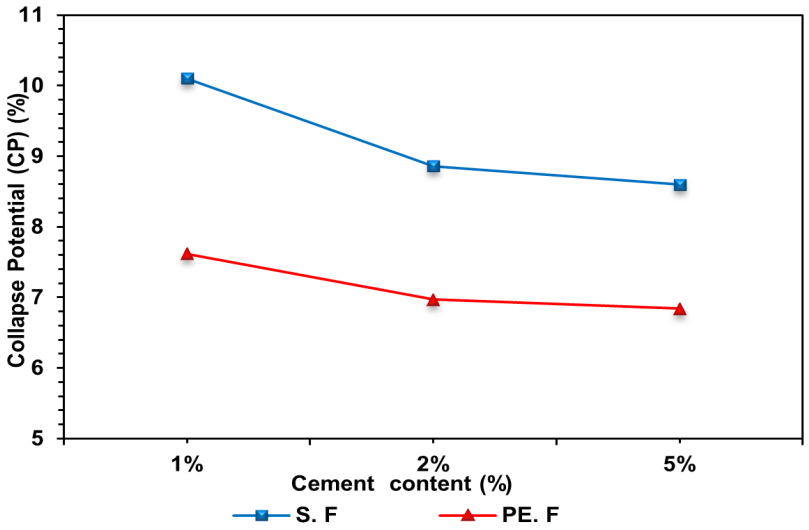

Figure5. Effect of cement content on the collapse potential

Table3. Effect of cement (APC) content on the collapse potential of reinforced soil with fiber

APC (%), 3 B/L	1	2	5
CP [%] (PE. Fiber)	7,62	6.97	6.84
CP [%] (Sisal. Fiber)	10.4	9.52	8.20

In this study, polyethylene fiber content of 15% of 5 mm long, and sisal fiber content of 0.5% of 5 mm long were used. Samples were simply compacted under 3 blows/layer, in two layers. It can be noted that the collapse potential is clearly affected by the added cement content, as illustrate in Fig. 5.

Taking into account table 3 and Fig 5, it is clearly observed that the collapse potential was decreased up to about 60%, but the goal of our study has not been reached yet.
For the soil reinforced with sisal fibers, as illustrate in Fig. 5 and Tables 3, the effect of the cement content on the collapse potential is insignificant; the decrease is about 52%. This reduction did not achieve the goal of getting a non-collapsible soil.
For sisal fibers reinforced soil, the adding of APC content of 5%, has reduced the collapse potential from 17.28% for non-treated soil to 8.20% (Table 3), the reduction is in order of about 53%. It can be seen that the difference between the 2% and 5% cement additions is small, but the study will depend on the value that gave the smallest collapse potential because this difference will be increased when the addition of cement combined with compaction.
This reduction is caused by the effect of cement which prevents destroying intergranular bonds at the time of wetting.

3.3 Effect of Combination of Three Methods of Treatment on the Collapse Potential

Table 4. Effect of blows on the collapse potential of treated soil with polyethylene fibers and APC

Number of blows/ layer	5	10	15	20	25	30	40	50	60
Compacter Energy [KJ/dm3]	0.065	0.13	0.195	0.261	0.326	0.391	0.522	0.652	0.783
CP [%]	6.42	4.37	4.04	3.65	2.88	2.73	2.14	1.96	0,9

Now, the objective of this study is to obtain a CP less than 1%. The soil treated with PE fibers and compacted under 60 blows /layer, has a reduction in CP value of about 94% (CP= 0,9%) (See table 4 and Fig. 6). For sisal fibers content of 0.5% of 5 mm long, and APC content of 5%, the number of blows is increased upto 40 blows/ layer. The obtained collapse potential of 0, 9 % and 0.69% is now considered to cause no problem according to Jennings and Knight classification[15].

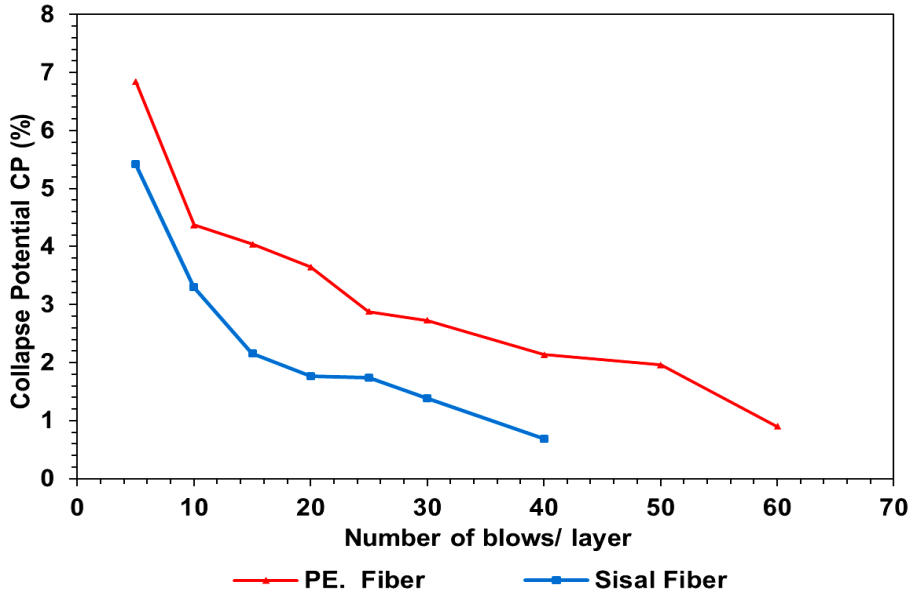

Figure 6. Effect of cement content and compaction energy on the collapse potential of soil reinforced with Polyethylene fibers and sisal fibers

Table 5. Effect of compaction energy on the collapse potential of treated soil with sisal fibers and APC

Number of blows/ layer	5	10	15	20	25	30	40
Compacter Energy[KJ/dm3]	0.065	0.13	0.195	0.261	0.326	0.391	0.522
CP [%]	5,42	3,3	2,16	1.76	1.74	1.39	0.69

The results are indicated in Table 5 and Fig. 6. This reduction is due to the effect of compaction which renders the soil dense and the cement which prevents the destruction of intergranular bonds upon wetting.

Scanning electron microscope is used to determine the morphology characteristics of the mixture of fibers reinforced clayey sand soil and Artificial Portland Cement.
The microstructure examination shows that the sample in both magnifications shows an open structure (see Fig 7).

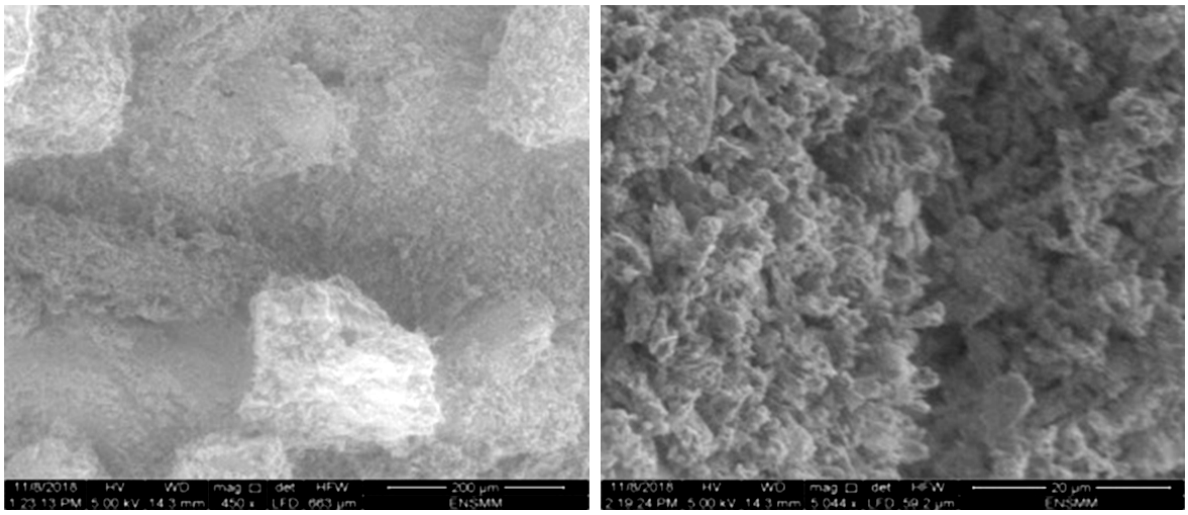

Figure7. Scanning electron micrograph of clayey sand sample showing an open structure of soil particles.

Microstructure of the clayey sand samples and Artificial Portland Cement mixture (5 %) is shown in Fig 8(b) and Fig 9(b). It is indicated that the voids of the mixtures were progressively reduced as a result of reactions between soil particles and cement aggregates.

Comparing Fig. 8(a) with Fig. 8 (b) for polyethylene fiber treatment and comparing also Fig. 9 (a) and Fig. 9(b) for sisal fiber treatment, it can be also seen that the formation of agglomeration where fine particles are bonded to larger ones, as a result of reactions between the cement and the clayey sand material. This is probably caused by a new formation of cementitious material that fills the porous areas within the mixture, leading to an increase in the density of the treated soil and a decrease in the collapse potential [16].

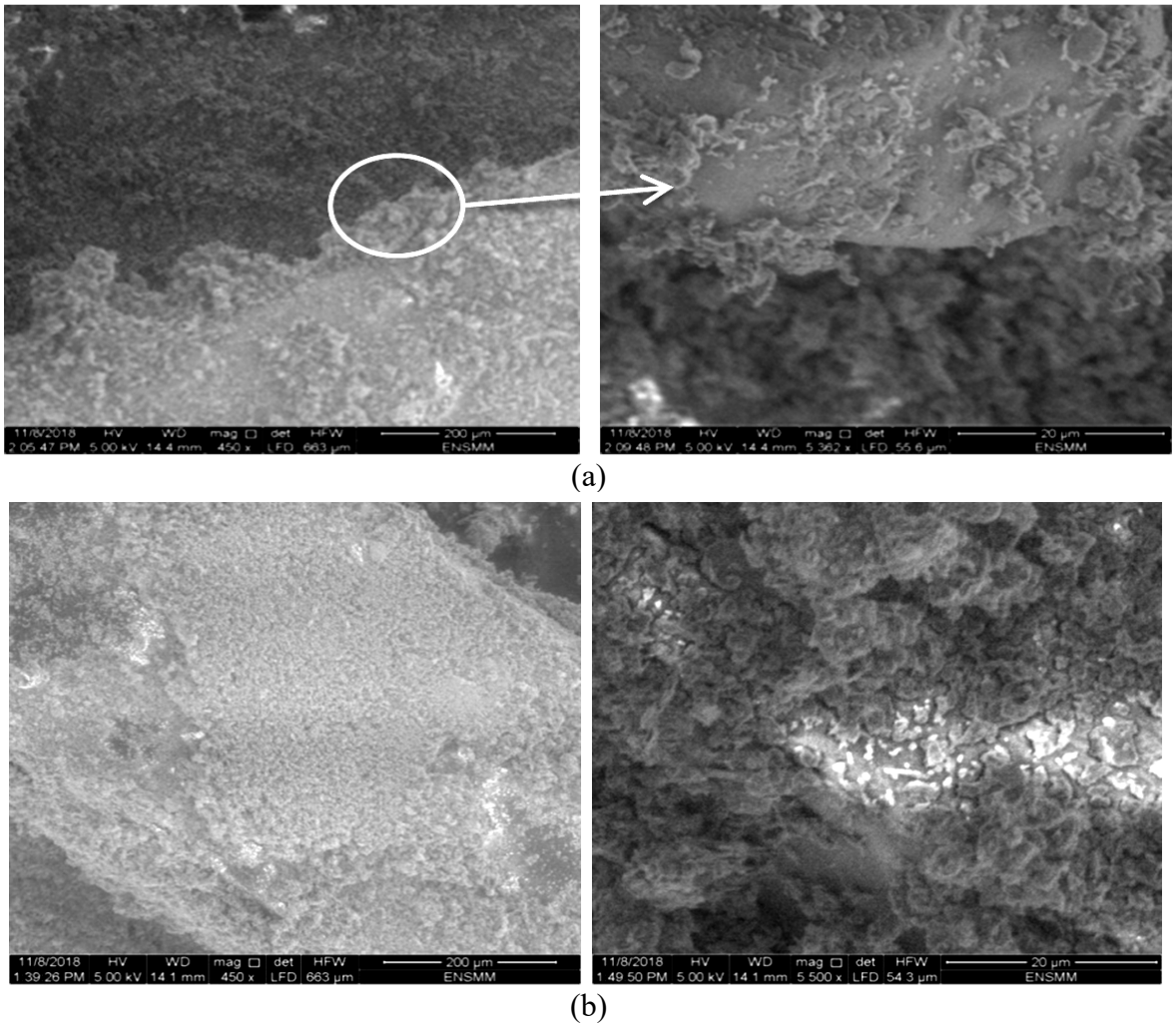

Figure8. SEM micrographs of: (a): polyethylene fibers in the matrix of soil, (b): clayey sand and Artificial Portland Cement mixture (5 %) reinforced with polyethylene fibers.

This is found to be in concordance with what has been outlined by Rashid et al. (2014) [17], who have reported that reactions of calcium ions with silica from sand and alumina from clay, resulted in the formation of pozzolanic products and produced a new soil matrix that is more dense and stable.

According to Fig. 9(a) and Fig. 9(b), some of the small particles adhere to fiber. This phenomenon may be responsible for increasing the stiffness and strength of the mixture samples. Therefore, the 5% cement content is able to effectively establish the stable cementation and the bonds between the different clay particles in comparison with the low cement contents used, where they may be responsible for the lack of bonds. Then, it can be mentioned to propose 5% as an optimal value for the decrease of collapse potential (CP).

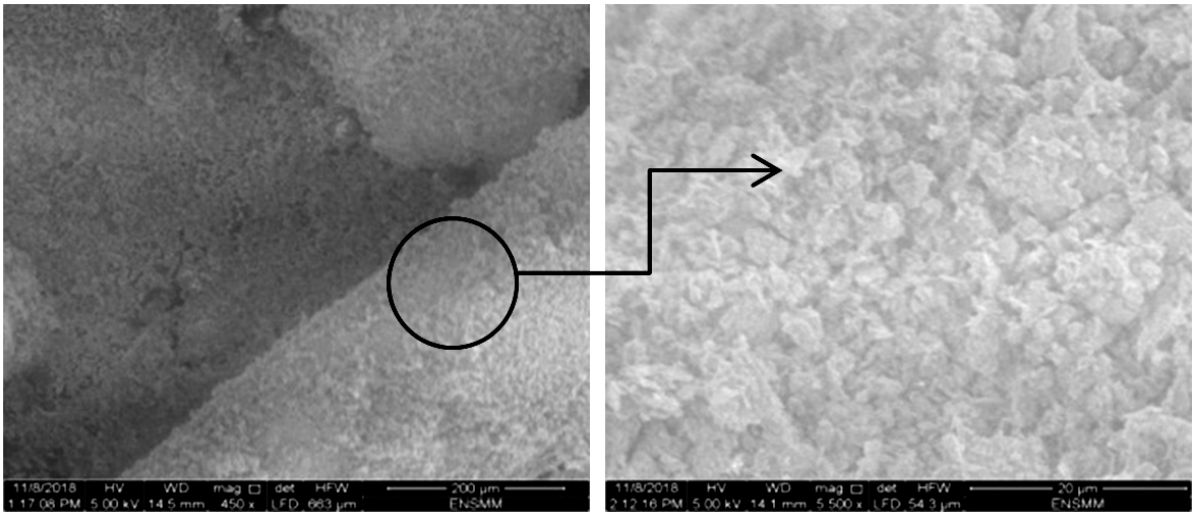

(a)

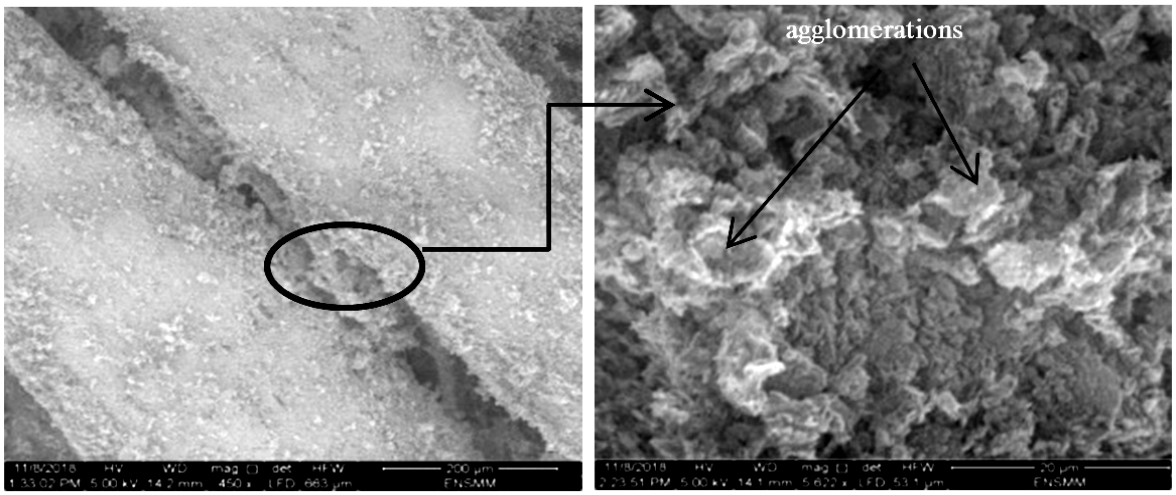

(b)

Figure9. SEM micrographs of: (a) Sisal fibers in the matrix of soil, (b) Clayey sand and Artificial Portland Cement mixture (5 %) reinforced with sisal fibers.

3.4 Shear Strength test

From the direct shear test it was found that there was not a large change in shear stress for untreated soil and treated soil with sisal fibers and polyethylene ones; for unsaturated soil, as shown in Fig. 10(a). After saturation, there was a decrease in shear stress for soil treated with polyethylene fibers and sisal fibers. It is noticed that the decrease of shear stress for soil treated with polyethylene fibers is larger than that in soil treated by sisal fibers (Fig.10 (b)).
The results of the direct shear tests are regroups in Fig.10. It can be seen that all the samples in the unsaturated case have almost the same behaviour with regard to the shear stress, but this stress is slightly higher in treated soils than in untreated soils. Tests on wetted samples show that water reduces shear stress, but this decrease is higher in cement-treated soils and polyethylene fibers. Treated soil with cement and sisal fiber produces the greatest

shear stress, so sisal fibers and cement increase the shear strength of the samples. The soil treated with polyethylene fibers and the cement gives the lowest value of shear strength, this is due to the flexibility of the fibers and their placement parallel to the shear plane.

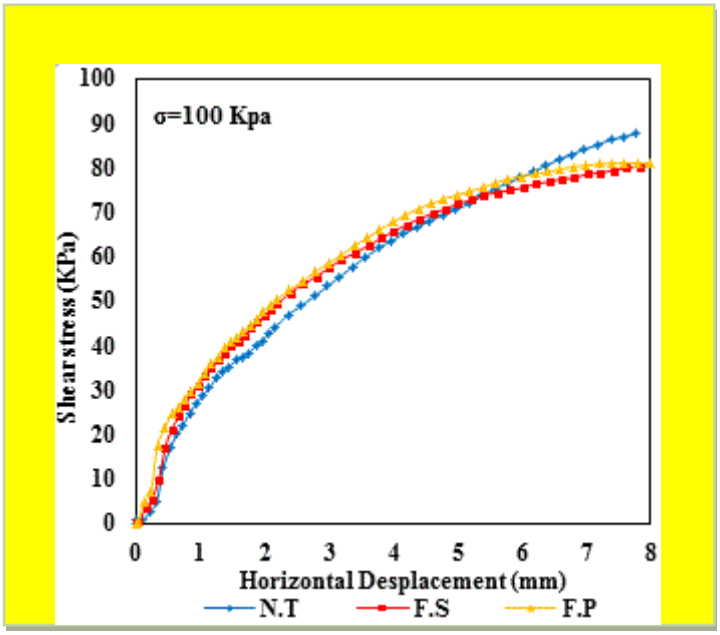

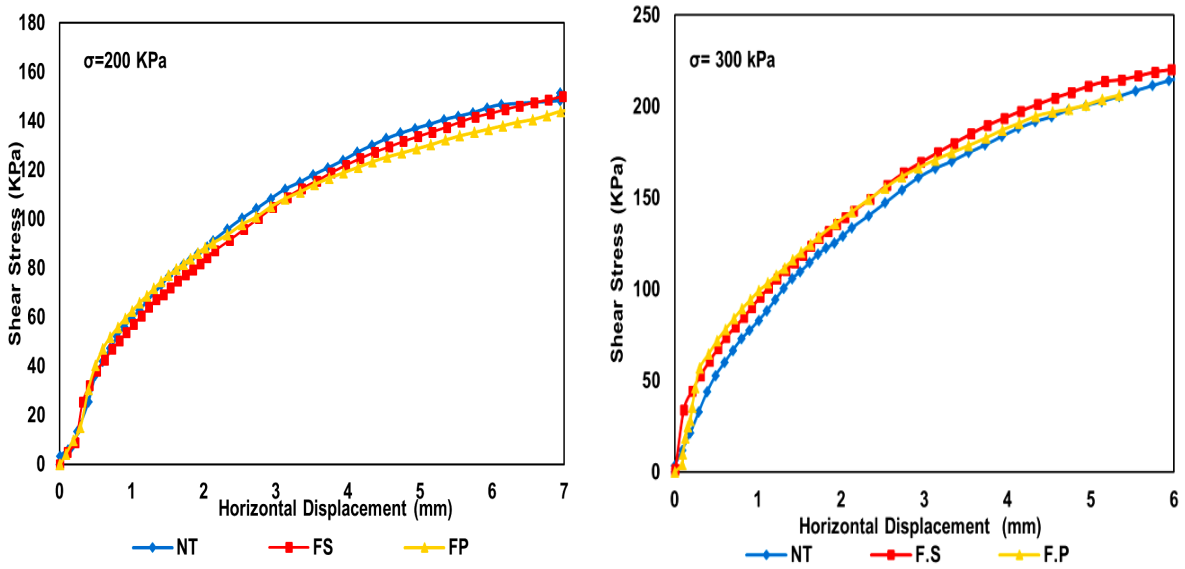

10(a). Before wetting

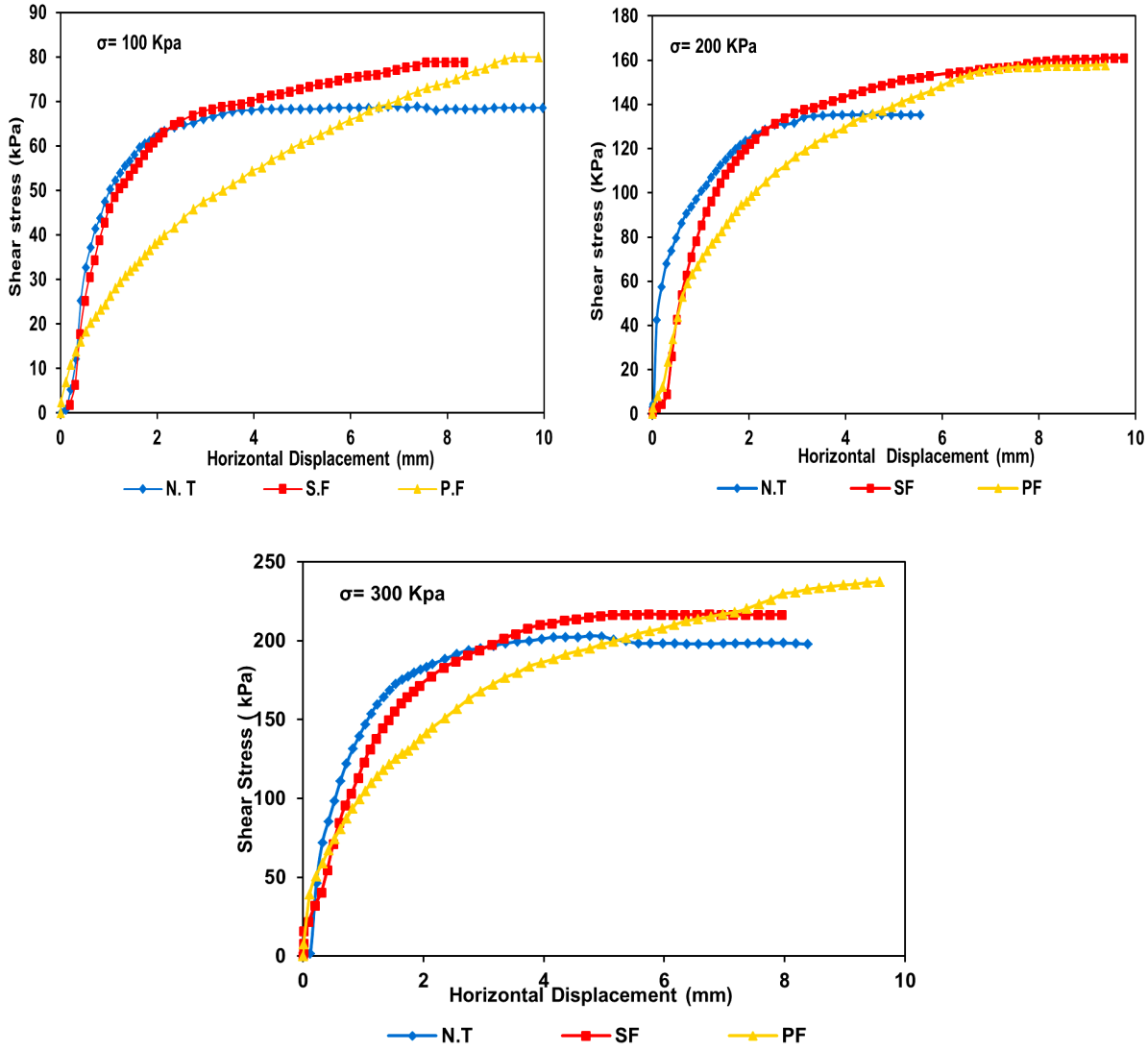

10(b). After wetting

Figure10. Shear strength of cemented soil treated with polyethylene and sisal fibers, (a). Before wetting, (b). After wetting

Table 6. Cohesion C and internal friction angle φ values for all shear testes.

	Non treated soil	Polyethylene Fibers	Sisal Fibers
C[KPa] Before wetting	16,76	3,23	16,76
φ [°]Before wetting	34,67	31,94	37, 87
C [KPa] After wetting	4,72	0,92	11,48
φ [°] After wetting	32,86	38,22	35,41

From Table 6 and Fig. 11, it is noted that the compacted soil and treated with cement and polyethylene fibers has the same behavior as the untreated soil in the unsaturated case and

after wetting there is a reduction in cohesion of about 94% and a small increase of 20% for the internal friction angle. In case of the compacted soil treated with, cement and sisal fiber, after wetting, there is an increase of about 72% in cohesion and a reduction of 6% in the internal friction angle. One of the most important factors affecting the strength of soil is the Bonding between particles [18], it can be said, that in wetting case of samples, the aggregates are more attached to the sisal fibers, which increase the value of the cohesion. In the case of polyethylene fibers, after wetting, there is a reduction of bond between the particles and fibers because of the smooth surface of this type of fiber, but this latter does not allow the movement of fine grains from one level to another. This explains the effectiveness of this type of fiber on the collapse and no influence on the cohesion.

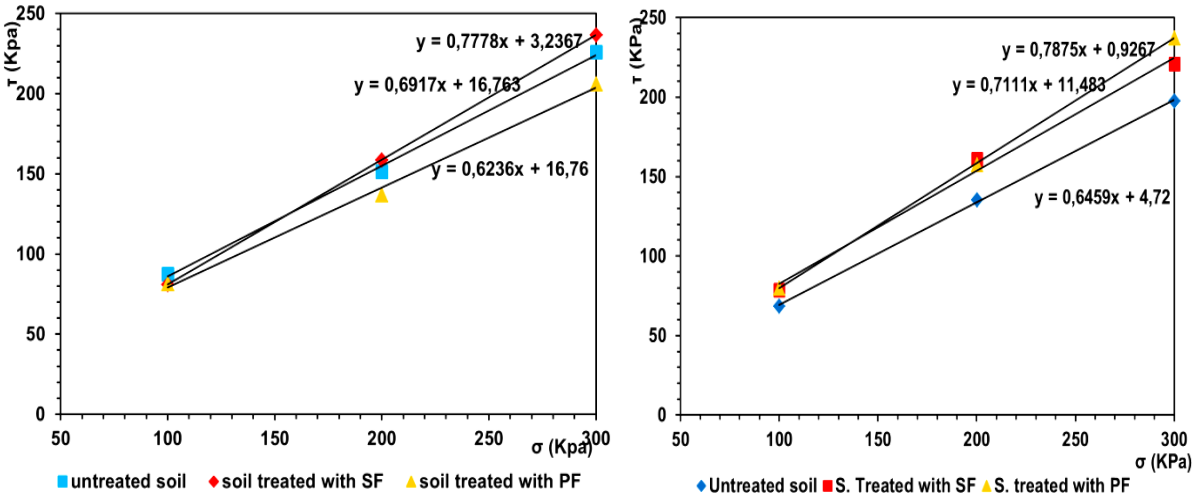

Figure11. Coulomb lines for treated samples

4 Conclusions

To preserve the environment from pollution resulted in the use of water plastic bottles thrown in nature, the polyethylene fibers are in general used rather than sisal fibers because these latter does not harm the environment. Reinforcing a collapsible soil with polyethylene fibers reduced the collapse potential up to 44%. The goal of this investigation is to improve the behaviour of a collapsible soil with the inclusion of sisal fibers and polyethylene fibers and treating this reinforced soil with the addition of cement and compaction technique. The next conclusions can be drawn:

- The combination of the fiber reinforcement of the collapsible soil, and the compaction technique gives interesting results. The collapse potential was decreased up to about 70% for PE fibers and 47.5 % for sisal fibers, but our objective has not yet attained because the collapse potential was still relatively high as indicated in Table2.
- To reduce collapse potential, the given cement content and PE fibers or sisal fibers were mixed with soil. Adding Artificial Portland Cement (APC) mixed with PE fibers reduced CP up to about 60%, and decreased the CP up to about 52% for sisal fibers.

• To have a non-collapsible soil, it is necessary to reduce the CP to a reasonable value. For this instance, the cement and the technique of compaction are combined with the reinforcement by PE fibers. Adding Artificial Portland Cement (APC) with compaction energy of 60 blows /layer decreased the CP to about 95% for PE fibers (CP=0,9%).

• In order to further reduce the collapse potential, the compaction energy applied to the samples is increased, which are prepared by the mixture of clayey sand with sisal fibers and cement. In this case, the value of CP decreased to 0, 69%. As a result, it can be concluded that there is no collapse problem according to the Jennings and Knight classification [15].

• These findings confirm the effectiveness of the compaction, cement, and fibers of sisal or polyethylene on the intrinsic parameters. Furthermore, the cohesion of collapsible soil is much more sensitive to wetting than its friction angle and it is thought to be responsible for the shear strength increase or decrease of the collapsible soil after wetting.

Acknowledgements

The authors wish to thank the LGCH laboratory of the University 8 May 1945 of Guelma where the experimental work was performed.

References

[1] M. Maher, Y. Ho, and H. Pincus, "Behavior of Fiber-Reinforced Cemented Sand Under Static and Cyclic Loads," *Geotech. Test. J.*, vol. 16, no. 3, p. 330, 1993, doi: 10.1520/gtj10054j.

[2] N. C. Consoli, P. D. M. Prietto, and L. A. Ulbrich, "Influence of fiber and cement addition on behavior of sandy soil," *J. Geotech. Geoenvironmental Eng.*, vol. 124, no. 12, pp. 1211–1214, 1998.

[3] T. Ayadat, M. Dahili, and K. M. H. Ahmed, "Traitement d'un sol effondrable par un liant hydrocarboné (bitume)," *Rev. française géotechnique*, no. 85, pp. 57–64, 1998.

[4] T. Yetimoglu and O. Salbas, "A study on shear strength of sands reinforced with randomly distributed discrete fibers," *Geotext. Geomembranes*, vol. 21, no. 2, pp. 103–110, 2003, doi: 10.1016/S0266-1144(03)00003-7.

[5] M. S. Chauhan, S. Mittal, and B. Mohanty, "Performance evaluation of silty sand subgrade reinforced with fly ash and fibre," *Geotext. Geomembranes*, vol. 26, no. 5, pp. 429–435, 2008, doi: 10.1016/j.geotexmem.2008.02.001.

[6] F. Ahmad, F. Bateni, and M. Azmi, "Performance evaluation of silty sand reinforced with fibres," *Geotext. Geomembranes*, vol. 28, no. 1, pp. 93–99, 2010.

[7] A. Al Adili, R. Azzam, G. Spagnoli, and J. Schrader, "Strength of soil reinforced with fiber materials (Papyrus)," *Soil Mech. Found. Eng.*, vol. 48, no. 6, pp. 241–247, 2012, doi: 10.1007/s11204-012-9154-z.

[8] A. Chegenizadeh and P. H. Nikraz, "Study on Sand and paper reinforcement," *Int. J. Emerg. Technol. Adv. Eng.*, vol. 2, no. 6, pp. 199–202, 2012.

[9] N. Cristelo, S. Glendinning, T. Miranda, D. Oliveira, and R. Silva, "Soil stabilisation using alkaline activation of fly ash for self compacting rammed earth construction," *Constr. Build. Mater.*, vol. 36, pp. 727–735, 2012.

[10] M. Zhang, H. Guo, T. El-Korchi, G. Zhang, and M. Tao, "Experimental feasibility study of geopolymer as the next-generation soil stabilizer," *Constr. Build. Mater.*, vol. 47, pp. 1468–1478, 2013, doi: 10.1016/j.conbuildmat.2013.06.017.

[11] E. Botero, A. Ossa, G. Sherwell, and E. Ovando-Shelley, "Stress-strain behavior of a silty soil reinforced with polyethylene terephthalate (PET)," *Geotext. Geomembranes*, vol. 43, no. 4, pp. 363–369, 2015, doi: 10.1016/j.geotexmem.2015.04.003.

[12] S. Adjabi, M. S. Nouaouria, and C. Betehi, "Effect of reinforcement fibers on the collapse potential of clayey sands," in *MATEC Web of Conferences*, 2018, vol. 149, doi: 10.1051/matecconf/201714901034.

[13] E. C. Lawton, R. J. Fragaszy, and M. D. Hetherington, "Review of wetting-induced collapse in compacted soil," *J. Geotech. Eng.*, vol. 118, no. 9, pp. 1376–1394, 1992.

[14] M. S. NOVAOURIA, O. HARIRECHE, and A. ROUAIGUIA, "Comportement de l'affaissement de

loess," *Ann. du bâtiment des Trav. publics*, no. 3, pp. 37–41, 2002.
[15] J. E. Jennings, "A GUIDE TO CONSTRUCTION ON OR WITH MATERIALS EXHIBITING ADDITONAL SETTLEMENT DUE TO COLLAPSE" OF GRAIN STRUCTURE.," 1975.
[16] M. S. Ouf, "Effect of using pozzolanic materials on the properties of Egyptian soils," *Life Sci. J.*, vol. 9, no. 1, pp. 554–560, 2012.
[17] A. S. A. Rashid, R. Kalatehjari, N. M. Noor, H. Yaacob, H. Moayedi, and L. K. Sing, "Relationship between liquidity index and stabilized strength of local subgrade materials in a tropical area," *Measurement*, vol. 55, pp. 231–237, 2014.
[18] B. B. K. Huat, A. A. Aziz, F. H. Ali, and N. A. Azmi, "Effect of wetting on collapsibility and shear strength of tropical residual soils," *Electron. J. Geotech. Eng.*, vol. 13, pp. 1–44, 2008.

DOI: 10.1515/sspjce-2021-0008

Analyzing the leachability of selected heavy metals from cement composites by long-term and cyclic tests

Adriana Eštoková, Jozef Oravec

Technical University of Košice, Slovakia
Faculty of Civil Engineering, Institute of Environmental Engineering
e-mail: adriana.estokova@tuke.sk

Abstract

Using of waste materials and secondary products from other industries in building industry to manufacturing building materials is one way to the sustainability. However, application of various waste requires serious monitoring and investigation of the safety of the new composites. Heavy metals presence and their releasing from the building materials can pose a potential risk to the environment and human health. The paper presents the results of a study of concrete composites with blast furnace granulated slag and special hybrid cement based on secondary mineral admixtures in relation to their heavy metals leachability. Selected metals (Cr, Pb, Ba, Ni, As) have been analysed using long-term tank and cyclic testing. The concretes with slag addition and hybrid cement proved more intensive releasing of analysed metals compared to the reference concrete. The aggressiveness of extracting media was strongly affected not only by pH but by the quantity of the ions presented in the liquids before the experiment as well. Although the leached quantities were not extremely high, results confirmed the need to monitor the building products with the incorporated waste.

Key words: concrete, hexavalent chromium, supplementary cementitious materials, waste materials in concrete, heavy metals, human health risk

1 Introduction

The use of secondary raw materials in construction products is stimulated in most EU countries in terms of recycling, conservation of natural resources and energy savings [1]. The main concern is the protection of the environment (air, water and soil quality) and human health, which requires an assessment of the environmental impact of the application of these composite materials based on cementitious matrices [2]. The use of waste in the production of cement composites may on the one hand improve the primary properties of cement composites and immobilize heavy metals [3], but on the other hand may under certain conditions cause increased leachability of some heavy metals [4].
Schmukat et al. [5] focused on the leaching of metals from various construction materials. The authors conclude that specific surface area measurement is an adequate tool to study the

release of metals from structural materials. Leaching experiments emphasize the influence of the leachate composition on the leachability of metals from construction materials, as evidenced by the significant influence of ionic strength when water structures are the intended end use. Xiaolu [6] focused on the characterization of the leachability of cement pastes containing solid wastes for the purpose of long-term assessment of the environmental load. He points to the important role of the pH at which leaching takes place. Yu et al. [7] studied the leachability of heavy metals from hardened cement mixtures with the addition of various types of fly ash. The amount of leached heavy metals from cement-stabilized fly ash depended strongly on the type of fly ash used. The highest concentrations were detected for the hexavalent chromium. With the addition of finely ground granulated slag, the content of leached hexavalent chromium decreased. Kayhanian et al. have also studied the leachability of metals from asphalt and concrete surface materials [8]. It was found that the ion concentrations of most metals were below the limit, but the presence of chromium was found in the leachate of the concrete sample. According to the study, the leachability of chromium is influenced by the age of the concrete, permeability, temperature, pH value and contact time with the leachate. Krol [9] paid also special attention to the chromium leaching from the concrete composites and studying its mechanisms. Even though, various leaching tests are used in different countries, e.g. Toxicity Characteristic Leaching Procedure (TCLP) in the USA [10], single-stage batch leaching procedure to waste leaching characterisation in EU [11-14] or Dutch tank test NEN 7375 [15], the main attention is focused only on the leaching of waste itself. There is a lack of systematic knowledge and a valid method for predicting the emissions from cement-based building materials with incorporated waste into the environment. The European standard [16] dealing with a study of the characteristic leaching behaviour of hardened concrete for use in the natural environment partially suits for the purposes of assessing the potential risk of concrete materials. The test procedure must be developed as a characteristic test designed to determine the leachability of new building products.

The paper focuses on examination the leachability of selected heavy metals from cement composites with incorporated waste materials by long-term and cyclic tests. The relationships between conductivity, pH and heavy metal concentration in leachates are studied and the leachability of heavy metals and the resistance of analysed cement composites exposed to several media are compared.

2 Material and Methods

2.1 Concrete materials

The following materials were used to prepare samples of cement composites for the experimental study of heavy metal leachability: Portland cement CEM I 42.5N (Považská cementáreň, a.s., Ladce); hybrid cement based on by-products and waste, (Považská cementáreň, a.s., Ladce); an admixture based on finely ground granulated blast furnace slag (Považská cementáreň, a.s., Ladce) serving as a substitute for a part of Portland cement. A total of 6 formulations were proposed for the experimental study of the leachability of heavy metals from cement composites, of which reference formulation without the addition of

additives. The concrete samples with blast furnace granulated slag were marked B1 (65 wt.% of slag); B2 (75 wt.% of slag); B3 (85 wt.% of slag); and B4 (95 wt.% of slag). The reference sample B0 did not contain any slag substitution and the H sample represented concrete with 100% of hybrid cement based on the various mineral waste. The manufactured concrete samples were cut to smaller dimensions of 40 × 40 × 20 mm and these samples were subsequently used for the testing of their leaching performance. Two samples of each formula were tested in the leaching experiments.

2.2 Leaching procedures

Two types of leaching tests, based on the [16], were configured: long-term tank tests under static conditions, and cyclic immersion tests. Different environments were chosen for individual types of tests (long-term and cyclic experiments), since according to literary it was proven that the deterioration of concrete samples is accelerated by alternating between wetting and drying within the cyclic tests. So the aim of the work was not to compare the resistance of samples tested according to the individual type of tests, but the resistance of concrete samples with waste and secondary materials to the particular medium and each other. Prior to the experiment itself, all concrete samples were dried in a laboratory oven at 105 ° C to constant weight.

2.2.1 Long-term tank tests

Long-term tests were performed for a period of 500 days. Based on the sample weights, the leachate volume was calculated to maintain a sample-to-leachate ratio of 1:10. The samples were immersed into liquid media to glass containers with a volume of 720 mL. A pre-calculated volume of the extracting liquid medium was poured into these vessels and then a sample was placed in them. The glass containers were covered with aluminium foil throughout the experiment to prevent evaporation and also the ingress of impurities. The extracting media were not renewed during the experiment, thus the experimental procedure represented static conditions and a steady state of concrete materials.
Three different extracting media were modelled in the study: distilled water (DW) with pH = 7.08 and conductivity of 2.71 $\mu S.cm^{-1}$; natural rainwater (RW) of pH = 6.54 (conductivity C = 99.3 $\mu S.cm^{-1}$); and Britton-Robison solution (BRS) with concentration 0.04M H_3BO_3 + 0.04M CH_3COOH + 0.04M H_3PO_4 (pH = 2.16; C = 2850 $\mu S.cm^{-1}$).
At the indicated intervals (30, 240, 300, and 500 days), the pH and also the conductivity have been measured by Mettler Toledo equipment. At the end of the experiment, liquid media were analysed to determine the concentrations of selected heavy metals by absorption atomic spectrometry (AAS) using equipment SpectrAA-30 (Varian).

2.2.2 Cyclic tests

The concrete samples of the same composition as in the long-term experiments were subjected to a 7-day experimental cycle: they were first immersed in a solution simulating

acid rain (H_2SO_4 + HNO_3 solution, pH = 3.5, C = 97.0 µS.cm^{-1}) for five days and then naturally dried at room temperature for two days. The samples were tested in this way for five consecutive cycles. The experiments were performed at room temperature (approximately 24 ± 1 °C). The constant pH of 3.5 was kept in the liquid media during the experiment. At the beginning of each experiment, the pH of the extracts was monitored once an hour and adjusted to the initial values every day with a 6 M solution of HNO_3 using a pH meter (Toledo Mettler). The conductivity of solutions and the concentrations of selected heavy metals was analysed by spectrometric analysis on DR 2800 (Hach Lange, Germany).

3 Results and discussion

3.1 Long-term tests

3.1.1 Concentrations of heavy metals due to long-term exposition

The concentrations of the measured extracted heavy metals in the individual extraction media after the 500-day leaching interval are presented in Figures 1-5.

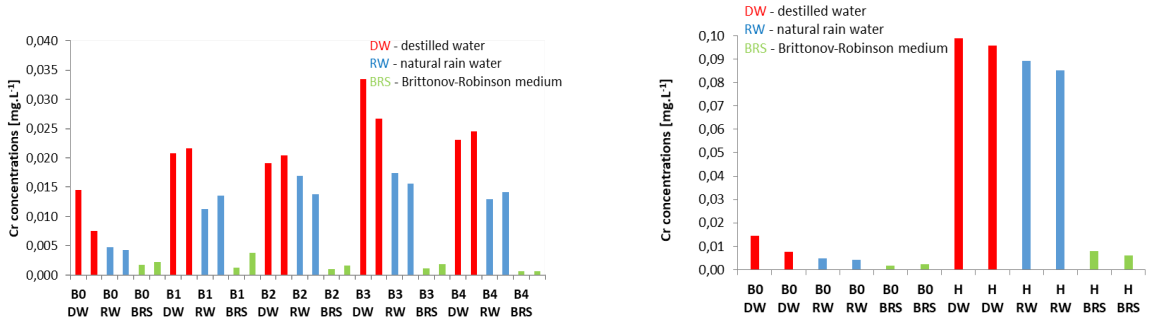

a) b)

Figure 1: Leached-out amounts of chromium per individual concrete samples a) with granulated slag; b) with hybrid cement

As can be seen in Figure 1, the concentrations of chromium ions extracted from slag-based and hybrid cement-based concrete samples immersed in distilled water are up to 8.8-fold higher than for reference samples in the same leachate; in rainwater 17.4 times higher than the reference samples in the same leachate; in Britton-Robinson solution 3.5-fold higher than the reference samples in the same leachate. From the point of view of the aggressiveness of the leachate, distilled water appears to be the strongest leachate, rainwater to be the weaker leachate and the Britton-Robinson solution to appear to be the weakest leachate. This seems surprising at first sight, as distilled water had the highest pH and several authors report a significant effect of pH on metal leaching [6]. This is true, but primarily when comparing

solutions of the same composition but with different acidity [17]. In our case the more important role likely played the quantity of the already presented ions in extraction media and stated equilibrium in ion concentrations. When comparing the conductivity of the extraction media, the values increased in order DW < RW < BRS. This could partially explain the worse leachability of solid chromium-based compounds from the concretes in the more acidic media. Another reason for the lower concentrations of chromium in the more acidic solutions could be based on the observation, that chromium was initially leached from the samples into Britton-Robinson solution was subsequently incorporated into the precipitates formed on the surface of the samples. The highest chromium leached-out quantities have been observed for the H samples followed by B3 samples.

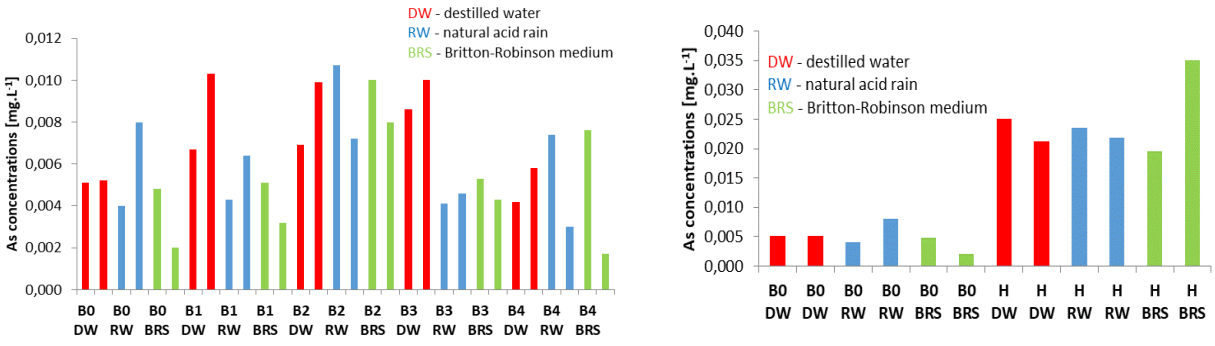

a) b)

Figure 2: Leached-out amounts of arsenic per individual concrete samples a) with granulated slag; b) with hybrid cement

As can be seen in Figure 2, a larger amount of arsenic ions was leached from the concrete samples with ground slag as a substitute for the Portland cement than from the reference samples. The leachability of arsenic ions from samples with hybrid cement was approximately five times higher than from reference samples.

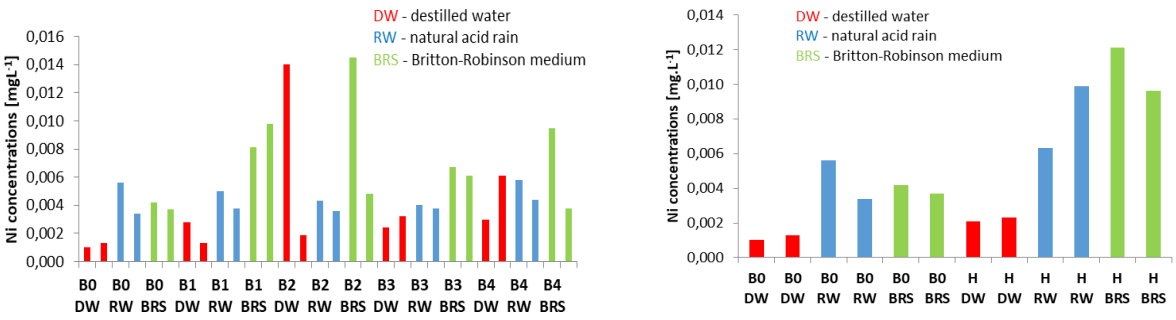

a) b)

Figure 3: Leached-out amounts of nickel per individual concrete samples a) with granulated

slag; b) with hybrid cement

The lowest leachability of nickel ions was observed in the reference samples (Figure 3), the largest in B2 samples with 75% slag addition. When comparing the leachability of nickel ions from slag-based samples and hybrid cement-samples (Figure 3) separately in individual environments, it is clear that from the samples with hybrid cement, a larger amount of nickel ions was leached in each case.

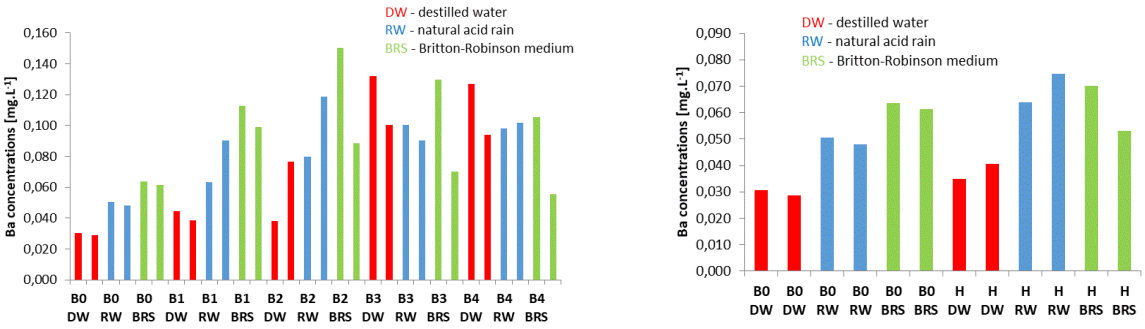

a) b)

Figure 4: Leached-out amounts of barium per individual concrete samples a) with granulated slag; b) with hybrid cement

From the point of view of leachability of barium, the reference sample was again the most resistant and, conversely, the samples with the slag were the least resistant (Figure 4). It should be noted that the barium ions dissolved in the leachate react very rapidly even with a minimal amount of sulphate ions leached from the cement matrix, forming a precipitate of almost insoluble barium sulphate. The concentrations of barium ions in the extracts from the hybrid cement samples are only slightly higher compared to the concentrations of the reference samples (Figure 4).

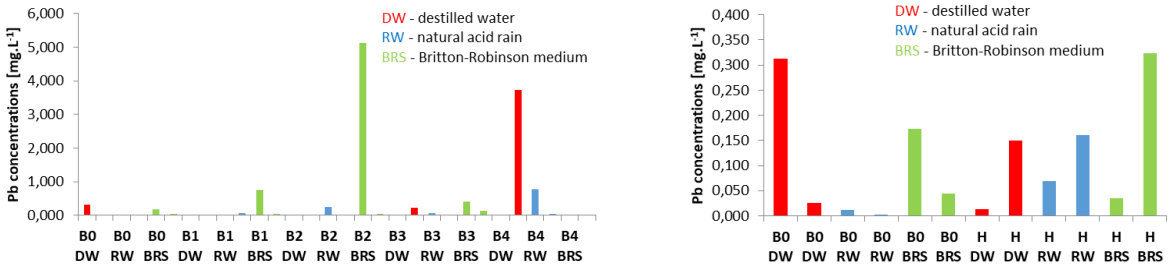

a) b)

Figure 5: Leached-out amounts of lead per individual concrete samples a) with granulated slag; b) with hybrid cement

When evaluating the results of measuring the concentrations of lead ions in extracts from reference samples, samples with slag and hybrid cement (Figure 5), no dependence on the composition of the samples or the environment was observed. In the case of sample B2 in Britton-Robinson solution, a value of 5.118 $mg.L^{-1}$ was measured, while according to the American method "EPA Test Method 1311 - TCLP, Toxicity Characteristic Leaching Procedure" the limit value for lead content is 5 $mg.L^{-1}$ and exceeding this value is considered waste as hazardous.

3.1.2 pH changes in liquid media

At the beginning of the experiment, the pH of distilled water (7.08) was measured before immersing the samples in various leachers; rainwater (6.54) and Britton-Robinson solution (2.16). The most significant increase in pH values was recorded within 30 days from the beginning of the experiment, which was caused by the leaching of hydroxide ions from the matrix into the leachate (Figure 6). After 240 days, the dispersion of pH values narrowed from 7.65 for sample B2 in Britton-Robinson solution to 8.83 for sample B0 in rainwater. After 300 days, the dispersion of the pH values narrowed even further, from 7.95 for sample B4 in distilled water to 8.79 for sample B0 in rainwater. The narrowest variance of pH values was recorded after 500 days, ranging from 8.61 for sample B4 in rainwater to 9.18 for sample B0 in the same medium.

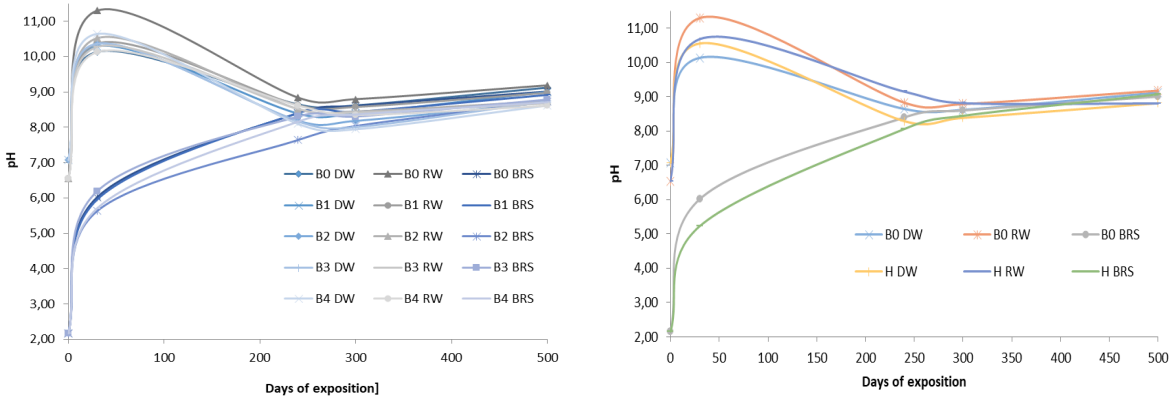

a) b)

Figure 6: Trends in pH in solutions of concrete samples a) with granulated slag; b) with hybrid cement

3.1.3 Changes in conductivity of liquid media

When monitoring the changes in the conductivity of the extracts from the hybrid cement samples compared to the conductivity of the extracts from the reference sample, an enormous difference in the conductivity values was found (Figure 7). The conductivity value of the extract of the H samples in distilled water after 500 days was 4.54 times higher than that of the reference sample in the same medium; the H samples in rainwater 4.43 times higher than the reference sample in the same medium and the H samples in Britton-Robinson solution

4.61 times higher than the reference sample in the same medium.

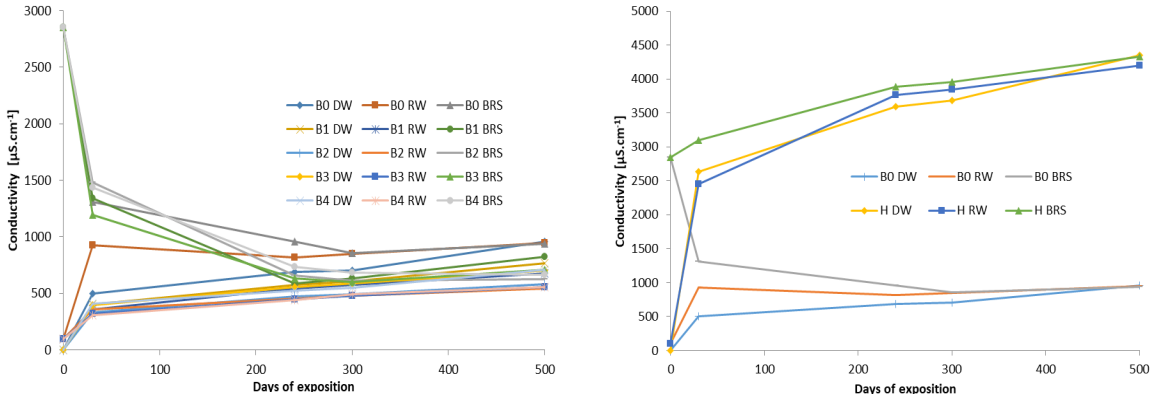

a) b)

Figure 7: Trends in conductivity of solutions of concrete samples a) with granulated slag; b) with hybrid cement

3.2 Cyclic tests

Chromium leaching was chosen as indicative testing for the analysed concrete samples using the cyclic tests. In the environment simulating acid rain, a significant part of hexavalent chromium Cr(VI) was leached already in the first days of the experiment, as can be seen in Figure 8.

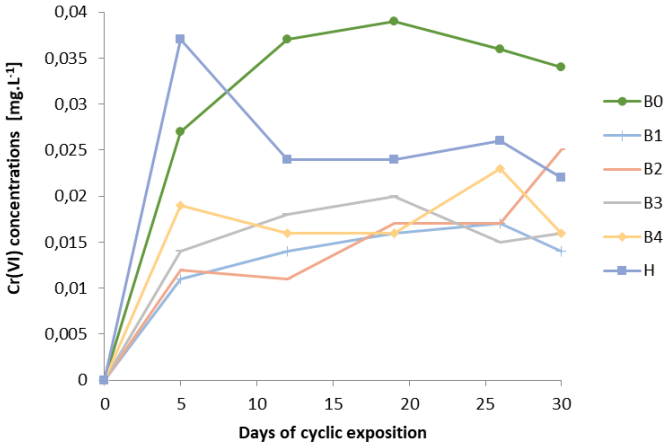

Figure 8: Leached amounts of hexavalent chromium in the cyclic experiment from concrete samples with granulated slag (B1-B4) and with hybrid cement (H)

The least resistant sample for Cr(VI) leaching was the B0 sample. The course of the curve of the sample with hybrid cement was different in comparison with the course of the other curves, while after five days the concentration of Cr(VI) reached the highest value among all samples. The lowest values of Cr(VI) concentrations were reached by the extract from the B1

sample with the lowest slag content. The leachability coefficients LC [$\mu g.h^{-1}.m^{-2}$] in simulated acid rain was calculated per each analysed concrete sample and the comparison of the values of the coefficients is given in Figure 9.

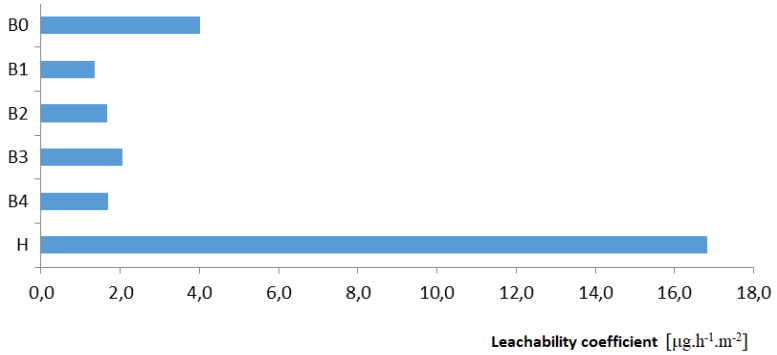

Figure 9: Comparison of the LC per the individual samples

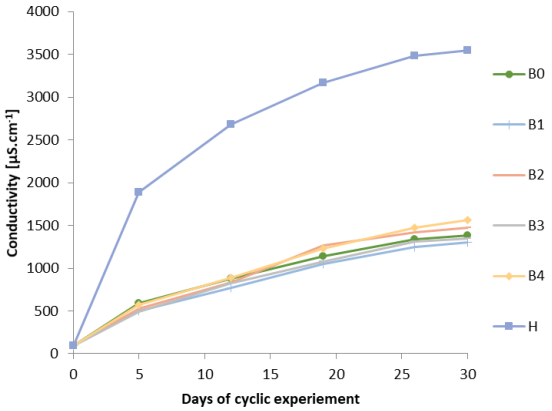

Figure 10: Trends in conductivity of the concrete samples with granulated slag (B1-B4) and hybrid cement (H) in the cyclic experiment

The conductivity of all extracts increased over time. The extracts from the samples with the admixture of blast furnace ground slag had very similar conductivity values and the course of the curves of the conductivity of the extracts from time was also very similar. Significantly different conductivity values were recorded for the hybrid cement sample. This means that more intensive leaching was proven in case of the hybrid cement concrete, probably not connected only to heavy metals leaching but also to the deterioration processes of cement matrix as reported in [18,19].

4 Conclusion

From an experimental study of the leachability of heavy metals from cement composites in various environments, it appears to be the most aggressive environment simulating acid rain, whose e.g. leachability of hexavalent chromium was several times higher than the coefficients

for other environments. Distilled water and natural acid rain appeared to be less aggressive environments. The least aggressive environment appears to be Britton-Robinson's solution, although in fact metals were leached-out in this medium, but precipitated back from the solution in the form of precipitates on the samples´ surfaces.
The concretes with the addition of ground slag were found to be more resistant than the concretes with hybrid cement. However, much more heavy metals were leached in the individual environments from all concretes containing waste and secondary materials than from concretes without waste. Although the concentrations of heavy metals in leachates were often low, it should be borne in mind that the negative impact of heavy metals on human health and the environment is marked even at very low concentrations.

Acknowledgment

The research was supported by VEGA grant, project No. 1/0230/21.

References

[1] Camilleri, MA. 2020. European environment policy for the circular economy: Implications for business and industry stakeholders. *Sustainable Development, 28,* 1804–1812. DOI: 10.1002/sd.2113M
[2] Hohberg, I. et al. 2020. Development of a Leaching Protocol for Concrete. *Studies in Environmental Science, 71(2-3)*, 217–228. DOI: 10.1016/S0166-1116(97)80205-1
[3] Ravindra, KD. et al. 2018. *8 - Environmental Assessment*, *Sustainable Construction Materials* Editor(s): Ravindra K. Dhir, Jorge de Brito, Ciarán J. Lynn, Rui V. Silva, Woodhead Publishing, 2018, 277–330, ISBN 9780081009970.
[4] Lu H. et al. 2016. Leaching of metals from cement under simulated environmental conditions. *Journal of Environmental Management, 169,* 319–327.
[5] Schmukat, A. et al. 2012. Leaching of metal(loid)s from a construction material: Influence of the particle size, specific surface area and ionic strength. *Journal of Hazardous Materials, 227,* 257–264. DOI: 10.1016/j.jhazmat.2012.05.045.
[6] Xiaolu, Y. 2018. Leaching Behavior of Heavy Metals from Cement Pastes Containing Solid Wastes. IOP Conf. Ser.: Earth Environ. Sci.186 012043. DOI: 10.1088/1755-1315/186/3/012043
[7] Yu, Q. et al. 2005. The leachability of heavy metals in hardened fly ash cement and cement-solidified fly ash. *Cement and Concrete Research, 35,* 1056–1063. DOI: 10.1016/j.cemconres.2004.03.031.
[8] Kayhanian, M. 2009. Leachability of dissolved chromium in asphalt and concrete surfacing materials. *Journal of Environmental Management, 90,* 3574–3580. DOI: 10.1016/j.jenvman.2009.06.011.
[9] Król, A. 2020. Mechanisms Accompanying Chromium Release from Concrete. *Materials (Basel, Switzerland)*, *13*(8), 1891. DOI: 10.3390/ma13081891
[10] EPA TEST METHOD 1311 – TCLP, Toxicity Characteristic Leaching Procedure: 1992.
[11] EN 12457-2:2002 Characterisation of waste - Leaching - Compliance test for leaching of granular waste materials and sludges - Part 2: One stage batch test at a liquid to solid ratio of 10 l/kg for materials with particle size below 4 mm (without or with size reduction).
[12] CEN/TS 15862:2012 Characterisation of waste - Compliance leaching test - One stage batch leaching test for monoliths at fixed liquid to surface area ratio (L/A) for test portions with fixed minimum dimensions.
[13] CEN EN 14405:2017 Characterization of waste - Leaching behaviour test - Up-flow percolation test (under specified conditions).
[14] CEN EN 14429:2015 Characterization of waste - Leaching behaviour test - Influence of pH on leaching with initial acid/base addition.
[15] NEN 7375: 2004 Leaching characteristics - determination of the leaching of inorganic components from moulded or monolithic materials with a diffusion test - solid earthy and stony materials.
[16] CEN/TR 16142:2011. Concrete – A study of the characteristic leaching behaviour of hardened concrete for

use in the natural environment.

[17] Fan, YF. et al. 2010. Deterioration of compressive property of concrete under simulated acid rain environment. *Construction and Building Materials, 24,* 1975–1983.

[18] Chen, R. et al. 2017. Degradation mechanism of CA mortar in CRTS I slab ballastless railway track in the Southwest acid rain region of China – Materials analysis. *Construction and Building Materials, 149,* 921–933.

[19] X. Zeng et al. 2018. Deterioration mechanism of CA mortar due to simulated acid rain. *Construction and Building Materials, 168,* 1008–1015.

DOI: 10.1515/sspjce-2021-0009

Analysis of CO_2 emissions in municipality Most pri Bratislave

Miroslav Garaj[1], Martina Zeleňáková[1]

[1]Technical University of Košice, Faculty of Civil Engineering, Institute of Environmental Engineering
e-mail: miro@dimatz.com, martina.zelenakova@tuke.sk

Abstract

The most discussed topics in the 21st century at the global level include climate change, carbon neutrality, digitization and globalization. They have impact on the lives of all people, the quality of the environment in which we live, the health of the whole population, the development of cities and urban areas, the development and direction of industry and its new technologies, and last but not least, they shape humanity to which they are giving direction. Regional self-governments, as elementary elements of the state, therefore play a key role in achieving the EU's environmental and climate change goals and objectives. The issue of digitization is changing human approaches to address global challenges, including the call for a proper assessment of the impacts of climate change on urban and suburban areas as a tool for identifying and subsequently integrating early actions. Digital technologies and their potential can make a huge contribution to sustainable development, and to re-addressing global challenges. According to the OECD, in an era of digitization, climate change and ageing, it is important to see cities as engines for economic growth.

Key words: climate change, carbon neutrality, new technologies, urban zones, digitization, global challenge

1 Introduction

Climate change in our Central European region also brings with it a change in the thinking of the individual setting of each of us. As humanity, we are in the process of climate change affecting the quality of our lives in urban and sub-urban areas. The steps we take together today to stop and avert this process will only be felt in the generations coming after us. Due to climate change, we can already feel fluctuations in extreme weather, less rainfall during the summer and subsequent torrential rains in the continental Central European region, where Slovakia is located, which brings with it an increased risk of floods [1]. Deforestation is also a major problem, with an increased risk of forest fires, the migration of forest species to lower areas, the loss of native biodiversity, a smaller area of agricultural land as well as the loss of originally grown agricultural products. Another important topic is the extremely high temperature of our urban zones, which brings with it a directly proportional increase in energy consumption for cooling households with air conditioning, higher energy consumption and higher household expenses. In the last two decades, we have experienced the 18 warmest years since the beginning of measurements, and extremes of weather such as forest fires, heat

and floods are increasingly occurring in Europe and around the world [2]. Europe's forests are ageing and more and more trees are unable to absorb carbon dioxide emissions [3]. All these indicators represent a global challenge, to which we must also respond globally, but in response we can also work individually. In December 2019, EU leaders endorsed the objective of achieving a climate-neutral EU by 2050 [4]. Slovakia must also adapt and honour its commitment to implementing the agreement and setting out a long-term strategy in a socially just and cost-effective way. This background document is a commitment for all of us, and for me personally it is key to further explicitly defining indicators by sector, and by volume of CO_2 production. In terms of the urban zone, six sectoral producers and their subsectors predominate, with which we work further.

Figure 1: Sectoral breakdown of CO_2 producers taken into account

2 Study area and data

2.1 Study area

According to the Statistical Office, 54% of the Slovak population lives in towns, only 46% in the countryside (2018). The share of the urban population has even fallen slightly over the last 20 years – by 3 percentage points [5]. Municipalities are basic territorial-self-governing units of public administration. Due to the statistical recalculation of the total population of municipalities, which currently represents approximately 2.5 million. population living in the countryside and the growing trend of urbanization, I decided to choose a village near a large residential conglomeration. The benchmark village is called Most pri Bratislave, located in Western Slovakia, only 3 kilometers from Bratislava. The village with an area of 19.01 km^2, is located in the Danubian Lowlands in the north-west part of the Žitný ostrov on the river Little Danube and consists of two cadastral areas: Most pri Bratislave and Studené /48°08'32" and 17°16'19"/. The village Most is currently experiencing a large construction progress and thanks to the relatively short distance and excellent accessibility to the Capital City, the small provincial village is becoming a satellite town with a current population of 3,716.
The economic structure of the inhabitants of the village and low unemployment rate result in a significant migration of inhabitants to the nearby Capital City, respectively neighbouring towns Senec, Šamorín, and Dunajská Streda. Also, the strategic position of the mentioned village on the secondary road number 572, provides conditions for the migration of the population for employment purposes and so the daily frequency of cars is at the level of 6 to 7 thousand cars per day, which is why the transport sector was evaluated as one of the main producers of CO_2.

2.2 Input data

An important key aspect for the processing and correct calculation of the volume of CO_2 production for the benchmark village is to obtain data from publicly available sources, or from the municipality itself, based on which we can take into account several aspects in the

recalculation itself. The most important input data to be taken into account is the combination of geographical, demographic and geo-spatial dataset of information. By combining and taking into account these three factors, and by their subsequent analysis, we can move to and reach the most accurate measurable result of production.

In terms of geomorphological predisposition, the village is mostly flat, formed by agricultural land, surrounded by the Little Danube in the north of the territory, in the protected water management area Žitný ostrov. In terms of the location, Most pri Bratislave is part of a warm climate area, which belongs to the group endangered by the warmest climate, while the average annual temperature is around 10.4°C. Its location within the micro-region results in the flow of warm air from the Danubian Lowland, and therefore the village has an average of up to 70 summer days. Demography is a basic factor determining the state and development of society. There are two ways in which population trends manifest themselves: one is the demographic decline of the population, the other is the growing migratory pressures, which we cannot be avoided by society. Demographic development is one of the main determinants determining the volume of traffic both in individual regions and in the whole territory of the Slovak Republic. The analysis of the demographic structure of the population was crucial to fill the statistics on pre-productive, productive and post-productive age, as each category of the population is characterized by a different form of transport. It is also directly proportional to the fact that they take into account their habits, the form and manner of human interaction with the environment, especially the causes and consequences of the distribution of human activity in the studied area. The methodology applied uses, as a relevant basis for further calculation, digital data processed and prepared for further classification and division according to types into various maps, based on sectoral division with relevant conversion to square meters, cubic meters, distances, spacings, traffic frequency or traffic signs such, such as street lighting, high voltage poles, or transmitters and others.

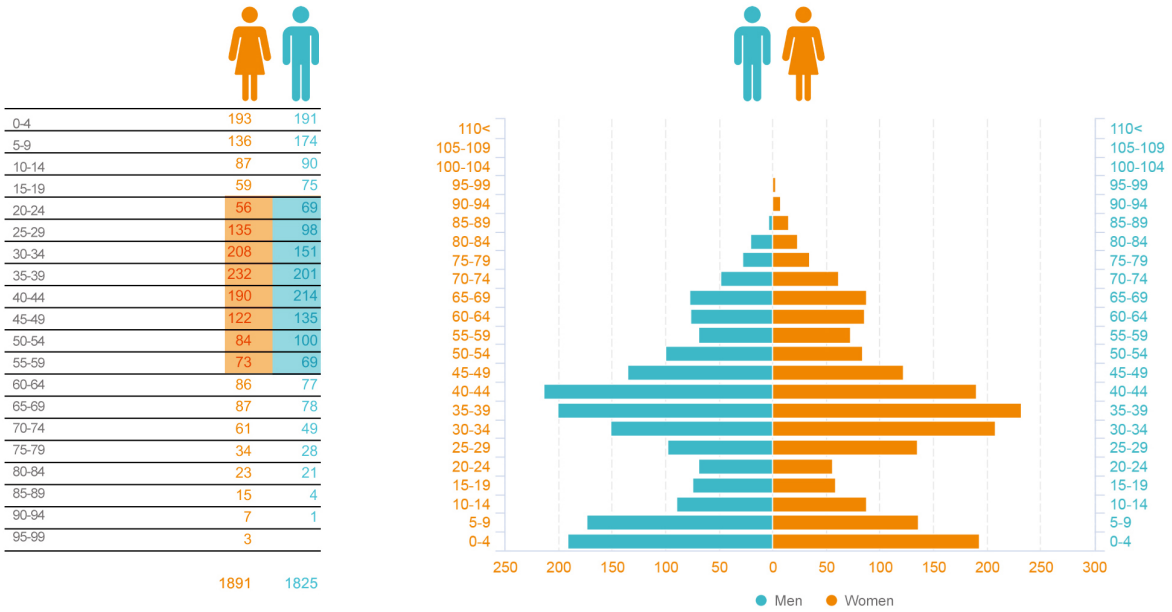

Figure 2: Productivity statistics of the inhabitants in the village / Age structure of the population

Other factors that affect air pollution and its temperature are the nature of the earth's surface,

especially its geographical configuration – mountains, plains, valleys, rivers and lakes, etc. Geographical factor as well as uneven terrain cause swirling of the flowing air, which we also call mechanical turbulence. This phenomenon affects the transport and dispersion of harmful substances in the air as well as their sedimentation. Mechanical turbulence can also be seen in cities, where due to tall buildings the air flow is much more complicated than in nature and in

open spaces. By comparing the balance of individual aspects and geo-spatial mathematical arrangement of the map data of the cadastral area of Most pri Bratislave on the basis of distribution by national sectors, we reached the stage of recalculation of production volume, which was not a completely explicit value, as it was limiting redistribution based on sector diversification.

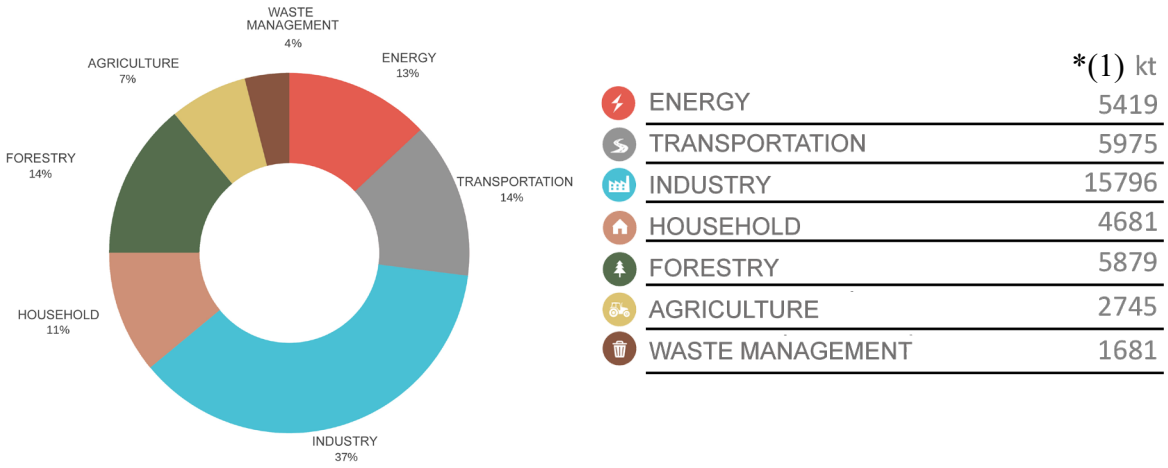

	*(1) kt
ENERGY	5419
TRANSPORTATION	5975
INDUSTRY	15796
HOUSEHOLD	4681
FORESTRY	5879
AGRICULTURE	2745
WASTE MANAGEMENT	1681

Figure 3: Overview of Slovak sectors graphically and in tables

*(1) – kiloton (unit of weight)

This process of application of seven sectors demonstrably does not correspond to the urban creative arrangement of villages and towns, but serves as a very fast and comprehensive identification of the volume of CO_2 production.

The advantage of this methodology is fast applicability, information from publicly available sources, universal and functional, easily combinable data with other indicators such as geographical and demographic aspects, which specifies this error rate and thus approaches the real number of production volume. The level of detail and error rate of such a recalculation and the whole process can be denoted as LOD 1 (Level of detail No. 1), which is typical for simple volume information.

Waste Management

Waste management is a set of activities aimed at preventing and reducing the generation of waste and reducing its danger to the environment and at waste disposal in accordance with Act No. 79/2015 Coll. on waste and on amendments to certain other acts, as amended (hereinafter referred to as the "Act"). In 2019, the inhabitants of Slovakia produced a total of 2.37 million tons of municipal waste. In terms of per capita, this means that in 2018 the average citizen threw 435 kg of municipal waste into waste bins. Approximately 1.2 kilograms per day [6].

Agriculture

Agriculture is one of the sectors of the national economy, whose main task is to ensure the nutrition of the population. These include human activities aimed at the production of food and feed or other agricultural products. Although agriculture accounts for only 3.4% of the world economy, it contributes to global warming directly by up to 17% and indirectly by another 7 to 14 percent [7].

Forestry

Forestry is a professional activity focused on forest cultivation, forest protection and other activities necessary to ensure the functions of forests. It is part of the national economy. The current increase in harvesting opportunities and the resulting increase in wood harvesting is mainly related to the development and current state of the age composition of forests [8]. Due to its gradual change, there should be a decrease in total timber production after 2030. Gradually, the area of age levels of forest stands will begin to decrease, which will eventually come to the restoration below the specified normal, which will also reduce their wood harvesting potential in favour of pre-cutting – raised forest stands.

Households

The term household means the coexistence of several natural persons. According to Section 115 of the Civil Code, a household consists of two or more natural persons living together permanently (not occasionally, or in the form of visits only), and at the same time pay the costs of their needs together (e.g., food, rent, etc.). Both conditions must be met cumulatively. Households are currently, with their standards, a large producer of CO_2 in urban areas with a huge impact outside the region.

Industry

The sector of manufacture and industry, referred to as the secondary sector, sometimes also the processing or manufacturing sector, includes all branches of human activity that converts raw materials into products or goods. Industry and industrial production are still large producers of CO_2 in Slovakia.

Transportation

Transportation can be defined as a branch of the national economy that provides for the transport (i.e., relocation) of people, things, messages, etc. It also means the intentional and targeted movement of means of transport on traffic routes and thus the operation of the transport facilities by which the transport takes place, which contributes greatly to CO_2 production.

Energy

Energy is a scientific department that deals with the economical use of all energy sources and supplies, as well as the energy supply industry [9]. Slovakia produces 54% of its electricity from nuclear energy, 24% from renewable sources, 15% from coal and 6% from natural gas. The energy sector is still the largest producer of CO_2, and the integration of renewable energy sources will help us reduce it.

3 Methods and methodology

3.1 Geometric research

Geometric research of spatial urban structure must always take into account geographical and geospatial predispositions, demographic methods of data collection such as UPI (UPI – ground plan) statistics of socio-economic indicators, community development strategy, transport accessibility etc. From the geographical point of view, especially the natural landscape predisposition, morphology, climate, geological, climatic information, and other data provided by the municipality or self-government. In the absence of specific information for further analysis, we requested these data from other sources or they have been added by us.

Geospatial-mathematical mapping is a method that is based on the quantification of objects using vectors expressed in a coordinate system (x-, y-, and z-axes). Often, the use of simplified geospatial information will help to better classify data information and its subsequent use in the accurate conversion of unit values. This process is the most important for the calculation and integration of the solution as it provides us with absolutely accurate data, which serves as a relevant basis for further processing. Digitization of geospatial information in real scale into digital can also be understood as a "digital twin" – a carrier of data and a large amount of information, which means that it is essentially a virtual model of the real factual situation. Currently, the term Digital Twin means a virtual representation of physical and non-physical objects and entities [10], such as buildings, networks, manufacturing and transportation facilities, but also processes, systems, workers, data, or the entire environment.

The area concerned in the form of a 3D polygon or a mesh with high resolution map / base texture results in the extraction of objects according to our own procedure so that we reach the most accurate unit values. This process is repeated for all sectors, from residential to multifunctional, to industrial buildings within LOD 1.

Subsequent identification of altitude points helps us to obtain more accurate numbers and values of CO_2 corresponding to each sector. The whole extraction is carried out using the method of division and quantification of data, based on the sectors defined by us and their morphological relationship to the surrounding area. Spatial quantitative data using the perimeter boundaries of individual objects divide the space into sectors whose relationship is identified by shape, area, material and structure, as well as volume, and then we can identify the smallest statistical units. Another process is the process of redistribution of data by sectors and their occupancy with conversion to square meters, and the height point that is provided by a 3D low poly model. The data adjusted in this way are mathematically recalculated in relation to the total surroundings of the area concerned. An essential step is the filling in of other attributes as subgroups that produce CO_2 for households, i.e., energy burden, such as energy connection point, natural gas kWh = 0, natural gas m3 = 0, extra light heating oil l = 0, coal/coke kg = 0, district heating kWh = 0, district heating from biomass kWh = 0, heat pump kWh = 0, chopped wood (logs) prm = 0, wood chips plm = 0, pellets kg = 0, household electricity, excluding photovoltaics kWh = 0, photovoltaics kWh = 0, solar collectors,

appliances, heating and architectural indicators, age of construction, insulation, replacement of windows, energy certification and disposition, number of cars belonging to households, number of members in the household, etc. In the absence of this information, the recalculation takes place on the basis of publicly available data, i.e., map data with elevation in the 3D geometry converted to sqm of usable area. We process similar attributes for each typing of the map data, such as, multifunctional zone, civic amenities, facilities for sports and recreation, areas of agricultural production, horticultural and cottage settlements, technical infrastructure facilities and protection zones. Furthermore, roads, service roads, paved areas, water bodies and streams, landscaped greenery, accompanying and protective greenery, greenery of watercourses etc. Raster redistribution of the map data and their functional use in relation to the proportion of the area on which the individual subsector indicators operate x load factor per square meter helps us to find the real value of consumption, which is based on the function of space and subsequent production of CO_2. Functional conversion is as follows:

Sub-sector sqm: 1.20%* × kWh/(sqm) × 0.00065 kgC**

* the coefficient of the difference between the built-up and usable area is equal to 1.20%
** average value for subsector kWh/(m)

3.2 Level of detail

Level of detail is the geometric relationship of the x, y, z coordinate system and its complexity of representation in the form of a 3D model polygon mesh. In general, there is a positive correlation, i.e., the lower level of detail of the displayed 3D object is, the faster the display in the software interface is. The level of detail can also be defined as the relationship between the observer and the observed object and their focal length, i.e., the further away the observer is from the object, the lower the level of detail is the displayed. From the point of view of a 3D polygon, the lowest level of detail of the model must meet the basic attributes, which are “x, y, z”, i.e., width, length, and height dimensions, and the correct position on the map. The level of detail is the bearer of data levels and the so-called classification, i.e., classification into categories in terms of purpose or use.

LOD 1
Level of detail 1 which is characterized by a lower quality display of a 3D object formed by a small polygon network, without text and materials with basic “x, y, z” information, i.e., width, length and height dimensions and orientation information about square meters and volume information in cubic meters in the correct position in the map data. This display can be called a simplified volumetric 3D model, which, however, contains all types of roofs such as saddle, hip, sloping, tent, rugged, attic and arched, cantilever, flat roofs (Figure 9: Basic types of roofs).

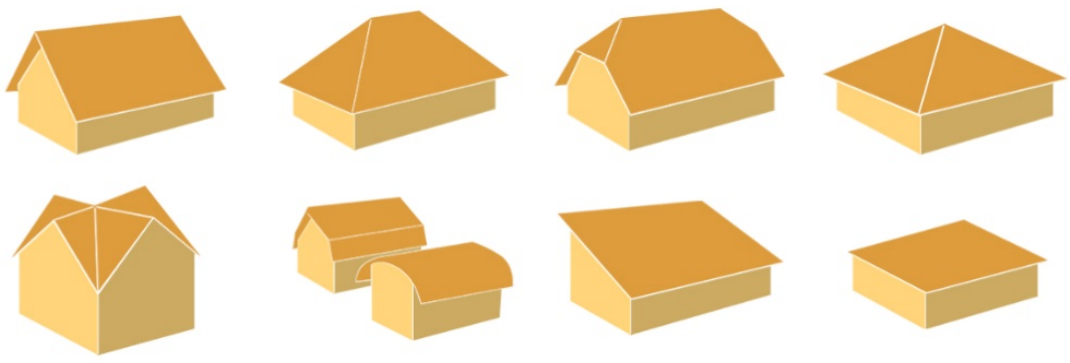

Figure 4: Basic types of roofs

LOD 2

Level of detail 2 is a representation of the model in a significantly higher quality, where the tectonics of the facade, division and building openings are visible. LOD 2 is a model formed by a medium polygonal network, the type of material used, a higher accuracy of "x, y, z", and thus, a precise definition of width, length, and height. The model is classified in class 2 due to a predefined classification, the bearer of information characteristics, type of manufacturer and/or the trademark, with which the object can be traced. Level 2 also includes an itemized tabular report in square meters and cubic meters.

LOD 3

It consists of a real depiction of the facade, building openings, technological equipment, building carpentry and all items that correspond to it in real scale so, as from the position of an observer we can perceive the detail of the facade and the architecture itself. The 3D model at level 3 is formed by a high polygon network, which is optimized, classified and included in classes in terms of the assignment, and thus, it is possible to switch the individual levels corresponding to the individual components on and off or combine them. Each object carries a texture in real UVW scale, which is standardized by the surface mapping technique using a raster matrix. Level 3 provides high accuracy that is characteristic of the category of BIM models, which carry the primary attributes as the size of individual objects: nature, material structure, type of manufacturer, trademark or www link, etc. The model contains GPS coordinates of our territory in the coordinate system S-JTSK and is, therefore, georeferenced and placed in the correct location and position on the map. All dimensions are given with absolute accuracy in square meters and cubic meters.

Figure 5: Digital model Most pri Bratislave

Figure 6: Digital model LC (Land cover map)

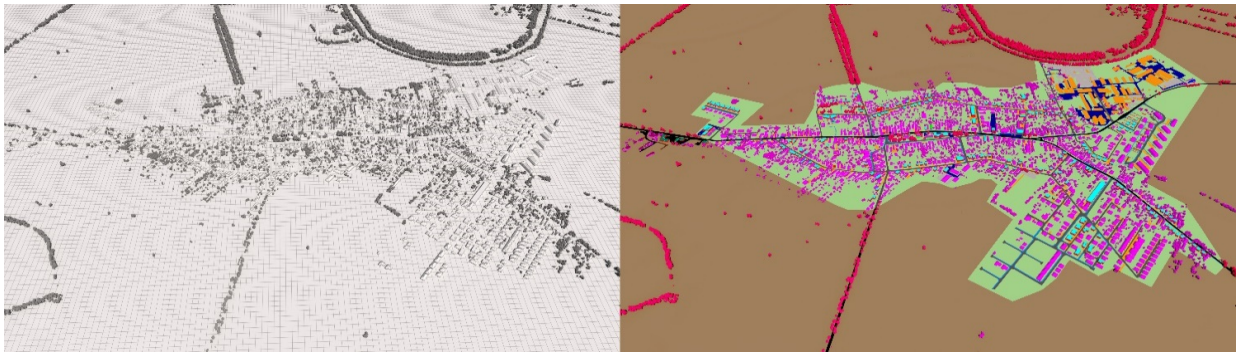

Figure 7: Digital model wire + DTM

Figure 8: Digital model LC LOD 1

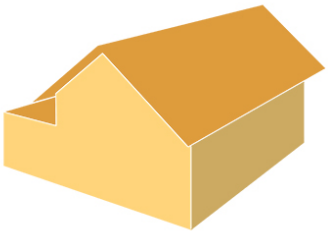

Figure 9: LOD 1

Figure 10: LOD 2

Figure 11: LOD 3

Transport as a separate chapter was analysed by entering the village via secondary road and with one output, we were able to identify, using the differential protocol, the number of cars leaving the village and the number of cars passing through the village. By combining the digital map data of the raster structure of space in combination with individual sectors, it is possible to determine the depth and exactly general spatial arrangements. It serves as a basis for further processing in the extent of the application of the problem and further interpretation.

We carry out the analysis of green areas on the basis of their diversification into four categories of wood species and their average value of annual wood growth for one vegetation period. Based on measuring the diameter of the trunk at a height of 1.30 meters above ground level and measuring the growth pattern of the crown part, as well as the total height of the tree, we were able to recalculate the coefficient Y. We work with this coefficient further as with the absolute weight of the tree during the growing season. When multiplying this value by a constant of 120%, which means a multiple of its weight +20% of the root system, - (minus) the point of fiber saturation, which means the moisture content in the wood mass - 72.5%, - 50% wood dry matter we get the CO_2 value contained in wood. The real supply of CO_2 in wood is 3.67 times smaller than the value of CO_2 in the atmosphere and therefore the equation applies that to one tonne of carbon in biomass 3.67 tonnes of CO_2 is consumed from the atmosphere [11]. Based on the average of the values of the crown system expressed in square meters, it was possible to define the area that the trees represent in terms of the category defined by us. By simply recalculating the offset of the area in square meters and the total area that the greenery occupies in terms of the map of the land cover, we were able to identify the quantity of trees for each category and the number of pieces.

Coniferous trees – spruce, larch, pine, yew, fir, microbiota, juniper, duglaska
Deciduous / Volunteers (scattered porous) – birch, hornbeam, maple, rowanberries, shapeless, sumac, ailanthus
Deciduous / Planting (circular porous) – oak, acacia, elm, ash, chestnut
Fruit trees – apples, pears, cherries, apricots, peaches, nectarines, plums, greengages, nuts

[12] year / increment* × Ø² × height × 120% × 72.5% × 50% = CO_2 × 3,67 CO_2 in the atmosphere

* average annual increment per growing season

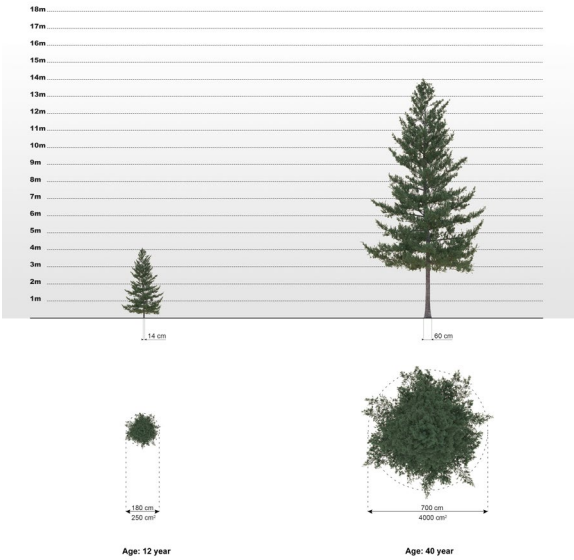

Figure 12: Coniferous trees / average

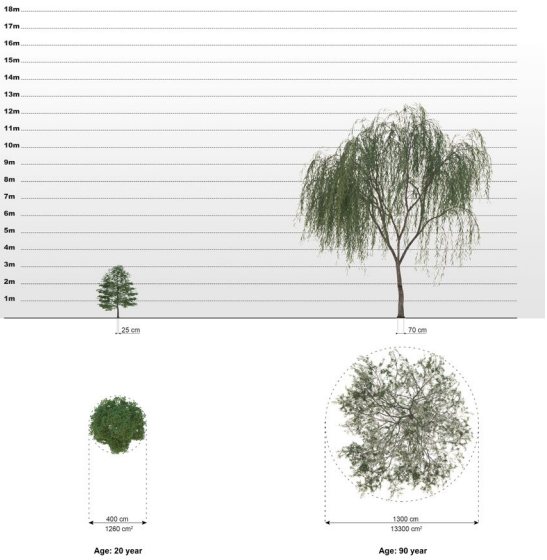

Figure 13: Volunteer trees / average

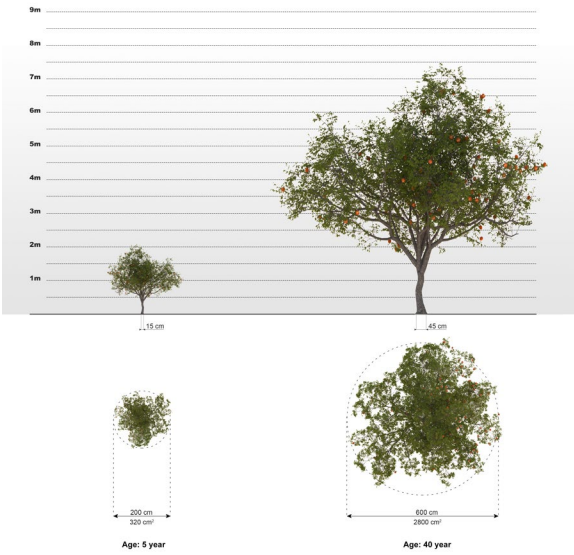

Figure 14: Fruit trees / average

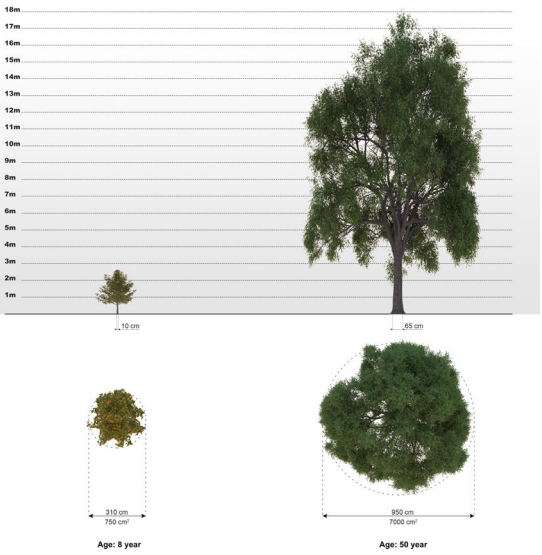

Figure 15: Deciduous tree – planting / average

Modern technologies form a very important part of smart cities, and should contribute to more efficient transport management, greener energy, and well-thought-out waste management, which will increase the sustainability of the local economy. When recalculating the volume of CO_2 production, I took into account the demographic factor – the number of the population and multiplied it by the unit value of waste production. According to the Statistical Office of the Slovak Republic, in 2019 the average Slovak produced 435 kg of municipal waste (MW), which was 35% more than ten years ago [13]. The inventory of emissions from the waste

sector includes direct greenhouse gas emissions (CH_4, CO_2, N_2O) and indirect emissions (NMVOC), an equally important study in terms of the percentage of CO_2 is [14] a waste management method that also has a significant impact on the carbon footprint.

4 Results and discussion

Technological progress will continue to be an integral part of the global progress and we simply cannot avoid this development. The carbon footprint is one of the most important tools for monitoring the impact of human activities on the environment, and we can even say that it is one of the most recent tools for society to make the environmental characteristics of products and services visible. In our work, we tried to draw attention to the environmental issues that move the world, which to a greater or lesser extent also affect our country, as well as the region that we focused on in this work. The aim was to calculate and record the most accurate emissions data, especially carbon dioxide in the village of Most pri Bratislave, produced by households as such, transport, other contributors to the production in question, which will subsequently help prepare and implement strategies to reduce greenhouse gases in our territory.
Applying the research methodology, where we used, among other things, the analysis and synthesis of specialised information, we were able to recalculate specific results of CO_2 production per person, car, aircraft or production hall of the food industry, based on the formula:

$$\mathbf{33{,}200{,}313\ kgCO^2 \times 1{,}419{,}763\ kgCO^2 \times 1{,}078{,}383\ kgCO_2 - 895{,}451\ kgCO_2 = \underline{34{,}802{,}265.00\ kgCO^2}}$$

*× Transport × Waste - Greenery = CO^2 of the municipality of Most pri Bratislave

*LC – Land cover map

while we included in the input data various aspects and factors that contribute to the increased result of the emissions concerned in any way whatsoever. In this scientific study, the result of the annual emission production from the cadastral area of Most pri Bratislave, taking into account all aspects and factors, was 34 802 265.00 kg CO_2. In the process of processing the described aspects and factors, I tried to reach the result of this scientific study by pointing to the main producers of CO_2, but also to highlight the need to address emissions not only from transport as one of the main producers, but also from agriculture, waste management or as already mentioned households as such.
As part of CO_2 reduction, cities and municipalities should focus primarily on reducing emissions from the production of various components in industry and, secondly, on electricity generation, as the energy industry is one of the largest producers of greenhouse gases. The general fact is that countries today have an ecological deficit, which means that their management is environmentally unsustainable from a long-term perspective. In this work, we pointed out several indicators of environmental sustainability, which provide information on how humanity, states, cities, municipalities, households and individuals live on the verge of said sustainability. Despite our findings and efforts to reduce the impact on global warming, this process is irreversible, and we will not feel the effects of its slowdown until many years later. Nevertheless, we believe that the data from our work will help in the preparation of low-carbon to carbon-free strategies for municipalities and cities, which will then act for the

benefit of nature for future generations.

Average Slovak 5.888 tCO_2

Average inhabitant of Most pri Bratislave 9.364 tCO_2

5 Conclusion

Research and development, comparison of our data and confrontation with the individual values of producers by sectors helped us to identify precisely the volume of CO2 production. The greatest benefit is the recognition that the impact of the CO2 production affects the nature and density of the population, transport interval and the general quality of the environment, geographical, demographic and social- economic predisposition.

The key, most important, default factor is the identification of the CO volume production. The methodology described in the article above stated precisely how to define the volume of the CO2 production. The identification of the problem is always primary and only then can various measures be integrated.

References

[1] MARCINČIN, A. (2019, March 29). Vidiek aj mestá majú spoločného nepriateľa. Retrieved November 13, 2020, from https://dennikn.sk/blog/1426478/vidiek-aj-mesta-maju-spolocneho-nepriatela/

[2] © Európska únia, 2019. (2020, December 22). Opatrenia EÚ v oblasti zmeny klímy, Retrieved November 15, 2020, from https://www.consilium.europa.eu/sk/policies/climate-change/

[3] EurActiv/Reuters, (2019, August 19). Schopnosť európskych lesov absorbovať CO_2 sa blíži k limitu, from https://euractiv.sk/section/zivotne-prostredie/news/schopnost-europskych-lesov-absorbovat-co2-sa-blizi-k-hranici-021422/

[4] CABUZEL, T. (2020, March 04). European Climate Law. Retrieved November 15, 2020, from https://ec.europa.eu/clima/policies/eu-climate-action/law_en

[5] MARCINČIN, A. (2019, March 29). Vidiek aj mestá majú spoločného nepriateľa. Retrieved November 13, 2020, from https://dennikn.sk/blog/1426478/vidiek-aj-mesta-maju-spolocneho-nepriatela/

[6] MARCINČIN, A. (2019, March 29). Vidiek aj mestá majú spoločného nepriateľa. Retrieved November 13, 2020, from https://dennikn.sk/blog/1426478/vidiek-aj-mesta-maju-spolocneho-nepriatela/

[7] DennikN. (2019, September 20). Vplyv poľnohospodárstva je v debate o klíme. Retrieved December 08, 2020, from https://e.dennikn.sk/minuta/1591730

[8] KAPUSTA, P. (2019, December 22). Ťažba dreva. Retrieved December 05, 2020, from https://www.enviroportal.sk/indicator/detail?id=781

[9] © 1999 Jozef Piaček & Miloš Kravčík, FILIT, OTVORENÁ FILOZOFICKÁ ENCYKLOPÉDIA, Verzia 3.0, http://dai.fmph.uniba.sk/~filit/fve/energetika.html

[10] Digitálne dvojča: Vedúca technológia inteligentného priemyslu. (2019, September 16). Retrieved November 17, 2020, from https://www.anasoft.com/emans/sk/home/Novinky-blog/blog/digitalne-dvojca-veduca-technologia-inteligentneho-priemyslu

[11] Majerský, I. (2019, December 05). Slovenské lesy pohltia čoraz menej emisií. Retrieved December 12, 2020, from https://ekonomika.pravda.sk/ludia/clanok/534411-slovenske-lesy-pohltia-coraz-menej-emisii/

[12] How to calculate the amount of CO_2 sequestered in a tree per year. (2003, June 24).Retrieved December 15, 2020, from https://www.unm.edu/~jbrink/365/Documents/Calculating_tree_carbon.pdf

[13] PROPERTY & ENVIRONMENT s. r. o. (2020, July 23). Slováci dosahujú rekordy, ktoré nepotešia (Analýza). Retrieved December 14, 2020, from https://www.odpady-portal.sk/Dokument/105461/slovaci-dosahuju-rekordy-ktore-nepotesia-analyza.aspx

[14] Nízkouhlíková stratégia rozvoja Slovenskej republiky do roku 2030 s výhľadom do roku 2050. (n.d.). Retrieved December 20, 2020, from https://www.minzp.sk/files/oblasti/politika-zmeny-klimy/nus-sr-do-roku-2030-finalna-verzia.pdf

DOI: 10.1515/sspjce-2021-0010

Techniques for Optimizing Parameters of Soil Nailed Vertical Cut

Fadila Benayoun [1], Djamalddine Boumezerane[2], Souhila Rehab Bekkouche[3]

[1]Department of Civil Engineering, Faculty of sciences and applied sciences, University Oum El Bouaghi, Algeria
[2]School of Computing, Engineering and Physical Sciences, University of the West of Scotland, United Kingdom
[3]Department of Civil Engineering, Faculty of technology, University 20 Août 1955, Skikda, Algeria
e-mail: benayounfadila@yahoo.fr, Djamalddine.Boumezerane@uws.ac.uk

Abstract

In this paper a finite-element analysis was carried out using Plaxis[2D] software to model a vertical cut reinforced by nails. Optimization of the effect of three input parameters on stability design is a key element of the analysis. We compare results obtained by three techniques of design optimization; Taguchi's Design of Experiment (DOE), Genetic Algorithm (GA) and Particle Swarm Optimization (PSO). The effect of three input factors on stability design was considered: nail length to wall height ratio (A), nail inclination (B) and vertical spacing (C). By altering the parameter variables, the design served to build and acquire a statistically significant mathematical model for optimizing soil nailing wall parameters. The aim is to minimize a single objective function of safety factor and identify the optimal parameters of design among all possibilities. DOE method and result analysis were carried out using MINITAB 18 software, while GA and PSO algorithm analysis were implemented by coding in MATLAB. According to the results, it was found that 9m of length, 2m of vertical spacing and 10° of inclination is the optimal combination minimizing safety factor. The results produced from this study show that all three techniques arrive at the same optimal combination of minimum response.

Key words: optimization, Taguchi method, genetic algorithm, particle swarm optimization

1 Introduction

Depending on the type of soil considered and the type of work to be carried out, an appropriate reinforcement solution should be chosen which matches both the nature of the soil in place and its environment. Two major techniques can be used to increase the mechanical characteristics of soils: by modifying the internal structure of the soil in place [1,2] and strengthening the soil by adding inclusions. More specifically, soil improvement techniques make it possible to increase the compactness of the soil in place, either by reducing the volume of voids…etc. [3]. Soil reinforcement is a special and recent field of soil improvement, it covers a range of techniques which consist of placing resisting inclusions in

the soil, now it is accepted as a more general concept which includes such techniques as micro -piles, stone columns, in-situ stabilized columns, soil nailing, texsol and membranes...etc. [4]
Most problems in soil reinforcement engineering involve analysis for stability. Thus, retaining walls, geosynthetics, slopes and soil nailing are designed for safety against failure.
Soil nailing is a ground stabilization technique that can be used on either natural or excavated slopes and retaining walls to make them more stable as construction proceeds from the top to bottom [5]. Soil nailing is an efficient and economical technique compared to other reinforcement techniques. Nails inclusions within a soil mass can operate as a reinforcement function by developing tensile forces which contribute to the stability of excavation [6].
Optimization problem is defined as finding the best solution from the feasible solution in a pool which contains all solutions **[**7**]**. In the field of geotechnical engineering optimization has become increasingly important, in the recent literature, researchers have applied the advanced optimization techniques to different purposes: finding the best design with regard to geometry, shape, weight and cost ...etc.
The geometric parameters adopted for nails such as their number, length, diameter, and inclination to stabilize a soil nailing wall present the main considerations for engineers to decide whether optimal design will be appropriate regarding stability and economy. One of the main reasons in failing to perform accurate calculations when dealing with excavations is the adoption of inappropriate constitutive models [8]. For optimum design of nailed wall, it is necessary to cast the problem in an optimization framework.
Presently, optimization techniques such as Genetic Algorithm (GA) [9,10], Particles Swarm Optimization (PSO) [11], Ant Colony Optimization (ACO) [12], Topology [13] and Artificial Neural Networks (ANNs) [14] are widely used in civil engineering. Generally, each optimization technique has its advantages and disadvantages, which means that not all optimization problems can be solved effectively by a given optimization method [15].
In this study we propose to approach the problem of optimizing parameters of soil nailed vertical cuts by using three techniques. The proposed methods discussed here are Taguchi's design of experiment (DOE), Genetic Algorithm (GA) and Particle Swarm Optimization (PSO). Each of the methods will be explained in the context of our problem and a comparison between their results of optimization is carried out.

2 Finite elements model for soil nailed wall

The soil nail wall system was numerically simulated, using a two-dimensional finite element Plaxis^{2D} software version 8.2, with a plane strain problem and long-term behavior simulated using drained analysis conditions. To provide information for the performance of the soil nailing wall, the soil was modelled using Mohr-Coulomb model, an elastic perfectly plastic model, which in general can be considered as a first order approximation of real soil behaviour (sandy soil). The model requires five basic input parameters: Young's modulus E, Poisson's ratio ν, cohesion C, friction angle ϕ, and dilatancy angle ψ. Fifteen (15) - noded triangular elements are used for generating finite element mesh of appropriate density. Coarse mesh density is adopted globally, which is refined to fine density mesh around nails. Left and right boundary of the model were fixed in horizontal direction while the bottom boundary was fixed in all directions.

Using the staged construction technique available in Plaxis^{2D}, top-down construction sequence was simulated in calculation stage of soil nailing [16].

Figure 1 shows the simulated soil nail wall with dimensions and mesh boundaries and fixity conditions.

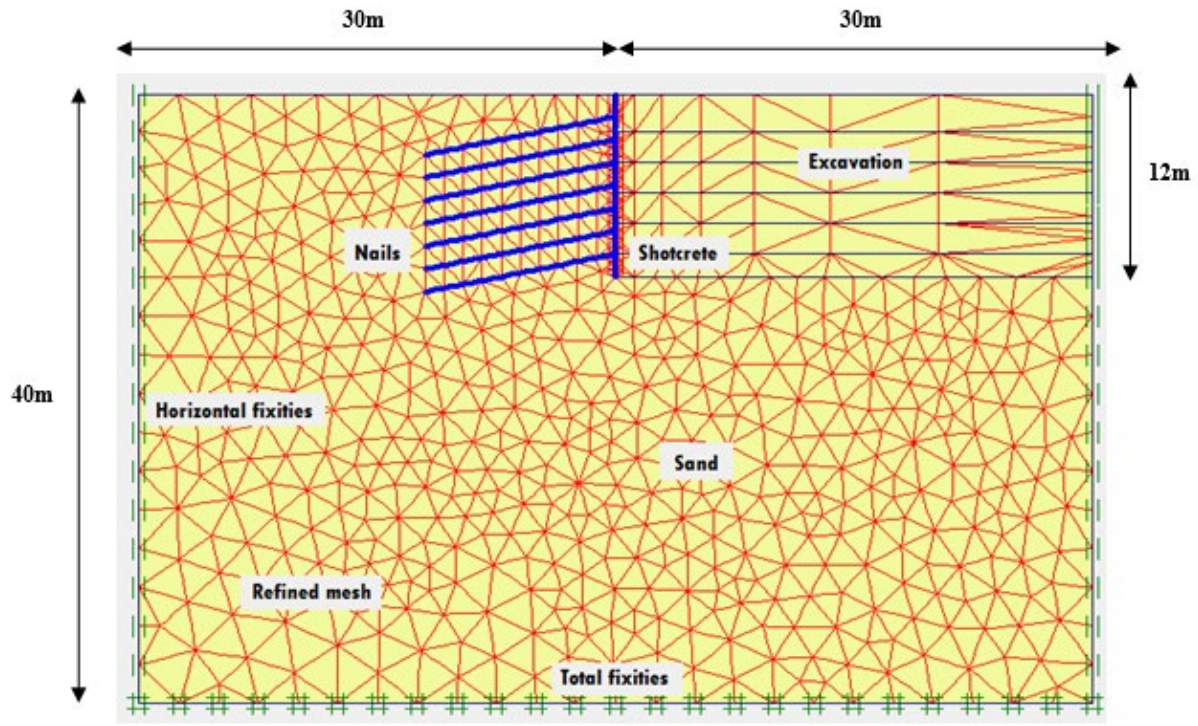

Figure 1: Geometry and FE mesh of soil nailing case in Plaxis^{2D} [16,17]

The physical and mechanical properties of the soil model are shown in Table 1:

Table 1. The physical and mechanical properties of soil layer

Soil properties	Sand
Unit weight γ (kN/m^3)	18.0
Cohesion C (kN/m^2)	10
Friction angle φ (deg)	35
Dilatancy angle ψ (deg)	5
Young's modulus E (kN/m^2)	6.5 10^4
Poisson's ratio ν	0.3

Plate elements were used to model the nails and the shotcrete (facing); the most important parameters of plates are flexural rigidity (bending stiffness) EI and axial stiffness EA [17], their stiffness values are shown in Table 2.

Table 2. Material properties input for modeling

	Axial stiffness EA (kN / m)	Bending stiffness EI (kN.m^2/m)
Grouted soil nail	6.8 x 10^4	12.5
Shotcrete	2.5 x 10^6	1.22 x 10^4

3 Parametric analysis

Several studies have been carried out detailing the effect of parametric variation on the stability of soil nailed wall, slope stability, and excavation, such as, nail inclination [18,19], nail length [20,21], vertical and horizontal spacing [22], surcharge load [23], excavation height [24], grouting pressure [25,26], hole diameter, soil cohesion, internal, friction angle Ground Surface [10], inclination and thickness of shotcrete …etc.

Length of nails, vertical spacing and nail inclination are chosen in these optimization techniques among the factors of soil nailing wall that may influence the stability. The stability of nailed wall is evaluated in terms of factor of safety, so in this case one response is evaluated. The goal of this optimization from computerized simulation models was to obtain the minimum response safety factor and to find the optimal combination of soil nailing inputs factors. The safety factor was calculated using the phi reduction technique available in Plaxis^{2D}, in which the shear resistance parameters are reduced by steps until the soil body fails as in Eq. (1) [20].

$$\sum Msf = \frac{tan\emptyset_{input}}{tan\emptyset_{reduced}} = \frac{C_{input}}{C_{reduced}} \quad (1)$$

Where:
$\emptyset_{input}$= input value of angle of internal friction (°)
$\emptyset_{reduced}$= reduced value of angle of internal friction at failure (°)
C_{input}= input value of cohesion (kPa)
$C_{reduced}$= reduced value of cohesion at failure (kPa).

In this case study, the length to height ratio will be considered for lengths of 9m, 12m and 14.5m whose excavation height is constant and equal to 12m.

Table 3: Length to height ratio values

Length (m)	Length to height ratio (A)
9	0.75
12	1
14.5	1.2

Table 4: Selected parameters and levels

Control Factors		Levels		
		1	2	3
A	Length to height ratio	0.75	1	1.2
B	Vertical spacing (m)	1	1.5	2
C	Inclination (Degree)	10	15	20

3.1 Mathematical model

The simulation of input-output data collected after modeling are used to establish the relation between input factors and response variable according to some modeling algorithm by combining techniques such as regression model. It is necessary to determine the appropriate function, and the focus is now on the nature of the relationship between the response and the factors, rather than on identifying important factors.
The regression equation is calculated by the mean values of safety factor under different conditions of input parameters.
Using ANOVA analysis, it is possible to evaluate the significance of the regression model selected. The main idea is to compare if the residues present normal distribution [27].
A multiple regression model is adopted as shown in equation (2), it is used as the objective function for applying the two algorithms Particle swarm Optimization (PSO) and Genetic Algorithm (GA).

$$F_s = +1.02532\,A - 0.124717\,B + 0.00855556\,C + 1.13475 \quad (2)$$

Table 5: Model summary

S	R-sq	R-sq(adj)	R-sq(pred)
0.0046	95.44%	94.85%	93.89%

From the regression model the R-squared value obtained is 95.44%. This value is high enough to show good agreement and great significance of the predicted model. The standard deviation S is used to evaluate the effectiveness of the regression model, S is equal to 0.0465 which represent the distance between the data values and the fitted values, it clearly confirms that the model can certainly predict the safety factor well [28].

4 Optimization Techniques

4.1 Taguchi's design of experiments

Design of Experiments (DOE) is one of the most famous optimization techniques. In the 1920's in England, Ronald Aylmer Fisher introduced a powerful statistical technique to study

the effect of multiple variables simultaneously [29]. In the late 1940's Dr. Taguchi's standardized a version of DOE, popularly known as the Taguchi method. In the early 1980's it was introduced in the USA. Today it is one of the most effective quality construction tools in all types of manufacturing activities used by engineers [29-30]. There are five types in Design of experiments:(1) Screening design, (2) Factorial design, (3) Response surface method designs, (4) Mixture, (5) Taguchi.

DOE using the Taguchi approach has become a much more attractive tool to practicing engineers and scientists [31]. It is a systematic method to determine the relationship between factors affecting a process and the output. In other words, it is used to find cause-and-effect relationships [32]. This information is needed to manage processing inputs to optimize the output. DOE can show how to carry out the fewest number of experiments while maintaining the most important information [33].

Taguchi experimental designs, often called orthogonal arrays (OA) use the signal to noise (S/N) ratio as the measurable value of the quality characteristics of the choice [27].

When using the Taguchi method with three levels an L27 or L18 orthogonal array are the most commonly used. L9 is usually adopted also. However, this requires many experiments (27 or 18 runs, respectively), consuming time, and resources compared to nine trials. An experiment can be defined as a series of tests in which a set of input variables is modified in a controlled manner to observe and identify the response of the model affected by these changes [27].
In this section, L9 orthogonal array is adopted. When minimizing the objective function, the smaller-the-better quality characteristic was used to get the minimum factor of safety and the optimal vertical cut parameters, we will compute the following S/N ratio.

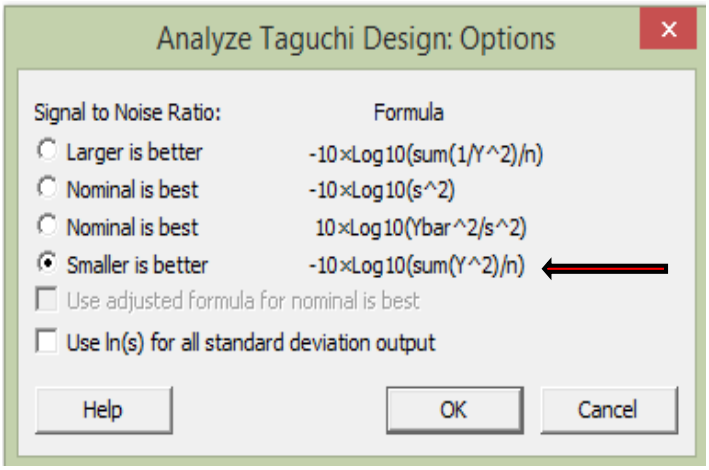

Figure 2: Smaller the better equation

Where n is the number of experiments and Y is the response in that run.

Table 6 shows the transformation result of data from the experiments into a proper S/N ratio.

Table 6: L9 orthogonal design array and measured responses and S/N ratios.

N°	Input factor			Response FS	S/N (dB)
	A	B	C		
1	0.75	1.2	10	1.84	-5.30
2	0.75	1.5	15	1.82	-5.20
3	0.75	2	20	1.8	-5.10
4	1	1.2	15	2.18	-6.77
5	1	1.5	20	2.18	-6.77
6	1	2	10	2.00	-6.02
7	1.2	1.2	20	2.35	-7.42
8	1.2	1.5	10	2.21	-6.89
9	1.2	2	15	2.22	-6.93

The analysis of data was carried out using MINITAB 18 software. Based on the analysis, one optimum parameter run is selected among nine of the suggested runs.

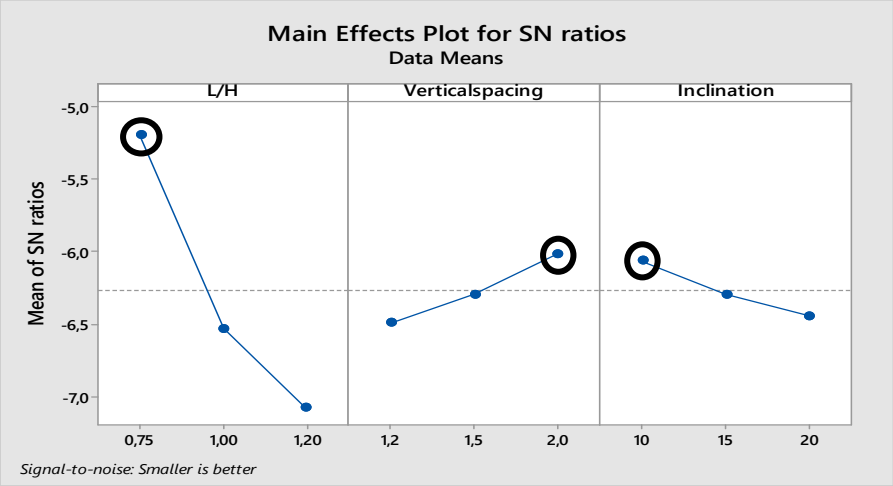

Figure 3: Main effects plot for S/N ratios

It is clear from Figure 3 that minimum safety factor is achieved at the combination of controls parameter 9m ,2m and 10° which represent length, vertical spacing and inclination respectively. The optimal combination (A1-B3-C1) was selected with the highest signal-to nose ratio.

4.1.1 Confirmation test

Once the optimal level of the design parameters has been obtained, the next step is to predict and verify the required improvement using the optimal combination of design parameters. Table 7 shows the comparison of the predicted safety factor value with the actual safety factor using the optimal soil nailing parameters, good agreement between the predicted and experimental safety factor was observed.

Table 7: Results of the Confirmation Experiment

Input and output parameters	Prediction combination A1B3C3	Experimental combination A1B3C3
A: Length to height	0.75	0.75
B: Vertical spacing (m)	2 m	2 m
C: Inclination (°)	10°	10°
Fs	1.71	1.68
S/N ratio (dB)	-4.72	-4.51

4.2 Optimization using Genetic algorithm (GA)

Genetic algorithm (GA) is a powerful metaheuristic algorithm it is perhaps the most well-known of all evolution-based search algorithms [28].

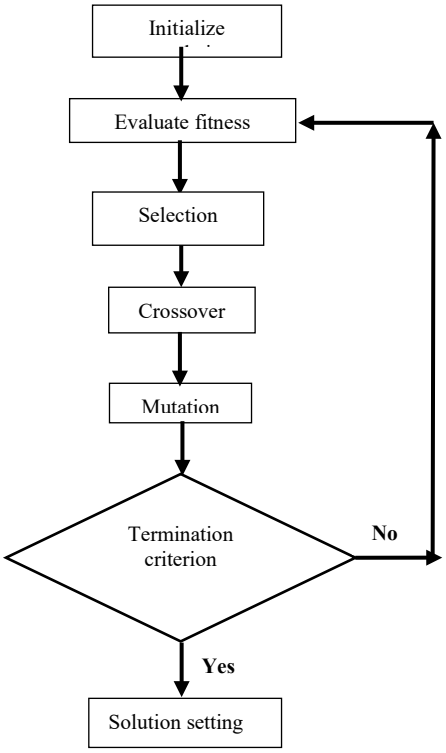

Figure 4: Flowchart of Genetic Algorithm (GA) [17]

This algorithm is created based on the theory of evolution of organisms in nature. It was first introduced by John Holland 1962. GA is executed iteratively on a set of coded chromosomes,called a population ,with three basic genetic operators :selection,crossover and mutation [34]. Each member of the population is called a chromosome or individual and is represented by a string. The flowchart for GA is given in Figure 4.

In GA, a population is created with a random group of individuals. The individuals in this population will then be evaluated based on the function provided. Through this evaluation

function, the performance of each individual will be scored. Then, two individuals with the highest performance will be selected to perform crossover and mutation to create better individual, this process continues until a suitable solution has been found [28].
The parameters for GA are set as follows: Population size is 100, crossover fraction is 0.8, mutation rate 0.05, roulette wheel is used as selection method [17]. MATLAB provides an optimization toolbox that includes a GA-based solver. The obtained optimal values of vertical cut parameters are shown in Table 8.

Table 8: Optimum parameter with Genetic Algorithm

Variables	A	B	C	Fs
Optimal value	0.75	1.99	10	1.69

4.3 Optimization using particle swarm optimization (PSO)

Particle Swarm Optimization is a metaheuristic search algorithm which was originally introduced by the scientists Eberhart and Kennedy in 1995, to find optimal solution in engineering design optimization [29]. The structure of PSO is based on the concept of social models, swarm theories and the composite practice of social insects such as bees, ants, bird flocking and fish schooling, to search for a food source and avoid a predator by applying information sharing phenomena.

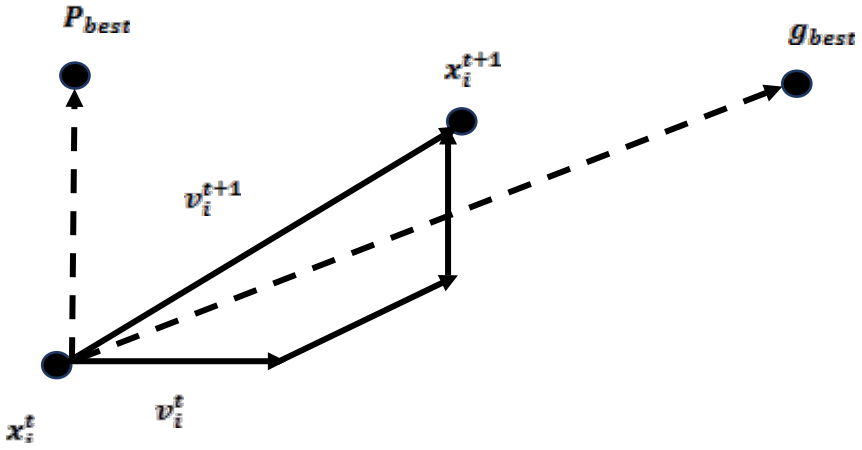

Figure 5: The movement of the particle by basic PSO [33]

For an optimization problem, the optimization of the swarm of PSO particles contains a population of candidates called swarm, this can be translated in the population which is made up of individual particles which mutually try to find an optimal solution in the multidimensional search zone by contracting between them [35]. The path of the particle in the search space is adjusted by updating the velocity of the particle and the information gain from the highest performing individual [28]

At each iteration, the individuals (particles) move towards the best solution that is experienced by them (best staff) and at the same time towards the best solution obtained by the other particles (best overall) [36]. Each particle is constantly updated via pbest and gbest to create a new population and the entire population searches for the region of the solution completely.
The new location of the particle is calculated as:

$$X_i^{t+1} = X_i^t + V_i^{t+1} \quad (3)$$

Each repetition of particle speed is updated using:

$$V_i^{t+1} = wV_i^t + c_1 \times r_1 \times \left(X_{pbest} - X_i^t\right) + c_2 \times r_2 \times \left(X_{gbest} - X_i^t\right) \quad (4)$$

Where X(t+1) denotes a new position of the particle.
V(t) defines the velocity of the particle, r1, r2 is the random number generated between 0 and 1. "w" inertia weight has been added to control the velocity, C1and C2 are the acceleration factors to compute Xpbest particle's personal best position and Xgbest global best position.
Swarm has a solution candidate called a particle, each particle in the PSO algorithm represents a possible solution, each individual particle flies in the search space with a speed which is dynamically adjusted according to its own flight experience and the experiences of flight of his companions.

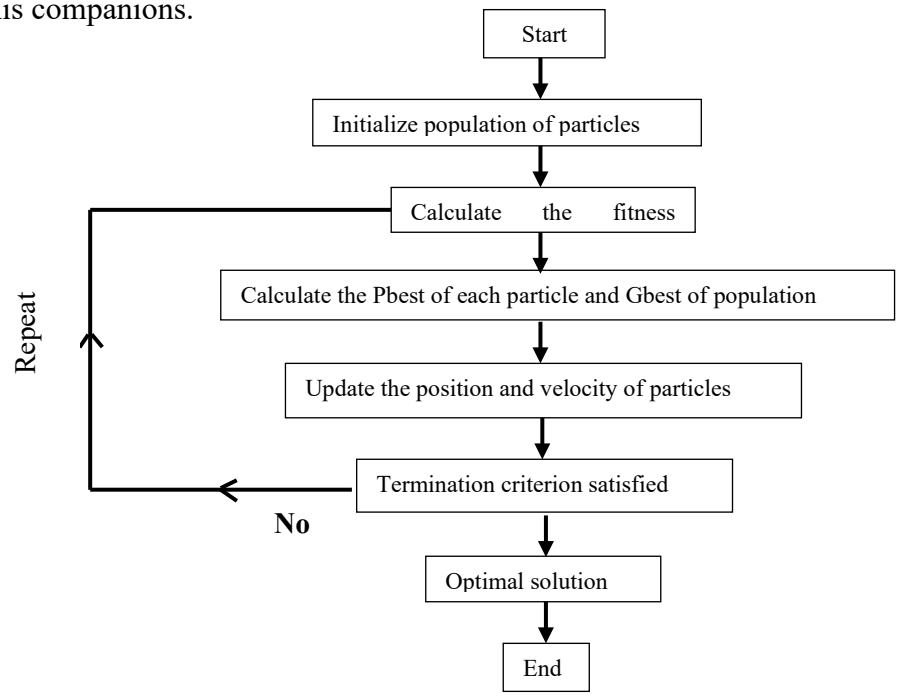

Figure 6: Particle Swarm Optimization (PSO)

The best position of each particle throughout the optimization process is the best solution found by the particle, then the best position experienced by the whole group is the currently best solution found by the whole of the group [37].
For particle cooperation in the PSO algorithm there are two principles:

- Communication: inform the best solution of a particular particle to the other particles of the swarm.

- Learning: when the particles get closer to each other, they really learn the best localization solution.

The simplified steps of the PSO algorithm for the single objective case are illustrated in Figure 6.

To get the optimal solution, particle swarm optimization can be used also in minimizing the objective function of this problem [35]. The appropriate choice of parameters improves the speed of convergence of the algorithm. To compare two specific algorithms (GA and PSO), the population size and the number of iterations should be the same, so population size and number of iterations are considered 100 and 50 respectively. The following parameters are adopted in the present PSO optimization using MATLAB.

Table 9. The parameters for PSO optimization

Variable	Value
Swarm population size	100
Maximum N° iterations	50
Inertia coefficient	0.5
Personal acceleration coefficient C1	2
Social acceleration coefficient C1	2

In Figure 7 is shown the fast convergence characteristic of the proposed PSO for the best result in 100 iteration.

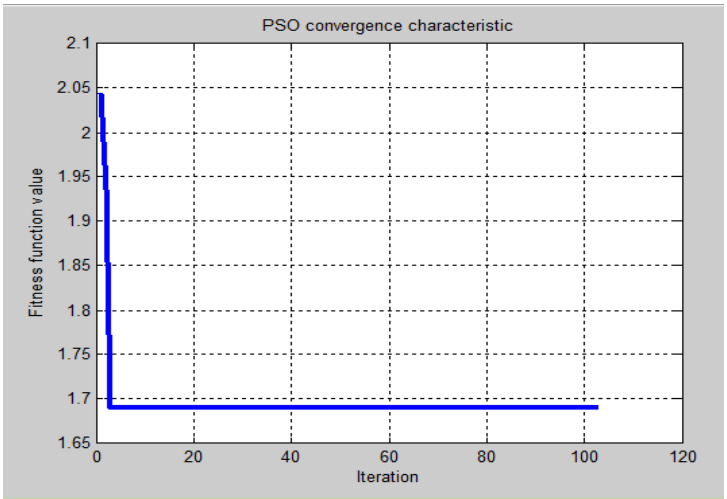

Figure 7: Convergence characteristics of PSO optimization

5 Results and discussions

By integrating the finite element analysis and the different optimization techniques an efficient design methodology can be developed. The optimum parameters obtained with three optimization techniques are summarized in Table 10.

Table 10: Results of optimal parameters of vertical cut using different optimization methods

Optimization Method		Input factors			
		A	B	C	F_S
Taguchi	L9	0.75	2	10	1.71
GA		0.75	2	10	1.69
PSO		0.75	2	10	1.67

From the results obtained, it is found that the parameter design of orthogonal array L9 provides a simple, systematic, and efficient methodology for optimizing the process parameter.

From this study, the optimal parameter values of our design consist of:

- Length of nails: all three techniques provided the same value of length 9 m i.e. (0.75 H), it is revealed that the overall safety factor increases with the increase of nail length indicating additional stability of the soil nailed wall, from (Clouterre Recommendations 1991) [38], nail lengths are usually in the range of 0.8H to 1.2H, where H is the retained height of the wall.
- Vertical spacing: the three methods gave the same value of 2 m, typically from [38], [39] and [22], spacing of 1 m to 2m between nails is adopted, it depends on soil type, from simulation results when the vertical spacing increases safety factor decreases this is due to the increase in the area served by the nail [16].
- Inclination: the three techniques agreed that the optimal value is 10°, according to [39] and [22], it was found that the effectiveness of the nail tends to decrease when the inclination of the nail exceeds 15° below the horizontal.
- The prediction model deduced for soil nailing wall parameters is in very good agreement with the values obtained experimentally (simulations) and confirm our results.

6 Conclusion

In this article we applied an optimization methodology for parameters of soil nailed vertical cut by comparing three methods: the Taguchi method, the Genetic Algorithm and Particle Swarm Optimization. The potentials of the three methods in estimating optimal parameters were explored and conclusions drawn.

- It has been demonstrated that the presented techniques are all capable of quickly finding the optimal solution.
- The optimal parameter values adopted for our design corresponding to the lowest factor safety, consisting of: 10° of nail inclination, 2 m vertical spacing between nails and 9 m of nail's length are satisfactory and in accordance with the recommendations Clouterre 1991 and consulted research.
- We noticed that PSO shares many similarities with the GA genetic algorithm, the

system is initialized with a population of random solutions and searches for optima by updating the generations, unlike PSO which does not have evolution operators such as crossover and mutation [36], the value of the safety factor resulting from the two methods is closely similar.

- The effectiveness of the Taguchi optimization method was conducted and verified using confirmation experiment.
- The advantages of Taguchi method over the other methods are that numerous factors can be simultaneously optimized, and more quantitative information can be extracted from fewer experimental trials.
- Application of DOE for Taguchi method can reduce the number of simulations, thereby reducing the computational cost significantly.
- The three methods can constitute a valuable tool for optimization of soil nailed walls in general, more parameters and different geometries can be considered in future analyses
- It should be noted that the obtained model is only valid in the selected ranges of the parameters.

References

[1] Patil, P., Mena, I., Goski, S. & Urs, Y. (2016). Soil reinforcement techniques. International Journal of Engineering Research and Application. 6(8), 25-31.

[2] Rouhanifar, S., Afrazi, M., Fakhimi, A. & Yazdani, M. (2020). Strength and deformation behaviour of sand-rubber mixture. International Journal of Geotechnical Engineering. 1-15.

[3] Villard, P., Briançon, L. (2018). Le renforcement des sols : des techniques devenues indispensables. In Encyclopédie de l'environnement, Université de Grenoble Alpes.

[4] Schlosser, F., Juran, I. & Jacobsen, H.M., 1983. Soil Reinforcement: general report: session no. 5. In Proc. of VIII ECSMFE: Helsinki, 1983, 1159-1180.

[5] Basudhar, P.K. (2008). Application of optimization and other evolutionary techniques in geotechnical engineering, The 12th International Conference of International Association for Computer Methods and Advances in Geomechanics (IACMAG). 1-6 October, 1-13, Goa, India.

[6] Budania, R., Arora, R.P. & CE, C. (2016). Soil nailing for slope stabilization: An overview. International Journal of Engineering Science.6(12),3877-3882.

[7] Dede, T., Kripka, M., Togan, V., Yepes, V. & Rao, R.V. (2019). Usage of optimization techniques in civil engineering during the last two decades. Current Trends in Civil & Structural Engineering. 1(1), 1-17.

[8] Babu, G.L.S., Singh, V.P. (2007). Stabilization of vertical cut using soil nailing, PLAXIS Bulletin. (22), 6-9.

[9] Hashemi, S.M., Rahmani, I. (2018). Numerical comparison of the performance of genetic algorithm and particle swarm optimization in excavations. Civil Engineering Journal. 4(9), 2186-2196.

[10] Imani, M., Pouya, O.B. (2021). Seismic Stability Analysis of Soil Nail Walls Using the Upper Bound Method. Transportation Infrastructure Geotechnology, 1-24.

[11] Hosseini, M., Naeini, S.A.M., Dehghani A.A. & Khaledian, Y. (2016). Estimation of soil mechanical resistance parameter by using particle swarm optimization, genetic algorithm and multiple regression methods. Soil and Tillage Research. 157(2016), 32-42.

[12] Gao, W., Zhang, L.Y. & Zhang, F. J. (2012). Critical slip surface searching for slope based on premium-penalty ant colony optimization. Shuili Xuebao, Journal of Hydraulic Engineering.43(2),209-215.

[13] Seitz, K.F., Grabe, J. (2016). Three-dimensional topology optimization for geotechnical foundations in granular soil. Computers and Geotechnics, 80(2016),41-48.

[14] Garg, A., Garg, A., Tai, K., Sreedeep, S. (2014). An integrated SRM-multi-gene genetic programming approach for prediction of factor of safety of 3-D soil nailed slopes. Engineering Applications of

Artificial Intelligence.30(2014), 30-40.
[15] Yin, Z.Y., Jin, Y.F. (2019). Practice of Optimisation Theory in Geotechnical Engineering, Springer. Shanghai, China.
[16] Mohamed, A.A.E.Z. (2010). Design charts for soil nailing, Master of Science in Civil Engineering, Shobra Benha University, Cairo.
[17] Benayoun, F., Boumezerane, D., Bekkouche, S.R., Bendada, L. (2020). Application of genetic algorithm method for soil nailing parameters optimization. IOP Conference Series: Materials Science and Engineering.800(1),1-8.
[18] Askari, A., Gholami, A. (2017). Effect of nail's orientation and length on soil-nailed retaining structures stability. DFI Journal-The Journal of the Deep Foundations Institute. 11(1),30-38.
[19] Jelušič, P., Žlender, B. (2013). Soil-nail wall stability analysis using ANFIS. Acta Geotechnica Slovenica. 10(1), 61-73.
[20] Sharma, A., Ramkrishnan, R. (2020). Parametric Optimization and Multi-regression Analysis for Soil Nailing Using Numerical Approaches. Geotechnical and Geological Engineering.38, 3505-3523.
[21] Mohamed, M.S., Sagitaningrum, F.H. & Kamaruddin, S.A. (2019). Optimization of Soil-Nailed Wall Design using SLOPE/W Software, Open International Journal of Informatics (OIJI), 7(1), 74-83.
[22] Villalobos, S.A., Villalobos, F.A. (2021). Effect of nail spacing on the global stability of soil nailed walls using limit equilibrium and finite element methods, Transportation Geotechnics, 26, p.100454.
[23] Kalehsar, R.I., Khodaei, M., Dehghan, A.N. & Najafi, N. (2021). Numerical modeling of effect of surcharge load on the stability of nailed soil slopes, Modeling Earth Systems and Environment, 1-12.
[24] Deng, D.P., Li, L. & Zhao, L.H. (2017). Limit equilibrium analysis for stability of soil nailed slope and optimum design of soil nailing parameters, Journal of Central South University, 24(11), 2496-2503.
[25] Zhou, W.-H., Yin, J.-H., & Hong, C.-Y. (2011). Finite element modelling of pullout testing on a soil nail in a pullout box under different overburden and grouting pressures. Canadian Geotechnical Journal, 48(4), 557–567.
[26] Yin, J.-H., Zhou, W.-H. (2009). Influence of Grouting Pressure and Overburden Stress on the Interface Resistance of a Soil Nail. Journal of Geotechnical and Geoenvironmental Engineering, 135(9), 1198–1208.
[27] Fukuda, I.M., Pinto, C.F.F., Moreira, C.D.S. & Saviano, A.M., Lourenço, F.R. (2018). Design of Experiments (DoE) applied to pharmaceutical and analytical Quality by Design (QbD), Brazilian Journal of Pharmaceutical Sciences, 54(SPE).
[28] Ahmad, N., Janahiraman, T.V. (2014). A comparison on optimization of surface roughness in machining AISI 1045 steel using Taguchi method, genetic algorithm and particle swarm optimization, In :2015 IEEE Conference on Systems, Process and Control (ICSPC), Bandar Sunway, Malaysia, 18 - 20 December.
[29] Roy, R.K. (2001). Design of experiments using the Taguchi approach: 16 steps to product and process improvement, John Wiley & Sons.
[30] Karna, S.K., Sahai, R. (2012). An overview on Taguchi method, International journal of engineering and mathematical sciences, 1(1), 1-7.
[31] Davis, R., John, P. (2018). Application of Taguchi-Based Design of Experiments for Industrial Chemical Processes, Valter Silva. Statistical Approaches with Emphasis on Design of Experiments Applied to chemical process,137-155, Intech, Janeza Trdine 9,51000 Rijeka, Croatia.
[32] Nurulhuda, A., Hafizzal, Y., Izzuddin, MZM., Sulawati, MRN., Rafidah, A., Suhaila Y. & Fauziah, AR. (2017). Analysis of flexural strength of A36 mild steel by design of experiment (DOE), IOP Conf. Series: Materials Science and Engineering, 226, 1- 7.
[33] Athreya, S., Venkatesh, Y.D. (2012). Application of Taguchi method for optimization of process parameters in improving the surface roughness of lathe facing operation, International Refereed Journal of Engineering and Science, 1(3), 13-19.
[34] Ashish, G. (2004). Evolutionary algorithms for multi- criterion optimization: A survey, International journal of computing and information sciences, 2(1), 38-57.
[35] Shi, Y. (2001). Particle swarm optimization: developments, applications and resources. Proceedings of the 2001 congress on evolutionary computation (IEEE Cat. No. 01TH8546), 1, 81-86.
[36] Bai, Q. (2010). Analysis of particle swarm optimization algorithm, Computer and information

science, 3(1), 1-5.

[37] Zhang, X., Zou, D. & Shen, X. (2018). A novel simple particle swarm optimization algorithm for global optimization", Mathematics,6(12), 1-34.

[38] Recommendations CLOUTERRE 1991, Soil Nailing Recommendations 1991 For Designing, Calculating, Constructing and Inspecting Earth Support Systems Using Soil Nailing, French National Research Project CLOUTERRE.

[39] Phear, A., Dew, C., Ozsoy, B., Wharmby, NJ., Judge, J. & Barley, AD. (2005). Soil nailing-best practice guidance, Construction Industry Research & Information Association, CIRIA, London.

DOI: 10.1515/sspjce-2021-0011

Production of non-traditional concrete based on steel slag as a way to reduce the environmental impacts

Vojtěch Václavík, Marcela Ondová, Jozef Junák, Natália Junáková

VŠB-TU Ostrava, Department of Environmental Engineering, Czech Republic;
Technical University of Kosice, Civil Engineering Faculty, Institute of Environmental Engineering, Slovakia
e-mail: vojtech.vaclavik@vsb.cz, marcela.ondova@tuke.sk

Abstract

Concrete is as a significant building material. Due to the fact that it is possible to incorporate by-products and industry waste into its structure, concrete represents an important sustainable material. Steel slag has a great potential for its reuse in concrete production. Despite that it is subject to volume changes over time, it can be used in concrete as a cement replacement or as a substitute for natural aggregates. The paper is focused at investigation the concretes with steel slag as a substitute of natural gravel aggregate of 4/8 mm and 8/16 mm fractions. In addition, a life cycle assessment within the system boundaries cradle-to-gate was performed. Results showed that some samples with slag have better mechanical parameters than samples with natural aggregate and significantly affect the utilization rate of non-renewable raw materials and reduce the overall negative environmental impacts of concrete up to 7 %.

Key words: concrete, steel slag, sustainability, LCA

1 Introduction

Rapid industrialization results in increased use of natural resources bring along serious ecological and environmental imbalance due to the dumping of industrial wastes. Principles of sustainable construction have to be accepted with regard to the consumption of natural resources and the production of harmful emissions. To reduce this environmental impact people all over the world are looking for a solution. Building materials were and are indispensable elements of each period. One of the most revolutionary materials of the 20th is especially the concrete. From construction elements to urban furniture, a large variety of concrete objects surround us nowadays [1]. However, it is true that a concrete and its composition have the significant influence on quality of environment. One of the possible solutions is incorporation of recycled industrial wastes in the mix-design of concrete [2&3], without reducing the quality of the final product. Many manuscripts indicate variousness and

a positive role of the waste incorporated into building materials [4&5]. Steel slag is a product of the metallurgical process, where active molten slag is used to separate undesirable adulterants and excess carbon. The potential for utilization of steel slag is huge, primarily including a cement replacement in the production of concrete [6] or untraditionally, a replacement the natural aggregates in the concrete and mortar production [7–9]. In addition, these concrete materials could be more beneficial for the environment.

The objective of the presented paper was to analyze and compare the technical properties and environmental impacts of concrete with steel slag as a substitute for natural aggregates of various fractions.

2 Material and Methods

2.1 Inputs - Raw materials

Steel slag (SS) fractions of 4/8 and 8/16 mm from Siemens-Martin furnaces stored on a heap, which had been produced by Trinecke zelezarny, a.s. company, was used to substitute natural gravel aggregates in concrete during the production of concrete. The above-mentioned fractions of steel slag were subjected to grain analysis according to CSN EN 933-1 as well as to: shape index (CSN EN 933-3), resistance to crushing (CSN EN 1097-2), density (CSN EN 1097-6), absorption capacity (CSN EN 1097-6), specific weight (CSN EN 1097-7), powder density (CSN EN 1097-3), and determination of impurities (CSN 72 1180). All results of monitored parameters can be seen in Table 1.

Table 1: Characterization of steel slag

Monitored parameter	Fraction	
	4/8 mm	8/16 mm
Shape index	SI = 2	SI = 1
Resistance to crushing	LA = 23	LA = 25
Absorption capacity [wt. %]	WA_{24} = 1.7	WA_{24} = 1.8
Density [Mg·m^{-3}]	ρ_a = 3.44 ρ_{rd} = 3.26 ρ_{ssd} = 3.30	ρ_a = 3.16 ρ_{rd} = 2.99 ρ_{ssd} = 3.05
Specific weight [Mg·m^{-3}]	-	ρ_f = 3.29
Powder density [Mg·m^{-3}]	ρ_b = 1.63	ρ_b = 1.51
Content of impurities [wt.] %]	0.0	0.0

Natural gravel aggregates – NGA, (0/4 mm from Bohumín and 4/8 and 8/16 from Valšov) were used for the production of plain concrete based on steel slag. The results of the tested properties of NGA of the aforementioned fractions are presented in Table 2. They are: powder density determined (CSN EN 1097-3), density (CSN EN 1097-6), absorption capacity (CSN EN 1097-6), shape index (CSN EN 933-3), resistance to crushing (CSN EN 1097-2), specific weight (CSN EN 1097-7), determination of impurities (CSN 72 1180), resistance to freezing and de-freezing (CSN 73 1322), quality of fine particles (CSN EN 933-8), presence of organic

substances (CSN EN 1744-1), and resistance to freezing and de-freezing (CSN 72 1176).

Table 2: Characterization of NGA

Monitored parameter	Fraction		
	0/4 mm	4/8 mm	8/16 mm
Shape index	-	SI = 10	SI = 31
Resistance to crushing	-	LA = 23	LA = 17
Absorption capacity [wt. %]	-	WA_{24} = 0.6	WA_{24} = 0.4
Density [Mg·m^{-3}]	-	ρ_a = 2.73 ρ_{rd} = 2.69 ρ_{ssd} = 2.70	ρ_a = 2.70 ρ_{rd} = 2.67 ρ_{ssd} = 2.68
Specific weight [Mg·m^{-3}]	-	ρ_f = 3.28	
Powder density [Mg·m^{-3}]	ρ_b = 1.71	ρ_b = 1.23	ρ_b = 1.36
Content of impurities [wt. %]	0.0	0.0	0.0
Resistance to freezing and de-freezing – magnesium sulphate test ($MgSO_4$)	-	MS = 1	MS = 4
Quality of fine particles – value of sand eq.	SE = 94	-	-
Presence of organic substances (Components affecting concrete solidification and hardening)	Solution colour – lighter than standard	-	-
Resistance to freezing and de-freezing – sodium sulphate test (Na_2SO_4) [wt. %]	-	-	0.9

All fractions of NGA were also subjected to grain analysis (CSN EN 933-1). Compatibility in size of the NGA and steel slag substitutes was investigated by a sieve analysis (Figure 1).

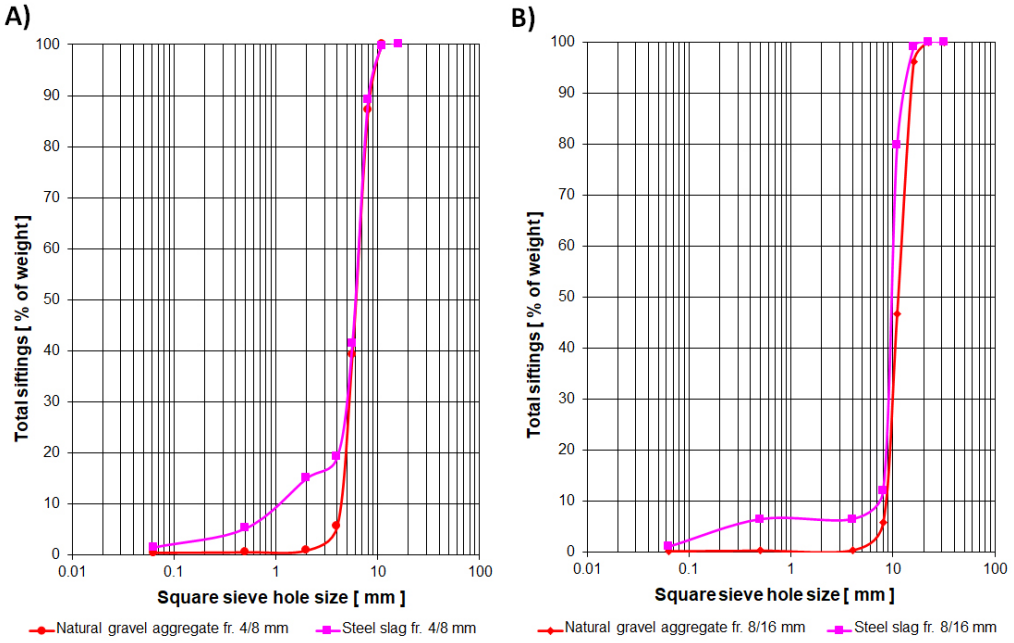

Figure 1: Grain fineness curves of NGA and SS for the fractions (A) 4/8 mm, (B) 8/16 mm.

The sieving tests were performed to determine the grading of the coarse fractions of NGA and SS used in this study. The fraction of 4/8 mm of steel slag proved a higher content of grains

within the range of 0.1–4 mm. In spite of this, both SS and NGA curves were identical in the interval of the grain size of 4–8 mm (Figure 1A). A higher share of fine grains within the range of 0.1–8 mm is clearly visible also in the steel slag fraction of 8/16 mm (Figure 1B).

Portland cement CEM I 42.5 R from Cement Hranice, a.s. was used as the binding component for production of concrete based on steel slag. The cement properties declared by the manufacturer are listed in Table 3.

Table 3: Characterization of Portland cement CEM I 42.5 R

Basic characteristics	Value
Strength in compression – initial strength [MPa]	≥ 20.0
Strength in compression – standardized strength [MPa]	≥ 42.5 ≤ 62.5
The beginning of setting [min.]	≥ 60
Stability of volume [mm]	≤ 10.0
Insoluble residue [wt. %]	≤ 5.0
Annealing loss [wt. %]	≤ 5.0
Content of sulphates (such as SO_3) [wt. %]	≤ 4.0
Content of chlorides [wt. %]	≤ 0.1

Drinking water from the water supply network was used to produce concrete based on steel slag. Superplasticizer MELMENT L10/40 based on melamine formaldehyde resin, produced by SKW TRONSBERG, was used as the plasticizing additive in mixtures used for the production of concrete based on steel slag.

2.2 Concrete mixtures

The tested concrete mixtures consisted of the same amount of Portland cement, tap water, superplasticizer, and three fractions of aggregates. Water to cement ratio was 0.55. A volume ratio of fine aggregates to coarse aggregates 0/4 : 4/8 : 8/16 (mm) was set to 4:3:3. The mixture marked as R0 was designed without a steel slag, only with NGA, and represented a reference concrete mixture. The concrete with the replacement of natural aggregate with steel slag was designed in three variants. In the first variant (R1), only the middle fraction of natural gravel aggregates with dimensions of 4/8 mm was replaced by steel slag, the other two fractions were represented by NGA. A substitution of a coarse fraction (8/16 mm) by the same fraction of steel slag was performed in the mixture R2. A complete substitution of all fractions (4/8 and 8/16) of NGA by SS was performed in mixture R3. The cubic and prism concrete samples with sizes of 150 mm × 150 mm × 150 mm, and 100 mm × 100 mm × 400 mm, respectively were prepared in a standard manner. After 24 h, the concrete samples were demolded and cured in water at 20 °C for 28 days.

2.3 Determination of physical-mechanical properties of concrete

Hardened concrete samples were tested in order to determine compressive strength, depth of penetration, frost resistance, and static modulus of elasticity. The determination of compressive strength and depth of penetration were performed for all experimental mixtures after 28 days on the cubic specimens (3 pcs of concrete cubic in total). Frost resistance of

concrete samples was tested on two sets of concrete prism specimens (6 pcs of concrete prisms in total), which were subjected to 100 cycles of freezing. Freezing and de-freezing of the test specimens was performed in freezing cycles within the range of −15 °C to 20 °C. One freezing cycle consisted of 4 h of freezing and 2 h of de-freezing. To determine the static modulus of elasticity, concrete prism specimens (2 sets) were tested. One set of test specimens (3 pieces) was used to determine the prism strength in compression and the other set (3 pieces) to determine the static modulus of elasticity in compression. The average value of prism strength in compression was applied to determine the tension used to measure the static modulus of elasticity.

2.4 Environmental assessment methodology

Environmental impact assessments were performed using the LCA (Life Cycle Assessment) method. This method belongs to a group of analytical instruments for environmental management that evaluate potential environmental impacts independent on the place of manufacture or product use. The method integrates time and space and thus all former, current, and future impacts of the life cycle all over the world. Moreover, LCA evaluates under a functional perspective. Thus, the functional unit is crucial because it defines all of the functions that the object under consideration will fulfil throughout its life cycle. When deciding between two or more alternatives, LCA can help to compare all major environmental impacts caused by products, processes, or services. Figure 2 illustrates the possible life cycle stages that can be considered in LCA and the typical inputs/outputs measured.

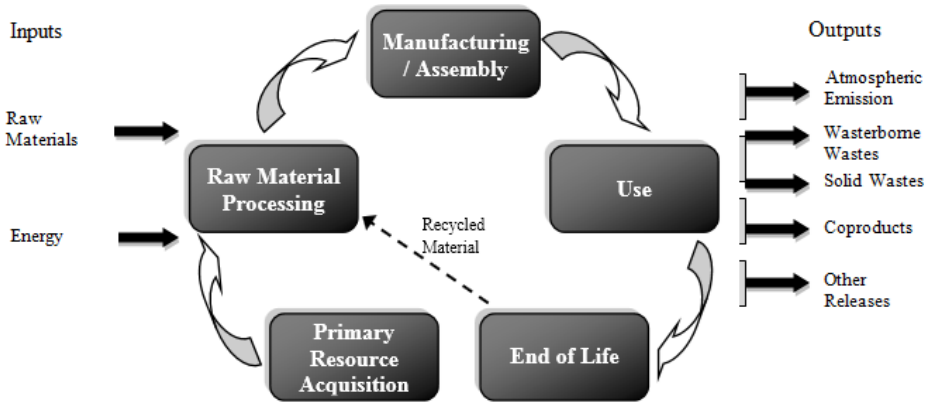

Figure 2: The possible life cycle stages with the typical inputs/outputs measured

The evaluation process itself is a systematic, phased approach, and consists of four steps according to series of standard 14040: goal definition and scoping, inventory analysis, impact assessment, and interpretation. The calculation of concrete´s environmental impacts was performed according to the above procedure by SimaPro software, with Eco-indicator 99 method and Ecoinvent database within the cradle to gate system boundaries. Functional unit was set at 1m^3 of concrete mixture.

3 Results and discussion

The results of physical-mechanical properties of concretes with slag substitutes (Table 4) confirmed the possibility of using slag as a partial replacement of natural aggregate in the production of non-traditional concrete. In order to take into account all tested mechanical parameters, it can be stated that the best properties were achieved by concretes R1.

Table 4: Characterization of Portland cement CEM I 42.5 R

Mixture	Cube strength of 28 [MPa]	Waterproof resistance [mm]	Frost resistance coefficient	Modulus of elasticity [GPa]
R0	44.0	23	0.89	25.8
R1	45.0	13	0.97	35.3
R2	46.0	19	0.81	25.5
R3	39.5	17	0.94	29.0

Partially: The results of the compressive strength tests showed that substitution of only one fraction of NGA by SS of the same fraction had not led to reduction in the initial strength of concretes. The R1 and R2 mixtures even achieved slightly higher values in the compressive strength tests of concrete comparing to mixture R0. The highest increase in strength of 4.4 % was recorded for the sample R2. A decrease in compressive strength was recorded for the concrete sample R3.
Based on the obtained results of waterproof resistance test, it is clear that the substitution of NGA of 4/8 and 8/16mm fractions by the same fractions of the SS is possible, without compromising the waterproof resistance of concrete.
After 100 cycles of concrete freezing and thawing test, it can be said that there was a decrease of all specimen's weight, ranged from 0.49 % to 1.01 %.
Obtained data also show that the results of the determination the modulus of elasticity of slag-based samples reached higher (R1 and R3) or comparable (R2) values than those measured for the R0. Percentage, there was found an increase by 27 % (R1) and by 11 % (R3). It is assumed that the proportion of fine slag particles affected the bulk density of the composite and filled its structure more.

Complete overview of results of LCA per $1m^3$ of the analyzed concrete samples are presented according to impact and damage categories in Figure 3-5. These figures present results in individual impact categories according to the substituted fraction of steel slag. It was found, that mixtures with the steel slag (R1, R2 and R3) the environmental indicators in human health damage category were reduced (except for carcinogens and respiratory organics indicators). The most significant decrease to $1m^3$ (7 %), was observed in the ozone layer category. In the damage category "Ecosystem quality", improvement of environmental impacts with steel slag substitution was observed. It was the same in the category "Acidification/eutrophication" - improvement was represented by 3.6 %. In Resources, the steel slag as NGA replacement has had a positive effect in reducing the environmental burden in both considered categories.

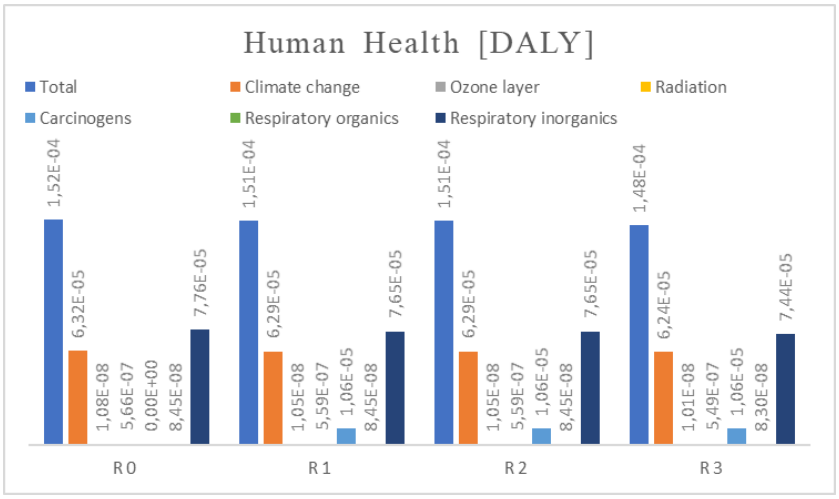

Figure 3: LCA results/damage category: Human Health [DALY]

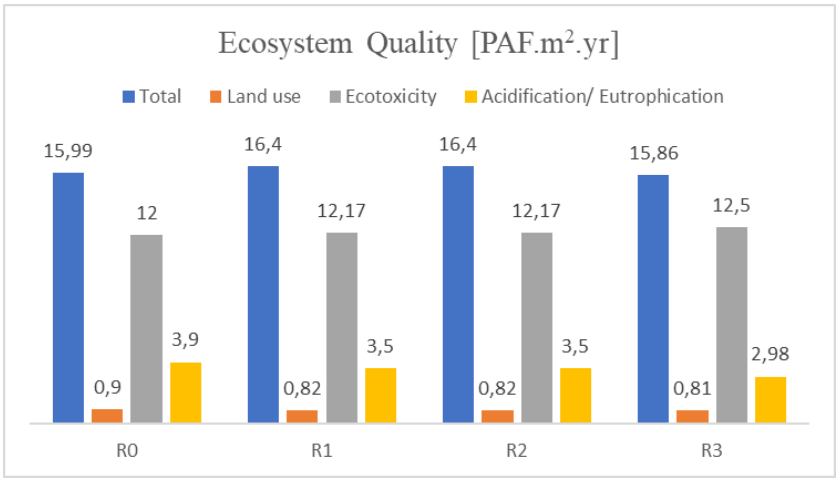

Figure 4: LCA results/damage category: Ecosystem Quality [PAF.m^2.yr]

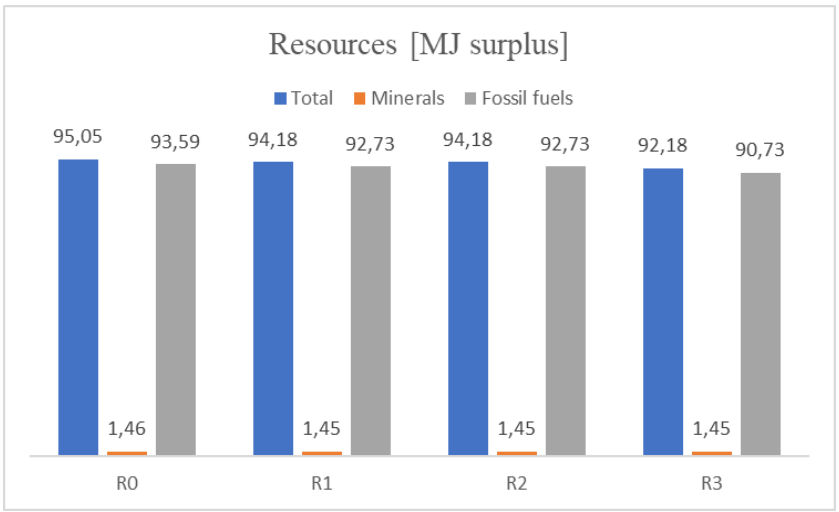

Figure 5: LCA results/damage category: Resources [MJ surplus]

4 Conclusion

The paper was focused on the evaluation of the sustainability (with regard to technical and environmental indicators) of non-traditional concrete with the replacement of natural gravel aggregates by steel slag. Based on the all presented results, the following conclusions can be formulated:

- Testing of technical parameters of non-traditional concretes through their physical-mechanical properties confirmed that steel slag can be effectively applied as a substitute for a part of natural aggregate in the production of concretes.
- Based on the tested mechanical parameters, it can be stated that the best properties were achieved by concretes with replacement of the natural aggregate fraction of 4/8 mm with the ratio of fine to coarse aggregate of 40:30:30. Its substitution led also to improved water tightness, frost resistance and static modulus of elasticity of concrete mixture, while maintaining the strength parameters.
- The results of the LCA analysis show a reduction in the negative environmental effects of non-traditional concretes compared to concrete without natural aggregate replacement. The most significant decrease was observed in concretes with replacement of both natural aggregate fractions by steel slag.

Acknowledgements

This research was funded by the Scientific Grant Agency of the Ministry of Education, Science, Research and Sport of the Slovak Republic and the Slovak Academy of Sciences (VEGA), grant number 1/0524/18.

References

[1] Sicakova A., Sliwinski J., Hager I., Tracz T., Zdeb T., Zych T., Hela R. & Bodnarova, L. (2008). *New generation cement concretes: ideas, design, technology and applications.* Kosice: Technical University. p. 156.

[2] Polettini A., Pomi R. & Fortuna E. (2009). Chemical activation in view of MSWI bottom ash recycling in cement-based systems. *Journal of Hazardous Materials*. *162*, p. 1292 - 1299.

[3] Draganovska M., Sicakova A. (2014). Selected parameters of concretes containing sludge from wet aggregates grading. In: ICEE-2014 - International Conference on Environmental Engineering: International Conference on Environmental Engineering; ICEE; Vilnius. Vol. 22, p. 1–6.

[4] Kr. Pati, P., Kr. Sahu, S. (2020). Innovative utilization of fly ash in concrete tiles for sustainable construction. *Mater. Today Proc. 33* (8), 2020, p. 5301-5305.

[5] Siddique R. (2003). Effect of fine aggregate replacement with Class F fly ash on the mechanical properties of concrete. *Cem. Concr. Res*. *33*, 539–547.

[6] Tsuji D., Kojima M., Kuroda M. & Sakata N. (2013). Study on the basic properties of concrete using high amount of ground-granulated blast-furnace slag. *Proc. Jpn. Concr. Inst*., *35*, p. 145–150.

[7] Srinivasarao Ch., Vijaya Bhaskar Reddy S. (2020). Study of standard grade concrete consisting of granulated blast furnace slag as a fine aggregate. *Mater. Today Proc*. *27*, p. 859–865, doi: 10.1016/j.matpr.2020.01.024.

[8] Oren O.H., Gholampour A,. Gencel O. & Ozbakkaloglu T. (2020). Physical and mechanical properties of foam concretes containing granulated blast furnace slag as fine aggregate. *Constr. Build. Mater*. *238*, 117774.

[9] Pasetto M., Baliello A., Pasquini E., Skaf M. & Ortega-López V. (2020). Performance-Based Characterization of Bituminous Mortars Prepared With Ladle Furnace Steel Slag. *Sustainability*. *12*,

1777.

European Technical standards:

CSN 72 1180, (1968). Determination of different particles in aggregates.

CSN 72 1176, (1968). Test of durability and frost resistance of aggregates.

CSN 73 1322, (1969). Determination of frost resistance of concrete.

CSN EN 933-1, (2012). Tests for geometrical properties of aggregates - Part 1: Determination of particle size distribution - Sieving method.

CSN EN 933-3, (2012). Tests for geometrical properties of aggregates - Part 3: Determination of particle shape - Flakiness index.

CSN EN 933-8, (2012). Tests for geometrical properties of aggregates - Part 8: Assessment of fines - Sand equivalent test.

CSN EN 1097-2, (2010). Tests for mechanical and physical properties of aggregates - Part 2: Methods for the determination of resistance to fragmentation.

CSN EN 1097-3, (1999). Tests for mechanical and physical properties of aggregates - Part 3: Determination of loose bulk density and voids.

CSN EN 1097-6, (2013). Tests for mechanical and physical properties of aggregates - Part 6: Determination of particle density and water absorption.

CSN EN 1097-7, (2008). Tests for mechanical and physical properties of aggregates - Part 7: Determination of the particle density of filer - Pyknometer method.

CSN EN 12350-2, (2009). Testing fresh concrete - Part 2: Slump-test.

CSN EN 12390-3, (2009). Testing hardened concrete - Part 3: Compressive strength of test specimens.

CSN EN 12390-5, (2009). Testing hardened concrete - Part 5: Flexural strength of test specimens.

CSN EN 12390-8, (2009). Testing hardened concrete - Part 8: Depth of penetration of water under pressure.

CSN EN 1367-2, (2010). Tests for thermal and weathering properties of aggregates - Part 2: Magnesium sulfate test.

CSN EN 1744-1, (2013). Tests for chemical properties of aggregates - Part 1: Chemical analysis.

STN EN ISO 14044: 2007, Environmental management. Life cycle assessment - Requirements and guidelines.

DOI: 10.1515/sspjce-2021-0012

3D Analysis interaction of piles groups under vertical load

Noura Houssou, Salah Messast and Assia Abdelouahed

University of 20 Août 1955-Skikda
Faculty of Technology, Department of Civil Engineering
Laboratory LMGHU
e-mail: n.houssou@univskikda.dz, msalah2007msalah@gmail.com, a.abdelouahed@univ-skikda.dz

Abstract

The study of the response of deep foundations under different types of stress was the subject of several studies, but it is always very useful to understand the phenomena accompanying the behavior of these foundations in contact with the ground, and to propose simple and more efficient approaches.

This paper presents a numerical analysis of the response of a pile foundation subjected to axial load with taking account the soil-pile interaction. The analysis of the composite pile–soil system was performed using the Finite Element Method (FEM) using software Plaxis 3D tunnel. The pile- soil analyses and design is an interaction three dimensional problem, wherein, the applied load is transferred by a complicated interaction process between the piles and the soil. To reduce the analysis volume of interaction problems, it is necessary to have a relatively simple design procedure so that the preliminary design can provide adequate but reasonably accurate data for the final analysis. The method consists to replacing two configurations of pile group with a single equivalent pier of the same length and an equivalent diameter. This equivalent pier is described by his material properties that result of the homogenisation of the piles and the surrounding soil. In this study, two types of symmetric and asymmetric pile group configurations are examined. The numerical results of settlements were compared with the field measurements collected from case history, which showed good agreement. The pier equivalent method can decrease the interaction factor of 2×2 pile groups by 16% than the interaction factor of single pile group.

Key words: pile group settlements, interaction factor, numerical modelling, equivalent pier, finite element method

1 Introduction

In recent years, many efforts have been devoted to the development of theoretical methods to analyze the behavior of a group of piles [1, 2, 3]. In many cases, the settlement of the pile groups is the determining factor in the design of deep foundations because the main purpose of the pile groups is to limit structural deformations. As a result, many researchers have proposed different methods to study the behavior and settlement of pile groups.
In the analysis and design of piles groups located close enough to each other, their individual responses differ from those of a single pile due to the group effect, to estimate the vertical

displacements of piles groups subjected to vertical loads, various methods have been proposed. These methods include the finite element method [4], the boundary element method [5, 6], the interaction factor method [7, 8, 9], and the pier equivalent method [8].

The effect of the interaction between the piles of group under axial loading has been the subject of many researchers during the past three decades. Based on the experience gained through these studies, empirical relationships were proposed to estimate the reduction factors on both, the bearing capacity and the stiffness of a group due the interaction between the piles. Moreover, specific values for these factors have been proposed in tabular form resulting from simplified analyses based on elastic continuum analysis and the principle of superposition Poulos and Davis [8]; Chen, S. L and al [10]; Poulos [11,12]. An alternative approach has been proposed by Lee (1993) [13] in which the response of single pile is simulated using the load transfer (t-z) method. Costanzo and Lancellota [14] proposed an approximate solution to evaluate the interaction factors taking into account the characteristic of non-linearity of the soil around the piles. Wong and Poulos [15] changed the interaction factors that can support the specifications of different types of piles.

Many subsequent studies have been carried out using the simplified concept of the interaction factor [16,17,18]; the simplified approach uses the nonlinear analysis of the load-displacement response of groups of piles [19]. Mahmoud and al. [20] analyzed analytically and numerically the interaction between groups of inclined piles. Rotta and Laloui [21]; Balakumar, V. and al[22] and Fatih, Celik .[23] present a method for estimating the average vertical displacement, of groups of energetic piles subjected to thermal loads. The method consists of replacing any group of regularly shaped piles with a single pier equivalent of the same length and equivalent diameter.

Simplified methods and computer-based approximate methods both have simplifications for considering the interaction between elements and soil behaviour modeling. Therefore, these methods are used as an initial estimation in design and then use available 3D-FEM software for reliable results. 3D finite element methods are of the most reliable methods for the analysis of piled raft foundations which can consider complex interaction between elements in these systems. Sinha and Hanna [24] performed a parametric study on piled raft foundations using ABAQUS software and the modified Drucker–Prager constitutive law. Deb and Kumar Pal [25] used ABAQUS software package to study the response of a piled raft foundation under combined lateral and vertical loading and analyse the influence of vertical load on the lateral response of a piled raft foundation. Mali and Singh [26] simulated a large piled raft through 3-D finite element modelling with PLAXIS 3D. Deb and Kumar Pal [27] used 3D finite element modelling by ABAQUS FEM package to study the complex load sharing behaviour due to the presence of interaction effects. Based on this study they proposed a simplified model for the design of the piled raft foundation considering both the safety and serviceability conditions. Abdolrezayi, A. Khayat, N. [28] considers the complex interaction between soil and structure using 3D FEM software available for modeling pield raft foundations.

The piled soil analyses and design is three dimensional interaction problems, wherein, the applied load is transferred by a complicated interaction process between the piles and the soil.

The paper presents such a simple design process in the form of equivalent pier approach by establishing its applicability by applying it to two configurations of piles groups.
The aims of this study, is to present selected numerical results which are:
(1) To verify the validity of the proposed solution via comparison with existing solutions.
(2) To demonstrate the effect of considering the pile group geometry in the solution, using the proposed interaction factor.
(3) Development of new prediction model for interaction factor of piles- groups foundations.

The foundation concept where the piles are considered as an equivalent pier simplified the analysis and opens up the margin of economy in the design solution. The prediction of these interaction factors holds prime importance in the design. Finite element based numerical methodology is used to obtain these interaction factors.

2 Behavior of the piles groups

Pile foundations have the dual purpose of strengthening the soil and transferring applied loads to deep and more rigid soil layers. In most cases, pile foundations consist of piles groups installed close together, center-to-center spacing is about 4 to 6 diameters, and joined by a molded cap on the top of the piles.
Failure of piles groups can occur by either failure of individual piles or failure of the overall block of soil enclosing the piles. If block failure occurs, the soil between the piles may move with the piles resulting from the failure plans that follow the periphery of the group or parts of the group [9]. When studying the failure mechanism of individual piles, it is necessary to consider the interaction effects between adjacent piles so that the capacity of each pile can be changed. The effects of installing neighboring piles may be relevant in loose soils, where the soil between piles becomes highly compacted leading to higher pile capacities than for single piles [29].
It has been experimentally proven by several researchers that the capacity of the group depends on several parameters, in addition to type of sandy or clay soil, the nature of drained or undrained behavior, pile construction method can have a critical influence on the capacity of a pile foundation, the value of the rigidity of the soil and piles, and the depth of the soil layer [9].

3 Concept of interaction factor

The degree of interaction between two identical, equally loaded piles may be expressed as an interaction factor, α, defined as the additional settlement ratio induced in the isolated pile due to loading an adjacent pile w_{ij}, by settlement of the isolated pile under its own load w_{ii}.
The interaction factor (α), as defined by Poulos [11], can be expressed by equation (1):

$$\alpha = \frac{w_{ij}}{w_{ii}} \tag{1}$$

For the calculation of the interaction factors, the displacement of a single pile under its own load was first determined. Then we calculate the displacement due to the loading of the two piles loaded identically for different diameter spacing ratio (s / d), where (s) is the distance between the axis and d is the diameter of the pile.

4 Numerical results

4.1 Piles embedded in a homogeneous soil layer

To verify the proposed solution, a simple problem with an axially loaded pile in a homogeneous elastic half-space is first selected.
The behavior of an axially loaded pile in an elastic soil is governed largely by the following dimensionless parameters:

(a) - The length-diameter ratio L/d;
(b) - The pile-ground stiffness ratio $K = E_P / E_s$, where E_P is the Young's pile modulus and Es is the Young's soil modulus.
Settlement of the head of a floating pile characterized by different values of $K = E_P / E_s$ K and L/d were determined. The pile diameter is 0.5 m, P is the applied load on the pile head taken p= $10\,MN$, E_s Young's modulus of soil taken $E_s = 1GPa$ and ν= 0.3.The results presented in table 1.

Table 1 Settlements at the head (mm) of a single pile in homogeneous soil

K	PGROUPN Basile1999	Poulos and Davis (1980)	Present study	PGROUPN Basile1999	Poulos and Davis (1980)	Present study
	L/d=25	L/d=25	L/d=25	L/d=10	L/d=10	L/d=10
10000	1.53	1.52	1.53	2.93	2.86	2.95
5000	1.55	1.54	1.56	2.94	2.86	2.96
1000	1.74	1.72	1.72	3.02	2.93	3.05

According to the results, it can be observed that the results obtained by this study are in good agreement with the different solutions published in the literature.

4.2 4.2. Pile embedded in a multi-layered soil

To analyze the settlement of a single pile in non-homogeneous soil profiles, the cases presented by Poulos [30] and Lee [31] will be considered in this study. The solutions are given in terms of an influence factor I_w defined by (2):

$$Iw = \frac{E_{s,ref} D \cdot w_t}{P} \tag{2}$$

Where $E_{s,ref} = 1GPa$: is the soil Young's modulus, D: is the diameter of the pile taken 0.5 m, wt

is the settlement at the pile head, and P is the applied load$10MN$. In this analysis, three cases are considered (Figure 1).

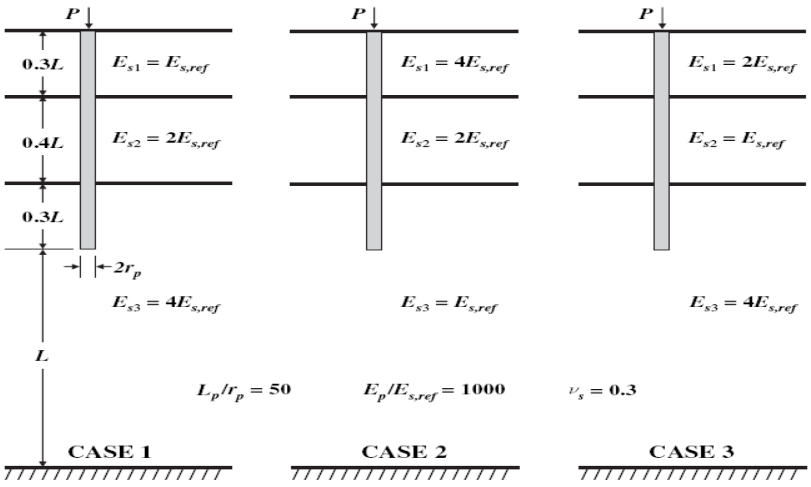

Figure 1: Non-homogeneous soil profiles modified by Poulos [20]

Randolph and Wroth [9] analysis is based on the concept of the r_m, radius at which the displacement becomes negligible, Lee and Xiao [32] developed the approach of Randolph and Wroth [9] to a three-layer stratified soil, see Figure 1, the analytical method of Hoyoung and Monica [33] is based on the soil profile divided into five layers, shear resistance the bottom of the third layer flush with the base of the pile. The fourth layer extends from a depth of L to 2L for the same Young's modulus; the fifth layer extends from 2L to the rigid base infinity and gives the ground along the direction and soil resistance to vertical compression. Numerical predictions from Plaxis3DT are compared with published results from alternative analyses (Table 2).

Table 2: Comparisons between different solutions in inhomogeneous soil

Case	Poulos 1979	Poulos 1979(FEM)	Lee 1991	Hoyoung Seo et al	Present study
1	0,0386	0,0377	0,0361	0,0336	0,0364
2	0,0330	0,0430	0,0372	0,0309	0,0303
3	0,0366	0,0382	0,0358	0,0323	0,0331

We can notice that there is an excellent agreement between the different solutions.

4.3 Pile embedded in a homogeneous soil of non-linear behaviour

The validation of the proposed approach (three-dimensional modeling using FEM) for the response of a single pile under axial load in a homogeneous soil was verified by comparison with numerical solutions, Poulos [27]; Basile PGROUPN (BEM) approach [28] and the LPC2

model described by Jardine et al. [29].

The pile is 30 m long; diameter 0.75 m, embedded in a homogeneous soil layer 50 m deep. The Young's modulus decreases markedly from an initial value of 1056 MPa to a constant limiting shaft resistance of the pile of 220 kPa, Poisson's ratio is assumed to be 0.49.The Young modulus of pile is taken as $E_p = 30GPa$.

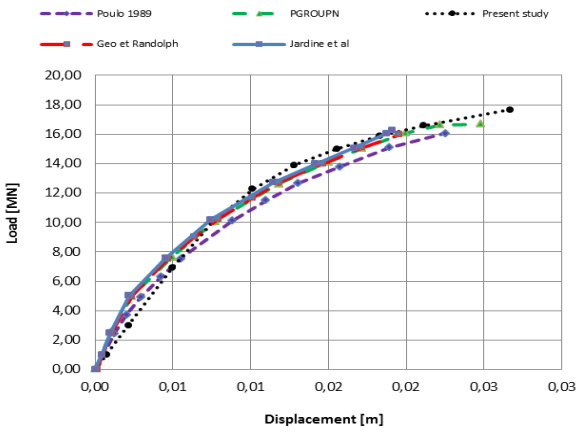

Figure 2: Load -Displacement of single pile in a homogeneous soil of non-linear behavior

Figure 2, illustrate all the numerical solutions, Poulos; Basile PGROUPN (BEM) approach and the LPC2 model (Jardine and al) are capable of predicting a very similar load-settlement response obtained from the FEM analysis (present study) which utilizes a non-linear constitutive model of soil behavior.

4.4 Interaction between two piles embedded in a linear homogeneous soil

The analysis of the interaction between piles is made in terms of the interaction factor (α) with respect to the normalized pile spacing (s/d), for different values of the slenderness ratio (L/d) and the relative stiffness ratio between the pile and the ground ($K = E_P / E_s$).

It has been found that the interaction effect is greater for more rigid piles and for reduced pile spacing.

In this section, the circular piles of diameter d are modeled as piles with square piles having an equivalent side B_{eq}, equation (3).

$$B_{eq} = \frac{1}{2}\sqrt{\pi} \tag{3}$$

Figure 3 and Figure 4 present a comparison of the results obtained by the present study (in homogeneous soil) with those predicted by Basile [8], and the analysis by the BEM method presented by Poulos and Davis [9] for different report slenderness ($L/d = 25{,}50$) and pile-soil stiffness ratio ($K = 100{,}1000$ and 10000).

The solutions are in good agreement, except for long and highly compressible piles

(i.e. $L/d = 50, K = 100$), where the present analysis gives interaction factors slightly lower than the analysis done by Poulos and Davis [9].

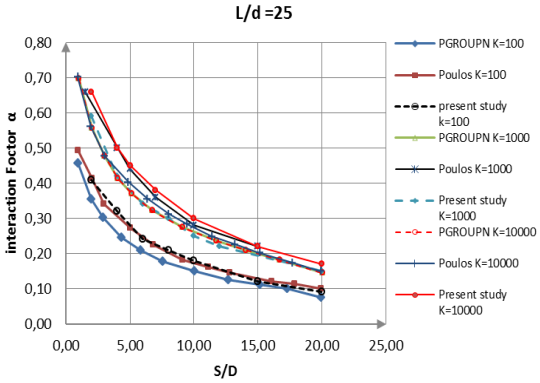

Figure 3: Interaction factor soil ($L/d = 25$)

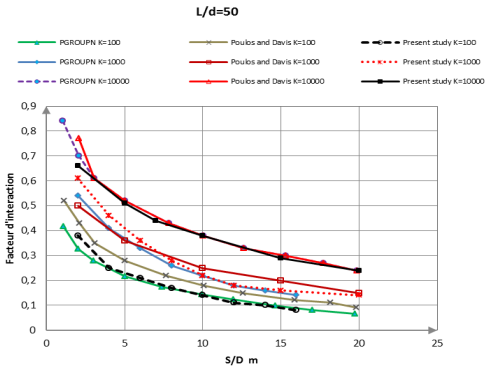

Figure 4: Interaction factor soil ($L/d = 50$)

4.5 Interaction between two piles embedded in nonlinear homogeneous soil

Interaction factors (α) are studied as a function of the applied load level P_g / P_u (where P_g is the total axial load acting on the group of two piles and P_u is its axial capacity of the ultimate load) for a slenderness ratio ($L/d = 50$), the relative stiffness pile-soil ($K = E_P / E_s = 100,1000$) and low spacing dimension of the piles (s/d = 2.5).
Pile diameter d=1 m, $E_p = 25GPa$, Soil undrained shear strength $C_u = 50KPa$

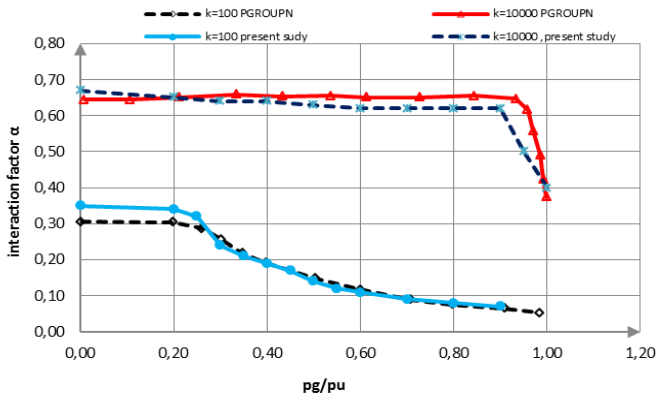

Figure 5: Interaction factor in homogeneous soil non-linear behavior ($L/d = 50, s/d = 2.5$)

Figure 5 shows that, at a standardized pile distance (s/d) of 2.5, the interaction factor (α) begins to decrease to a level of P_g / P_u of 0.2, for long piles, and for rigidity ($K = E_P / E_s = 100,1000$), the values of α are larger and constant up to a load level P_g / P_u of about 0.9 in a row.

5 The effect of group configuration

In this section, the variation of the interaction factor for various pile group configurations is studied. Two configuration cases are considered as illustrated in Figure 6.
Configuration I, corresponds to a group of 4 piles with an isolated pile. Configuration II, represents two groups of piles each of 4 piles, the characteristics of piles and soil are the same for both configurations, the load applied to each pile is from $10MN$ (uniformly distributed compression load).
All piles have the same diameter (1m) and the same length of 25m. The pile's properties are: $E_p = 25GPa; \nu = 0.2$.
The behavior of the soil is linear elastic, with a soil rigidity ratio pile $K = E_P / E_s = 1000$, the spacing between the piles of the group of 4 piles is (3d), the depth of the soil mass is considered finished equals h/L = 2.

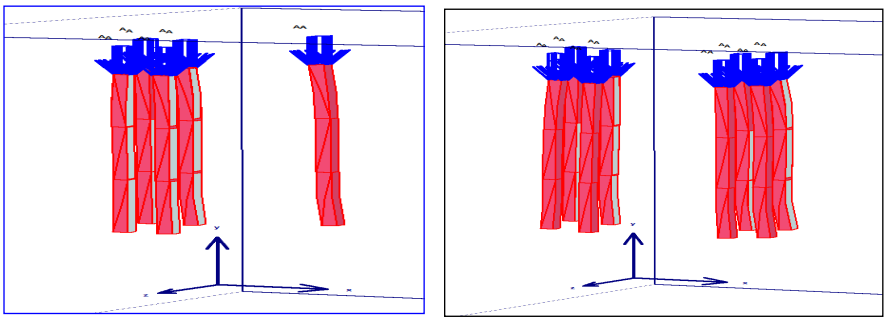

Configuration.1 Configuration.2

Figure 6: Configuration of two groups of piles

5.1 Configuration I

Two cases will be presented: Case 1 represents the effect of the loaded group on the isolated pile; case 2 illustrates the effect of the loaded single pile on the pile group.
In order to determine the interaction factor of the configuration I, w0 the settlement at the head of the single pile under its own load must be calculated, and the additional settlement due to the loading of the adjacent pile group w1, then determined.
The settlement of the head pile group w_{0A}, w_{0B}, w_{0C}, w_{0D} and w_{0E} (center), then calculates the additional settlements w_{1A}, w_{1B}, w_{1C}, w_{1D} and w_{1E} under load of the adjacent, the different points A, B, C, D , E (middle of group) and single pile (F) are shown in Figure 7.

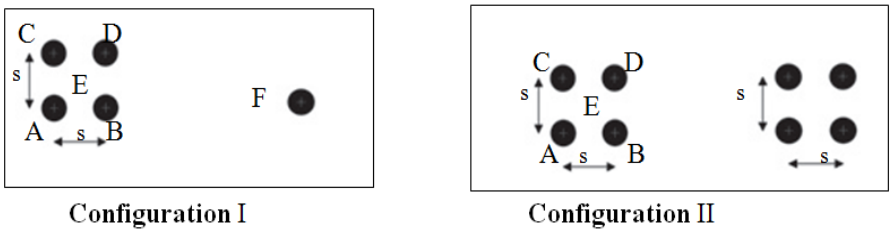

Figure 7: Plan of the two configurations piles groups

The results are shown in Figure 8.

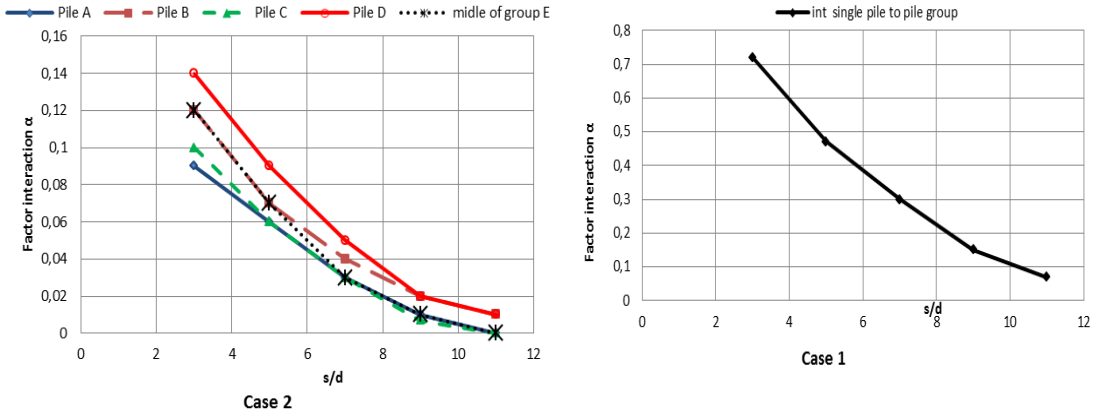

Figure 8: Configuration I: Interaction factor of the group of 4 piles and the single pile

Interaction factor for the two cases of the pile group configuration I is relatively significant for a low s/d = 3 spacing and decreases with the increase in spacing up to a value greater spacing as s/d> 10 (Figure 8).

Figure 8, illustrate the interaction factor a single pile between middle 4 pile groups (E) is very important (case1) while the interaction factor of head 4 piles groups to single pile are less significant.

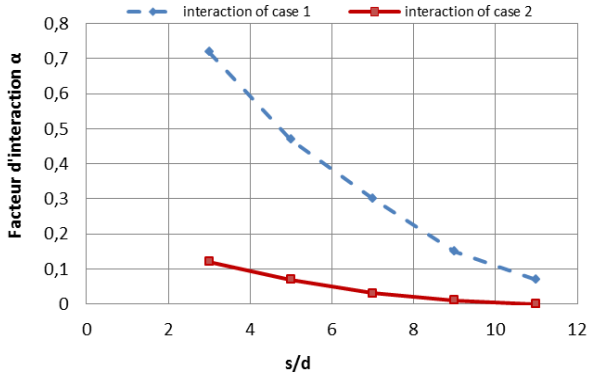

Fig. 9 Comparison between two cases of configuration I

Figure 9, illustrate a comparison with results obtained through the interaction factor two cases of configuration I, we notice a big difference in the interaction factor of the two cases, we conclude that when an isolated pile is placed near a group of piles becomes more interactive.

5.2 Configuration II

The configuration II represents the case of two groups of piles, each group of 4 piles are spaced from 3d, the geometry of the two groups is symmetrical, and the interaction factor between the two groups is the same i.e. $\alpha_{ij} = \alpha_{ji}$.

The settlement at the head of each pile of the first group due to the loading of all piles , w0A, w_{0B}, w_{0C}, w_{0D} and w_{0E} (middle), the additional settlement due to the loading of the second group of Adjacent piles , w_{1A}, w_{1B}, w_{1C}, w_{1D} and w_{1E}. Loads to all piles $10MN$, interaction factor are calculated for different spacing of two groups, results are shown in Figure 10.

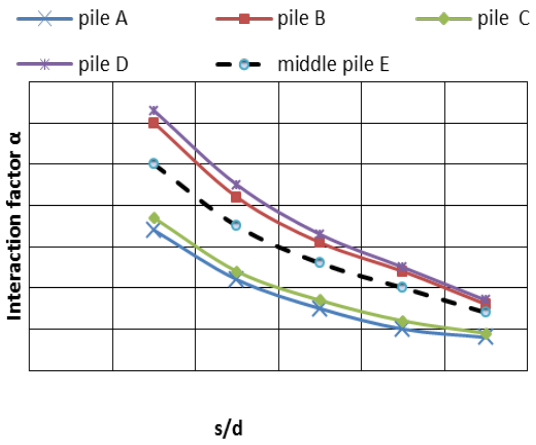

Figure 10: Interaction factor for configuration II

Figure10, illustrate the interaction factor between two groups of piles is very important at the head of piles B and D which are all near the second group of piles with respect to pile A and

C to the most distant piles, then the interaction factor of the middle of the group is the average value of the group interaction factor that we can take into consideration.

6 Simplification of piles groups

Poulos and Davis [8] have proposed a so-called equivalent pile method for estimating settlement of a group of piles. In this method several piles are replaced by a single pile considering the soil in which the piles are integrated as homogenized continuum "equivalent pile". The equivalent pile is characterized by a length which coincides with the average length of piles and of equivalent diameter this can be calculated as follows [36].

$$D_{eq} = \frac{2}{\sqrt{\pi}}\sqrt{A_g} \approx 1.13\sqrt{A_g} \tag{4}$$

Where A_g, is the area of the group plan. For any general configuration of piles, A_g can be determined as in equation 5:

$$A_g = A_{t,EP} + A_{soil} \tag{5}$$

Where $A_{t,EP}$ is the total section of the piles making up the group. If n_{EP} is the number of piles in the group and A_{EP} is the cross section of a single pile) and A_{soil} is the ground plan area surrounding the piles delimited by the simplest polygon reproducing the shape of the pile group. For a square geometry of the piles, A_g can be calculated as (6):

$$A_g = \left[\left(\sqrt{n_{EP}} - 1\right)s + d\right]^2 \tag{6}$$

Where s is the center-to-center spacing of the piles and d is the diameter of the pile. L_P Is the pile length, E_s, E_P and E_{eq} are the Young's modulus of the soil, pile and pier equivalent respectively, D_{eq} is the equivalent pile diameter and Ag is the flat surface of the pile group of the block.

The total cross section of the piles defined as (7):

$$A_{t,EP} = \pi\frac{D^2}{4}n_{EP} \tag{7}$$

Is replaced by a single pile equivalent cross-section defined by (8):

$$A_{eq} = \pi\frac{D_{eq}^{\ 2}}{4} \tag{8}$$

The shape of the pile group can be categorized by the 'aspect ratio' (AR) (formula 9), which can be determined for a square geometry of piles in the plan view as [37].

$$AR = \sqrt{\frac{n_{EP} \cdot s}{L}} \tag{9}$$

Here L is the length (average) of the piles. The equivalent pile approach (Figure 11) has been proven to provide a representative description of the behavior (eg. deformation and

capacitance) of conventional pile groups subjected to mechanical loads for AR values smaller than 4 and certainly less than 2.

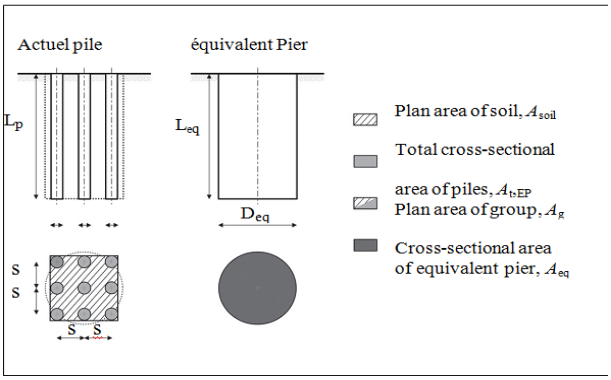

Figure 11: modeling of the approach

The equivalent pile can be characterized by an equivalent Young's modulus efficiently homogenizes that of the piles and the ground embedded between them which can be calculated as the weighted average of the Young's modulus (formulas 10 and 11) of these bodies as [36] (Figure12).

$$E_{eq} = \frac{A_{t,EP}E_{EP} + A_{soil}E_{soil}}{A_{t,EP} + A_{soil}} \tag{10}$$

$$E_{eq} = E_{EP}\frac{A_{t,EP}}{A_g} + E_{soil}\left(1 - \frac{A_{t,EP}}{A_g}\right) \tag{11}$$

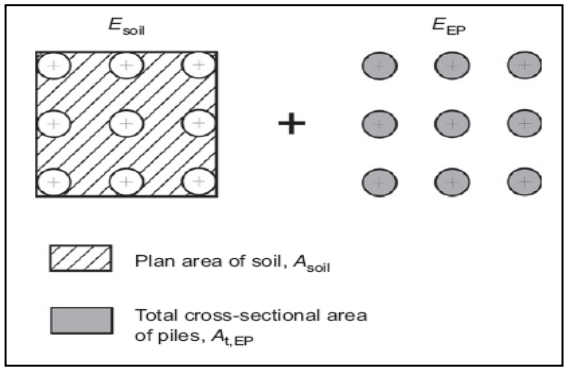

Figure 12: Young's module representation of the equivalent pile

In order to study the effect of the interaction factor between two groups of piles, the configurations of section 6 are repeated, each group of piles replaced by a single equivalent pile.

The configuration I, corresponds to a group of 4 piles with an single pile, the group of 4 piles is replaced by a pile equivalent, we must determine the various parameters of the group system of homogenized ground piles, L_p is the average length, E_{eq} and D_{eq} are the Young's modulus and the equivalent pile diameter respectively.

The modeling of the interaction factor of the configuration I extends to the modeling of the interaction between two piles of the same length and of different diameter (axisymmetric system), the single pile is loaded by $10MN$ whereas the equivalent pile is loaded with ($10MN \times 4$) for different values of the spacing between the two equivalent piles. The results obtained are compared with those of conventional pile group results (section 5.1) (Figure13).

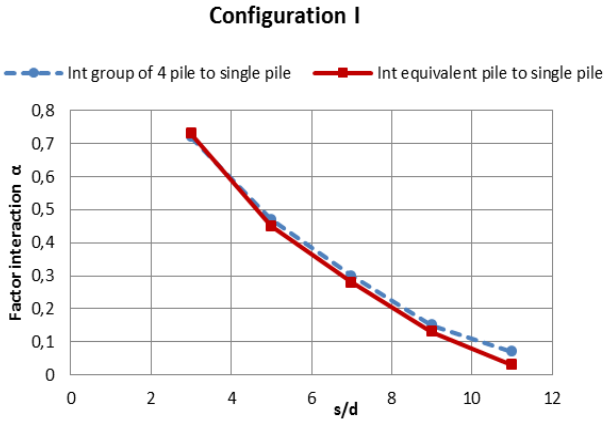

Figure 13: Comparison between the equivalent pier interactions factors with the isolated pile of configuration I

Figure 13, illustrate a comparison between the equivalent pier interactions factors with the isolated pile of configuration I. The negligible influence on interaction factor with change in configuration from 2×2 to single pile was observed.

The configuration II, represents two groups of piles each of 4 piles, the group of 4 piles is replaced by a pile equivalent, the parameters of the group system of homogenized ground piles, L_p is the average length, E_{eq} and D_{eq} are the module of Young and the equivalent pile diameter respectively. The modeling of the interaction factor of the configuration II, extends to the modeling of the interaction between two piles, of the same length and of the same diameter (symmetric system), each equivalent pier is loaded by a force 10 MN times the number of piles ie (10× 4 = 40MN), for different values of the spacing between the two equivalent piles. The results obtained are compared with those of conventional pile group results (section 5.2) (Figure 14).

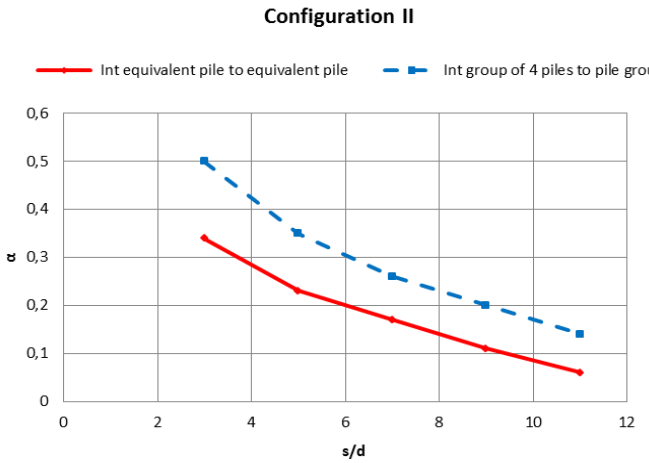

Figure 14: Comparison between the interactions factors between two piles equivalents (configuration II)

Figure 14, illustrate a comparison between the interactions factors between two piles equivalents (configuration II). The pier equivalent method can decrease the interaction factor of 2 × 2 pile groups to 16% than the interaction factor of single pile group.

7 Conclusion

A three-dimensional numerical modeling using Plaxis 3DT based on the finite element method has been established to predict the behavior of large pile groups. The method of analysis of the interaction factor has been briefly described, and some parametric studies have discussed. The consideration of inhomogeneous soil modulus with depth; taking into account the influence of the stiffness ratio pile-sol is presented.

The purpose of this work was to contribute to the modeling of the interaction behavior between two piles, which significantly conditions the behavior of many engineering works. It emerges from this study that numerical modeling of geotechnical structures requires a precise knowledge of the behavior of the soil and the contact zones, between solids of different types.

To estimate the interaction between pile-pile, two piles of the same length and diameter were loaded identically, which could be used to predict the settlement of groups of piles.

The validity of the current method has been verified by comparisons with solutions obtained using other methods such as the boundary elements method (PGROUPN) studied by Basile and those of Poulos and Davis.

This paper proposes a simplified new prediction model for the interaction factor evaluation for the piles group. Finite element modeling was used to achieve this aim. The proposed methods were validated with the centrifuge test and numerical results available in the literature. From the study, it has been found that the equivalent pier can be predicted the factor interaction of a pile group. The procedure of the current solution is effective in solving the problem of 3D interaction of vertically loaded pile groups.

The values of interaction factor α is increasing with decrease the escapement s/d and

converging to unity.
Negligible influence on α with change in configuration from 2×2 to single pile was observed.
The obtained interaction factors for various configurations followed a certain trend; hence, a simplified model was defined through the method of equivalent pier. The predicted values of interaction factors were limited to unity.
This study can be extended to the dynamic and cyclical case and the examination of different cases of soils and piles.

References

[1] Brian, B. S. and Bryan, A. M. (2014). A finite element–based approach for predictions of rigid pile group stiffness efficiency in clays. *Acta Geotechnica, 9*, 469–484.
doi: https://doi.org/10.1007/s11440-013-0240-9

[2] McCabe, B. A. and Lehane, B. M. (2006). Behavior of axially loaded pile groups driven in clayey silt. *J. Geotech. Geoenviron. Eng. 132(3)*, 401–410.
doi: https://doi.org/10.1061/(ASCE)1090-0241(2006)132:3(401)

[3] Comodromos, E.M. and Bareka, S. V. (2009). Response evaluation of axially loaded fixed-head pile groups in clayey soils. *Int. J. Numer. Anal. Methods Geomech. 33(17)*, 1839–1865.
doi: https://doi.org/10.1002/nag.787

[4] Majid, H. Buse, E. Hanifi, C.and Abdulazim, Y. (2020). 3D Numerical Modeling of a Single Pipe Pile Under Axial Compression Embedded in Organic Soil. *Geotech Geol Eng. 38*,4423–4434.
doi: https://doi.org/10.1007/s10706-020-01299-1

[5] Butterfield, R.and Banerjee, P. (1971). The elastic analysis of compressible piles and pile groups. *Géotechnique. 21(1),* 43–60.
doi: https://doi.org/10.1680/geot.1971.21.1.43

[6] Jeramy, C. Ashlock, A. M. ASCE; and Zhiyan Jiang. (2017). Three-dimensional soil-pile group interaction in layered soil with disturbed zone by Boundary Element Analysis, *Geotechnical Frontiers. GSP 279*, 334-344.
doi: https://doi.org/10.1061/9780784480465.035

[7] Basile, F. (1999). Non-linear analysis of pile groups. *Proc. Inst. Civ. Eng. Geotech. Eng. 137(2)*, 105–15.
doi: https://doi.org/10.1680/gt.1999.370205

[8] Poulos, H.G and Davis, E. H. (1980). *Pile foundation analysis and design*. New York, John Wiley.

[9] Randolph, M. F and Wroth, C. (1979). An analysis of the vertical deformation of pile groups. *Géotechnique. 29(4)*, 423–39.
doi: https://doi.org/10.1680/geot.1979.29.4.423

[10] Chen, S. L, Song, C. Y and Chen, L. Z. (2011). Two-pile interaction factor revisited. *Can. Geotech. J. 48(5)*, 754–766.
doi: https://doi.org/10.1139/t10-095

[11] Poulos, H. G. (1968). Analysis of the settlement of pile groups. *Geotechnique, 18(4)*, 49−471.
doi: https://doi.org/10.1680/geot.1968.18.4.449

[12] Poulos. H. G. (1989). Pile behaviour- theory and application. *Geotechnique. 39(3),* 365-415.
doi: https://doi.org/10.1680/geot.1989.39.3.365

[13] Lee, C. Y. (1993). Pile group settlement analysis by hybrid layer approach. Journal of the Geotechnical Engineering, ASCE.119(6), 984−997.
doi: https://doi.org/10.1061/(ASCE)0733-9410(1993)119:6(984)

[14] Costanzo, D and Lancellota, R. (1998). A note on pile interaction factors. *Soils and Foundation. 38(4)*, 251−253.
doi: https://doi.org/10.3208/sandf.38.4_251

[15] Wong, S.C and Poulos, H.G.(2005). Approximate pile-to-pile interaction factors between two dissimilar piles. *Computers and Geotechnics, 32(8),* 613−618.
doi: https://doi.org/10.1016/j.compgeo.2005.11.001

[16] Poulos, H.G and Mattes, N. S. (1971). Settlement and load distribution of pile groups. Aust. Geomech. J. G1(1), 18-28.

[17] Lee, C. Y. (1993). Settlement of pile group-practical approach. *J.Geotech. Eng. 119(9)*, 1449-1461. doi: https://doi.org/10.1061/(ASCE)0733-9410(1993)119:9(1449)

[18] Qian-qing, Z, Shi-min, Z, Fa-yun, L, Qian Z and Fei, X. (2015). Some observations of the influence factors on the response of pile groups, *KSCE Journal of Civil Engineering. 19(6)*, 1667-1674. doi: https://doi.org/10.1007/s12205-014-1550-7

[19] Sheil, B.B, McCabe, B.A, Comodromos, E. M, Lehane, B. M. (2019). Pile groups under axial loading: an appraisal of simplified nonlinear prediction models, *Geotechnique. Vol.69*, No. 7, 565-579. doi: https://doi.org/10.1680/jgeot.17.R.040

[20] Mahmoud, G, Pedram, R and Arash, A. L. (2014). Analytical and numerical solution for interaction between batter pile group. *KSCE Journal of Civil Engineering.18(7)*, 2051-2063. doi: https://doi.org/10.1007/s12205-014-0082-5

[21] Rotta, Loria, A. F and Laloui, L. (2017). The equivalent pier method for energy pile groups. *Géotechnique. 67 (8)*, 691–702. doi: https://doi.org/10.1680/jgeot.16.P.139

[22] Balakumar, V. Huangand , Min.and Erwin ,Oh .(2013).Equivalent pier theory for piled raft design .Proceedings of the 18th International Conference on Soil Mechanics and Geotechnical Engineering, Paris.

[23] Celik, F. (2019). An Analytical Approach for Piled-Raft Foundation Design Based on Equivalent Pier and Raft Analyses by Using 2D Finite Element Method. *Arabian Journal of Geosciences . 12(429)*:1-16 doi: https://doi.org/10.1007/s12517-019-4579-6

[24] Sinha, A. Hanna, AM. (2019). 3D numerical model for piled raft foundation. *Int J Geomech . 17:*1–9. doi: https://doi.org/10.1061/(ASCE)GM.1943-5622.0001066

[25] Deb P, Pal SK. (2019). Numerical analysis of piled raft foundation under combined vertical and lateral loading. *Ocean Eng; 190:106431*. doi: https://doi.org/10.1016/j.oceaneng.2019.106431

[26] Mali, S. and Singh, B. (2018). Behavior of large piled-raft foundation on clay soil. *Ocean Eng. 149:*205–216. doi: https://doi.org/10.1016/j.oceaneng.2017.12.029

[27] Deb, P., Pal, S.K. Analysis of Load Sharing Response and Prediction of Interaction Behaviour in Piled Raft Foundation. *Arab J Sci Eng* 44: 8527–8543 doi: https://doi.org/10.1007/s13369-019-03936-1

[28] Abdolrezayi, A. Khayat, N.(2021). Comparative Three-Dimensional Finite Element Analysis of Piled Raft Foundations. *Computational Engineering and Physical Modeling* 4(1): 19-36. doi: https://dx.doi.org/10.22115/cepm.2020.234834.1111

[29] Vesic, A. S. (1969). Experiments with instrumented pile groups in sand. Performance of deep Foundations. *ASTM STP 444*, 177-222. doi: https://doi.org/10.1520/STP47286S

[30] Poulos, H.G. (1979). Settlement of single piles in non-homogeneous soil. *J. Geotech. Eng. Div. ASCE. 105(5),* 627-641. doi: https://doi.org/10.1061/AJGEB6.0000799

[31] Lee, C. Y. (1991). Discrete layer analysis of axially loaded piles and pile groups. *Computers Geotech.11(4)*, 295-313. doi: https://doi.org/10.1016/0266-352X(91)90014-7

[32] Lee, K.M and Xiao, Z.R. (2001). A simplified nonlinear approach for pile group settlement analysis in multilayered soils. *Canadian Geotechnical Journal. 38(5)*, 1063−1080. doi: https://doi.org/10.1139/t01-034

[33] Hoyoung, S and Monica, P. (2006). Analytical solutions for a vertically loaded pile in multilayered soil. *Geomechanics and Geoengineering: An International Journal. 00(00)*, 1-10. doi: https://doi.org/10.1080/17486020601099380

[34] Guo, W.D and Randolph, M. F.(1997). Vertically loaded piles in non-homogeneous media. *Int. J. Numer . Anal. Meth. Geomechs. 21*, 507-532. doi:https://doi.org/10.1002/(SICI)1096-9853(199708)21:8%3C507::AID-NAG888%3E3.0.CO;2-V

[35] Jardine, R. J, Potts, D. M, Fourie, A. B and Burland, J. B. (1986). Studies of the influence of nonlinear stress-S1rain characteristics in soil-structure interaction. *Geotechnique. 36(3)*, 377-396.

doi: https://doi.org/10.1680/geot.1986.36.3.377

[36] Poulos, H.G.(1993). Settlement prediction for bored pile groups. In Proceedings of deep foundations on bored and auger piles .(ed.W. F. Van Impe). 103–117.

[37] Randolph, M. and Clancy, P. (1993). Efficient design of piled rafts. In Deep foundations on bored and auger piles – bap II (ed. W. F.Van Impe).119–130.